UNIVERSITY OF HELSINKI
DIVISION OF GEOPHYSICS

REPORT SERIES IN GEOPHYSICS

No 48

SNOW PACK STRUCTURE CHARACTERISTICS IN FINLAND – MEASUREMENTS AND MODELLING

Sirpa Rasmus

HELSINKI 2005

UNIVERSITY OF HELSINKI
DIVISION OF GEOPHYSICS

REPORT SERIES IN GEOPHYSICS

No 48

Cover photo: A view of the Saana-Jeahkats fell plateau in Kilpisjärvi (K. Rasmus)

SNOW PACK STRUCTURE CHARACTERISTICS IN FINLAND – MEASUREMENTS AND MODELLING

Sirpa Rasmus

HELSINKI 2005

Report Series in Geophysics No. 48
ISBN (printed version) 952-10-2378-3
ISBN (pdf-version) 952-10-2379-1
ISSN 0355-8630

SNOW PACK STRUCTURE CHARACTERISTICS IN FINLAND – MEASUREMENTS AND MODELLING

Sirpa Rasmus

Academic dissertation in Geophysics, to be presented, with the permission of the Faculty of Science of the University of Helsinki, for public criticism in the Auditorium E 204 of Physicum, Gustav Hällströminkatu 2, Helsinki, on May 27th, 2005, at 12 o'clock.

Helsinki 2005

Contents

’Tell me about the snow,’ Moomintroll said and seated himself in Moominpappa’s sun-bleached garden chair. ’I don’t understand it.’
’I don’t neither,’ said Too-ticky. ’You believe it’s cold, but if you build yourself a snowhouse it’s warm. You think it’s white, but at times it looks pink, and another time it’s blue. It can be softer than anything, and then again harder than stone. Nothing is certain.’

(Tove Jansson, Moominland midwinter)

Acknowledgements

Measuring the snow pack structure using traditional methods is time consuming and laborious work. Many people have helped me in the huge effort of finding out the local variability of the snow pack structure in different parts of our country. Especially during my maternity leave continuation of the field work would not have been possible without the help from my parents and from my husband in taking care of the kids and from my colleagues in digging the snow pits and driving thousands of kilometres with the faithful car of the Division of Geophysics. So thanks to Riitta Lehmusjärvi, Olli Huttunen, Kai Rasmus, Tiia Grönholm and to many students in courses Geophysics of snow and ice and Winter ecology.

I would like to thank the Swiss Federal Institute for Snow and Avalanche Research for the opportunity to use the SNOWPACK -model, SMEAR II station and Rossby Centre for making the essential input data available for my use and CSC Scientific Computing for the computer time. Thanks to Kai and Tiia for technical support... Weather and snow water equivalent data have been provided by Finnish Meteorological Institute and Finnish Environment Institute. Special thanks to Veijo Hiltunen and Toivo Pohja at the Hyytiälä Forest Station for everything, especially collecting of new snow density data, which were also provided by the staff of Oulanka Biological Station. Thanks to the staffs of all the different field stations I have visited during the measurement campaigns (Tvärminne, Lammi, Hyytiälä, Mekrijärvi, Oulanka, Kilpisjärvi). Food has been excellent, beds have been warm and the help has always been there when it has been needed!

Thanks to many people, who have helped to plan the measurement campaign and motivated me to carry on with the work and with whom I have had discussions about snow, climate and other important things: William Pruitt, Philip Marsh, Don Gray, Michael Lehning, Timo Helle, Tim Carter, Reijo Solantie, Jouni Räisänen, Markku Kulmala, Timo Vesala, Heikki Hänninen and Timo Saarinen just to mention some. Many othes have answered my numerous e-mailed questions. Thanks to the fellow-students and researchers at the Division of Geophysics, especially for the “joyful sounds of the young generation”, and for the support of the other Graduate School participants: Anja, Jari, Mats, Nadja, Tari. Matti Leppäranta is acknowledged for the supervision of the work.

Parts of chapter 5 and chapter 6 have also been formed as articles, Tiia Grönholm, Michael Lehning, Kai Rasmus and Markku Kulmala being co-writers in the first one and Jouni Räisänen and Michael Lehning in the second. I thank them all for the help with the articles, and for the permission to use the articles also as a material for this work. National Land Survey of Finland has given permission to use their maps as a basis for some figures (permission no. 49/MYY/04). Following instances have supported the work: Snow and Ice Graduate School, financed by the Academy of Finland; Yrjö, Kalle and Vilho Väisälä Foundation; Sohlberg Delegation; Magnus Ehrnrooth Foundation; Friends of Finland in Switzerland Association; Alfred Kordelin Foundation. Business language teacher Mariel Pilois checked the language of the work.

Greatest thanks go of course to my own family: to Aino, who wanted to come and dig snow pits with me, to Sauli, who gave me a joint materinity leave and time to think my research through in the middle of the Graduate School, to Matias who set the final dead-line I needed to finish my work - and to Kai, who has bravely taken all that one has to take in a family of two field-working scientists and small children and still loves me!

Summary

In this work theoretical background for snow distribution and the structure of snow cover as well as its evolution during the winter is presented. Snow pack structure modelling is discussed and the SNOWPACK model is described in detail.

The present day snow climatology in Finland is shortly described, as well as measurements and methodology of the field work of this study. The snow conditions in Finland are studied using long-term statistics of snow depth and water equivalent and variation in snow pack structure especially using field measurements in Santala, Lammi, Mekrijärvi, Oulanka and Kilpisjärvi. The variation of the snow pack structure inside and between the different study locations and inside and between the main biotypes (forest and open field) in these sites are the most important subjects of this study. The variations of snow depth and snow pack structure were observed to be small inside individual biotypes. More variation was seen between the forest and open area; normally effects of more efficient metamorphic processes in the open area were seen. Distinguished coefficient of variation ranges were found for the snow depth in different locations, especially in the forested conditions. Based on the study of agreement scores between the observed snow profiles inside individual biotypes it can be said that the highest agreement scores and lowest variability is seen in grain size and temperature. Lowest agreement scores and highest variability is seen in density and grain type. Fraction of faceted grain snow and that of icy or melting snow during the early and mid-winter divide Finland into two areas. Differences were seen in bulk properties, like bulk density or grain size, between different locations and different biotypes in a individual location. Differences were also found in density, hardness and grain size between different grain types of snow.

As a model tool a Swiss snow pack structure model SNOWPACK has been chosen. Model is developed in the Swiss Federal Institute for Snow and Avalanche Research. The validation of the SNOWPACK –model in Finland is described in this study, and also results concerning the reliability and sensitivity of the model in Finnish climate. Sensitivity of the model was studied especially in Hyytiälä and in Kilpisjärvi, as well as model parameterisation in Finnish conditions. The snow depth is simulated well during the accumulation periods, during the melt the snow depth is overestimated. Modelled snow water equivalent is most often overestimated. Visual agreement between the snow pack structure observations and simulations is reasonably good throughout the country. Agreement scores between the observed and simulated snow profiles are highest for temperature and grain size, and lowest for grain type and density. Most sensitive snow parameters in this study were snow water equivalent, temperature, grain form and size, snow depth and timing of the snow melt. The model sensitivity grows towards the melting period, and also the choices of the input data and boundary conditions become more important.

The SNOWPACK model is used together with output of a regional climate model to give estimates of future snow conditions around the year 2080 in Finland. The reliability of this new method for climate change work is also discussed. Climate model used was Rossby Centre regional climate model (RCA) for Northern Europe. Using control run and scenario run data as input, a set of snow winter conditions was calculated for most of the study locations for "present day" and "future" case. In a climate represented by the RCA scenario runs around 2080s, snow cover thickness and duration are likely to decrease. Snow properties are also likely to change: snow will be denser, warmer and coarser; fraction of depth hoar in the snow pack will decrease and fraction of icy or wet snow will increase. Also the standard deviations for many of the studied snow cover parameters will change.

Yhteenveto

Tässä työssä lumipeitteen jakautumisen ja lumipeitteen rakenteen ja sen talven aikaisen kehityksen teoreettinen tausta on esitetty. Lumipeitteen rakenteen mallinnusta esitellään, ja lumipeitteen rakenteen malli, SNOWPACK, käydään läpi yksityiskohtaisesti.

Suomen nykyinen lumi-ilmasto kuvaillaan lyhyesti, samoin kuin tutkimuksen mittausmenetelmät. Suomen lumioloja on tutkittu käyttämällä lumen syvyyden ja vesiarvon pitkiä aikasarjoja, ja lumipeitteen rakenteen vaihtelua käyttämällä kenttämittauksia Santalassa, Lammilla, Mekrijärvellä, Oulangalla ja Kilpisjärvellä. Lumipeitteen rakenteen havainnot Suomen eri osissa eri biotoopeilla ja eri talvina esitellään. Lumipeitteen rakenteen vaihtelu eri paikkojen välillä sekä saman paikan eri biotooppien (pääosin metsä ja avoin pelto) välillä on tutkimuksen tärkein aihe. Lumen syvyyden ja lumipeitteen rakenteen vaihtelun huomattiin olevan pientä yksittäisen biotyypin sisällä. Enemmän vaihtelua huomattiin metsän ja avoimen pellon välillä; yleensä avoimella alueella nähtiin tehokkaampien lumen metamorfoosien tulokset. Tunnusomaiset vaihteluvälit lumen syvyyden variaatiokertoimille havaittiin eri paikkakunnilla, erityisesti metsässä. Laskemalla vastaavuuskertoimia saman biotyypin eri havaituille lumiprofiileille huomattiin suurinta vaihtelua tiheydellä ja kidetyypillä; pienintä vaihtelua havaittiin kidekoolla ja lämpötilalla. Tahkokkaisten kiteiden osuus lumen syvyydestä sekä jäisen tai märän lumen osuus lumen syvyydestä jakoi tutkimustalvina Suomen kahteen osaan. Keskimääräisten lumipeitteen ominaisuuksien, kuten keskimääräinen tiheys tai kidekoko, huomattiin eroavan eri paikkakuntien ja biotyyppien välillä. Eroja havaittiin myös eri lumikidetyyppien tiheyden, kovuuden ja kidekoon välillä.

Lumipeitteen rakenteen malli nimeltään SNOWPACK, joka on kehitetty Sveitsissä SLF –tutkimuslaitoksessa, on valittu tutkimuksen mallinnustyökaluksi. Malli on eräs maailman johtavista lumipeitteen rakenteen malleista. Työssä kuvaillaan SNOWPACK –mallin testausta Suomessa, sekä tulokset mallin luotettavuudesta ja herkkyydestä Suomen oloissa. Joitakin suosituksia mallin käytöstä annetaan myös. Mallin herkkyyttä ja parametrisointia testattiin erityisesti Hyytiälässä ja Kilpisjärvellä. Malli simuloi lumen syvyyden hyvin kun lunta kertyi; sulannan aikana malli yliarvioi lumen syvyyden. Malli yleensä yliarvioi myös lumen vesiarvon. Mallinnettujen ja havaittujen lumipeitteen rakenteiden silmämääräinen vastaavuus oli kohtuullisen hyvä. Vastaavuuskertoimet havaintojen ja mallinnustulosten välillä olivat suurimpia lämpötilalle ja kidekoolle ja alhaisempia kidetyypille ja tiheydelle. Herkimmiksi parametreiksi tässä työssä nousivat lumen vesiarvo, lämpötila, kidekoko ja muoto sekä lumen syvyys. Mallin herkkyys lisääntyi sulamiskaudelle tultaessa, jolloin lähtötietojen ja reunaehtojen valinta nousee entistä tärkeämmäksi.

SNOWPACK-mallia on tässä työssä käytetty yhdessä alueellisen ilmastomallin tulosten kanssa arvioitaessa lumioloja vuoden 2080 tietämillä Suomessa. Tämän uuden ilmastonmuutoksen vaikutusten arviointimenetelmän luotettavuutta pohditaan myös. Käytetty ilmastomalli oli Rossby Centren RCA Pohjois-Euroopalle, joka on laskettu parempaan paikkaresoluutioon käyttämällä eri globaaleja laskennan reunaehtoina. Joukko eri paikkakuntien lumitalvia ”nykyhetkellä” ja ”tulevaisuudessa” simuloitiin käyttämällä RCA:n kontrolliajon ja skenaarioajon talvien sääoloja lähtötietoina. Tämän jälkeen keskimääräisiä lumipeitteen rakenteita ”nyt” ja ”tulevaisuudessa” verrattiin keskenään. RCA:n skenaarioajoa vuoden 2080 tietämillä vastaavassa ilmastossa lumipeite on nykyistä ohuempi ja kestää vähemmän aikaa. Lumen laatu mitä luultavimmin muuttuu (lumi on tiheämpää, lämpimämpää ja suurikiteisempää; tahkokkaisten kiteiden osuus vähenee ja jäisen lumen osuus kasvaa), ja keskihajonta kasvaa useilla lumiparametreilla.

1. Introduction

Snow is formed in the clouds when the temperature is less than 0 °C and supercooled water and suitable condensation nuclei are present. Ice crystals form around condensation nuclei. They grow through aggregation of small ice crystals and riming from water droplets into the snow flake form, and land to the ground as snow fall. The falling snow forms a porous cover consisting of ice crystals and moist air, in some cases also liquid water.

Snow pack is actually an ice skeleton, with liquid water and moist air in its pores. In case of seasonal snow cover, large fraction of the volumetric content of the snow is always air. Because of this, snow is a very efficient insulator. In snow covered areas relatively warm ground is insulated from the relatively cold air. Only a few tens of centimeters thick layer of this insulator is sufficient to dampen the daily temperature variation under the snow cover. The fact that energy exchange between the atmosphere and the ground is limited during the winter has an effect on for example the freezing of the ground: thick enough snow cover can keep the ground unfrozen even during long periods of low temperatures.

Snow has also larger-scale effects on the globe. Snow cover acts as a heat storage, and a lot of heat energy is needed for its phase changes. When the air temperature starts to rise, part of the heat energy is used for the increasing of the temperature of the snow cover to the melting point, and for the melting of snow. Only after this air masses close to the snow cover are able to warm up efficiently. This way the snow cover slows down the temperature variations both globally and locally. Saturation pressure for the water vapour is larger on the water surfaces than on the snow surfaces. Because of this the presence of the snow cover has an effect onto the areal evaporation.

Snow has a high albedo. New snow can reflect 90 % of the incoming short wave radiation back to the atmosphere. This leads to the other important role of the snow cover in the global climatic system: there is a positive feedback mechanism between the snow covered area and the rise of global air temperature. As mean global air temperature rises, there is a decrease in the snow covered area and the duration of the snow cover. This implies the decrease of global albedo, which leads to a greater amount of absorbed heat energy, a more efficient increase in mean air temperature and a more intense decrease in snow covered area. Naturally this feedback mechanism works also vice versa as mean global air temperature decreases.

Seasonal snow cover is also a water storage. In cold climates it is possible that the snow pack stores all of the precipitation fallen during the winter. This water is freed during the melting period, and this moisture is important for the beginning of the growing season. Also nutrition pulse consisting of the various chemicals scavenged by the falling snow flakes and affected by the different chemical reactions in the snow pack is freed to the soil and to the water bodies.

Snow is one of the most complex physical materials on Earth, which makes it a challenging habitat for life. As a substance it is crystalline at small scales ands porous at larger scales. It undergoes phase changes to liquid and vapour forms of water during a normal winter. The snow conditions may also be manipulated by life forms. (Pomeroy and Brun, 2001) For animal and plant life snow cover makes it in many cases easier to cope with coldness and drought during the winter. Under the snow cover air humidity and temperature change relatively little and are relatively high through the winter. On the other hand long lasting snow cover in the spring may slow down the starting of growth – solar radiation is dampened efficiently in the snow even in the first 10 cm of the snow surface. In the areas with variating snow depth, like fell plateaus in the Finnish Lapland, also the vegetation has been noticed to have a spatial variation: in some parts of the area the species with adaptations to short growth season and humid soils but no adaptations to frost are dominating (snow bed areas); in other parts the species coping with dry, cold and windy conditions but adapted to long growth season dominate (deflation areas). (Gjaerevoll, 1956; Eurola et al., 1980) The inter-relationships between snow properties and vegetation involve a series of feedbacks between vegetation structure and the snow structure. For example snow density in the Finnish fell plateau has an effect to the temperature regime in and under the snow cover, which in turn affects the vegetation type; on the other hand vegetation has an effect on the snow density (Eurola et al., 1980). Snow pack affects ecology, but it also can be controlled by the resulting vegetation. (Körner, 2003; Pomeroy and Brun, 2001)

A similar pattern is seen in the animal population in the areas with snowy winters: some species are physically adapted to the snow (chionophiles), for some the snow acts as a hindrance for spreading (chionophobes). For some species snow is essential: ringed seals of Lake Saimaa give birth to their pups in the snow caves on the lake ice; ptarmigans hide in the warm snow caves (kieppi) during the very low temperatures; forest hares are adapted to hide from predators with camouflage; wiesels are using the same methods to move unnoticed when looking for prey. A clear pattern can be found between the movement and feeding behavior of reindeers and caribous and snow conditions. During winters with difficult snow conditions reindeers may have difficulties in finding food under the hard snow cover, and when thick basal ice covers the ground, they may even die. (Formozov, 1946; Helle, 1984, 2001; Pruitt, 1959; Reimers, 1982)

As we remember that snow covers over 50 % of the northern hemisphere land area during the winter, and in many areas over half of the year, we understand how vital, or in some cases fateful, snow cover can be to plants and animal life. In southern Finland 30 – 40 % of annual precipitation is snow and in northern Finland even 40 – 50 % (Mustonen, 1965). Snow covers the northern part of the country from October until May or even June, the southern part from December until April or May. Snow is part of the landscape during the winter, it has high value for winter sports but on the other hand the costs of keeping roads, streets, roofs and other structures free from snow are high. For example real estates spend yearly up to 100 million euros for winter maintenance (Snow and ice geophysic course study, University of Helsinki, 1998, unpublished). In mountainous areas snow forms a risk to lives and property in the form of avalanches.

Most of the researchers and also some decision makers all over the world have admitted the fact that the global climate is slowly warming. There is evidence of increase in mean air temperature, precipitation and extremity of climate system, and also of most intense change in polar regions. There does not exist mutual understanding if the change is even partly due to mankind activities. It is still very probable that a huge increase in greenhouse gas emissions to the atmosphere during past centuries is a main reason for the climate warming. This is also called anthropogenic enhanced greenhouse effect. (Nakićenović et al., 2000; Houghton et al., 2001)

Solar radiation is the source of energy for all global weather phenomena. Approximately half of the radiation coming to the upper atmospheric boundary reaches the ground surface. During its way through the atmosphere radiation is absorbed to clouds and atmospheric gases, scattered from gases and particles and reflected back from clouds, particles and ground surface. To remain in thermal equilibrium, the Earth has to radiate out long way thermal radiation equivalent amount to the short wave radiation absorbed. Some of the atmospheric gases – water vapour, carbon dioxide, methane, oxidized nitrogen and ozone being the most important ones – absorb upwelling long wave radiation efficiently without preventing transmission of incoming short wave radiation. This is the basis to global greenhouse effect, which makes life possible on Earth. As mankind uses fossil fuels and cuts down large areas of forests, atmospheric greenhouse gas content keeps rising more rapidly than natural processes are able to bind these gases back to biosphere, geosphere and hydrosphere. This is causing a serious problem as the greenhouse effect is enhanced and the climate probably changing due to this. It is true that geologically thinking we are now living in a relatively cold spell in the Earths climatic history. It is still important to keep in mind that this is the first time the climate is changing because of other than natural causes; and as we do not fully understand mechanisms and processes in the Earth's climate system we should be prepared for changes and also for surprises. Surprises may be caused by nonlinearity of the climate system. Reaction of this kind may be unpredictable when the system is quickly diverted from the equilibrium state. (Nakićenović et al., 2000; Houghton et al., 2001)

Global circulation models (GCM) have been developed in several research institutes concentrating on climate research. Models have been used not only to simulate behavior of present day climate, but also to estimate how global climate will change under enhanced greenhouse effect. It is important to understand that GCMs are not always able to explain acceptably even the present day climate variation. It is also worth noticing that there are large deviations between predictions of different GCMs for example for global mean air temperature during the next century. And it is also good to remember the one basic problem in climate simulations: simulations are based not only on imperfectly understood physical phenomena in the atmosphere, but also for example on greenhouse gas emission scenarios, which are rather unreliable itself. Increase of emissions depend for example on international politics, global economy and suddenly breaking wars, all of which are extremely difficult to predict. Still, after filtering predictions given by GCM simulations through all of the uncertainties listed above, there are some estimates left which should be taken seriously.

The annual mean temperatures have increased about 0.7°C during the 20th century in Finland, with the greatest warming in spring. Mean daily minimum temperatures have risen more than maximum temperatures, possibly because of a increase in cloudiness. The winters and springs were exceptionally mild during the 1990s. There has also been a tendency towards a shorter snow cover season and reduced amounts of snow during recent decades in Southern Finland. (Carter et al., 2002)

The annual mean air temperature can be expected to rise during the following 100 years in Finland, many simulations predict a rise of approximately 4°C. Increase may be larger during the winter. Precipitation can be expected to increase, also liquid precipitation during the winter. Climate scenarios have more deviating predictions what comes to the other quantities, like wind velocities or cloudiness, by some of the scenarios both of these are expected to increase in the future. (Carter, 2002) As winter mean air temperature rises, duration of snow cover and amount of snow decreases. Because of the importance of snow to climate and living environment, it would be useful to estimate the intensity, timing and placing of the change. What is the effect of more frequent rain during the winter? How about the possible change in frequency of extreme events? Does the climate change affect also snow characteristics other than snow amount?

This work concentrates on seasonal snow cover. The greatest attention is not paid to the amount of snow, snow cover duration or evolution of snow water equivalent, as in most of the hydrological studies. Focus of this work is in the inner structure of the snow cover. What difference does it make to properties of snow cover listed earlier if the snow consists of different types of layers?

Snow pack structure means description of internal stratigraphy of snow cover. The description consists of information about the amount of layers, layer thickness and layer quality: temperature, density, hardness, grain size and grain form, for example. In addition, also snow microstructure can be described; this means information about grain size, bond size, amount of bonds per grain (coordination number). Also information about fractions of ice, water and air can be defined as part of the microstructure.

Combined properties of single layers define properties of the whole snow cover. On the other hand, the snow microstructure in single layers define those snow properties people are usually interested in. Snow heat conductivity, which determines temperatures inside the snow pack as well as snow insulating capacity, is mostly due to the grain bonding and fractions of different water phases; snow viscosity, which has an effect on snow settling and stability, is based on grain size, form and bonding; snow carrying capacity, which determines the animals' ability to move on the snow cover, is due to the grain bonding. During winter time (not taking the melting period into account) snow pack properties and the effects on its environment cannot be satisfyingly studied without taking the snow pack structure into account, and also snow microstructure if possible.

Finland can be roughly divided into five snow zones according to the snow pack structure. The south-western part is known as *ephemeral zone* and snow covers it irregularly. A strong layering structure caused by many warm and cold periods during a winter characterise the snow pack in the *thin maritime zone* and the *maritime zone* in southern and middle-Finland. It is also suggested to use term mild snow zone together with term maritime. *Taiga zone* with deep, usually homogenous snow pack reaches to the timberline. The most northern part of Finland, treeless Lapland, is known as *tundra zone*. The snow pack there, is characterised by wind packed dense layers and depth hoar. *Thin alpine zone, prairie snow zone* and *transition zone* between ephemeral and maritime zones can also be located in small areas in Finland. The location of snow zones will change with possible climate warming. (Oksanen, 1999; zones described originally by Sturm et al., 1995)

Snow cover research has long and diverse traditions. In many countries the systematic snow observations covering the whole country were started at the end of the 1880s or during the 1890s. Observations on snow morphology were started in the Swiss Alps during the 1930s by Seligman and Bader (Colbeck, 1987). Systematic observations on snow conditions (snow cover formation, melting and snow depth) were started in Finland in 1890. The Finnish Meteorological Institute and Finnish Geographical Society built observation networks, which were combined in 1909. The number of observers was 300-500. Also Hydrographic Office and Agricultural Administration conducted snow and ice observations during those early decades. (Lavila, 1949)

In Finland snow cover research has traditionally been the mapping of snow precipitation, accumulation and melting. The estimating of snow water equivalent has been studied intensively, as well as melt and runoff prediction (review by Vehviläinen, 1992). A snow scale developed by professor V. V. Korhonen in the beginning of the 1900s is worth noting: it is still in operative use in determining snow water equivalent. Hardness measurements were conducted during the 1950s in 20-30 locations (Angervo, 1952). Remote sensing of snow has been used to estimate snow water equivalent (for example Hallikainen et al., 1990). Studies concerning skiing have been conducted in Finland also by geophysicists (for example Palosuo et al., 1979).

Snow pack structure has been studied very little in Finland. Almost the only earlier study concerning snow pack structure is a snow density profile evolution study by Simojoki and Seppänen (1963).The studies by Oksanen (1999) and Rasmus (1999) were the first ones to collect thorough information on snow cover structure in Finland. In the first one the areal variation was studied using measurements from 19 locations; in the second the temporal variation of the structure was followed in two locations. So the most important result of this study will be the information of the variation of snow pack structure in time and space in Finland.

Above I stated a question regarding the effect of climatic change on snow pack properties. Increase in air temperature and precipitation as well as more frequent melting events during the winter will also certainly have an effect on the snow pack structure. Snow pack structure is due to repeated snowfalls during the winter. Weather conditions during and between the snowfalls modify the properties of the layers continuously until the snow melts. Size, form and bonding of the snow grains change as a function of meteorological factors, and with them also snow properties like heat conductivity and viscosity. It can be assumed that these will change if the winter climate will be warmer in the future. This in turn will have consequences for example to the welfare of animals and plants during the winter in a changed climate.

In this study the aim is to answer the following questions:

1. What are the present snow conditions like in the selected sites on different snow zones in Finland? Especially how does the snow pack structure vary between and inside the main biotypes (forest and open field) in these sites?
2. Can the selected snow pack structure model be reliably used in the Finnish conditions?
3. What estimates can be given about snow pack structure changes during the following 100 years using the snow pack structure model and climate scenario data as tools?

I also hope to be able to present estimates for the error limits and uncertainties connected to every aspect of the study.

Answer to question 1 will be looked at from a long-term statistics of snow conditions and especially by field measurements. Measurements have been made twice in winter during three winters: in Santala, Lammi, Mekrijärvi, Oulanka and Kilpisjärvi. Snow depth has been measured using snow surveys, and snow pack structure has been studied from the snow pits.

As a model tool a Swiss snow pack structure model SNOWPACK (Bartelt and Lehning, 2002) has been chosen. The model was developed in the Swiss Federal Institute for Snow and Avalanche Research, and it is one of the world leading snow pack structure models, together with the French model Crocus and North-American SNTHERM. The model was chosen to be used in this work because of its sophisticated microstructure description and ongoing development work.

Meteorological data as well as data about snow pack structure were collected from several locations in Finland to allow the validation of the SNOWPACK model. The sensitivity of the model was studied as well as model parameterisation in Finnish conditions.

In this study snow pack structures were simulated also by using climate scenario data as input for SNOWPACK model. The climate model used was Rossby Centre regional climate model (RCA) for Northern Europe, which is downscaled to a better resolution using different GCMs (HadAM3 and ECHAM4 with different emission scenarios) as boundary conditions for calculations. Using control run and scenario run data as input, a set of snow winter conditions was calculated for most of the study locations for “present day” and “future” case. Thereafter mean snow pack structure characteristics between “present day” and “future” cases were compared.

Snow can be studied in different scales: from micrometer scale in snow microstructure studies to the scale of hundreds of kilometers in snow cover distribution studies. In this study the most often used scale is between centimeter and a meter (snow pack structure), in some cases hundreds of meters (variation in snow depth and snow cover structure). Measurements presented in this study have been made in Finland and model runs have been planned keeping in mind conditions in Finland. The results can be representative also in areas with similar snow climate around the world, especially in the boreal forest zone.

In chapter 2 the theoretical background for snow distribution and snow pack structure as well as evolution of snow pack structure during the winter is presented. In chapter 3 the present day snow climatology in Finland is shortly described, as well as measurements and methodology of the field work of this study. Observations about snow pack structure in different parts of Finland in different biotypes and during different winters and times of the winter are also presented in chapter 3. Snow pack structure modelling is discussed in chapter 4. The SNOWPACK model is also described in detail here. In chapter 5 the validation of the SNOWPACK –model in Finland is described, and also results concerning the reliability and sensitivity of the model in Finnish climate. Some recommendations are also given for the model use in Finland. In chapter 6 the SNOWPACK model is used together with output of a regional climate model to give estimates of the possible future snow conditions around year 2080 in Finland. The reliability of this new method for climate change work is also discussed. Chapter 7 gives conclusions of the study.

2. Snow pack structure

Snow cover consists of the net accumulation of snow on the ground resulting from several precipitation events. It may include also hoar frost, hoar formed of the water vapour from the unfrozen soil, as well as frozen rain and melt water. Structure and dimensions of the snow pack are complex and highly variable, both in space and also in time. The variability depends on many factors: the variability of the weather bringing the snowfall, the nature and frequency of the storms, the weather conditions between the storms and other snowfall events and finally surface topography and vegetative cover. Snow cover is an end product of both accumulation and ablation, so it is also a product of complex processes and their interactions.

Snow pack structure means the description of internal stratigraphy of snow cover. The description consists of information about the amount of layers, their thickness and quality: for example temperature, density, hardness, grain size and grain shape. In addition also snow microstructure can be described; this means information about grain size, bond size, amount of bonds per grain (coordination number). Also information about fractions of ice, water and air can be defined as part of the microstructure.

Properties of falling snow are determined by temperature and humidity conditions inside the cloud, where ice crystal nucleation takes place, and along its flow path where the crystal grows. This study concentrates on snow on the ground, snow formation in the atmosphere is not discussed further.

Snow stratification results from successive snow falls over the winter and processes that transform the snow cover between snow falls. Snow crystals transform their shapes under the effect of thermodynamics. This is called metamorphism. Transformations of snow cover are controlled by two interacting processes: snow settling and metamorphism. (Pomeroy and Brun, 2001)

2.1 Distribution and properties of falling snow

The areal variability of snow cover is considered on three geometric scales:
1) Regional scale, areas up to 10^6 km^2 with characteristic linear distances of 10 to 100 km. Meteorological effects of mountains and lakes are important in this scale.
2) Local scale, with characteristic linear distances of 100 m to 1 km. Here redistribution of snow may occur because of wind or avalanches. Accumulation may also be related to elevation and canopy effects.
3) Microscale, with characteristic linear distances of less than 100 m. Accumulation patterns result mainly from interactions between surface roughness and transport phenomena in this scale. (McKay and Gray, 1981)

The shape of the snow cover depth distribution can be summarised using the coefficient of variation. In a study conducted in Canada the coefficient of variation was noted to be 0.44 in the snow cover on a ploughed field, 0.57 on lawn and 0.29 in the forest. The greater the variability, the greater the impact the snow cover depletion curve (SDC) will have on snow cover estimation. SDC is being used in hydrologic models, and it summarises the relationship between snow cover distribution and average snow depth or water equivalent. Depending on the coefficient of variation of a snow depth in a certain area, very different reductions in average snow depth result to the same area of exposed ground. Snow covers with different variability have different impacts on energy balance and snow melt. When the variability is small, the response to reduction in average snow depth approaches the instant bare ground effect, while the large variability results in more gradual snow cover ablation and different snow melt runoff patterns. (Donald et al., 1995)

Snow cover is not even in all parts of an certain area. It is redistributed by wind during and after the snowfall. Efficiency of accumulation and erosion is affected by topography and vegetation. The properties of falling snow also vary during different times, due to the different weather conditions. In below snow properties and distribution are discussed in relation to the weather, topography and vegetation.

2.1.1 Weather

Factors controlling snow cover distribution and characteristics are atmospheric conditions together with the state of the land surface. The most important meteorological factors connected to this are temperature and wind speed.

The temperature at the time of the snowfall controls the dryness, hardness and crystalline form of the new snow and also its erodability by wind. In a study by Eagleson (1970) it was observed, that increase in air temperature of 1°C causes new snow density to increase by 6.5 kgm^{-3}.

The wind redistribution of snow includes erosion of snow cover by the shear force of the wind, transport of blowing snow from exposed sites with low aerodynamic roughness, sublimation of blowing snow in transit, and deposition of snow to sites with higher aerodynamic roughness or less exposure to wind. (McKay and Gray, 1981)

Blowing snow transport involves three modes of movement: creep (rolling movement on the surface), saltation (skipping along the surface) and turbulent diffusion or suspension (the movement in suspended flow in the air). Saltation is the source of all other snow particle movement and it is derived from the eroded snow. Sublimation from blowing snow is a significant loss to the surface snow pack during the dry winter season. The magnitude of sublimation loss depends on blowing snow mass concentration, wind speed, air temperature and relative humidity, and can be several tens of per cents of annual snowfall. Erosion prevails where the wind accelerates (e.g. at the crest of a ridge) and deposition occurs where the wind velocity decreases (e.g. along the edges of forests). Other sources of blowing snow in the arctic are for example tundra and exposed soil, sinks including shrub tundra, sparse forest and drifts (Pomeroy and Brun, 2001).

The roughness of the land surface affects the structure of wind and its velocity distribution. The wind flow near the ground is normally turbulent, and snow cover patterns reflect the turbulent structure. The wind moves the snow crystals, changing their shape and properties and redeposits them as drifts or banks with greater density. Very slight perturbations in the air flow may induce drift formation. Wind transports loose snow causing erosion and packing into wind slab and crust. The rate of transport is greatest over flat, extensive open areas. Snow can be transported more than 50 km on polar ice caps; in complex topography the average transport distance has been observed to vary between 100 and 500m (McKay and Gray, 1981).

There is a strong positive correlation between wind speed and density of the accumulating snow. This is mainly due to the fact that wind sorts the material by size: the largest particles move near to the surface, while the smallest ones float relatively high. The snow crystals are also deposited onto the surface in similar manner. Strong wind during a snow fall may cause new snow density to increase even to 340 kgm^{-3} (Kuusisto, 1973).

Exposure to wind also hardens snow. The higher hardness values are associated with conditions of high wind speeds, greater age and concurrent blowing snow during deposition. Snow deposited within exposed vegetation cover has lower hardness and density (Pomeroy and Brun, 2001).

2.1.2 Topography

Snow cover reaches the greatest depths in areas to the lee of open water areas and on windward slopes which stimulate the precipitation process. The physiographic features related to snow cover variations are elevation, slope, aspect, roughness and the optical and thermal properties of the underlying materials (McKay and Gray, 1981).

In areas where snow is mostly due to frontal activity and strong winds prevail, slope and aspect are important in snow distribution. Snow depth along a slope oriented in the direction of the prevailing wind speed tends to decrease with distance. Hilltops may be free of snow, while the lee of steep slopes and gullies are major accumulation areas. There is a large difference between windward and leeward slopes of especially coastal mountain ranges. The aspect is also related to the frequency of snow fall and the energy exchange processes influencing the snowmelt (McKay and Gray, 1981).

The underlying surface as well as the physical properties of the snow cover and its surroundings affect the radiative flux to the snow. The albedo, the ratio of the reflected to the incident short wave radiation, directly affects the solar energy absorbed by the snow. The spatial changes in albedo relate to the snow properties to the snow depth; under 20 cm of snow depth the snow is becoming transparent. Albedo of snow covered area varies between over 0.80 (continuous snow cover, new snow) and 0.15 (wet, melting snow) (McKay and Gray, 1981).

Different landscape types accumulate different amounts of snow. In an open grassland, where level plains accumulate 100% snow water equivalent, for example ridges and hilltops accumulate about 50% and small shallow drainageways 200 % of that (Pomeroy and Brun, 2001). Landscape type and land use affect also the variation of the snow depth when the vegetative cover is short. For example the coefficient of variation increased when going from plain (0.15) via different slope types (0.2) to toplands (0.3). Also inside a certain landscape type the land use has an effect; in most of the cases stubble had the lowest values for coefficient of variation, whereas the values for pasture were highest, fallow being in the middle (McKay and Gray, 1981).

2.1.3 Vegetation

Vegetation influences the surface roughness and wind velocity affecting the erosional, transport and depositional characteristics of the surface. The biomass affects the energy exchange process, when extending above the snow cover, as well as the magnitude of the energy change components and the position of the most active exchange surface. It also affects the amount of snow reaching the ground. Vegetative patterns also affect the average density of snow and snow hardness. The lowest densities occur over forested areas that are least subject to wind action (McKay and Gray, 1981). Studies on interaction between snow and vegetation are divided into studies of forests and short vegetative cover ecosystems.

Over the highly exposed and flat terrain the increased aerodynamic roughness resulting in variation in vegetation may produce wide variations in accumulation patterns. The depth of snow collected by scrub is higher than that collected by fallow, stubble or pasture. A strong dependency exist between vegetation and terrain in relation to the comparative amounts of snow retained by fallow, stubble and pasture (McKay and Gray, 1981).

The forest provides a large intercepting and radiating biomass above the snow surface. Several interactions in a forest environment have an effect on snow distribution. Forest cover intercepts falling snow, serves as a wind break and shelters the snow cover from solar radiation extending the duration of the snow cover. Maximum accumulation of snow often occurs at the edge of a forest where snow is blowing. Generally the snow cover distribution is more uniform within hardwoods than within coniferous forest. The accumulation depends on the species of tree, and it is inversely related to canopy density (McKay and Gray, 1981). More snow is normally found within forest openings than within the stands. Snow accumulation in clear cuts range from 4 to 118 percent more than in an adjacent coniferous forest. In any case, increase in the size of a clearing decreases the average snow depth (Pomeroy and Brun, 2001). Snow accumulation was studied by Golding and Swansson (1986) in clearings and adjacent forest in Canada. It was found that the maximum snow water equivalent was greater (more than 10%) both in small and large clearings compared to the forest. Maximum accumulation occurs in clearings with width 2 to 5 times the height of surrounding trees. The reason for greater snow accumulation in the clearings is snow interception in the forest and snow redistribution from the canopy and from beneath it to the clearing.

Snow interception is the accumulation of falling snow in the canopy. The interception efficiency is affected by air temperature and wind speed, as well as the type of forest and tree species. The snow is affected by sublimation, melt and unloading. Intercepted snow may reach the ground as a solid, liquid or vapour, but not all intercepted snow reaches the ground. Mass fluxes associated with the disposition of snowfall in forest are sublimation, unloading from branches, resuspension from branches to the atmosphere, vapour deposition to the intercepted snow, redistribution of the intercepted snow and melt and drip of the snow. The collection efficiency of a branch is limited by elastic rebound of snow crystals (depends on temperature), branch bending under a snow load and strength of a snow structure (Pomeroy and Brun, 2001). The transport of intercepted snow, mostly because of wind, also has an effect. The process is complicated by the complexity of the air flow patterns and velocity distribution within different forest covers, and also by cohesion and adhesion properties of different vegetation types and snow (McKay and Gray, 1981).

Sublimation of snow can consume great amounts of energy from a forest environment. Measurements in boreal zone in Canada showed that approximately one third of the annual snowfall is sublimated from intercepted snow from dense coniferous canopies (Pomeroy and Brun, 2001).

The interception of snow leads to variations in the snow depth in the forest. Snow depth and water equivalent decreases with decreasing distance to a coniferous tree trunk and slightly increase with decreasing distance to a deciduous tree trunk. There is higher accumulation under deciduous trees and smallest under coniferous trees. A roughly linear decrease is observed in snow water equivalent with increasing leaf area (Pomeroy and Brun, 2001).

In a study by Adams (1976) the snow depth, density and water equivalent were studied in different types of open areas and forests. The snow cover of the vegetation zones was most distinct in terms of water equivalent and least distinct in terms of density. The coefficients of variation were around 20 % in open area comparable to the measurements in Finland and around 40 % in the forest for depth; around 40 % in both areas for density; and around 60 % in open area and around 40 % in the forest for water equivalent.

The incoming solar radiation is normally smaller in the forest than in the open area, and net long wave radiation negative at least during the melt season. Wind speed is smaller under the forest canopy, and this causes also evaporation to decrease. Before the melt season the largest water equivalents are found in the sparse forest and after this in the clearings and in the dense forest. During the melt season the largest water equivalents are found in the dense forest, after this in sparse forest and in the open area (Kuusisto, 1973). Melting is slower in the forest than in the open area because the snow is shielded from the incoming solar radiation and from the wind, that is a turbulent exchange of sensible heat. The canopy emits on the other hand large amounts of long wave radiation (Vehviläinen, 1992).

The effect of topography and vegetation to the snow depth has been studied in Finland e.g. by Seppänen (1967). When the observed snow depth is assumed to be 100% in the flat, open area, the snow depth in an adjacent birch forest was 103% in southern Finland and 108% in northern Finland. The snow depth increased when going from southern slopes to the northern ones. There was also less snow on the hilltops when compared to the flat area – between 91 and 93% in the open area, and between 96 and 104% in the birch forest. The snow accumulated at the base of the hills was approximately 110% of the flat area value.

2.2 Processes governing the snow pack structure evolution

Snow is a fine-grained material with high specific surface area, it is normally close to its melting point and because of this active thermodynamically (Colbeck, 1982). Changes in snow properties are driven by the energy, mass and momentum exchange in the surface and bottom boundaries of the snow pack. As ground surface is mostly stable, cold and impenetrable by water and air because of ground frost, at least in many areas in Finland, surface boundary conditions are the most important. Driving forces for the changes are prevailing meteorological conditions. Air temperature, relative humidity, precipitation, wind velocity, short wave and long wave radiation all affect to the energy, mass and momentum exchanges in the snow-atmosphere interface. In this section the energy balance of the snow pack is discussed, as well as other main processes governing the snow pack structure evolution, and after this the theoretical background of the different metamorphoses is gone through.

2.2.1. Snow thermodynamics and snow melt

Important processes causing snow metamorphoses are heat exchanges between snow-air and snow-ground boundaries, percolation of rain and melt water, internal pressure caused by weight of snow, wind and variation of temperature and humidity in the snow cover. Environment (vegetation, altitude, topographical features, slope orientation) affects the significance of these factors.

The energy and mass exchange between the snow cover and the atmosphere involve sensible and latent turbulent heat transfer, radiative energy transfer and phase changes. The relative importance of the processes depend on weather conditions (air temperature, humidity, wind speed, incoming short and long wave radiation and precipitation) and state of the snow cover (albedo, snow surface temperature, surface roughness). The time of the year and latitude have strong effects on the snow energy balance (Pomeroy and Brun, 2001). In the figure 2.1 the different mass and energy fluxes forming the energetics of the snow cover are presented.

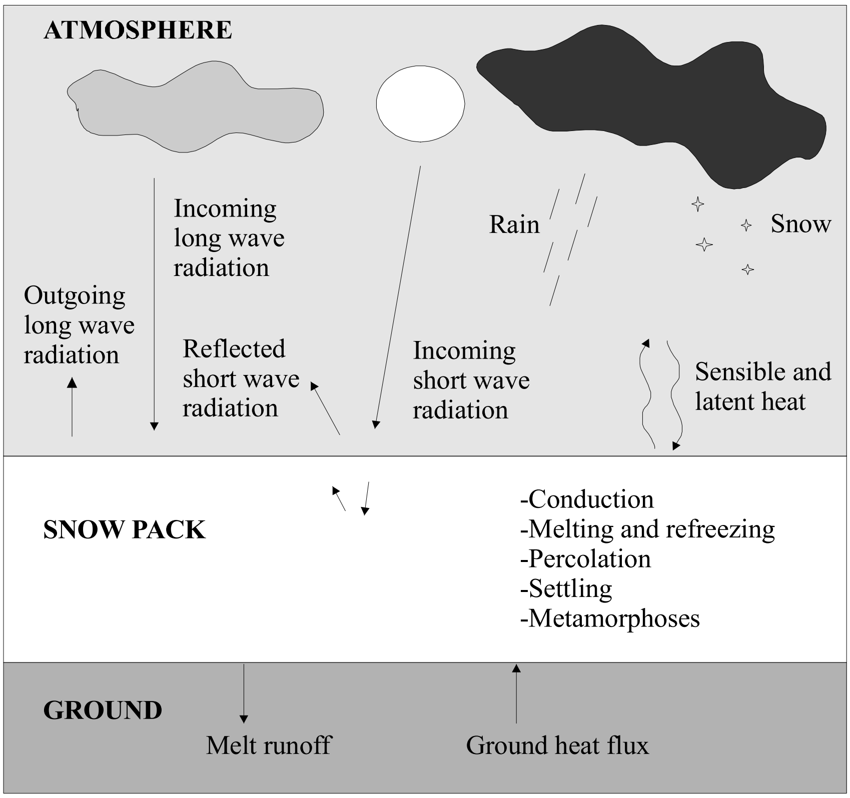

Figure 2.1. Mass and energy fluxes forming the energy budget of the snow cover.

There is normally a net loss of long wave radiation from the snow cover. Under a forest canopy however there may be a downward long wave flux from the branches, and this may lead to greater net radiation at the snow surface in the forest compared to the open area. The net short wave flux to snow decreases with increasing canopy density (Pomeroy and Brun, 2001).

Sensible heat flux is the rate at which heat is carried to or from the snow surface by atmospheric turbulence. Latent heat flux is the rate at which water vapour is carried to or from the snow surface by atmospheric turbulence. They depend on the temperature and humidity gradients in the atmosphere. For discontinuous snow covers the local advection of sensible energy from bare ground to snow patches is an important component of energy balance of a snow pack. The energy input increases with increase in patchiness. Patchiness can be described by using information of snow mean depth and coefficient of variation (Pomeroy and Brun, 2001).

The snow/ground interface is not an active partner in the reshaping of the snow cover, but temperature and humidity conditions there also have an effect on snow metamorphoses. Bottom boundary conditions include heat, mass and momentum transfer through the ground and snow interface. These include processes like heat flux from the ground and water vapour flux from the ground. Fluxes are rarely towards the ground, because in normal conditions the ground is warmer than overlying snow cover.

The ground heat flux is small but goes on all through the winter, and can have an important cumulative effect. When the soil is incompletely frozen, the flux is positive, in the arctic it is negative during late winter and it delays the snow melt. The flux is due to the temperature gradient in the soil as well as infiltration of melt water. Refreezing of the melt water at the soil-snow interface, forming a basal ice layer, releases a significant amount of latent heat (Pomeroy and Brun, 2001).

Vehviläinen (1992) has studied the contribution of different energy balance terms in Finland. The short wave term normally dominates in spring, and long wave radiation is mainly negative throughout the snow cover period. The latent heat term is most often negative in spring (evaporation) and positive in autumn (condensation). This term is normally smaller than the sensible heat term. Sensible and latent heat terms are most important during the mid-winter, and the precipitation heat greatest. (Vehviläinen, 1992)

Snow pack energy balance determining the temperature distribution in the snow cover can be written as:

$$\Delta Q = Q_{sw} - \alpha Q_{sw} + Q_{La} - Q_{Lo} + Q_c + Q_e + Q_{pc} \qquad (2.1)$$

where ΔQ is the total energy exchange, Q_{sw} the short wave radiation, Q_{La} the atmospheric long wave radiation, Q_{Lo} the long wave radiation emitted by the snow cover, Q_c the sensible heat flux, Q_e the latent heat flux and Q_{pc} a term accounting for melting and melt water refreezing. The left hand side of the energy equation can also be expressed as:

$$\Delta Q = \rho_s c_s \frac{\partial T_s}{\partial t} - k_e \frac{\partial^2 T_s}{\partial z^2} \tag{2.2}$$

where T_s is the snow temperature, ρ_s is the snow density and c_s is the specific heat capacity of snow at constant pressure. In all of the equations presented, z is a vertical coordinate (z=0 at the ground surface and z=h at the snow surface) and t is time. All the notation used can be found in Appendix I.

To solve the equation 2.2 an estimation of the heat transport, described by an effective thermal conductivity k_e of snow, is needed. It must be parameterized including all heat transfer processes like vapour transport across a pore space.

The components of heat conduction in natural snow cover are conduction through the ice skeleton, conduction through pore spaces and latent heat transport across pore spaces due to vapour sublimation and condensation. Also convection and radiation may occur. The ice skeleton provides a better path for heat transfer than pore space since the thermal conductivity of ice is about 100 times that of air/vapour. So the temperature gradient must exist largely across the pore spaces, and it is responsible for the transport of the water vapour. The flux of vapour depends also on the vapour density gradient that develops due to the temperature gradient. (Singh, 1999) Pore space temperature gradient enhancement increases the vapour pressure gradient and the transport of water vapour, and at the same time the transport of latent heat. The ice skeleton has at the same time a blocking effect that limits vapour movement to the pore spaces. (Sturm et al, 1997)

In a study by Adams and Sato (1993) the effective thermal conductivity of a snow cover is estimated assuming idealized collection of uniformly packed ice spheres. The snow cover is modelled as a collection of cells. Each cell is defined in terms of a single sphere, its neighbouring pore space and the ice bonds where the sphere contacts other spheres. Coordination number depends on the type of packing and the ice-volume fraction. All of the heat flow is assumed to be one dimensional. Heat transfer occurs through projected areas of the pores, ice/ice contacts and ice/pore contacts in series in the direction normal to the temperature gradient. Effective thermal conductivity is calculated by combining calculated heat flow through the ice network, ice and pores taken in series and conduction through the pore alone. (Adams and Sato, 1993)

The thermal conductivity is shown to depend strongly on the snow density and temperature, but also on intergranular bonding. The ratio of the neck radius to grain radius also plays a significant role: effective thermal conductivity decreases as the ratio of the contact radius to the radius of the ice grain sphere decreases. (Adams and Sato, 1993)

In a study by Sturm and others (1997) several data sets of snow effective thermal conductivity have been analysed. Rounded-grain and wind-blown snow showed strong density dependence. Under equilibrium growth conditions snow tended to densify and thermal conductivity increased. If kinetic growth process was prevailing, density and conductivity were not coupled. (Sturm et al, 1997)

A significant scatter was noted in the thermal conductivity data by Sturm and others (1997). The scatter is real, and it is due to differences in the microstructure of snow. At any given snow density there was an order-of-magnitude range of thermal conductivity, so density is not the most important controlling variable for thermal conductivity, but microstructure (bonding, shape and arrangement of snow grains) is more important. (Sturm et al, 1997)

In a study by Singh (1999) thermal conductivity of snow was measured in the field and in the laboratory. Thermal conductivity was increased with density and water content and also with temperature. The effect was most easily seen in temperatures between –15 and 0°C. Estimates of heat transport by vapour are in the range of 10-40% of total flux depending on the type of snow and its temperature. The effect of liquid water content has to be accounted for, because water conducts heat better than vapour. The scatter in the values is the result of natural variation in phase volume, packing, grain size and type and in temperature. The relationship between thermal conductivity and density can also be explained in terms of the complex relationship between microstructure and density. (Singh, 1999)

Temperature regimes in snow cover are controlled by a balance of the energy regimes at the top and bottom of the snow pack, radiation penetration, effective thermal conductivity of snow layers, water vapour transfer and latent heat exchange during metamorphism. The thermal regime in the snow pack depends strongly on the amount of snow fall early in the winter season. (Pomeroy and Brun, 2001)

Dry snow undergoes processes of thermal conduction, thermal convection and wind pumping. These processes govern the heat flux between the bottom and top of the snow cover. Significant amounts of the solar radiation penetrates the snow cover to approximately 20 cm below the surface. The preferential flow paths have coarser grains than the surrounding snow, and this leads to greater irradiances in these paths. (Pomeroy and Brun, 2001)

The internal energetics during melt are complex. Snow pack can undergo melt in upper layers, while snow temperatures are sustained below melt temperature in lower layers. Internal heat fluxes in wet snow are controlled by conduction and by latent heat releases due to refreezing. In most snow covers the flow initiates along preferential flow paths, in which flow fingers may penetrate the dry snow several days before the matrix flow reaches a certain layer. When percolating melt water reaches cold snow layer, a part of the water refreezes freeing latent heat. This warms the layer quickly toward melting point. The rate of snow melt is primarily controlled by the energy balance near the upper surface. In cold climates the change in the internal energy of the snow pack can be a significant term in the energy balance during melt. Net radiation and sensible heat largely govern the melt of shallow snow packs in open environments. (Pomeroy and Brun, 2001)

This work concentrates on snow pack structure during the winter period in Finland, so only a short introduction to spring snow melt is given here, based on Leppäranta (1995) and Pomeroy and Brun (2001).

The cold content of the snow cover is the quantity of heat, which is needed to rise the snow pack temperature to 0°C:

$$F_d = -\int_0^h \rho_s c_s T dz = -\rho_s c_s h T_s \tag{2.3}$$

Here h is the snow depth, T_s the average temperature of snow, ρ_s the snow density and c_s the specific heat of snow. Energy needed to melt snow layer with depth of h is:

$$F_m = \rho_s L h \tag{2.4}$$

Here L is the latent heat of melting.

Thermal quality of the snow cover is:

$$\Theta = \frac{[F_d + (1-\theta_w)F_m]}{F_m} \tag{2.5}$$

Here θ_w is the liquid water content of snow. Snow pack has a thermal quality under 1 during the melting period.

The melting of snow starts when snow pack heat storage becomes greater than the cold content of the snow cover. The melting starts depending on weather conditions either from the surface or under the surface. Sub-surface melting is common during clear weather, and the melt water can readily percolate into the snow pack. During cloudy conditions most of the melting takes place on the surface. (Granberg, 1998)

Like in all phase changes from solid to liquid, the temperature of the melting material, here the ice grains of the snow cover, has to rise to melting temperature. At first melting is slow, because the energy is needed to raise the snow cover temperature. When isothermal condition is reached the melting advances quickly. All of the gained energy is used to the ice grain phase change to liquid water.

There is also positive feedback mechanism in melting. When liquid water content increases the albedo decreases. This means that more of the incoming solar energy can be absorbed, more melting occurs and so on.

Snow melt can be estimated with an equation:

$$\frac{dh}{dt} = -\frac{\Delta Q}{\rho_s L} \tag{2.6}$$

Here ΔQ is the total energy coming to snow cover.

The liquid water content of the snow increases greatly during the melting season. The water holding capacity of the snow cover is not normally reached during short periods of melt in the winter time, and percolation through the snow pack is not extensive. During spring the melt water holding capacity is full for a long time, and all new rain and melt causes percolation and runoff. Also snow cover thinning has an effect on the decrease in water holding capacity. The water holding capacity of a certain snow cover depends on the snow depth and density, the amount of ice lenses and snow microstructure. (Kuusisto, 1973) The water holding capacity of snow in temperature of 0°C varies between 2 and 5%, according to Finnish studies. The melt water runoff starts when the liquid water content rises to 6% of the snow volume in the bottom layers of the snow cover. (Lemmelä, 1970).

When percolated melt water reaches the ground, it forms a melt water pond or surface runoff, depending on the topography, if the ground is frozen, or it percolates to the ground and forms bottom water or sub-surface runoff if the ground is unfrozen. In all cases melt water can refreeze if its temperature drops below freezing. (Pomeroy and Brun, 2001)

Snow has an impact on soil and aquatic ecosystems through infiltration of melt water into frozen and unfrozen soils. Even frozen soils that contain large cracks or macropores are able to accommodate infiltration of all melt water. Streamflow is generated by snow melt water that directly runs off. Deep snow packs in the forest cause soils to be warm and runoff to be small. (Pomeroy and Brun, 2001)

The snow melt does not occur evenly in all parts of the snow cover. The accumulation pattern is repeated in the pattern of the snow patches and snow free land area. Shadings of the vegetation and topographic features (aspect and slope) also play an important role in the timing and pattern of snow melt. (Pomeroy and Brun, 2001)

2.2.2. Compaction of snow

The settlement equation governing the density distribution in the snow cover is:

$$\frac{\partial \sigma_s}{\partial z} + \rho_s g \cos\phi = 0 \qquad (2.7)$$

Here σ_s is the overburden stress applied to snow, and ϕ is a slope angle.

The complete description of the snow deformation consists also of the following relations:

- A description of snow that relates the state of deformation to the total state of strain ε
- A formulation for Young's modulus that relates the stress to the elastic strain ε_e
- A formulation for the viscosity that relates the stress to the viscous strain ε_v (Bartelt and Lehning, 2002).

The material viscosity, η, relates the stress to the strain rate $d\varepsilon_v/dt$, when elastic deformations are small as in the case of snow settling:

$$\frac{\partial \varepsilon_v}{\partial t} = -\frac{\sigma_s}{\eta} \qquad (2.8)$$

In avalanche forecasting, new snow amounts and snow pack settling rates are the most interesting snow cover parameters. Many times a new snow mass is determined indirectly by automatically measuring the location of the snow cover surface. The settlement of the snow pack must be theoretically to determine the true amounts of new snow. The deformation rate is controlled by the viscous deformation, and snow elasticity is of minor importance. (Bartelt and Van Moos, 2000)

Work on snow mechanics has been done ever since the 1930s, and the objective of the studies has most often been to determine the parameters required for applying the linear elasticity, viscosity and viscoelasticity relationships to snow. These relationships use normally density as an important predictor of the snow strength. When the strength of snow is plotted against density, a large scatter is seen. It has been known since the 1970s that the influence of the snow microstructure should be taken into account in snow mechanical studies. (Shapiro et al., 1997)

The viscoelastic behaviour of snow was studied in work by Bartelt and Von Moos (2000). Both tension and compression were applied to the sample and volume changes were determined. It was shown that snow is a highly non-linear but ideal viscoelastic material with a strong strain rate dependency. Snow viscosity varies with density and strain rate. The measured stress showed a steep rise at the beginning of the experiment and a partly elastic behaviour was seen. After this the curve flattened because of the creep under constant strain rate. The stress decreased quickly during the relaxation. The effect of density and strain rate to the stress was seen. The Maxwell model can predict the loading but not the relaxation phase. Mahajan and Brown (1993) have proposed one constitutive relation, based on the dislocation of the grain bonds, but this theory is limited to small strains. (Bartelt and Van Moos, 2000)

Snow of a given density exhibited higher viscosity at lower strain rates. This is also seen in ice at high stresses. High stresses exist at the inter-granular bonds of the ice lattice. A constitutive law for snow viscosity could be formulated in terms of ice viscosity, where the strain rate is included via the ice viscosity law and the microstructural parameters via the Mahajan and Brown parameterisation. The constitutive theory did not work well for high density snow. (Bartelt and Van Moos, 2000)

In Bartelt and Van Moos (2000), a parameter indicating how much ice mass is resisting deformation was introduced. The parameter was found to have values between 2-20%. In Mahajan and Brown (1993), another parameter related the stress state of the bonds to the applied stress. The ratio between these two parameters indicates how much of the mechanical resistance of the sample is being controlled by dislocation straining of the ice bonds. This was found to be 80% or higher, so dislocation straining of the ice bonds seems to be the dominant mechanism of deformation. (Bartelt and Van Moos, 2000)

2.2.3. Transport of water vapour and liquid water

Two mass conservation equations are needed for the vapour and water phases. For conservation of mass on the air phase the vapour diffusion equation is:

$$\theta_a \frac{\partial p_a}{\partial t} + \theta_a \frac{\partial J_v}{\partial z} = M_{mm} \qquad (2.9)$$

Here θ_a is volume fraction of air in the snow cover, p_a water vapour partial pressure and J_v water vapour flux. M_{mm} is a mass sink or source term due to the deposition or sublimation of water vapour onto the ice matrix.

The mass transfer rate in the snow cover is proportional to the water vapour density gradient. This is a function of temperature gradient and mean temperature. The diffusion can account for 30% of the heat flux when snow is very porous. Water vapour diffusion, which is due to a temperature gradient, is the most important mechanism for the grain growth. (Satyawali, 2000)

By the early observations (Yosida et al. 1955) the effective diffusion coefficient is nearly constant between densities 80-510 kgm^{-3}. The grain growth rates obtained later do not support this, but diffusion mass transfer decreases with an increase in snow density. (Satyawali, 2000)

In the study by Satyawali (2000) the one dimensional grain growth model predicted the variation of diffusion coefficient with snow density. In the model ice cubes with certain dimensions and certain distance to each other represented a grain. Sink and source grains were represented as top and bottom grains. The microscopic temperature gradient between source and sink can be expressed by the geometric parameters, as well as porosity and equation for mass transfer between snow grains. It was assumed that the mass flux from regions of higher vapour concentration to the regions of lower affects the grain growth uniformly and that vapour deposits on the growing grain surface as a solid ice and that growing grains do not act as a vapour sink. A non-linear dependency of porosity was introduced by grain length modification factor, because the grain length does not vary linearly with porosity. The variation of grain length modification factor with density was found in the laboratory tests. (Satyawali, 2000)

For the water phase mass conservation the water transport equation is:

$$\frac{\partial \theta_w}{\partial t} - \frac{\partial J_w}{\partial z} = M_{pc} \tag{2.10}$$

Here θ_w is volume fraction of liquid water, J_w liquid water flux and M_{pc} a phase change sink or source term due to the melt water refreezing or subsurface melting.

The use of the equations 2.1-2.10 in snow cover modelling is described further in Chapter 4 and in Appendix III of this work.

2.3. Snow metamorphoses

As soon as snow has fallen to the ground or to the underlying snow surface, the snow grains start to reshape due to different physical processes. At the same time snow quickly reaches equilibrium state with the changing conditions surrounding it. Large fraction of the snow cover volume is moist air, and air pores will not close before snow has slowly turned into ice after decades of pressure from layers lying above. There can be found different layers in the snow pack, differing from each other but each having relatively homogenous properties inside the layers. There are layers, which consist of rounded snow grains bonded together; layers of weakly bonded cup-shaped crystals, and layers, where meltwater has percolated and refrozen forming large polycrystals. These three layer types are due to the three different snow metamorphoses changing the size and shape of the grains: equilibrium growth, kinetic growth and wet snow metamorphism.

2.3.1 Definitions and terminology used

During several decades many classifications with different terminology have been developed for the snow metamorphoses. Sampling of different snow types led to the earliest classification works by Wolley (1858), Bentley and Humpreys (1931) and Seligman (1936). In this work mainly classification presented by Colbeck (1982) has been used. Using his own words: "Like all seasonal snow morphologies, also this is an arbitrary attempt to categorise snow". The classification is shown in the table 2.1, together with the widely used synonyms for the metamorphism processes. Grain types associated with the different metamorphoses as well as their symbols are also listed in the table. It is worth noticing that in a natural snow cover there is a competition between the equilibrium and kinetic growth depending on the temperature gradient conditions. As the temperature gradient is not constant, the results are often intermediate or mixed snow types. (Pomeroy and Brun, 2001)

Table 2.1. Snow metamorphism classification used in this work (based on Colbeck, 1982). Observed grain types associated with the metamorphism processes are listed together with their generally used symbols in this table as well (by Colbeck et al, 1990). Terminology according to the classification by Sommerfeld and LaChapelle (1970) has been given in the table, in addition to some other widely used synonyms for the processes.

Process	*Grain type*	Symbol	*Sommerfeld and LaChapelle*	*Others*
Snow precipitation	Precipitation particles	1	Unmetamorphosed snow	
Decomposing	Partly rounded particles Packed fragments	2		
Dry snow				
Equilibrium growth metamorphism	Rounded grains	3	Equi-temperature metamorphism	Rounded-grain metamorphism, radius-of-curvature metamorphism
Kinetic growth metamorphism	Faceted crystals Depth hoar	4 5	Temperature-gradient metamorphism	Faceted-grain metamorphism
Wet snow metamorphism				Melt metamorphism
No melt-freeze cycles	Clustered rounded grains	7		
Melt-freeze cycles	Rounded polycrystals Ice masses	8	Firnification: Melt-freeze/ pressure metamorphism	
Surface processes				
Kinetic growth in air	Surface hoar	6		
Surface melt	Melt crusts			
Wind packing	Wind crusts			

The classification by Colbeck (1982) divides the snow metamorphic processes into dry and wet snow processes. The processes associated with snow precipitation and surface formations are also taken into account. The dry snow process type (equilibrium growth or kinetic growth) depends on the temperature gradient. The wet snow processes can be divided either using the liquid water content of the snow or using the presence of the melt-freeze cycles. Here the latter has been chosen. The classification by Sommerfeld and LaChapelle (1970) is based on the different physical processes going on in the snow cover, and in this way it is better than classifications based only on the appearance of the snow crystals. Terms destructive and constructive metamorphism used in the classification by Eugster (1952) also describe well the functions and effects of the metamorphoses. Also term rounded-grain metamorphism has been used for equilibrium growth metamorphism and term faceted-grain metamorphism for kinetic growth metamorphism. Melt metamorphism has been used instead of wet snow metamorphism.

Some of the microstructural parameters used in this chapter are shown in the figure 2.2. The two shape related qualities, dendricity and sphericity are defined as follows. Dendricity describes to what extent the snow may be described as consisting of new snow, fragmented or decomposing particles. It varies from 1 for new snow to 0 for snow with no dendrite particles. Sphericity describes how far snow grains are either faceted (0 for fully faceted) or rounded (1 for fully rounded). In the table 2.2 the snow microstructure terminology is being explained shortly. What comes to terms crystal and grain, I have tried to obey the advice by Marsh (1987): “Snow grain refers to the smallest distinguishable unit, whether single or polycrystalline.”

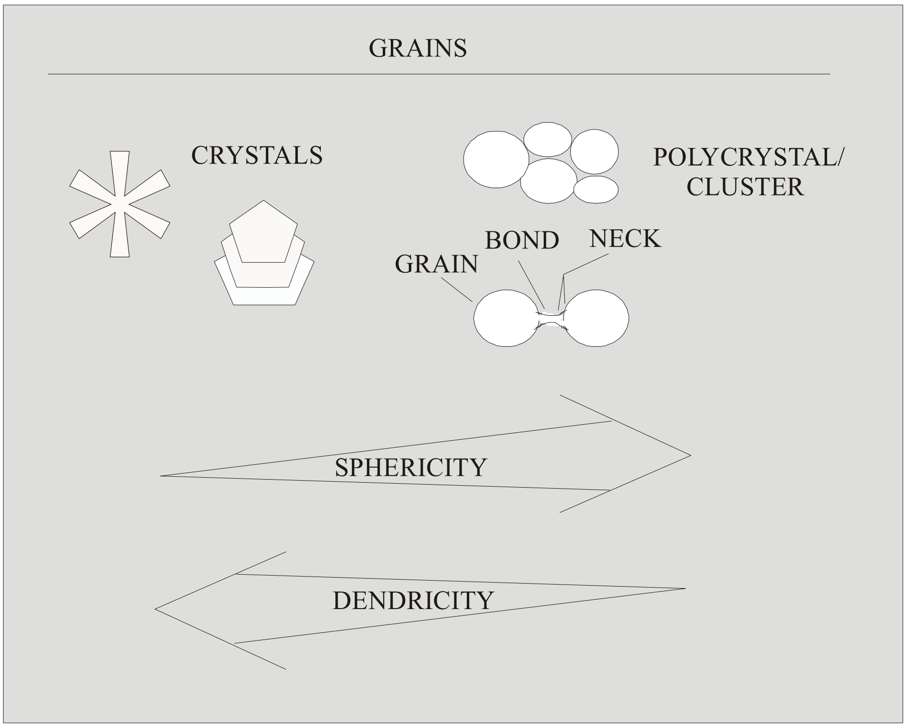

Figure 2.2. Schematic picture of snow microstructure.

Table 2.2 Snow microstructure terminology

Term	*What does it mean?*
Crystal	Ice particle formed by sublimation of water vapour
Grain	The smallest distinguishable unit in a snow pack, single or polycrystalline
Polycrystal; Cluster	Several grains bonded as one, normally through melt-freeze metamorphism
Bond	Ice bridge between the separate grains
Neck	The constricted regions connecting the ice grains / Area of the bond, where the bond is attached on the grain. The necks have negative radii of curvature.
Coordination number	Number of bonds per grain
Grain size	Maximum diameter of a grain (or average diameter, or average or maximum radius, depending on the definition)
Bond size	Diameter of a bond
Sphericity	Explains how far snow grains are faceted (0 for fully faceted) or rounded (1 for fully rounded)
Dendricity	Explains to what extent the snow may be described as consisting of new snow, fragmented or decomposing particles, varying from 1 for new snow to 0 for snow with no precipitation particles.

2.3.2. Equilibrium growth metamorphism

There is a clear disproportion between the studies on equilibrium growth and kinetic growth metamorphoses on the favour of kinetic growth. Because of this, the latter is more thoroughly discussed also in this work. Equilibrium growth is well described in the work by Perla (1978). There is an extensive review on sintering of snow by Colbeck (1997).

Equilibrium growth metamorphism is a subtype of the dry snow metamorphism. Distinction between dry and wet snow is necessary to describe the behaviour of snow layers. The liquid water is absent from the dry snow. Snow crystals may still be surrounded by a liquid-like layer (Pomeroy and Brun, 2001).

The type of metamorphism in the dry snow depends on the temperature gradient between the ground and the snow surface. When the temperature gradient is low, under 5 $°Cm^{-1}$, the equilibrium growth dominates the kinetic growth forms (Pomeroy and Brun, 2001). This is why the metamorphism is also called equi-temperature metamorphism. In any case, small temperature differences are present between different parts of the snow grains also during this process. The term destructive describes well what happens during this process: beautiful stellar shaped precipitation particles are broken and turned into rounded grains. At the same time bonds are formed between the grains. Normally this is the metamorphism that precipitation particles first go through; it is also possible that older grain types experience rounding later during the winter.

Fallen snow crystals are already smoothed towards rounded shape during the wind transportation. This is sometimes called mechanical metamorphism. As fallen crystals are packed together, they form complex net of concave air pores and convex grain boundaries. Water vapour pressure varies in the differently shaped parts on this ice/air – boundary. In the convex areas the water vapour pressure is relatively high, while in the concave areas it is relatively low. This leads to the sublimation from the convex grain surfaces and transport of water vapour to the concave parts between the grains. The average temperature of the snow layer is near constant during the process, but there is a decrease in temperature in the convex areas because of the heat of sublimation needed. In the concave areas the heat is released during the water vapour recrystallisation. The temperature difference between the different areas of the grain keeps the process going, when the heat flows back to the convex areas.

The shape of the crystals is lost during the process, and a layer consisting of rounded grains of different sizes is formed. The smallest grains merge with the larger ones when the process is continued. The vapour pressure is larger over the smaller ice grains, as it is larger over the dendrite branches with small radii of curvature (Colbeck, 1982). The longer the equilibrium growth metamorphism has been going on in a layer, the larger the average grain size. In the figure 2.3. the evolution of the grain shape during the equilibrium growth metamorphism is shown.

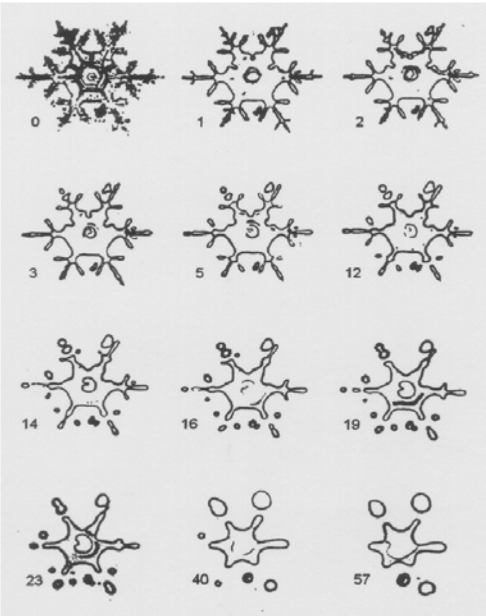

Figure 2.3. The evolution of grain shape during equilibrium growth metamorphism. The numbers refer to the number of days from the beginning of the experiment. (Bader et al., 1939)

Important part of the process is sintering: forming of strong ice bonds between the grains. Ice bonds form between the grains in most types of snow. In dry snow the bonds have been described as necks with a concave geometry where the growth of the bonds is driven by vapour pressure differences over the convex grain and concave bond surfaces (Colbeck, 1997). In the figure 2.4. the sintering between the snow grains during the equilibrium growth metamorphism is described.

The efficiency of the equilibrium growth metamorphism depends on the water vapour difference between the different parts of the grain, the temperature of the snow and the distance between the grains (depends on the shape of the grains). The process is efficient near the melting point, but when going towards -40°C it becomes negligible. The smaller the grains are in the beginning of the process the faster the sintering is happening. It is also possible to form more binds between the grains, when the grain size is small.

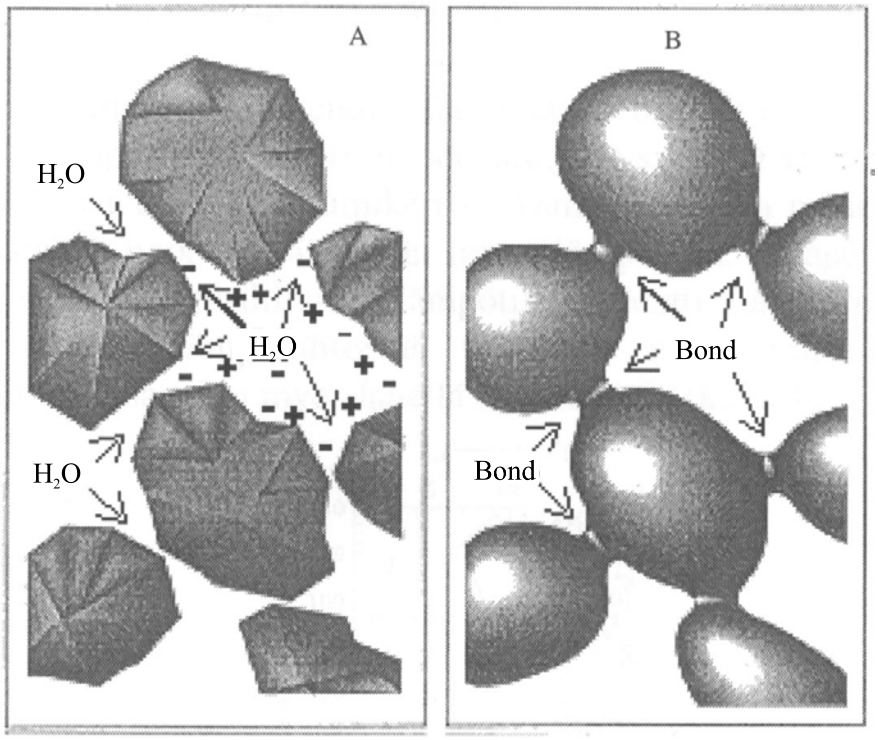

Figure 2.4. Forming of bonds and sintering between snow grains during the equilibrium growth metamorphism. Symbols – and + refer to the areas with relatively low or high water vapour pressure. (Lind and Sanders, 1996)

Wind crusts can be classified to equilibrium growth types of snow. Wind crust forms when ice particles are carried along the wind, broken into smaller fragments and packed densely together. Faster sintering of smaller particles also develops high strength in these layers. (Colbeck, 1982)

In work by Brown and others (1994) an attempt is made to predict the rates of changes of the snow microstructure, especially the rates at which equilibrium growth (here: radius-of-curvature) metamorphism proceeds in dry snow. This is done using the application of mixture theory. (Brown et al., 1994)

The radius-of-curvature metamorphism happens when there is an interchange of mass between two neighbouring ice grains that are assumed to be spherical but have different radii of curvature. The equilibrium vapour pressures over the two surfaces will be different resulting in a vapour pressure gradient between the two ice grains. This produces a flux of mass from a small grain to a larger one. This can result in a measurable alteration of mean grain size and the statistical distribution of grain sizes making up the material. (Brown et al., 1994)

Balance equations for mass, momentum and energy are used in the work in conjunction with constitutive relations governing the behaviour of the vapour phase. Two neighbouring ice surfaces are considered. They are separated by small space containing an air/vapour mixture which normally is vapour saturated. The exchange of mass between the two surfaces is determined. (Brown et al., 1994)

There is an additional process going on at the same time, thermodynamical sintering. This involves the exchange of mass between the ice grains and the bonds or necks connecting the grains. The radius of curvature changes from a positive value on the body of the ice grain to a negative value on the ice neck. So the necks have normally lower radii of curvature than the ice grains, so the equilibrium vapour pressure over the neck surfaces will differ from that over the grain. This produces a flux of vapour from the grain along the surface to the neck, where it is deposited on the neck. As a result the necks slowly grow with a resulting increase in the material strength and rigidity. When there is a sharp jump in curvature between the grain body and neck, most of the mass exchange takes place at the transition. When the radius changes gradually, the mass transfer is spread out over the region of the transition. (Brown et al., 1994)

The temperature would be expected to have a significant effect on the rate at which the two grains would exchange mass (the warmer the faster). Grain size also has an effect on the rate of metamorphism (the smaller the more efficient), as well as the relative size (the more difference the faster) of the two grains. The separation distance between particles also has an effect: as the distance is shortened, the rate of transfer increases markedly. Results from the laboratory tests show that microstructure of the material changes slowly with time while small grains lose mass to the larger ones and the process of sintering takes place at a slow rate. The movements of vapour along the grain surface to the neck is determined by the details of the surface curvature of the grain and neck. This process is assumed to be primarily due to the sublimation of vapour from the ice grain surface, diffusive transportation along the grain surface to the neck and subsequent deposition onto the neck. The exchange rate between grains of different surface curvature depend upon the radii of curvature, pore size and temperature. The rate of sintering is determined by temperature, grain curvature and neck curvature. (Brown et al., 1994)

In work by Brown and others (1997) the snow is modelled as a mixture of vapour occupying the pore spaces, dry air occupying the pore spaces, ice grains and ice necks which interconnect the ice grains. The time-dependent changes in grain size distribution and neck size distribution are calculated. The rate at which each constituent is interchanging mass with the others by means of phase changes is calculated. (Brown et al., 1997)

Each ice constituent exchanges mass only with the vapour phase, while the vapour phase can exchange mass simultaneously with all ice constituents. Free surface area determines how rapidly the interchange of mass happens, because available free surfaces are needed for sublimation and condensation of vapour to occur. These are determined by the density and the radii of curvature. (Brown et al., 1997)

When an initial state consists of a collection of ice grains of different sizes and a vapour phase, the ice grains will lose mass to the vapour until its energy begins to exceed the energies of some of the ice grains. Then the vapour will begin to supply mass to those grains with the lower energies, while the grains with higher energies will continue to lose mass to the vapour. The vapour will reach a stable configuration with an energy level where it is continuously acquiring mass from some grains while at the same time giving up mass to the grains. (Brown et al., 1997)

In one example analysed, five grain sizes with equal number density were assumed, so the mass density increases with grain size. The largest grains were noted to grow at the expense of all smaller ones. In other example there were five grain sizes with equal mass density. Here larger constituents did gain mass, but the activity between the smaller grains was much more substantial since they had more surface area to support mass exchange. Neither of these models could be considered to be very realistic. A normal distribution of grain sizes centered about the mean grain size should be assumed. (Brown et al., 1997)

In another example the distribution of grain sizes was altered by making each constituent smaller by a factor of 10. Free surface area was hence increased, and grain size redistribution proceeded much more rapidly. In the last example a distribution of both grain sizes and neck sizes was assumed, the necks were taken to be uniformly distributed in number density and have dimensions initially 10 % of the grain sizes. The presence of necks had very little effect upon the changes in the grain sizes. The necks, however, experienced significant growth. The rate of sintering was seen to decrease as the neck size grew. The smaller necks were seen to sinter more rapidly than the larger necks. (Brown et al., 1997)

2.3.3. Kinetic growth metamorphism

Extensive studies have been carried on the kinetic growth metamorphism, both theoretical and based on the observations either in the laboratories or in the field. A selection of these studies are reviewed here.

Kinetic growth metamorphism changes the rounded grains once again into hexagonal crystals under relatively high temperature gradients. Resulting forms are either faceted crystals, depth hoar crystals or hard depth hoar. Growth of the crystals occurs by the movement of molecular steps across the crystalline faces, and crystals develop distinctive shapes. Faceted crystals in the snow pack usually grow with a step structure. Basal planes of ice are connected by either prismatic or pyramidal faces (Colbeck, 1982). Equilibrium and kinetic growth metamorphoses can both work in a same layer, perhaps several times during a winter, depending on weather. So the same grains may show forms associated with both of the processes during different times of a winter. In any case, the faceted grains do not sinter rapidly because their rapid growth leaves little time for sintering (Colbeck, 1997).

When the rate of growth in a dry snow is limited by vapour diffusion, it is slow and the equilibrium form prevails. When temperature gradient increases the gradient in vapour pressure, the excess vapour pressure is much larger. Growth rate increases, and a transition to the faceted crystals of the kinetic growth form occurs. This happens when temperature gradient exceeds approximately 10-20 °Cm^{-1} (Colbeck, 1982). Between the clear equilibrium and kinetic growth metamorphoses there can be found a regime of medium temperature gradient between 5 and 15 °Cm^{-1}. Faceted crystals grow, but slowly, because gradient effects are partially balanced by curvature effects (Pomeroy and Brun, 2001). The growth of faceted crystals at the expense of the rounded ones can occur, if the vapour pressure is between that of a fully rounded crystal and that for a flat-face crystal (Colbeck, 1982b).

The kinetic growth metamorphism starts when there is large enough temperature difference between relatively warm ground and relatively cold snow surface. Because of this the water vapour pressure is higher near the ground surface than near the snow surface, and water vapour sublimates from the bottom layer of the snow cover. The water vapour is transported along the vapour pressure gradient, and it recrystallizes on the bottom surfaces of the above laying snow layer. In a layer the extensions pointing downwards tend to be colder than the surrounding air, while as the extensions pointing upwards tend to be warmer than that. So the extensions – cup shaped grains – tend to grow downwards. In the figure 2.5. the growth of the depth hoar crystals during the kinetic growth metamorphism is shown. The process can also start under an internal ice layer, when the temperature gradient between the ice layer and the ground is sufficient. Water vapour does not penetrate the ice layer, but the recrystallisation has to take place under the ice. In this way thick depth hoar layers form efficiently.

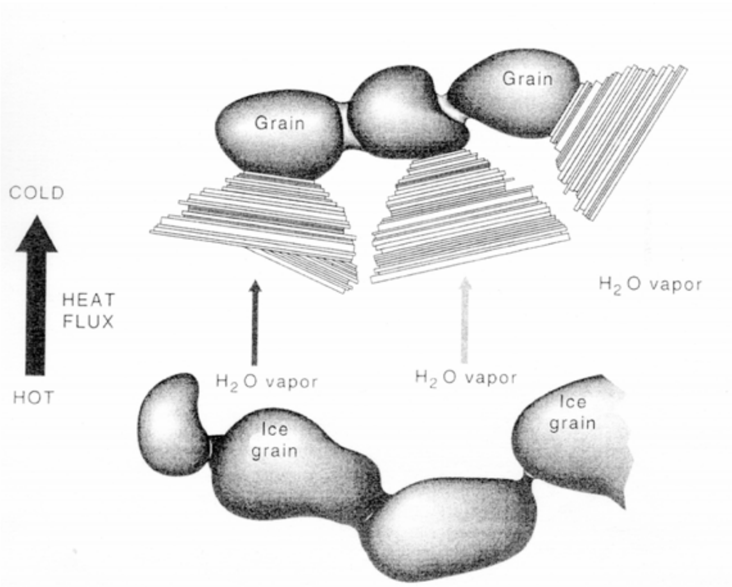

Figure 2.5. Growth of depth hoar crystals during the kinetic growth metamorphism. (Lind and Sanders, 1996)

Kinetic growth is slower than equilibrium growth. It can go on for several months if the large enough temperature gradient is present, and build up large cup-shaped crystals. In most of the cases rather shallow snow pack is required, as well as cold enough air temperatures.

The growth process in dry snow has been described as "the hand-to-hand delivery" of water vapour (Yosida et al. 1955), because water vapour moves through the snow cover from warmer parts to the colder parts by step-by-step transport of water from a grain to its coldest neighbour. In this model the water vapour molecules condense on the bottom of an ice grain, while other molecules sublimate from the top producing a continuous flow of vapour through the pore spaces. If the two rates do not balance, the grain grows or shrinks. (Sturm and Benson, 1997) This process enhances the rate of vapour diffusion because the flow path is shortened compared the vapour flowing across the pores only, and also because the temperature difference across the pores is increased. (The thermal conductivity is much higher for ice than for air.) (Colbeck, 1997)

Heat conductivity of the snow increases with density. This leads to a smaller temperature gradient in the dense snow compared to the porous one. More heat is being transported by conduction, and less by phase changes. This is why for example wind-packed snow with small grain size changes its shape slowly because of kinetic growth metamorphism.

The process does not change the density of a layer significantly, but it has an effect on the strength of the snow pack. This is because the single crystals grow without the bonds between.

The formation of faceted crystals is restricted near the snow surface because of the lower temperatures. Another type of faceted crystal known as surface hoar often forms there. These crystals form by condensation from atmosphere supersaturated as compared to snow surface. This happens normally during cold, clear nights, when surface is cooled by long wave radiation to the atmosphere. (Colbeck, 1982)

A classic series of cold room simulation tests were performed to study depth hoar grain growth by Marbouty (1980). Grain growth was found out to be an increasing function of the temperature gradient modulus with a lower limit of 25 °Cm^{-1}, and function of temperature with a maximum at –5°C. The metamorphism was found to take place at constant density between densities 150-350 kgm^{-3}. Parameters influencing the process were temperature gradient, temperature, density and crystal type. Very dense snow samples varied little. Round grains became sharp, but lack of space obstructed crystal growth. Fresh snow first underwent destructive metamorphism accompanied by packing, and after this kinetic growth metamorphism without packing. (Marbouty, 1980)

In the laboratory work by Fukuzawa and Akitaya (1993) snow samples were exposed to the temperature gradients between 100-300 °C/m. Depth hoar crystals were observed to grow linearly as function of time, and faster the greater the temperature gradient. The growth rate for the crystals was of order of 10^{-9} m/s.

In work by Sturm and Benson (1997) long time series of measurements from subarctic snow pack were used to study relationships between grain growth and water vapour flow. In the study high rates of condensation and sublimation were observed. A continuous flux of water vapour moved from the soil into the snow. Basal snow layers lost vapour to upper layers, leading to the development of a weak layer near the base of the snow. At the same time grains grew rapidly. Water molecules can travel distances as great as the snow depth during the winter in the series of hops from grain to grain. (Sturm and Benson, 1997)

New and recent snow changed slowly into solid type depth hoar, then into large pyramidal cups opening downward, then into hexagonal cylindrical prisms and later into long thin prisms. Layers at the base exhibited more advanced stages of depth hoar, because they had been subject to temperature gradients longer than the overlying layers, and also because they had experienced stronger gradients in the early winter. The steady increases in the average grain size and in the standard deviation were observed, as well as a gradual shift from unimodal to bimodal grain size distributions, then back to unimodal. Layers experienced an initial period of rapid densification followed by a period of slower or no densification. (Sturm and Benson, 1997)

The mass redistribution took place in a complicated and episodic manner. The short periods of peak fluxes early in the winter and just after the deposition of a layer seemed to be responsible of the most of the mass redistribution. Snow layers just above the base of the snow tend to lose mass, while the ones near the surface tended to gain mass. (Sturm and Benson, 1997)

Layer-to-layer fluxes were found out to be ten times higher than inter-particle fluxes. This accounts for depth hoar formation being observed in snow covers without changes in layer density. So the layer-to-layer net flux rates are unnecessary to maintain depth hoar growth. The limiting factor for depth hoar growth is not the rate at which vapour is being supplied to the growing grains. In some works the vapour flow is assumed to be the rate-limiting process in kinetic growth metamorphism (Colbeck, 1982b). Colbeck (1983, 1986) further concluded that kinetic growth forms result from the dynamics of crystal growth rather than from limitations in the rate at which vapour is supplied. There is a limiting factor, because the grain growth rate flattens and the inter-particle flux rate drops in some grain size. Thermal control and increase in geometric complexity of depth hoar can explain this. Large grains lose their thermal efficiency in cooling, and become less efficient for growth, also the amount of vapour bypassing grains and moving to higher layers in the snow cover increases. Depth hoar grains reach a maximum size yet their form continues to change. (Sturm and Benson, 1997)

Observations that depth hoar grains nearly always have growth features on the bottom and erosion features on the top support the hand-to-hand concept, and the process is also supported by grain growth limited by thermal control, not vapour supply. Still the net layer-to-layer flux rate is large and this could indicate excess water vapour bypassing grains.The grains gain and lose water molecules at the rate many times higher than the rate at which they grow. A growing grain is in the near-equilibrium throughout the winter but has a high rate of mass exchange and a high potential for metamorphism. (Sturm and Benson, 1997)

In work by Pfeffer and Mrugala (2002) the effect of temperature gradient and initial density on depth hoar growth was studied. Also the range of conditions under which cohesive or hard depth hoar forms was defined. Hard cohesive depth hoar was found to be formed from rounded grain snow with density 400 kgm^{-2} or greater, with exposure to a temperature gradient of 20 $°Cm^{-1}$ or greater. Hard depth hoar consists of solid type depth hoar grains connected by necks and organisation of grain-to-grain chains. Solid type depth hoar (anhedral) is formed of grains having flat surfaces and sharp corners, while skeleton type depth hoar (euhedral) grains exhibit well developed stepped surfaces and cup like shapes. Both have large grain size (over 1 mm) and sparse grain-to-grain bonding. Third type, very hard cohesive type of depth hoar, shows much greater strength characteristics. (Pfeffer and Mrugala, 2002)

The formation of hard depth hoar was dependent on snow density and on grain shape. At lower densities sintering and alteration occurred, but hardness was not increased. Incohesive solid type depth hoar formed in the low density samples of fresh snow. Hard depth hoar formed in the compacted snow under the snowmobile trail. Compaction of snow (snowmobiles etc.) causes increase in coordination number as well as pore collapse. This combined to increase in temperature gradient form ideal conditions for the development of hard depth hoar. (Pfeffer and Mrugala, 2002)

There is an inverse relationship between the diffusion coefficient for snow and average pore size. Since vapour flux is dependent on the magnitude of the diffusion coefficient and the temperature induced vapour pressure gradient, an increased effective diffusion coefficient, due to smaller pore size, has to cause the vapour flux to be high enough for the formation of hard depth hoar. (Pfeffer and Mrugala, 2002)

A major problem in the numerical snow cover models is the appropriate description of grain growth. In the work by Baunach et al. (2001) a model of kinetic grain growth is built based upon vapour transport and assuming a simple geometry to present snow texture. In the model a simple uniform geometry was chosen. The grains are initially arranged in a body-centred cubic lattice. The grain at the centre of the unit cell is considered to be the source of intralayer transport, whereas sinks – one per unit cell – are at the cell's corners. As time goes on, the source will be consumed and the texture of the cell will change accordingly. The sink grains are described as plates growing into two dimensions. An adjustable geometrical parameter takes into account the real grain shape. The lattice constant (distance between sinks) can be calculated using the volume fraction of ice in the layer. Grain growth rate and grain size can then be expressed in terms of temperature conditions and lattice geometry. (Baunach et al., 2001)

With large temperature gradients the model overestimated the grain growth because of the linear dependency on temperature gradient, but overall agreement was good. Marbouty formulation with non-linear dependency on temperature gradient usually underestimated the growth. Marbouty's growth rate is linear, whereas with the new model it decreases with both time and increasing grain size. This is observed by Sturm and Benson (1997). The model gave good results for snow densities between 100-200 kgm^{-3} and temperature gradients up to $200°Cm^{-1}$. It fails under extreme conditions but performs still at least as well as the Marbouty formulation. (Baunach et al., 2001)

2.3.4 Wet snow metamorphism

Wet snow is characterised by a significant amount of liquid water in snow. In wet snow the snow mass is macroscopically isothermal (mean snow temperature equal to the melting point) and the temperature variations occur only locally among the grains. The typical range of liquid water content in well drained layers is from 0.1 to 8 percent of the snow mass. Wet snow metamorphism is very efficient when the liquid water content is more than 5 percent of mass, because the heat and mass transfer needed for the phase changes is strong when liquid veins are found among the grains. (Pomeroy and Brun, 2001)

Liquid water content is normally expressed as a percentage by volume. It divides the metamorphism into two regimes: pendular with low liquid water content and funicular with high liquid water content. Highly unsaturated wet snow or pendular regime means that air occupies continuous paths throughout the pore space, and the snow grains are well bonded together. Highly saturated wet snow or funicular regime means that the liquid occupies continuous paths throughout the pore space, and the snow is cohesionless. There is a sharp transition at a critical liquid water content between the two regimes at liquid water content 8%; at the same time the material strength is reduced dramatically. Liquid water becomes mobile when the irreducible water content is exceeded; this is about 2-5 percent by volume, but depends on snow microstructure. The snow is flooded with water, when the liquid water content is more than 15 %. (Pomeroy and Brun, 2001) (Colbeck et al., 1990) (Colbeck, 1982; 1983)

Wet snow and dry snow are basically two different materials. Liquid water, present due to melt or rain, causes major reconfigurations of grains and bonds. Wet snow is active thermodynamically because of the high temperature and presence of the liquid phase, but vapour flow due to a macroscopic temperature gradient can only occur in dry snow. (Colbeck, 1997)

Smaller particles have lower melting temperatures in liquid saturated snow than the bigger ones, and heat flow to them causes their melting. Larger particles grow. Clusters of grains, not single spherical grains, characterise highly unsaturated wet snow. (Colbeck, 1982) The melting point at an ice-water interface depends on the radius of curvature of the interface. The sharpest parts of a snow crystal can be melting while the flat or concave parts are refreezing. This induces the microflow of water from sharp points to flat or concave points, rounding the crystals. (Pomeroy and Brun, 2001)

In wet snow at low liquid contents the single crystals join together by ice-to-ice contacts. Also neighbouring clusters are well bonded to each other. At higher liquid contents (slush) the volumetric air content can still be higher than the volumetric liquid content, but only the liquid phase is mobile. There is no intergranular bonding in slush, because bonds melt away by pressure melting. (Colbeck, 1997) Wet snow metamorphism induces at first a decrease in cohesion and hardness as liquid bonds form between the crystals at the expense of solid ones. The presence of liquid water increases the compaction rate because of the decrease in viscosity of wet snow and efficient metamorphism directly into spherical grains. (Pomeroy and Brun, 2001)

If the snow temperature once again falls under 0°C, the liquid water refreezes in the snow cover. In this way wet snow metamorphism, which can now be called melt-freeze metamorphism, causes extremely hard and strong layer to form. Melt-freeze layer consists of large polycrystals, sometimes it is almost clear ice.

Snow often undergoes freezing and thawing cycles, and this leads to multicrystalline grains. When there is long period of solar radiation, these grains may break down along the crystalline boundaries to original grain clusters. So clusters can be found even without a melt-freeze cycle. (Colbeck, 1982) With repeated melt-freeze cycles the grains in the clusters become an amorphous version of the cluster. These can break down later on along the grain boundaries. (Colbeck, 1983)

Melt-freeze layers can form on and below the surface while a thin surface layer melts during the day and refreezes at night, or when infiltrating melt water is refrozen. Repeated cycles of melt-freeze can lead even to impermeable icy layers in the snow cover. Crystals are normally large in these layers, because of crystal growth in the liquid-saturated snow before the refreezing. (Colbeck, 1982) Supercooled rain water can refreeze onto the surface and form smooth and impermeable glaze with crystal size about the same as grain size in the snow. (Colbeck, 1982)

Wet snow metamorphism is very fast compared to the other two metamorphoses: it does not take days but hours. Liquid water affects large areas inside the snow pack, either by percolation downwards, or spreading horizontally to form a layer.

In work by Marsh (1987) snow grain growth was observed in wet snow in the Canadian Arctic. In the study mean grain size and the range of grain sizes increased and the smaller grains disappeared. Occurrence of both pendular and funigular water saturations and melt-freeze events produce large variations in grain growth rates within a melting snow cover. Presence of large snow grains at snow layer boundaries can be explained by freezing of single grains to polycrystalline grains, followed by rapid grain growth under funicular conditions. Freezing followed by high liquid saturations occur at layer boundaries. (Marsh, 1987)

Liquid water percolates downward when its content exceeds the irreducible water content, which can be held in a snow layer by capillary forces. When the water flux is high, or when a layer lies upon an impermeable layer, the snow may become saturated. As water enters to cold, dry snow cover the following changes may occur: refreezing of melt water as ice layers and ice columns, the filling of liquid water storages and snow grain growth. (Pomeroy and Brun, 2001)

Spherical grains are unstable in the low liquid contents, like grain boundaries are in the high one. When the liquid is drained from the liquid-saturated snow, the tightly packed grain clusters appear. Also mass transfer among the particles in clusters is taking place through surface diffusion. The bulk density increases when the air-filled voids are reduced. Later the clusters are no longer individual units, but form a continuous ice phase. (Colbeck, 1982)

Water flow through snow is not stable and it is affected by flow instabilities like impermeable layers, zones of preferential flow and large melt water drains. These instabilities concentrate water within a melting pack, resulting in a great flux of water at the leading edge of the wetting front. On slopes, melt water may be diverted downslope by ice layers. (Pomeroy and Brun, 2001)

When a wetting front is stationary, the heat flux from wet to dry snow may be sufficient to refreeze water and form ice bodies within the snow pack. Flow fingers form ice columns, snow layer boundaries form ice layers and snow-soil boundary forms basal ice. Ice columns develop very large, rounded, clustered crystals. Basal ice forms where the melt water flux exceeds the infiltration rate of frozen soils and there is a strong negative heat flux from the snow to the soil. Rain on snow events are important in wetting the snow surface and in forming ice crusts. (Pomeroy and Brun, 2001)

Firnification is a process that is not dealt separately in the classification of metamorphoses by Colbeck (1982). It is a process that turns the seasonal snow slowly into glacier ice. Firnification is going on in all of the snow that survives at least one summer. Firnification consists of two separate processes: melt-freeze metamorphism and pressure metamorphism. Melt-freeze metamorphism has been discussed already above, but in the firn this process is repeated annually because of spring melt and refreezing during the autumn period. Every melt-freeze cycle turns the snow stronger and denser. The cycles also increase the snow grain size. When enough snow has accumulated on the firn, the pressure metamorphism begins to affect at a higher rate to the densification of the snow. Pressure reshapes the grains, and rearranges snow into denser mass. Slowly the grain boundaries become difficult to distinguish. Rounding and sintering by equilibrium metamorphism can increase the snow density to 600 kgm^{-3}. After the snow has turned into ice the snow density has reached the value 830 kgm^{-3}, and the air pores always present in the snow have closed and formed air bubbles. (Sommerfeld and LaChapelle, 1970; Paterson, 1994)

3. Present day snow conditions in Finland

In this chapter some long-term observations on Finnish snow climatology is presented. Different snow zonations in Finland are gone through briefly. Most of the theory of the snow distribution in the landscape and of the local variability of the snow cover is already discussed in Chapter 2.

Most of this chapter is devoted to the snow pack structure measurements carried out in this study, and especially to the results of the measurements. The results include observations on local snow pack structure and average snow conditions in different measurement location, as well as variation of snow cover in time and in space in different scales. Values for certain snow characteristics for different snow types, snow zonation testing and snow hardness measurements are also discussed in this chapter.

The results of the measurements have also been used for testing of the model SNOWPACK in Finland, discussed in Chapter 5.

3.1. Material and methods

3.1.1. Large scale observations on snow climatology in Finland

Snow cover is a normal, yearly phenomenon in Finland. Finland has a such winter climate that there is a certain period during each year when more snow is accumulating than melting. During this time the seasonal snow cover can be distinguished from the ephemeral snow cover during early and late winter. In our country 200-250 mm of yearly precipitation is snow. In southern and in middle Finland 30-40 % of yearly precipitation is snow, in Lapland the same fraction is 40-50 % (Mustonen, 1965). In the fells it can be even more. The amount of snow on the ground on March 15 compared to the total snow fall amount varies between 40 and 90 %, percentage increasing towards north (Lavila, 1949).

Permanent snow cover forms in Lapland on average during October, and in the southernmost Finland during December; snow melt takes place during March and April in southern Finland, in Lapland at least a month later. In the figures 3.1 and 3.2 the maps of snow cover formation and snow melt in Finland are shown, based on long-term statistics by the Finnish Meteorological Institute.

The snow water equivalent is measured using snow surveys. Snow surveys have been conducted in Finland since 1936 by the Finnish Environment Institute. For each survey 50-80 snow depth measurements are made, as well as 8-10 density measurements to find out the water equivalent of the area. The measurements are made in different biotypes in the area, typically different types of forest, bog and open area. Snow surveys are made on the 16th of each winter month. (Perälä and Reuna, 1990) In this study data from the following snow surveys have been used: Hanko, Santala; Siukolanpuro, Orivesi; Koppelonoja, Koski; Ilomantsi; Vääräjoki, Kuusamo; Iittovuoma.

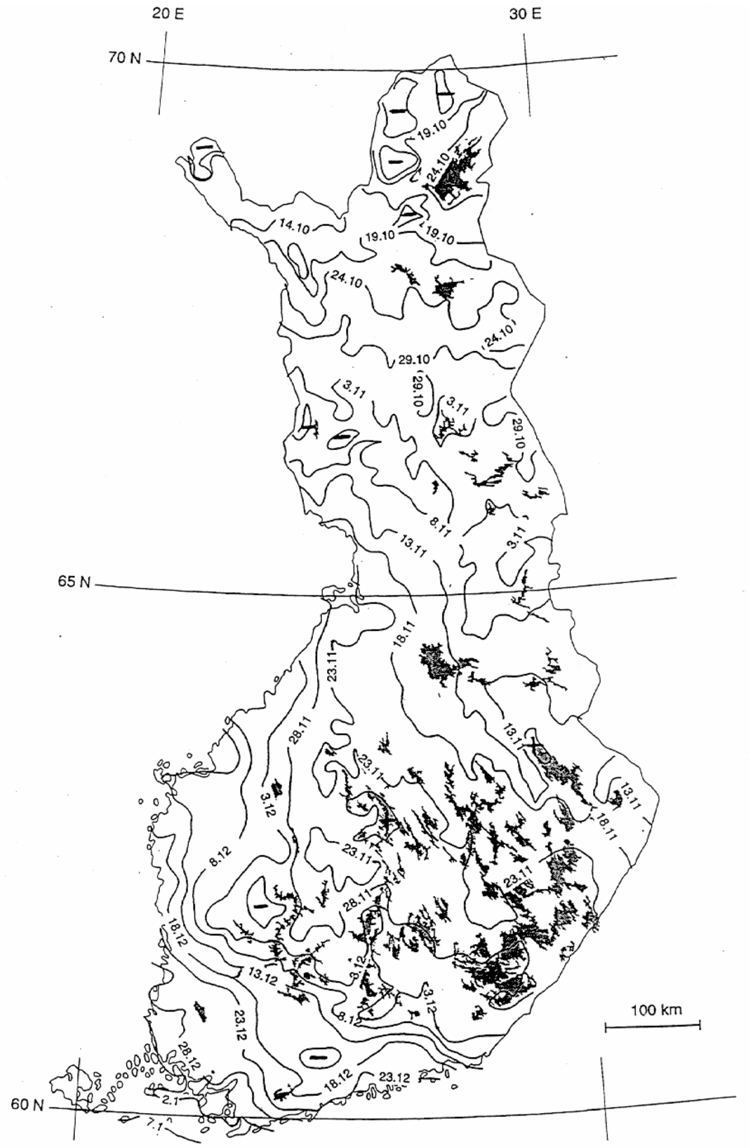

Figure 3.1. Average formation date of the seasonal snow cover during 1961-1990 (Solantie, 1996).

Snow cover formation, melt and depth are observed in several hundreds of locations by Finnish Meteorological Institute. The snow cover reaches its maximum depth in most of the country during March. Earlier this was true even in the southern part of Finland, but it seems that during the 1990s the snow depth maximum has shifted to late February in the south. Also snow cover has been thinner than before in southern and western Finland in the 1990s. During many winters the situation in the east and north has been reversed; thick snow covers have been observed. (Nordlund, 1999) In the figures 3.3, 3.4 and 3.5 the maps of the maximum date, maximum water equivalent and maximum depth of the Finnish snow cover are shown, based on long-term statistics by the Finnish Meteorological Institute and Finnish Environment Institute.

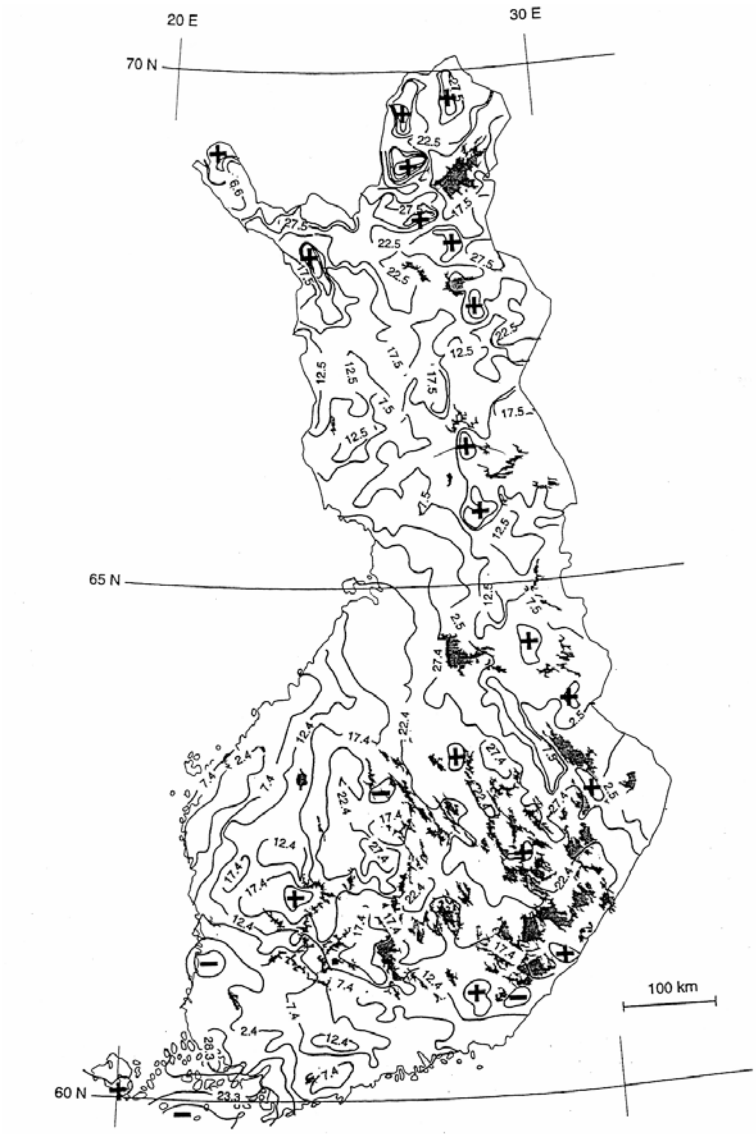

Figure 3.2. Average disappearance date of the seasonal snow cover during 1961-1990 (Solantie, 1996).

Solantie (2000) has reported the coefficients of variation of the snow depth observed in different areas in Finland. The coefficients for Lammi (southern Finland) area were around 0.56 in the forest and 0.61 in the open field. In Mekrijärvi (eastern Finland) area the coefficient for forest was around 0.23, and in Oulanka (northern Finland) area around 0.22 (Solantie, 2000). The greatest variation in the snow depth in Finland has been observed in Kilpisjärvi, where the maximum snow depth can vary between 60 and 250 cm, in the open fell plateau even more. The coefficients of variation for a snow water equivalent in large watersheds have been 0.3-0.4 in southern Finland and 0.2-0.25 in northern Finland (Kuusisto, 1984).

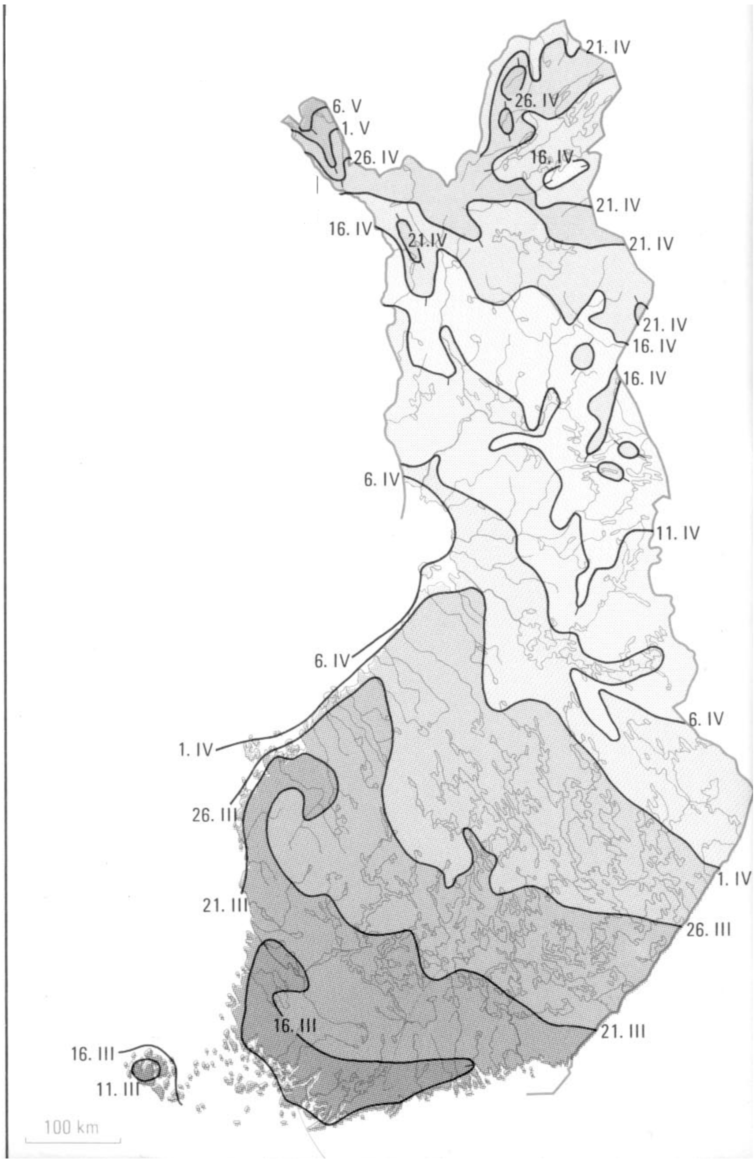

Figure 3.3 Average date of maximum water equivalent of the snow cover in Finland during 1961-1975 (Solantie, 1981)

3.1.2. Snow zonations for Finland

The basis of a snow zonation development is the wish to find snow conditions – this may include taking into account the amount of snow and/or type of snow – which can be distinguished from each other in different areas. The snow conditions should also be rather constant from winter to winter in these areas, so that the borders of the zones would remain the same. The first requirement is possible to meet, but the normal winter weather varies so much from winter to winter that large areas close to the borders of the zones are expected to fall into transitional or varying snow conditions category.

Several snow zonations have been developed for different areas of the world. Sturm and others (1995) have listed 14 of them, and at least three have been developed in Finland.

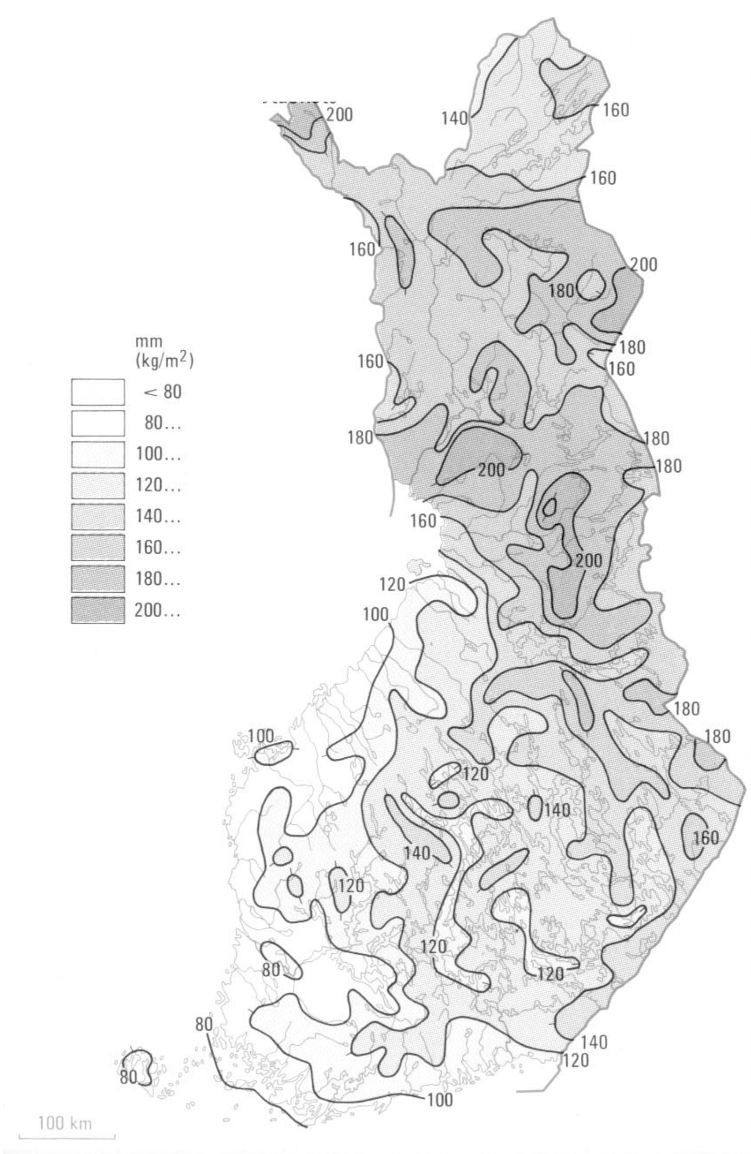

Figure 3.4 Average maximum water equivalent of the snow cover in Finland during 1961-1975 (Solantie, 1981)

In the earliest zonation the country was divided into 12 different snow types by snow crystal size and snow hardness (Angervo, 1952). In the study by Kuusisto (1984) Finland was divided into nine different snow areas by snow cover duration, duration of the period without melting, average maximum snow water equivalent and the coefficient of variation of the average maximum snow water equivalent. In the zonation by Solantie and others (1996) eight different zones with some sub-zones were found, mainly based on the snow cover formation, melt and duration. Snow cover structure has not been used as a tool in these zonations.

A scheme that has attempted to classify global snow cover using physically based measures is that by Sturm, Holmgren and Liston (1995). Climatic scheme is based on temperature, wind speed and snow fall, and snow cover is discriminated into seven classes (tundra, taiga, alpine, prairie, maritime, mountain and ephemeral). A transitional zone is found between each two of the neighbouring classes. Each class is defined by snow properties like snow layering, layer density, temperature, grain-size and type. Also characteristic bulk density versus time curves are observed to differ from one snow zone to another. Curves in tundra, taiga and the maritime zone seem to have similar slopes and intercepts but differ from class to class (Sturm and Holmgren, 1998). The strict use of climatic indicators can result in confusing classification. For example tundra snow can develop in a prairie environment if the climate falls within the tundra snow class (Sturm et al., 1995).

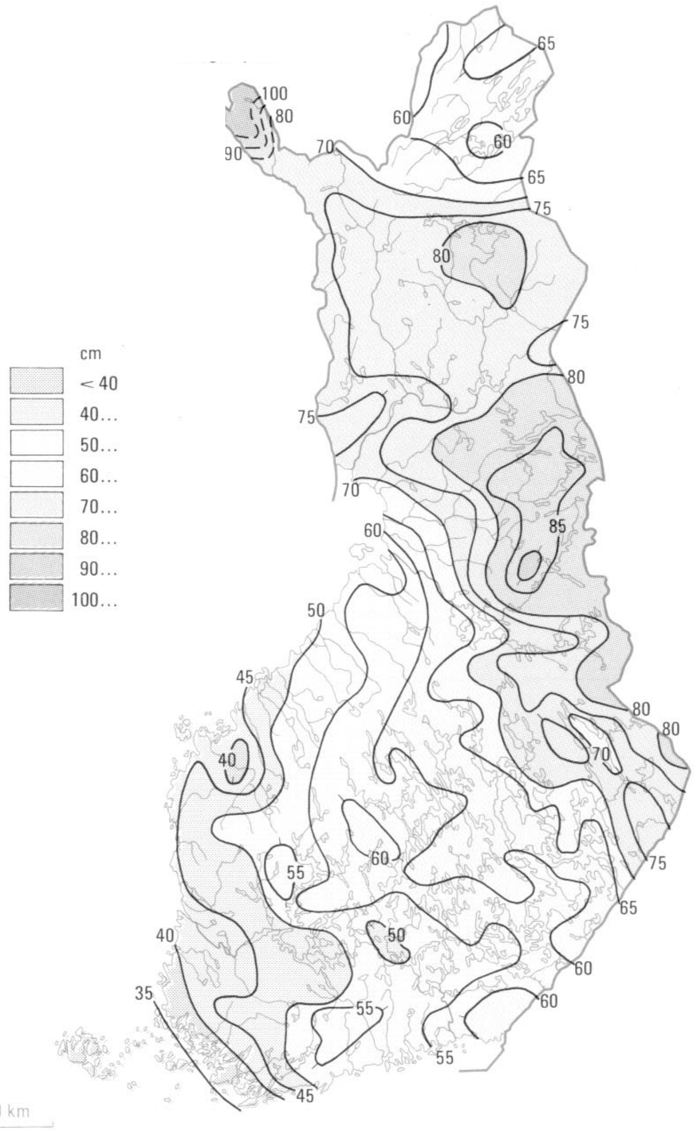

Figure 3.5 Average maximum depth of the snow cover in forest in Finland during 1921-1960 (Solantie, 1978)

Only tundra and taiga snow develop temperature gradients needed for kinetic metamorphism (Sturm et al., 1995). On the tundra zone in Alaska two different types of snow conditions have been observed: veneer surfaces and drift snow surfaces. The veneer surfaces are formed in the flat tundra, but drift snow surfaces are accumulated according the topography to hollows and leeward slopes. The veneer surfaces are thin, consisting of wind packed snow and depth hoar; they are "normal" tundra snow. On the other hand the depth of drift snow can be ten times the one of veneer surfaces, they are dense and have different stratigraphy than the veneer surface. Local variability of the snow pack structure is high in this kind of snow, the snow cover can be said to be a transition type between taiga and tundra snow. (Benson and Sturm, 1993)

In the latest snow zonation for Finland the global snow zonation by Sturm et al. (1995) has been validated for Finland, and the following snow zones were found: ephemeral snow zone, transition snow zone between ephemeral and maritime zones, maritime or mild snow zone consisting of thin maritime and maritime parts, taiga zone and tundra zone. Prairie zone and thin alpine snow zone were found in small areas in Finland, first in the large fields in Ostrobothnia in western Finland, latter in some hills in northern Finland. (Oksanen, 1999)

In the table 3.1 the description of the snow cover on each zone, as well as depth range, bulk density, number of layers, duration and average slopes and intercepts of the characteristic bulk density versus time curves are shown. Not enough information is available on mountain snow zones, and it has been left out from the study. The data collected here are from the measurements from America, and it is not always comparable to Finnish conditions. In the figure 3.6 the approximate snow zonation for Finland by this scheme is shown. The zonation shown results both from mapping from climate data (Sturm et al., 1995) and from the snow pack structural measurements (Oksanen, 1999). What comes to this map and other snow zonation results presented also in this work one has to keep in mind words by Sturm and others (1995): "Every static classification of snow cover is somewhat misleading, because snow is such a dynamic phenomenon."

Table 3.2. Measurement locations and their description. Snow zones by Sturm et al. (1995), physical geographic regions by Nordiska ministerrådet (1984), forest vegetation zones by Ahti et al. (1968).

Location	*Coordinates*	*Snow zone*	*Physical geographic region*	*Forest vegetation zone*	*Main vegetation types*
Santala	59°50' N; 23°15' E	Ephemeral	Oak region of Southwestern Finland	Hemiboreal	Mixed forest, field
Lammi	61°03' N; 25°03' E	Thin maritime	Lake district	Southern/ middle boreal	Mixed forest, spruce forest, field
Mekrijärvi	62°46' N; 30°59' E	Maritime	Southern hilly vaara-region	Southern/ middle boreal	Mixed forest, pine forest, field
Oulanka	66°22' N; 29°19' E	Tundra	Coniferous woodlands	Northern boreal	Mixed forest, pine forest, bog
Kilpisjärvi	69°03' N; 20°48' E	Taiga	Submaritime birch forests/ Northern high mountain area	Fjeld Lapland birch forest	Birch forest, fell plateau

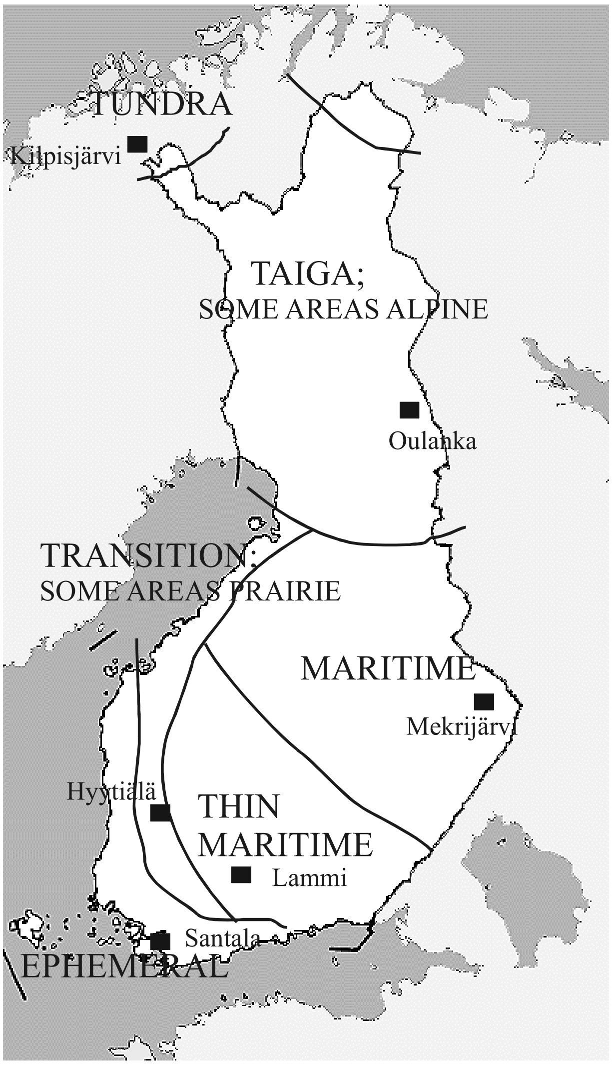

Figure 3.6 The approximate snow zonation for Finland from the scheme by Sturm et al. (1995). The zonation shown results both from mapping climate data (Sturm et al., 1995) and snow pack structural measurements (Oksanen, 1999).

3.1.3. Measurement locations

Locations of measurements for this study were tried and chosen so that all of the assumed snow zones in Finland would be covered, and also so that each location would clearly fall into a certain snow zone. In figure the 3.6 also the measurement locations of the regular snow pack structure observations are marked on the map, as well as Hyytiälä, where model testing discussed in chapter 5 was done. It is seen from the map that the transition zone (including also patches of prairie snow in large fields of Pohjanmaa) is not covered in this study. Also Hyytiälä is not clearly in a thin maritime snow zone.

The terminology of the zonation is somewhat problematic in Finland. The maritime snow zone is situated relatively far away from the Baltic sea, and for this reason also use of a term mild snow zone is suggested. In any case it is convenient to use the same terms all over the world when using the same classification; the snow conditions determine the zonation, not geographical facts.

In table 3.2 some basic data about the measurement locations (excluding Hyytiälä) is given. Below the different locations are gone through one by one with more details.

Santala

Santala is located in an ephemeral snow zone on the coast of the Gulf of Finland. In the figure 3.7 a map of Santala is shown, as well as the measurement areas in the forest and in the field. Typical forest and field snow conditions in Santala are shown in the figure 3.8.

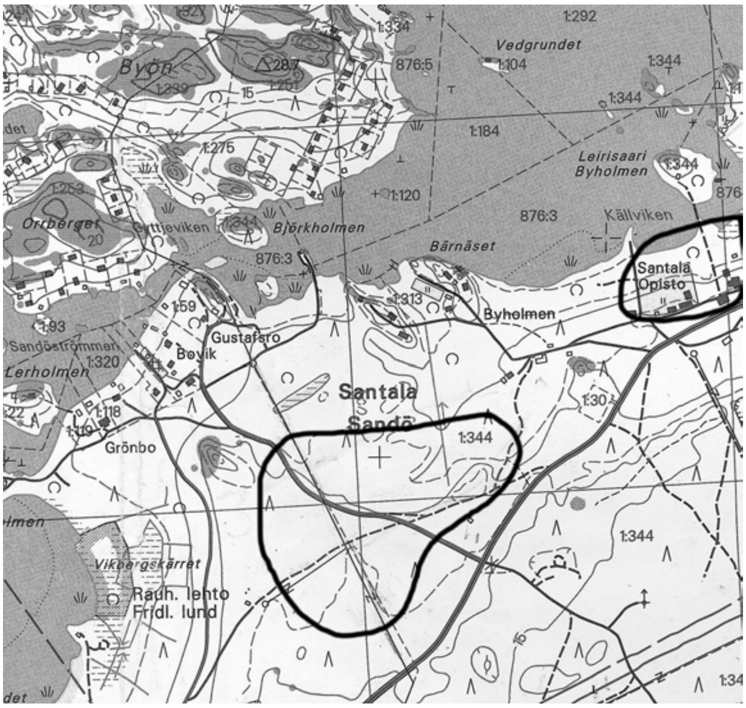

Figure 3.7. Map of Santala. Measurement areas are marked on the map. Grid size is 1 km. (Maanmittaushallitus, 1999)

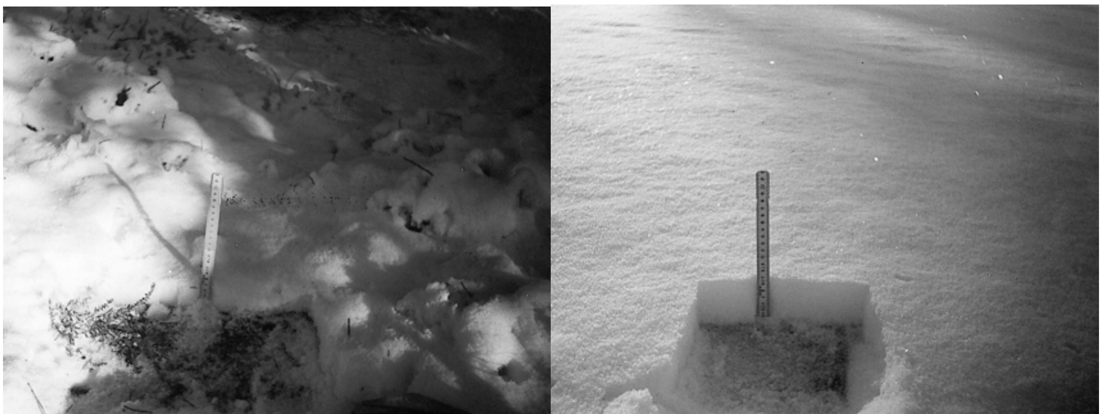

Figure 3.8. Forest and field snow in Santala.

Measurements in Santala were conducted in two main biotopes of the area: mixed forest and open field with short vegetation. Shore meadows with high vegetation were not taken into account. The forests and fields in Santala are rather small in scale, because of many roads, settlement and other infrastructure in the area. The terrain is fairly flat. The mixed forest is mainly coniferous and quite homogenous in age and in tree density.

Lammi

Lammi is found in a thin maritime snow zone in southern Finland. The landscape is dominated by mainly coniferous forests and large fields. There are also several lakes in the area. Measurements were conducted near Lammi biological station. A map of the area is in the figure 3.9. The measurement areas are also marked on the map.

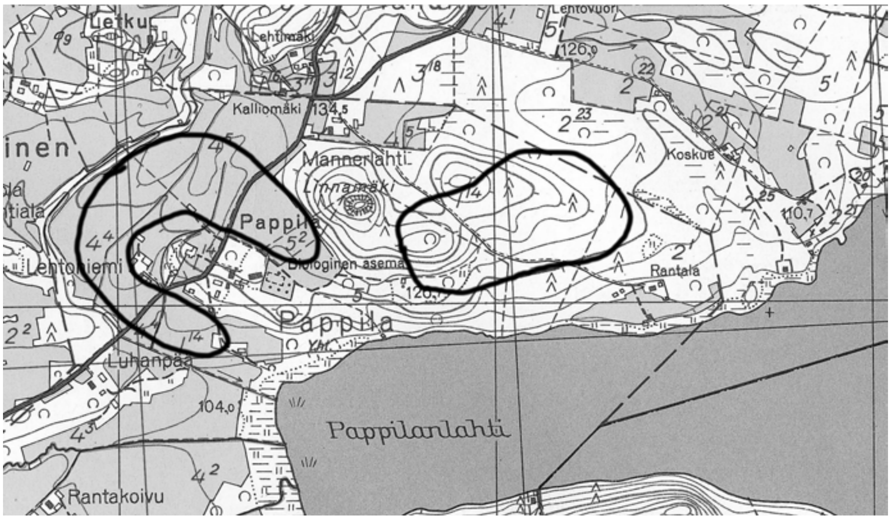

Figure 3.9. Map of the vicinity of Lammi Biological Station. Measurement areas are marked on the map. Grid size is 1 km. (Maanmittaushallitus, 1965)

Figure 3.10. Field work made by students in the forest and in the open field in Lammi

Measurements were made in large open fields with no vegetation. Wind packing can be seen in the snow cover, because of the large fields. The measurement forests were mostly old and dense spruce forest, where snow interception is notable. Parts of the forest were younger mixed forest. The terrain chosen is fairly flat. Figure 3.10 shows the forest and the open field near Lammi biological station.

Mekrijärvi

Mekrijärvi is situated in the eastern part of Finland near the Russian border, in the maritime snow zone where snow depths exceed those in Lammi, sometimes even those in Oulanka. There are large fields and bogs in the area, as well as mixed forests of different ages. Some forests are heavily cultivated having only pine trees with homogenous age and tree density. The field and forest measurement areas were rather far from each other in Mekrijärvi. These, and the vicinity of Mekrijärvi biological station, are shown in the figure 3.11. Views in the forest and open field are shown in the figure 3.12.

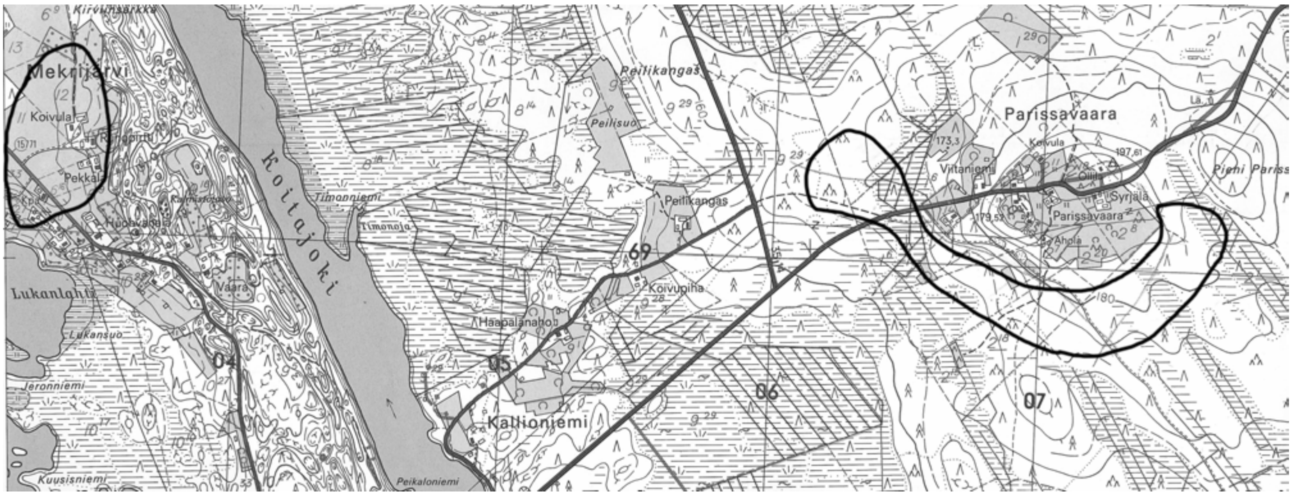

Figure 3.11. Map of Mekrijärvi. Measurement areas are marked on the map. Grid size is 1 km. (Maanmittaushallitus, 1974)

Figure 3.12. Forest and field view of Mekrijärvi

The fields were large, with wind effect notable, and with no vegetation. Two thirds of the measurement forests were rather dense and mixed, and the soil was drained with several ditches across the forest. Combined effects of interception and ice and melt water dripping from the canopy made the snow cover rather difficult to measure. One third of the forests was homogenous pine forest with smaller canopy effects. The terrain is fairly flat both in the forest and in the open field.

Oulanka

Oulanka is situated near the eastern border of Finland as well. However, the snow and vegetation zones are different from the ones in Mekrijärvi. Oulanka is found in the boreal vegetation zone and in taiga snow zone. In figure 3.13 the map of the vicinity of Oulanka biological station is shown. Measurement areas are marked on the map. The station is located in a nature reserve area with large, old forests, mainly coniferous, and quite small bogs. Views from the forest and bog are shown in the figure 3.14.

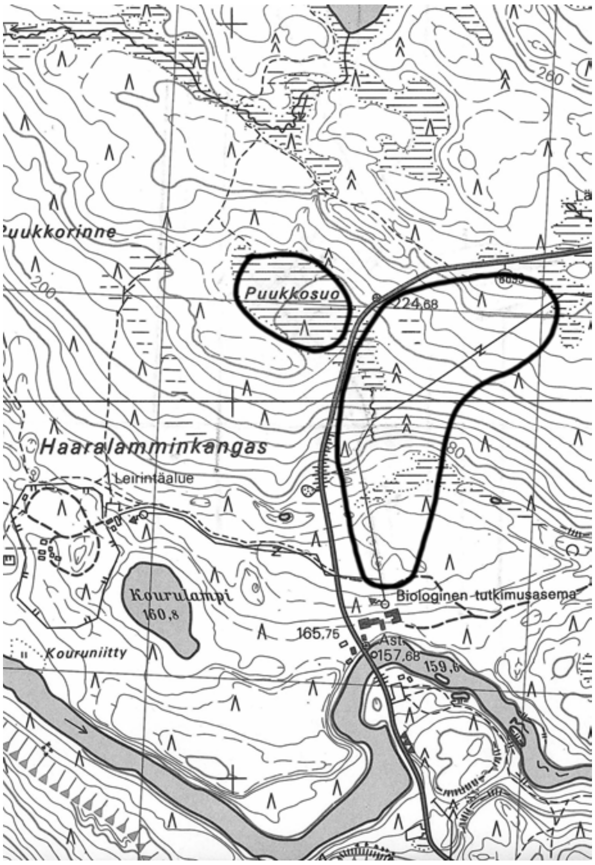

Figure 3.13. Map of vicinity of Oulanka Biological Station. Measurement areas are marked on the map. Grid size is 1 km. (Maanmittaushallitus, 1964)

Figure 3.14. View of the nature reserve area forest and of the Puukkosuo bog in Oulanka.

Measurements were conducted in mainly coniferous forest, pines being the main tree species. The forest was less dense than in Mekrijärvi, and the canopy effects were smaller because of this. Bog measurements were done in a small bog called Puukkosuo, with sparse pine tree vegetation. Wind effect is not probable in this bog. The terrain was naturally flat in the bog; in the forest there were some hills.

Kilpisjärvi

Kilpisjärvi is located in Finnish Lapland, in the far northwestern part of the "arm" of Finland. It also differs greatly from the rest of Lapland, which mainly belongs to the taiga snow zone and has boreal forest and fells with gentle slopes. Kilpisjärvi is almost alpine with steeps slopes and high fells. It is also totally located above coniferous tree line, and only birch forest is found there. The fell plateau is treeless. The Kilpisjärvi area can be divided into four distinct vegetational regions: mountain birch forest, subalpine region, lower alpine region and mid-alpine region (Eurola et al., 1980). The measurements of this study were made in the mountain birch forest and in the mid-alpine region. Kilpisjärvi is located in tundra snow zone.

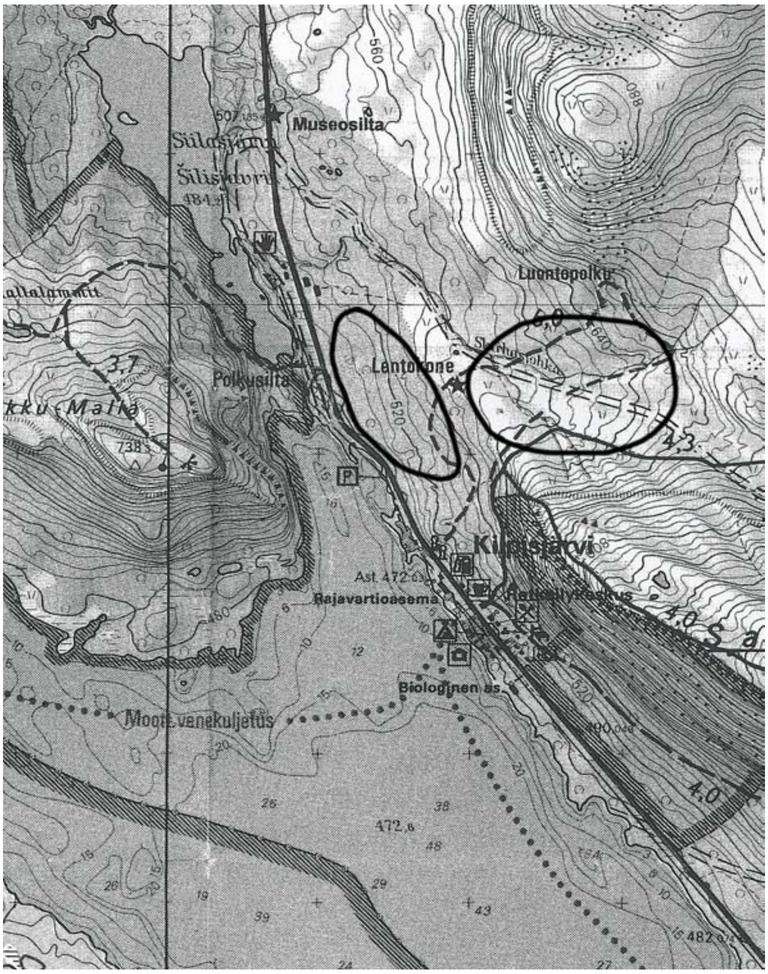

3.15. Map of Kilpisjärvi. Measurement areas are marked on the map. Grid size is 5 km. (Maanmittaushallitus, 1998)

A map of the vicinity of Kilpisjärvi biological station is in the figure 3.15. Measurement areas are also marked on the map, one below the tree line in the sparse birch forest with rather hilly terrain, and the other above the tree line in the fell plateau, also with sloping terrain. Only low vegetation is found in the plateau area. Wind and local topography have great effect on the snow distribution in the fell area. Snow beds with several meters of snow depth are found, as well as nearly snowless deflation areas. The deepest snow cover is found just above the tree line (approximately 600 masl). Most variation is seen in the snow depth above 900 masl, where almost all of the area can be grouped either as snow beds or deflation areas. Snow is denser higher up in the fell plateau area in the beginning of the winter and during the spring time. No great differences are seen in the midwinter. (Eurola et al., 1980) The snowless period is four months in the mountain birch forest, five months in the deflation areas and three months on the snow beds (Hiltunen, 1980). Field work in the birch forest is shown in the figure 3.16, as well as a view in the Saana-Jeahkats fell plateau.

Figure 3.16. Field work in the birch forest and view of the Saana-Jeahkats fell plateau in Kilpisjärvi.

3.1.4. Measurement winters and times

Measurements were carried out during the winters 1999/2000, 2000/2001 and 2001/2002 in all of the locations. The first measurement period was timed approximately from one to two months after the formation of snow cover; the second around the average water equivalent maximum of the location. Because of differences in winters and also timing problems the measurement times did not always match to the ideal times. In the table 3.3 the dates of the measurements for different locations are shown for each winter.

Table 3.3. Measurement dates for different locations for each winter.

Location	*1999/2000*		*2000/2001*		*2001/2002*	
Santala	22.2.	21.3.	12.2.	15.3.	13.2.	14.3.
Lammi	24.2.	16.3.	18.2.	18.3.	-	18.3.
Mekrijärvi	29.1.	17.4.	21.1.	12.4.	5.1.	25.3.
Oulanka	26.1.	20.4.	18.1.	9.4.	3.1.	27.3.
Kilpisjärvi	23.1.	23.4.	15.1.	16.4.	1.1.	19.4.

Below, some specific features of the measurement winters (weather and snow conditions) are gone through.

1999/2000

The end of the year 1999 was clearly colder than normal (when comparing to period 1961-1990). There were relatively large amounts of precipitation during October and December, but because it was most often liquid, the snow cover built up very slowly even in Lapland. (Finnish Meteorological Institute, 1999) In the end of the year 1999 more snow was found in southern and middle Finland than normally; the water equivalent of snow was in many places 1.5 times the normal amount. (Finnish Environment Institute, 1999)

The year 2000 was warm compared to normal. The winter months were especially warm. Slightly more precipitation was obtained than normal in the whole country. The snow cover was deeper than normal in the whole country in the beginning of the year 2000. Prolonged melt period in the January melted large portion of the snow in southern and western Finland, but large amounts of snow accumulated in eastern and northern Finland and the snow loads were greater than normal there. The snow melted rapidly at normal time. (Finnish Meteorological Institute, 2000; Finnish Environment Institute, 2000)

2000/2001

There was very little snow during November and December 2000. Warm and rainy weather lasted until December. The snow cover formed as late as at the end of the year even in Lapland. In southern and middle Finland the thin snow cover melted once again in the beginning of the year 2001. (Finnish Meteorological Institute, 2000; Finnish Environment Institute, 2000)

The year 2001 had monthly average temperatures close to normal, as well as precipitations. The snow water equivalent was smaller than normal in the whole country during the winter and spring 2001. (Finnish Meteorological Institute, 2001; Finnish Environment Institute, 2001)

2001/2002

Snow cover formed in southern Finland much earlier than normally. In the end of the year 2001 the snow water equivalent was close to the long term average in the whole country. (Finnish Meteorological Institute, 2001; Finnish Environment Institute, 2001)

The beginning of the year 2002 was warmer than normal almost everywhere in Finland. Of the winter months 2001/2002 December was the coldest one, which is very rarely the case. The precipitation amounts were very small. Precipitation was often rain, also in Lapland in January and February. There were normal amounts of snow in the winter and spring 2002, but spring was early in the whole country. The warm weather in March and April melted the snow rapidly 1-3 weeks earlier than normal. (Finnish Meteorological Institute, 2002; Finnish Environment Institute, 2002)

In the table 3.4a the average formation, melt and maximum snow depth dates as well as maximum snow depth are listed for measurement winters in four of the measurement locations, together with results of the long-term observations. In the table 3.4b the same is done monthly for some meteorological variables during the winter time: mean air temperature, monthly precipitation as well as the amount of "warm" days (days when maximum air temperature exceeds 0°C). Different shading is used in the tables to distinguish the notable deviations from the long-term mean. Deviations associated with the warm and moist winters producing deep snow covers in most of the country (early snow cover formation, late snow melt, late snow depth maximum, thick snow cover, warm temperature, large amount of precipitation, long periods of warm days) are marked with dark shade. Deviations associated with colder and dryer conditions producing thinner snow covers (late snow cover formation, early snow melt, early snow depth maximum, thin snow cover, cold temperature, small amount of precipitation, short periods of warm days) are marked with light shade. The observations without shading show no marked deviations from the long-term mean.

Table 3.4a Formation, melt, maximum snow depth dates and maximum snow depth for measurement winters in the measurement locations (data by Finnish Meteorological Institute), together with results of the long-term observations (Solantie, 1996; Finnish Meteorological Institute, 1991). Deviations associated with warm and moist winters are shaded in dark grey. Deviations associated with colder and dryer conditions are shaded in light grey.

	Santala				*Mekrijärvi*			
	61/90	*99/00*	*00/01*	*01/02*	***61/90***	*99/00*	*00/01*	*01/02*
Form date	**2.1.**	19.12.	29.12.	21.12.	**18.11.**	5.11.	14.11.	7.11.
Melt date	**25.3.**	19.3.	12.3.	14.3.	**2.5.**	26.4.	21.4.	27.4.
Max date	**16.3.**	30.12.	26.1.	29.12.	**1.4.**	17.3.	5.3.	6.3.
Max depth (cm)	**23**	9	14	14	**63**	111	59	84
	Oulanka				*Kilpisjärvi*			
	61/90	*99/00*	*00/01*	*01/02*	***61/90***	*99/00*	*00/01*	*01/02*
Form date	**29.10.**	11.11.	20.11.	22.10.	**14.10.**	9.10.	30.10.	20.10.
Melt date	**17.5.**	7.5.	2.5.	2.5.	**6.6.**	1.6.	13.5.	26.5.
Max date	**16.4.**	10.3.	5.4.	7.3.	**6.5.**	29.3.	12.4.	17.2.
Max depth (cm)	**68**	106	75	89	**95**	124	74	104

It is important to notice that the change in the snow depth is connected both to the average winter air temperature and to the change in it. Even if the mean monthly air temperature is several degrees higher than long-term mean, thicker than average snow cover can build up because of larger amounts of precipitation if the air temperature stays long periods below 0°C.

Winter North Atlantic Oscillation (NAO) index is NAO based on the difference of normalized sea level pressure (SLP) between Lisbon, Portugal and Stykkisholmur/Reykjavik, Iceland during December-March period. Positive values of the index indicate stronger-than-average westerlies over the middle latitudes, and result normally in warm, moist and snowy winter conditions in Finland; negative values result in colder and dryer conditions because of air masses coming mostly from the east. The NAO index was positive during winters 1999/2000 and 2001/2002: 2.8 and 0.76, respectively. During winter 2000/2001 the index was negative, -1.89. (North Atlantic Oscillation Indices Information, 2004)

The effect of positive NAO index is seen in the table 3.4b most easily in the mean monthly air temperature. Also high precipitation amounts and long periods of warm days are seen in the positive NAO index winters. During the positive NAO index winters more snow accumulated to most of the study locations than normal; in Mekrijärvi and in Oulanka almost double amount. Snow cover also formed earlier than normal. On the other hand, deviations associated with positive NAO index winters are also seen in the winter 2000/2001 weather, and deviations associated with colder and dryer negative NAO index winters during winters 1999/2000 and 2001/2002.

Table 3.4b. Mean monthly air temperature, monthly precipitation and amount of "warm" days (days when maximum air temperature exceeds 0°C) for measurement winters in the measurement locations (data by Finnish Meteorological Institute), together with results of the long-term observations (Finnish Meteorological Institute, 1991). Deviations associated with warm and moist winters are shaded in dark grey. Deviations associated with colder and dryer conditions are shaded in light grey.

	Santala				*Mekrijärvi*			
	61/90	*99/00*	*00/01*	*01/02*	***61/90***	*99/00*	*00/01*	*01/02*
T ave (°C)								
Dec	**-1.6**	0.7	3.6	-3.2	**-8.8**	-6.1	-4.9	-12.7
Jan	**-4.7**	0	0.8	-1.1	**-12.1**	-7.6	-5.8	-9.6
Feb	**-5.5**	-0.3	-5.3	0.4	**-10.6**	-6.7	-12.3	-4.2
Mar	**-2.4**	0.3	-1.6	1.1	**-5.1**	-3.1	-8.2	-3.1
Prec (mm)								
Dec	**59.6**	95.8	72.0	34.1	**50.2**	71.0	47.4	16.9
Jan	**41.4**	53.2	79.2	70.1	**38.3**	35.6	20.9	57.4
Feb	**30.8**	46.2	31.7	63.2	**29.6**	41.4	46.7	61.7
Mar	**32.3**	36.9	30.5	49.8	**34.2**	30.4	34.6	25.7
T > 0°C								
Dec	**20**	22	27	15	**7**	8	13	1
Jan	**13**	24	26	24	**5**	10	3	11
Feb	**10**	22	15	23	**3**	9	5	14
Mar	**20**	29	18	29	**15**	18	7	18
	Oulanka				*Kilpisjärvi*			
	61/90	*99/00*	*00/01*	*01/02*	***61/90***	*99/00*	*00/01*	*01/02*
T ave (°C)								
Dec	**-13.1**	-10.9	-8.4	-13.3	**-12.5**	-15.4	-12.1	-11
Jan	**-16.4**	-10.3	-6.8	-12.7	**-14.6**	-9.9	-8.8	-13.4
Feb	**-14.0**	-9.9	-13.8	-8.8	**-13.1**	-10.7	-14.3	-11.2
Mar	**-7.7**	-5.3	-11.2	-6.6	**-10.1**	-8.4	-15.2	-8.6
Prec (mm)								
Dec	**34.3**	50.5	66.4	15.0	**33.3**	34.1	30.5	29.8
Jan	**30.4**	37.6	29.9	53.9	**33.4**	98.6	60.5	109.7
Feb	**25.5**	37.6	31.6	54.3	**29.2**	50.2	60	61.6
Mar	**30.9**	33.8	26.8	26.3	**21.5**	72.6	9.9	24.5
T > 0°C								
Dec	**6**	2	6	0	**4**	1	5	9
Jan	**3**	3	2	4	**3**	3	8	8
Feb	**3**	3	4	4	**3**	0	5	2
Mar	**11**	10	2	11	**6**	5	0	7

During the negative NAO index winter 2000/2001 no large deviations are seen in the winter climate; little less than the normal snow was accumulated, and the snow season was shorter than normal in most of the country.

Because of the large variation in winter weather conditions, it is very difficult to get an average winter included in a short time series of measurement winters. The overall winter weather conditions during the three measurement winters were rather warm with relatively large amounts of precipitation. Naturally some very cold months were also experienced, as well as few months with very little precipitation in northern Finland. In southern Finland there were rather long warm periods during the measurement winters. On the other hand, in the northern part of the country the amount of warm days had no large deviations from normal and the snow pack structure can be expected to be close to the average one at least in these locations. In the south the situation may deviate from average snow pack structure towards warmer and denser snow cover.

3.1.5. Methods, error sources and error limits

The following measurements were carried out in every location and in every biotype:

Three line measurements of snow depth, most often 500 m with 25 m intervals and with three measurements at every point. In this way, approximately 180 depth measurements were made in every biotype. During some of the measurement periods, also the water equivalent of the snow cover was observed together with snow depth measurements.

It is worth noting that the spatial distribution of snow depth in prairie and arctic environments has been found out to be fractal at small scales, becoming random at scales beyond the cutoff length. The standard deviation of randomly sampled data is independent of the sample size, but for a fractal, the standard deviation is a function of the sample size. For flat surfaces, the cutoff length is between 20 and 100 meters, approximately 30 meters. When the sampling distance is greater than this length, the distribution becomes random (Shook and Gray, 1994; 1996)

One snow pit profile at each line. This includes:

- Observations of the site, snow and ground surfaces
- Snow depth and water equivalent at the snow pit site
- Snow stratigraphy including the estimation of the grain size and form in each layer
- Air temperature, snow surface temperature, temperatures below each layer
- Layer density
- Layer hardness

During every measurement period, approximately three snow pits were dug in every main biotype in each location. The total number of snow pit profiles collected during this study is approximately 180.

Traditional methods were used in all of the snow pack structure measurements. (See for example Colbeck and others, 1990, for details in methods.) In the table 3.5 information on the devices or methods used to measure different quantities is presented, together with the accuracy of the devices and also estimated error of the method.

A traditional tube scale (height 50 cm and diameter 11.5 cm) was used to determine the water equivalent of the snow cover. The scale is calibrated to give WE in mm. When the snow depth is known, also the bulk density can easily be calculated.

Grain size and form were estimated visually using a plate with 1 mm grid. Grain size is defined here as an average diameter of the snow grains in the sample; however it is noted (see later in the chapter 5) that visually estimated average equals closely with the maximum grain diameter from image processing. Mean grain size obtained by sieving agrees quite well with those inferred from area or diameter measurements. Fieldworkers also have a tendency to give a lower limit on grain size that matches quite well values that are objectively measured by either sieving or image analysis. (Fierz and Baunach, 2000)

Table 3.5. Snow quantities measured in this study, their units, devices or methods used, accuracy and estimated error of the devices or methods.

Quantity	*Unit*	*Device*	*Accuracy*	*Max error*
Depth	Cm	Avalanche sond with a scale	0.5 mm	1 cm
WE	Mm	Korhonen- Relander snow balance	1 mm	10 %
Grain size	Mm	Plate with mm scale	1 mm	20 %
Grain form		Plate with mm scale	-	-
Density	Kgm^{-3}	1 l box sampler and spring balance	1 kgm^{-3}	10 %
Hardness	Nm^{-2}	Penetrometers	1 Nm^{-2}	20 %
Temperature	°C	Digital thermometer	0,1 °C	0,2 °C

Layer density was observed using a Swedish design one litre box sampler with a removable lid and a turning and cutting front part. It has a height of only 5 cm, and this allows measuring of the thinner layers also. On the other hand the sampler is big enough not to be very sensitive to the snow cover inhomogeneities. The sample was weighed with a spring balance. In the figure 3.17 measurement of snow density using a one liter sampler and a spring balance is shown.

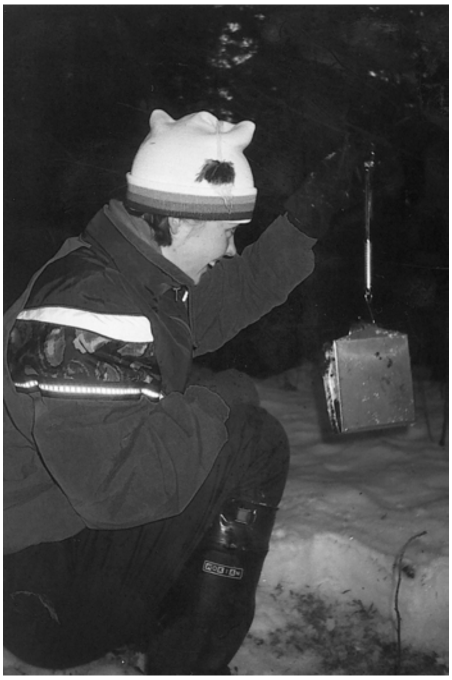

Figure 3.17. Measuring snow density by weighing a one-liter sampler.

Layer hardness was measured with a Canadian style penetrometers with a spring balance allowing the measurement of the pressure needed to break the snow structure in the layers. Measurements were done both horizontally and in the surface layer also vertically. Plates of different sizes were used to broaden the measurement ranges of the penetrometers. The hardness measurements are discussed further in Section 3.2.7.

Temperature measurements were conducted at the snow surface, and after this below each visible snow layer by sticking the thermometer 10 cm inside the pit wall.

The estimated error listed in the table 3.5 is based on the author's own experience, as well as discussions with other field researchers with longer experience. Some sources of error that are not taken into account in the table are listed below; the list is based on discussion by Lehmusjärvi (2001) about measurements of density and water equivalent, but it can be broadened also to other snow quantities.

- Problems with the devices
- Different devices or changes in devices between the measurements
- Different measurers
- Unrepresentative location of the snow pit
- Difficult snow conditions
- Difficult weather
- Ground surface variations and vegetation

3.2. Observed local snow conditions

3.2.1. Snow pack structure

The observed snow pack structure on measurement locations is shown in figures 3.18-3.28. In most of the places the early and late winter are treated separately on the opposite pages; observed snow pits from the three winters are collected on one page. On average three snow profiles form open area and three from the forest are placed together on to the pages. In Kilpisjärvi different winters are collected on separate pages. A code connecting the shades and different snow types is shown in the figures 3.18 and 3.19.

There are several different types of variation shown in the figures. First, the variation in time is seen both between early and late winter cases and also between different winters. Part of this variation is caused by differences in measurement times and points between the measurement periods. Second, spatial variability is seen in three scales: inside a biotype, between two biotypes in same location and between different locations. Below the observations from different locations are gone through separately. Some types of variations are also discussed in section 3.3.

When looking at the figures 3.18 – 3.28, snow pack structure, and also snow pack structure evolution, differing from each other is seen in different locations. In any case, the structure and evolution seem to have some common characteristics between different years in a single location. The measurement locations were chosen keeping in mind the snow zonation map (Figure 3.6): each of the locations was assumed to be located in a different snow zone with a different snow pack structure characteristics. In this section it is also tried to answer how well does the observed snow pack structure support the assumption.

Sometimes the observations in either forest or in open areas were done a day later than in the other biotypes. This explains a possible thin layer of precipitation particles on top of a snow pack in either of the biotypes, when it is missing from the other.

<u>Santala</u>

In figures 3.18 and 3.19 the observed snow pack structure in Santala, assumed to be located in the ephemeral snow zone, is shown for the three study winters.

Observations show that Santala clearly falls into ephemeral category. At maximum two layers of snow was present, and the snow cover consisted of new snow, melting snow or refrozen snow. Snow depth was below 20 cm during all of the measurement periods. On many occasions no snow was present during the winters.

Variation of snow pack structure was not very big between the winters, however, no snow was observed during the winter of 2002. This variation, as well as observation of new and melt-freeze snow, was rather random and depended on timing of the measurements. The snow cover changed towards more wet, warm and icy when going towards late winter. Snow depth also decreased, and density increased.

Spatial variability of depth and structure inside a biotope was quite small in Santala, and it decreased when going towards late winter observations. Variation in snow pack structure was seen only during early winter 2000, when in some places older refrozen snow was found under the recent snow. Spatial variability between the biotopes was seen only during winter 2000. Snow depth was smaller in open areas than in the forest, and in the late winter the melting of the snow occured sooner in open areas.

Lammi

Figures 3.20 and 3.21 show the snow pack structure observed in Lammi, assumed to lay on thin maritime/ thin mild snow zone. Two facts make the data series in Lammi rather difficult to use: late winter observations were partly made by students of the course Geophysics of snow and ice, and therefore include larger source of error than the other measurements. Also data from early winter 2002 are missing, and this sets some limitations to conclusions.

Snow covers in maritime/mild snow zone in Finland are very shallow and consist only of a few layers compared to those in America, where the snow zonation was developed. However the structure of the snow cover gives proof that Lammi really belongs to the thin maritime zone. The snow cover in this zone is assumed to be formed mainly of wetted snow, ice and of recent snow. This was true when looking at the figures; on the other hand quite large portions of the snow covers were rounded or even faceted snow, especially in late winter cases. This might give reason to set Lammi on a transition zone between maritime and taiga snow.

There were some differences seen between different winters. During winter 2000/2001 the snow cover was thinner than during the other two winters. The snow pack structure was however quite similar between the early winters 1999/2000 and 2000/2001. In late winter the snow season of 1999/2000 stands out because of more maritime structure, and thicker layers. During the other two late winter cases the snow pack consisted of several thin layers, where rounded, refrozen and faceted grains alternated. It is worth noticing that probably the same layers have been marked as faceted or melt-freeze layers during late winter 2002 – this implies to the effect of student measurers. Variation between early and late winter was seen as a slight increase in snow depth, and during 2000/2001 also in layer amount and portion of faceted grains. This was somewhat surprising, but the increase in temperature and density were assumed.

Spatial variability within a biotype was bigger in the late winter cases. In the early winter only a small variation in snow depth was seen; also variation in structure was restricted to single layers with possibly slightly different grain form. In late winter the variation of depth, layer amount and layer thickness was bigger. Especially during 2001/2002 there were big differences observed in grain forms of some layers; as mentioned before, this may have to do with the measurers ability to distinguish different snow types.

Snow pack structure did not differ a lot between forest and field in Lammi. During early winter 2001 the snow cover in the forest had more rounded grain snow, whereas in the open field almost all of the snow cover was formed of melt-freeze snow. In the late winter cases the same tendency of quicker processes in the open field is seen during the winters 2000 and 2001: rounded grains are more easily replaced by refrozen or faceted grains in the open field. It is very difficult to say anything based on the 2002 data.

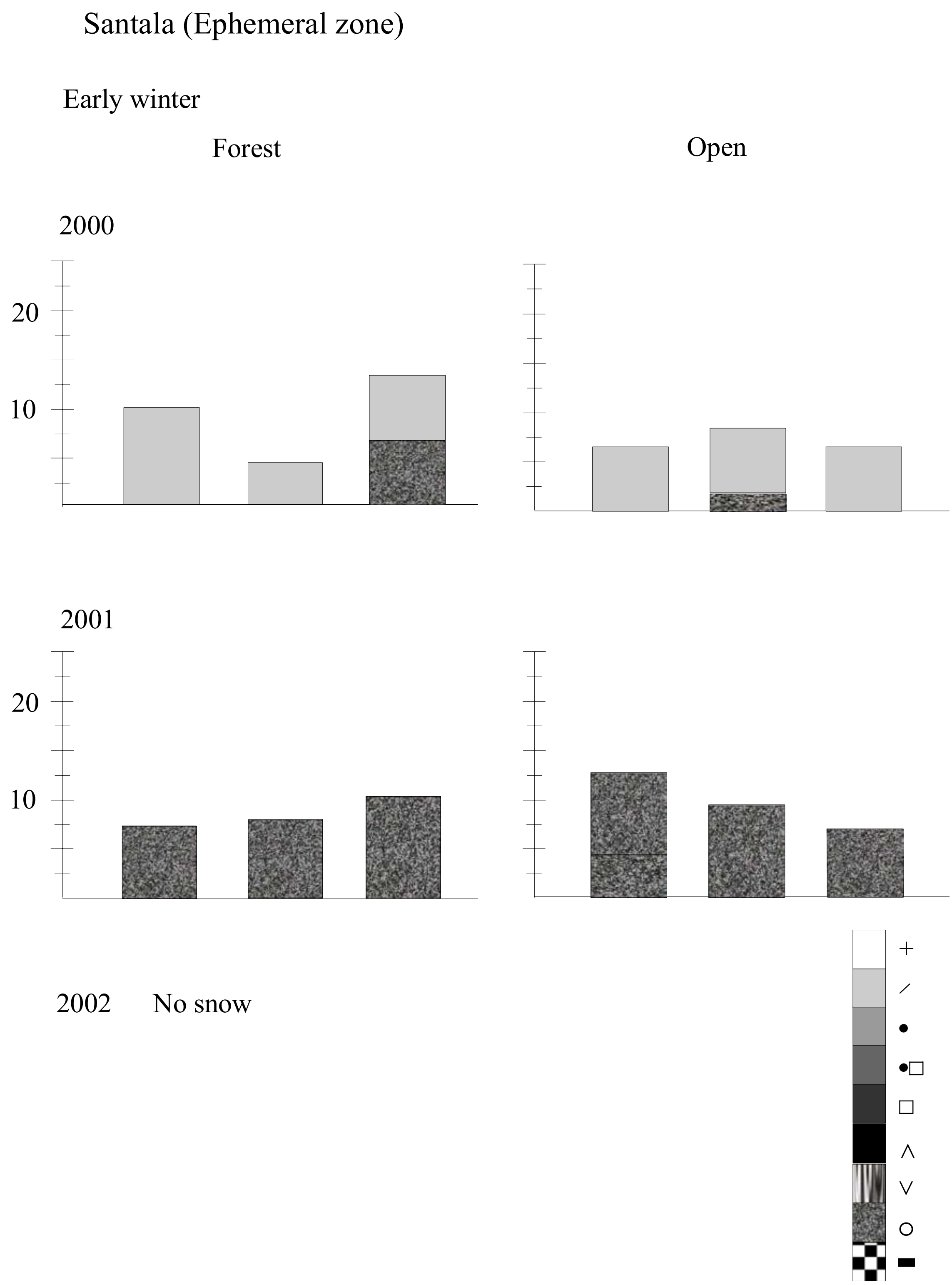

Figure 3.18. Observed snow pack structure in Santala in early winter.

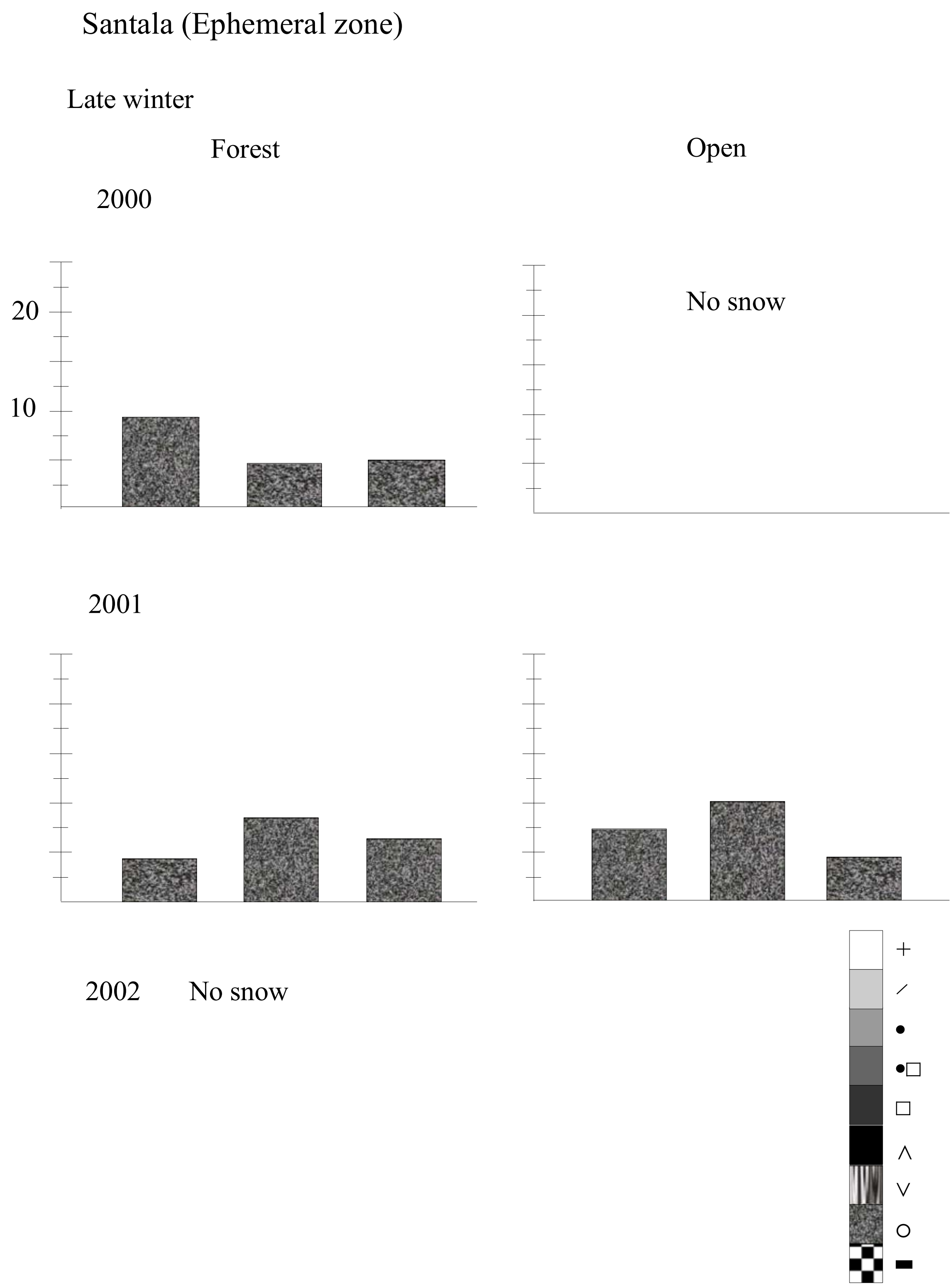

Figure 3.19. Observed snow pack structure in Santala in late winter.

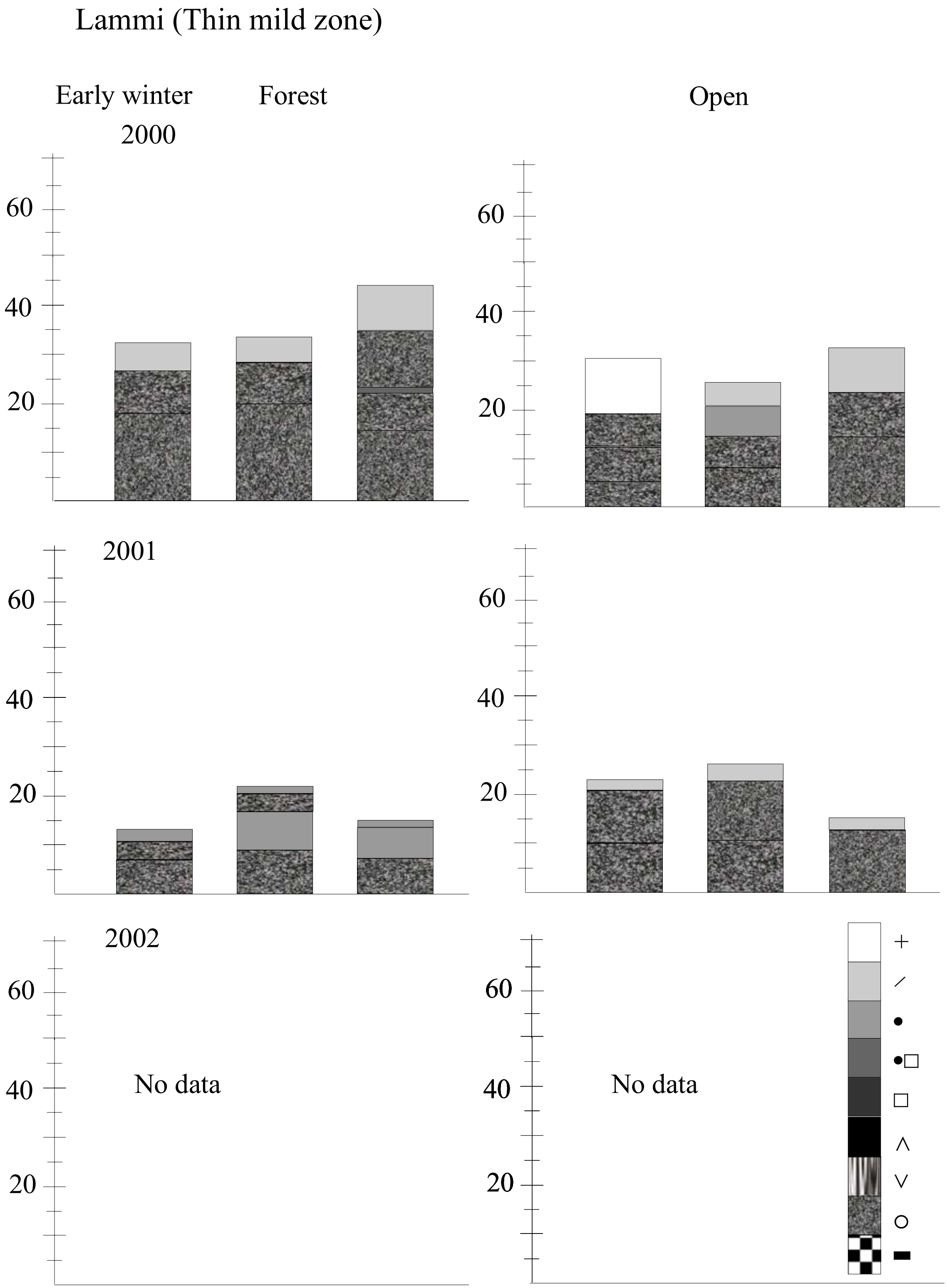

Figure 3.20. Observed snow pack structure in Lammi in early winter.

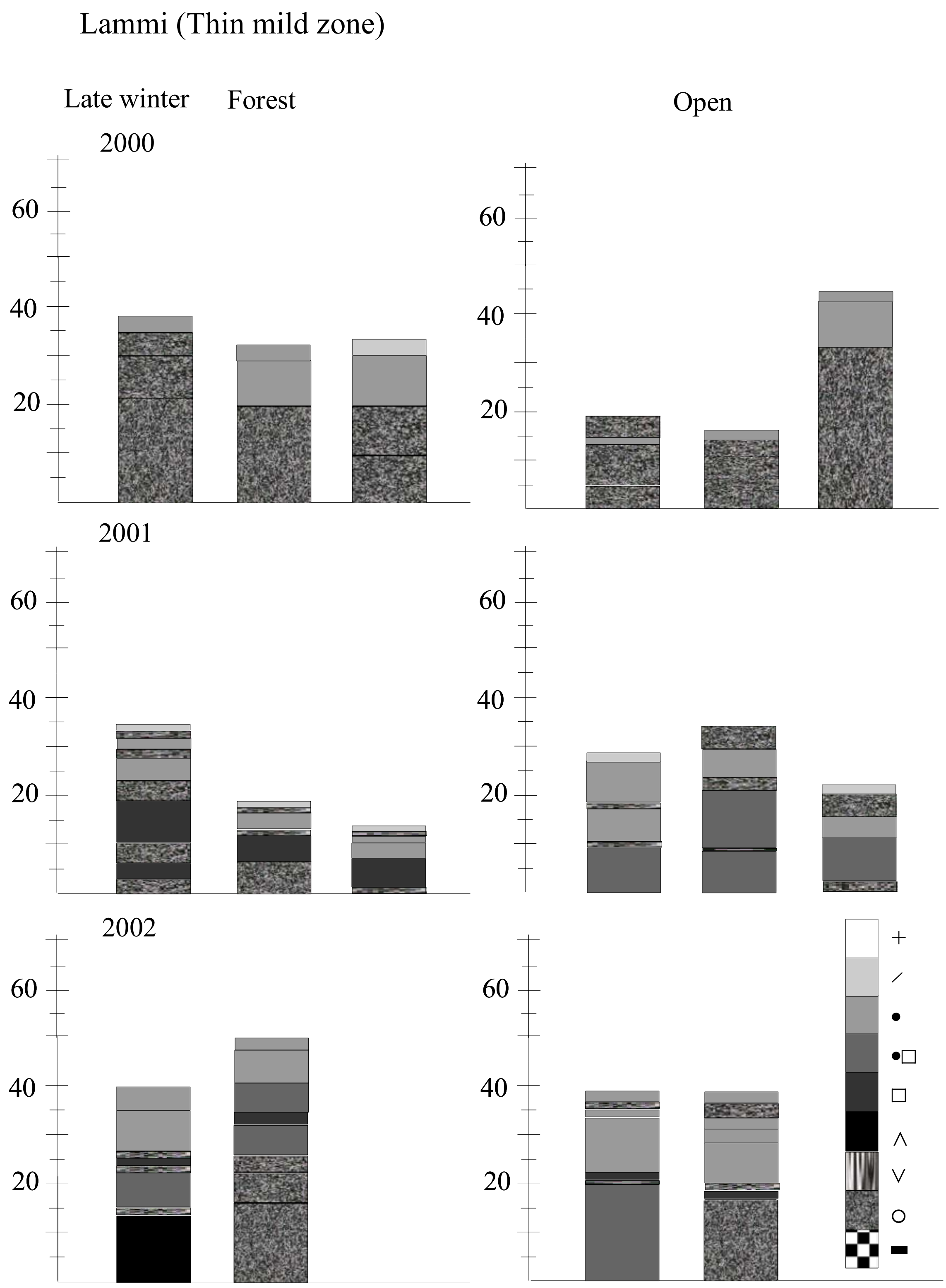

Figure 3.21. Observed snow pack structure in Lammi in late winter.

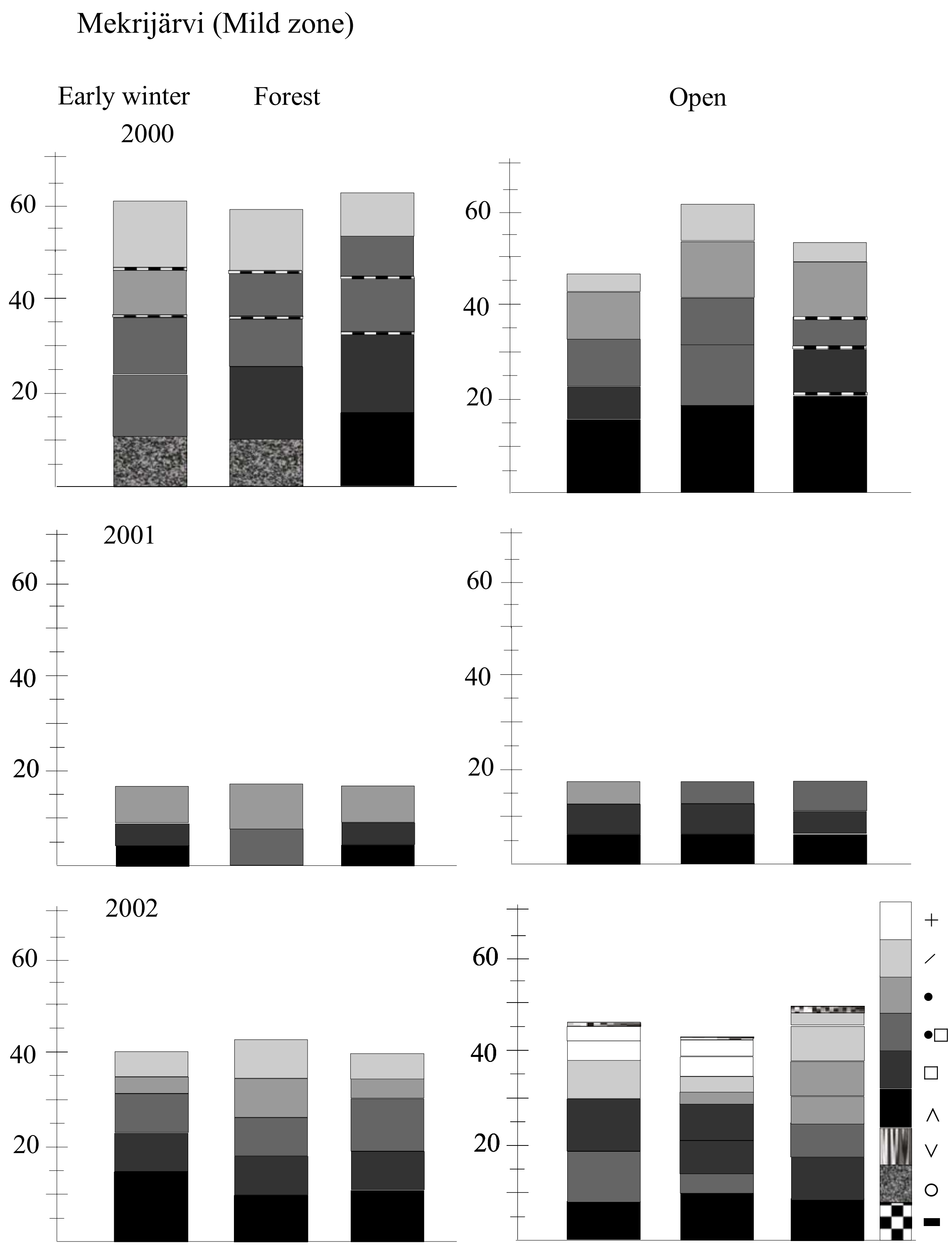

Figure 3.22. Observed snow pack structure in Mekrijärvi in early winter.

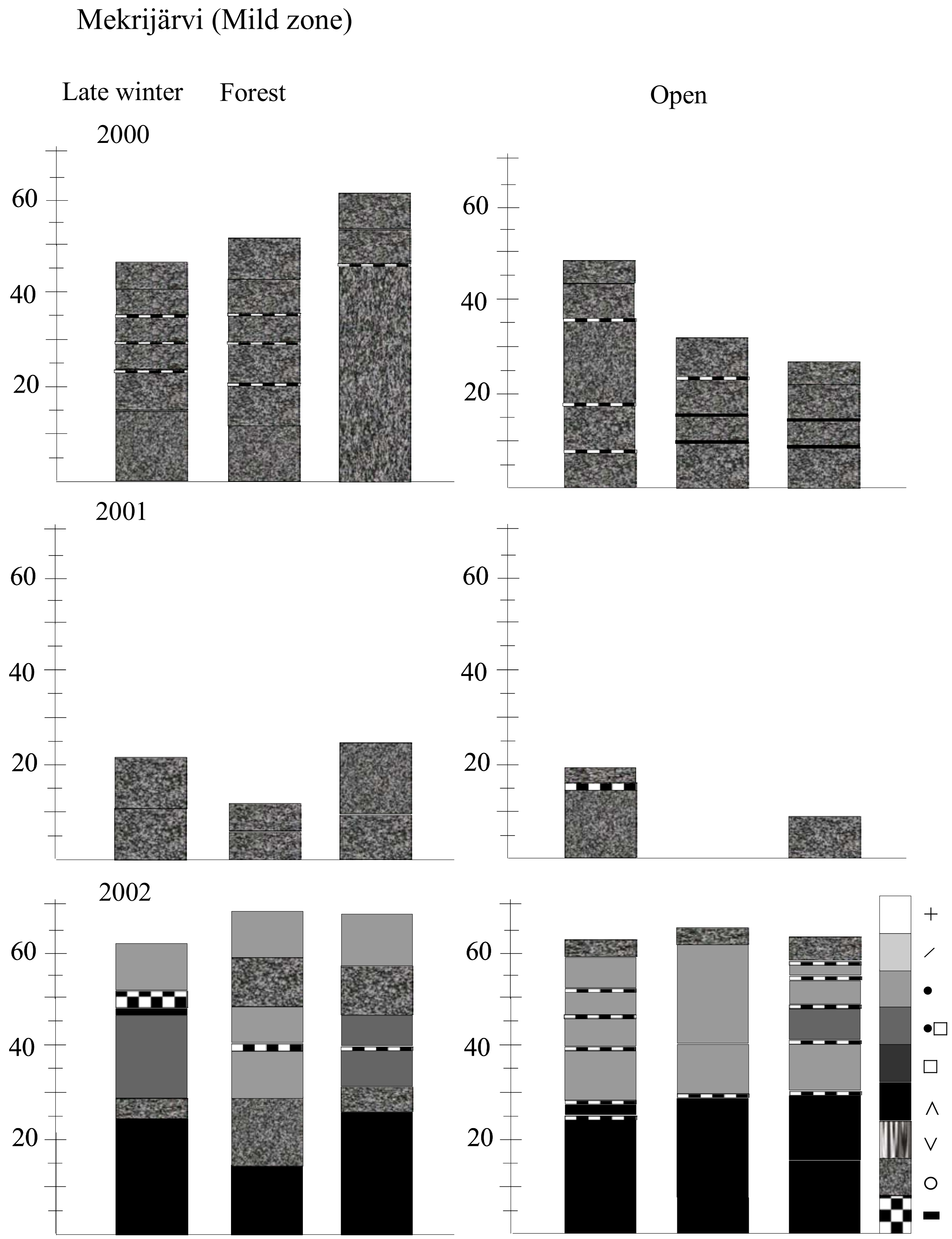

Figure 3.23. Observed snow pack structure in Mekrijärvi in late winter.

Mekrijärvi

Figures 3.22 and 3.23 show the observed snow pack structure in Mekrijärvi, maritime/mild zone.

Three main differences were found when comparing these figures to the ones from Lammi. Firstly, snow depth and the amount of snow layers was on average increasing when going away from the thin part of the maritime zone, and secondly (this can not be seen from these figures only) the duration of the snow cover was longer in Mekrijärvi. This leads to a third difference: the early winter measurements were done earlier and late winter measurements later than in Lammi. This together with the colder climate, in spite of assumed maritime zoning, is seen as rather large portions of faceted grain snow in Mekrijärvi. During the early winter melt features were rare in Mekrijärvi, which would allow situating Mekrijärvi to taiga zone. In any case ice layers also during the early winter and especially very common wet and icy snow and ice layers in late winter keep Mekrijärvi in maritime, or either in transition snow zone.

Winter 2000/2001 was peculiar because of small amounts of snow and early winter. Most melt features were observed during winter 1999/2000, and colder weather and longer spring during 2001/2002 allowed large amounts of faceted snow to remain also during late winter. The change in snow pack structure between early and late winter was quite remarkable during all of the winters: rather cold and porous snow cover turned into a truly maritime, warm and dense (density very close to maritime zone average) snow cover. Snow depth equalled or exceeded the one in early winter.

Spatial variability within a biotype was small, especially in early winter. Some layers had slightly different grain forms or thicknesses, some layer incontinuity was seen, and the ice layers might be absent in some places. During the late winter the variability of snow depth increased; this was clearly seen during early spring 2001, when part of the snow cover was already melted in the open field, and varying amounts of layers were observed together with snowless patches. Variability of layer amount, thickness and grain type seemed also to increase towards late winter.

Spatial variability between the biotypes was bigger than the one inside the biotypes. In early winter more melt features were seen in the forest than in the open field. More faceted snow was found in the open field than in the forest. This implies to colder local climate in the open area. In the late winter the snow depth was observed to be smaller in the open area because of more efficient melting. During springs 2000 and 2001 it was difficult to say anything about structure variation because of advanced melting. During spring 2002, however, thicker melt-freeze layers were observed in the forest compared to open field. In the field melt features consisted of common ice lenses and surface crust, which were missing in the forest. This was probably due to the more efficient surface melting in the open areas.

Oulanka

Figures 3.24 and 3.25 show observed snow pack structure in Oulanka, which is assumed to lay on taiga snow zone.

Measurements during late winter were a bit problematic, because during every spring the measurements were conducted too late; even if the earlier snow type was recognisable in the layers, the snow cover was wet and melting had started. Thus all layers fell into the category of melt-freeze snow. This leaves only early winter profiles to be studied. Looking at these profiles it is clear that Oulanka really belongs to taiga zone. During every research winter the snow cover was relatively cold, thin to moderately deep, and had low density. Most of the snow cover was formed of faceted snow or new snow, also some rounded snow was present. No melt features were observed during early winter.

Winters studied were quite similar together. The main differences were seen in snow depth in early winter; especially open area snow depths were quite constant during all the late winter cases. The snow pack was formed of recent snow, rounded grain snow, mixed layers and faceted snow. The efficiency of the faceting, which determines the height of the layer consisting of faceted crystals depends on the winter weather. Rounded grain snow formed the biggest fraction of the snow cover during winter 2000/2001; smallest during 2001/2002. Differences were more difficult to see in late winter cases; during spring 2001 more melt features were observed in the open area than during the other springs. The change between early and late winter was quite similar than in the Mekrijärvi case; the wet and melting snow was very maritime. In any case the density of the snow cover was lower than in Mekrijärvi, and traces of winter time grain types were seen in the layers. Snow depth increased somewhat when going towards late winter and some ice layers became visible.

Spatial variability inside a biotype was small. Some layer incontinuity was observed, and small variability in grain type in some of the layers. The variation was bigger in forest than in open area; reasons for this were very homogenous conditions in small bog were open area measurements were conducted. Spatial variability between the biotypes was not very big either. Snow pack structures in the open area and in the forest were very close together, but the average snow depths could differ from each other. During spring 2001 more melt features were observed in the open area. The wetness of the snow does not show in the figures, but naturally the base of the snow cover in bog was a lot wetter than the one in the forest.

Kilpisjärvi

Because of greater snow depths in Kilpisjärvi, tundra zone, and the effort to keep the same scale in all of the snow pit figures, the observations of snow pack structure in Kilpisjärvi are divided into three figures, figures 3.26, 3.27 and 3.28. In each figure the results of one winter measurements are collected. The amount of snow pits observed was a bit more variable here than in other locations, sometimes only two snow pits were dug per biotype, sometimes four.

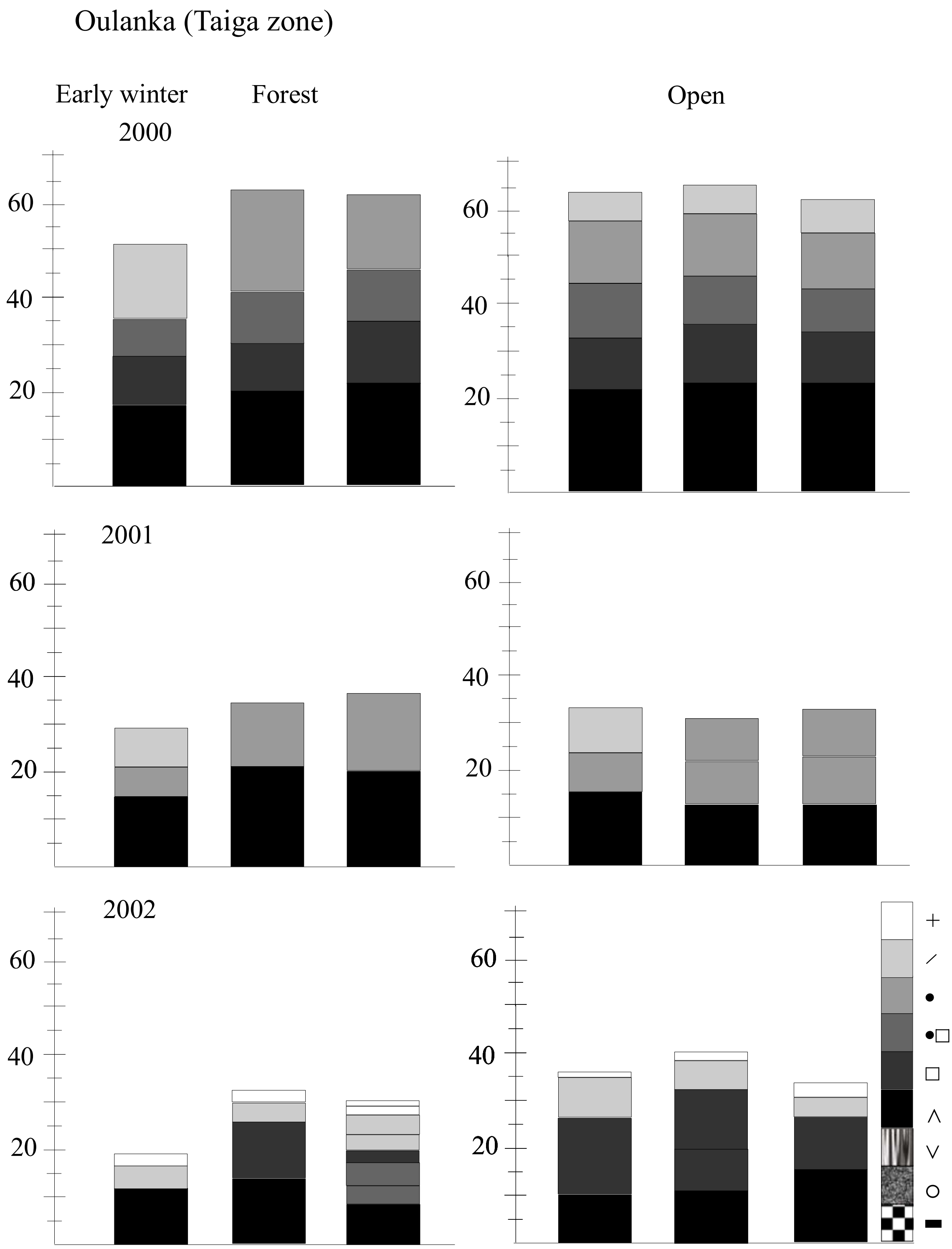

Figure 3.24. Observed snow pack structure in Oulanka in early winter.

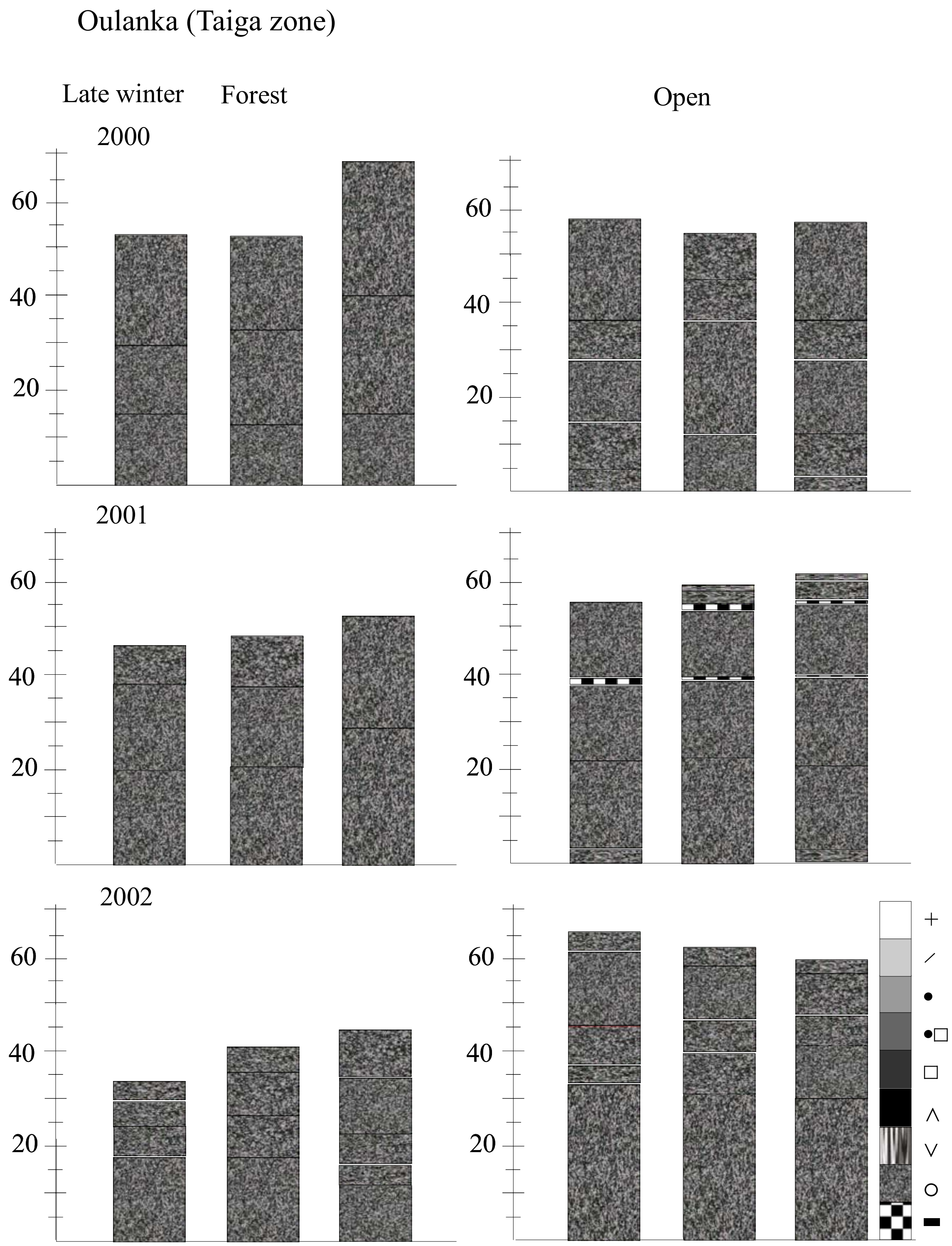

Figure 3.25. Observed snow pack structure in Oulanka in late winter.

The snow pack structure in Kilpisjärvi could be divided into two parts: the snow cover below the tree line, in sparse birch forest, differed from the one found above the tree line. Kilpisjärvi is located in tundra snow zone, but tundra snow is not found elsewhere in Finland than in open fell. The snow pack structure seen in the figures tells that the snow below the tree line is more taiga snow, and also its density and depth make it fall into this category. The snow cover above the tree line is closer to real tundra snow. In any case its depth is very variable, and in many places exceeds the assumed tundra snow depth. It consists mainly of depth hoar and hard wind slabs, but also melt features were seen in fell snow even in early winter during all of the study winters. This makes Kilpisjärvi tundra snow a bit untypical, but the occurrence of melt features can be explained by weather events coming from Norway, from the direction of the Arctic Ocean, which is located not more than 50 km from Kilpisjärvi. During suitable conditions the temperature might rise rapidly by more than 20 °C and it might even rain in Kilpisjärvi in midwinter, in spite of normally very cold weather. This makes Kilpisjärvi an untypical place in Finnish Lapland altogether.

The variation of snow depth between different winters was considerable. There was plenty of snow during winter 1999/2000, and very little during 2000/2001. The winter 2001/2002 was closer to the average. The snow pack structure did not vary that much between the winters. Naturally the amount and thickness of the layers were different, but the fractions of different snow types did not vary a lot.

The snow pack structure did not change a lot between early and late winter in the forest. There was perhaps double amount of snow during the late winter, but the structure was quite similar compared to the early winter situation. Snow depth increased also in open fell, and the variation of snow depth increased greatly. During the research winters the melt features were more common during the late winter than during the early winter in the open fell.

The spatial variability was small inside the forest, both for snow depth and for snow pack structure. On the other hand the variation of depth was very pronounced in the open fell. The variation in depth reflected itself also in the snow pack structure. If the snow was shallow, the snow pack consisted mostly of faceted snow and hard wind slab; if the snow was deep there were more layers, some of the rounded grain layers softer than the wind slabs. Also melt-freeze layers were thicker and more common in deep snow covers.

Spatial variability between the biotypes was rather big. During some of the measurement periods the average snow depth in the forest was close to the one in the open fell, but many times the snow pits in the open fell were much deeper than in the forest. This is also due to the large variability inside the fell biotype and relative homogeneity of the forest conditions. As said earlier, forest snow was more like taiga snow with porous new and rounded snow and faceted snow, whereas the fell snow was tundra snow with wind slabs and faceted snow. There were also more melt features seen in the open fell.

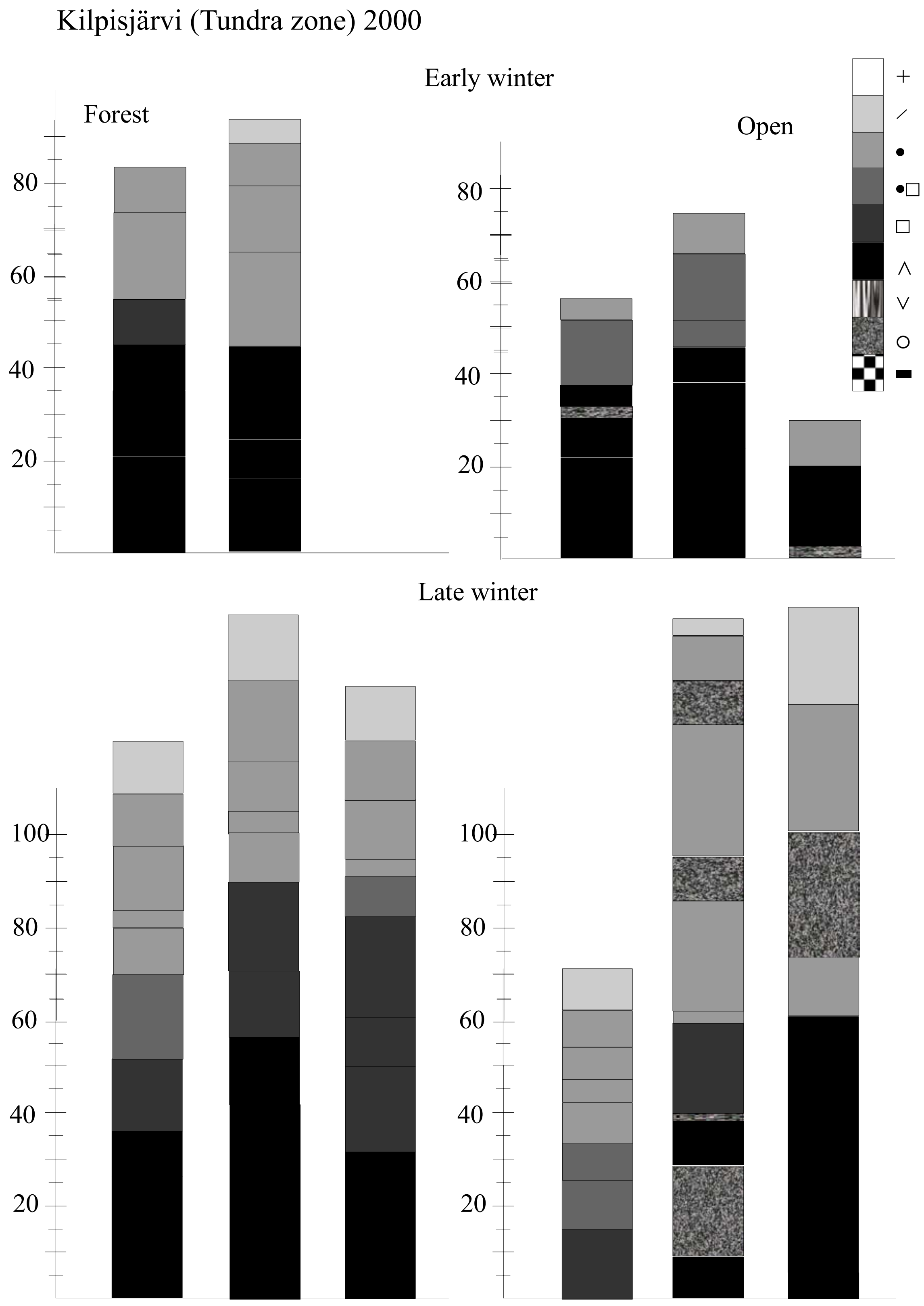

Figure 3.26. Observed snow pack structure in Kilpisjärvi during winter 1999/2000.

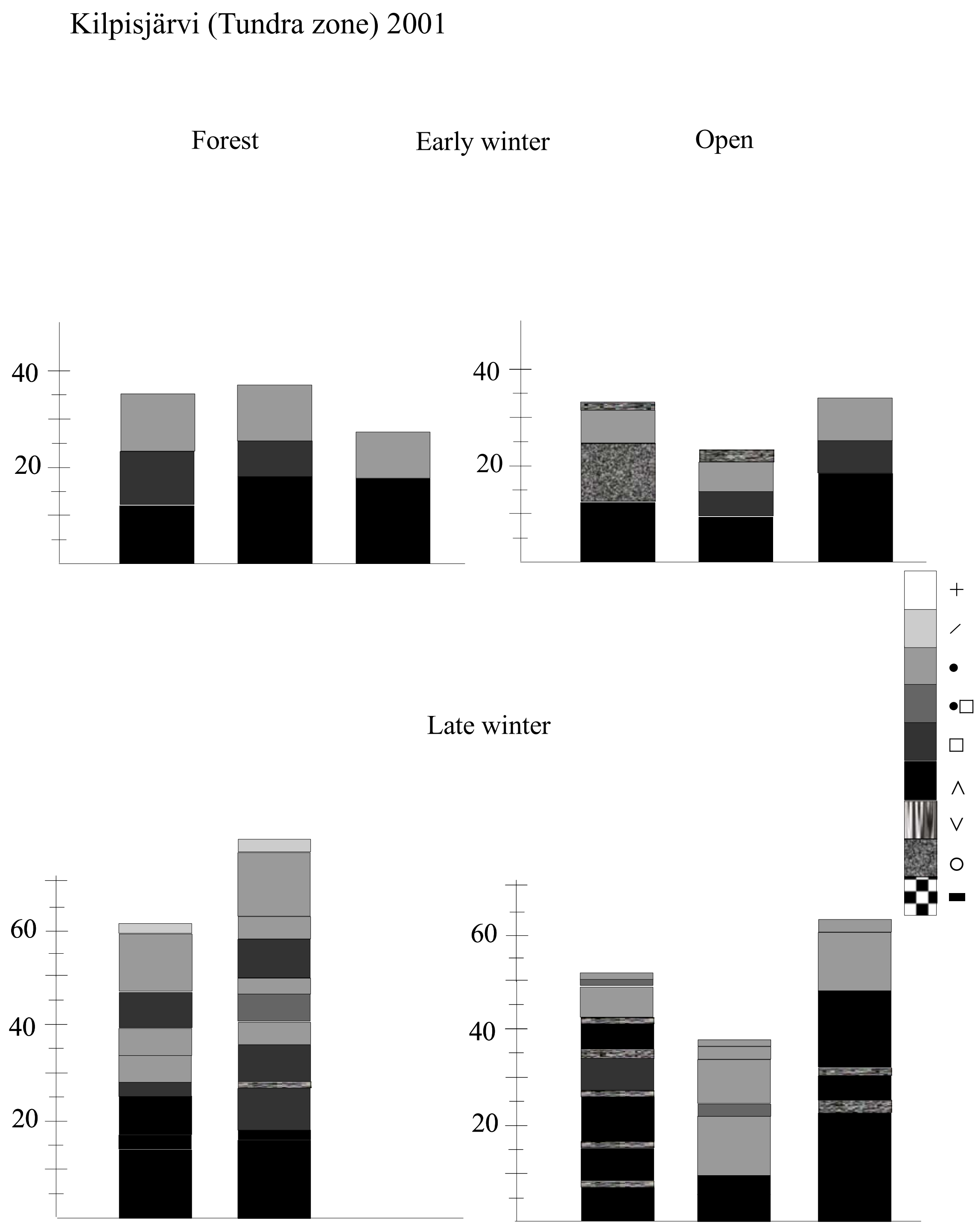

Figure 3.27. Observed snow pack structure in Kilpisjärvi during winter 2000/2001.

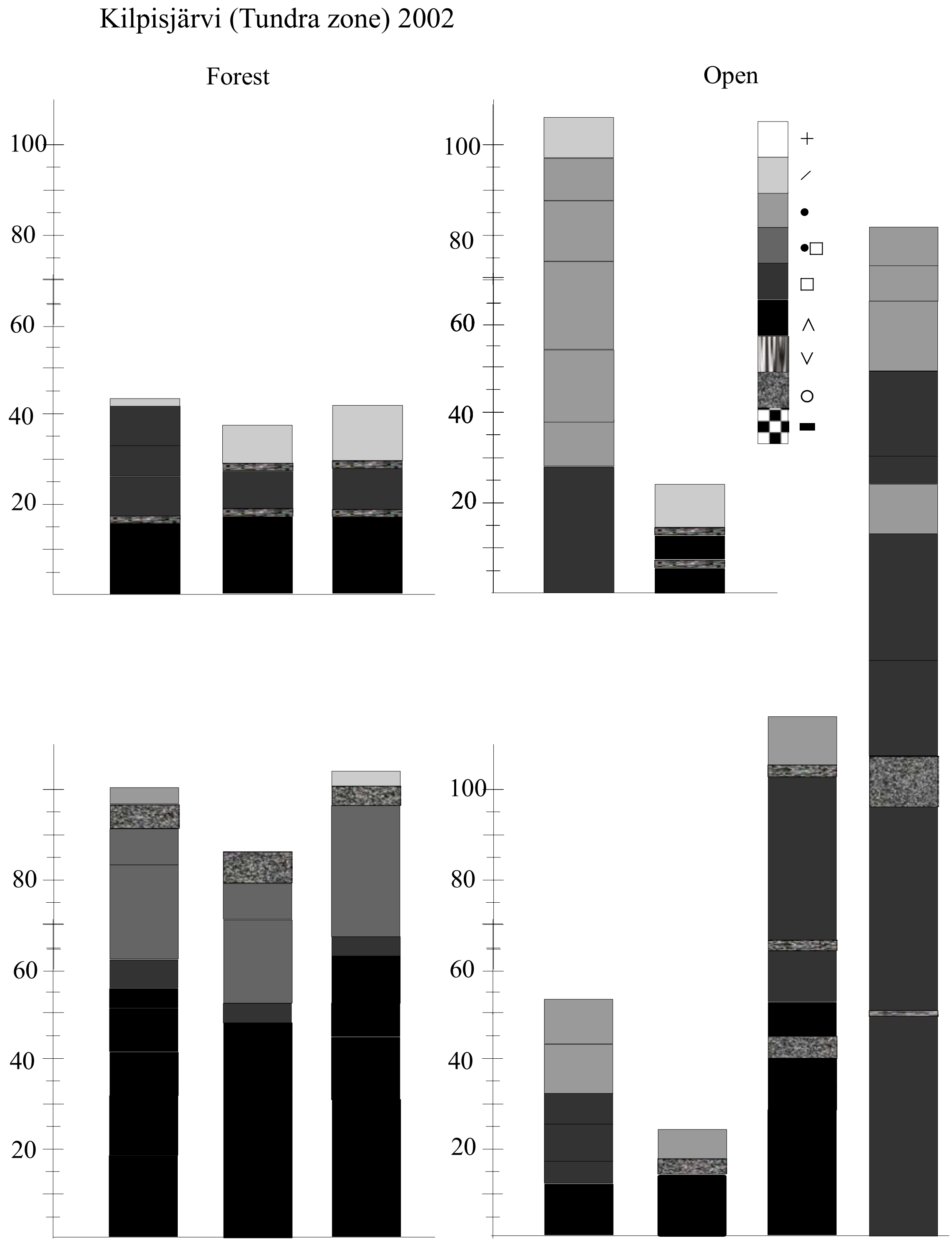

Figure 3.28. Observed snow pack structure in Kilpisjärvi during winter 2001/2002.

3.2.2. Examples of snow profiles

Density

In the graph series 3.29 the average density profiles from all locations except Santala are shown (in Santala there was normally only one layer of snow). The forest and field are treated separately, as well as early and late winter cases. The different colours represent average profiles for different winters.

In Lammi quite a large variation in the placement and shape of the density profiles is seen between the winters and also some between the biotypes. In most of the cases the surface layer density is smaller than the density of the ones below it. Most often the density ranges between 300 and 350 kgm^{-3}. More stratigraphy is seen in the late winter profiles, and the variation of density with depth is smaller.

In Mekrijärvi the variation of profile shape is smaller than in Lammi. In the early winter there is a trend of increasing density when going towards the bottom of the snow cover; not very much difference is seen between the open area and forest. During the late winter the profiles are quite homogenous in the forest, but in the open field trend of decreasing density with depth is seen. The density range is close to the one in Lammi.

In Oulanka the variation between some of the winters is remarkably large, especially in the forest. In bog most of the profiles fall together. No big differences are in any case seen between the open area and forest. Large gradients are seen in the density profiles during the early winter – density increases considerably with depth. In the spring profiles are quite homogenous. Density range is between 125 and 275 kgm^{-3} in the early winter; the range is shifted to 250 and 400 kgm^{-3} in the late winter.

In Kilpisjärvi the density profiles form tight groups with little variation in figure series 3.29. Only single layers stand out in the early winter profiles, more variation is seen in late winter. In most of the cases density is increasing with depth, but some of the late winter profiles are quite homogenous and only single layers show more or less dense snow. The densities are higher in the open fell than in the forest, and density ranges are large between soft surface snow and densely packed wind blown snow or ice lenses, varying between 100 and up to 600 kgm^{-3}.

Grain size

In the graph series 3.30 the average grain size profiles from all locations except Santala are shown (in Santala there was normally only one layer of snow). The forest and field are treated separately, as well as early and late winter cases. The different colours represent average profiles for different winters.

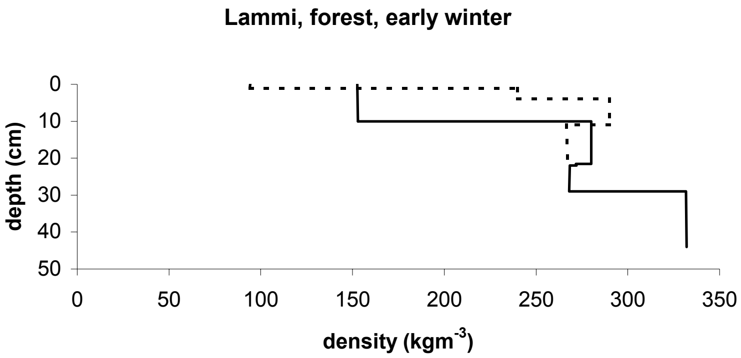

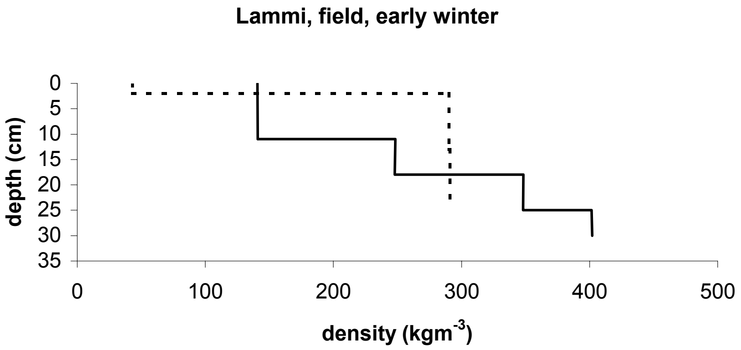

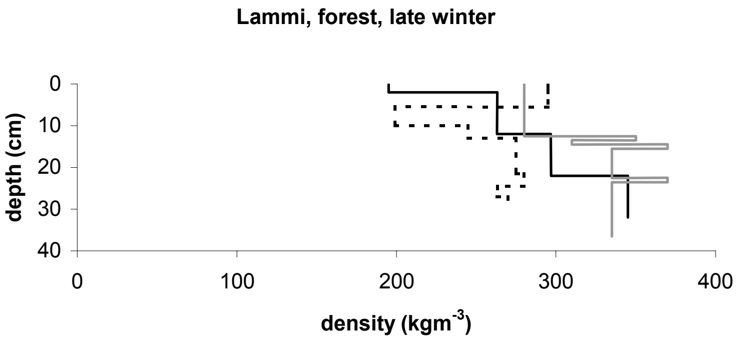

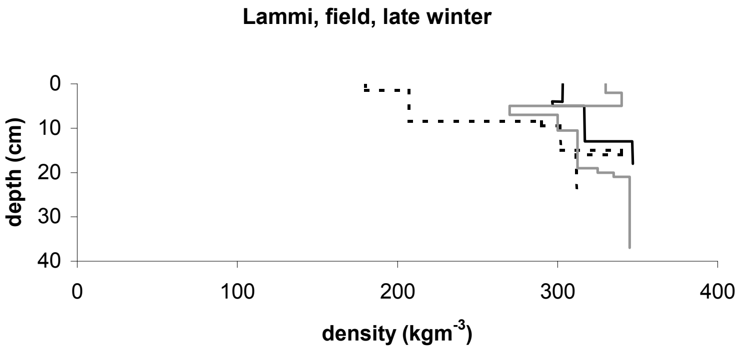

Figure series 3.29. Average density profiles during different winters. The black line refers to 1999/2000, the dotted line to 2000/2001 and the grey line to 2001/2002.

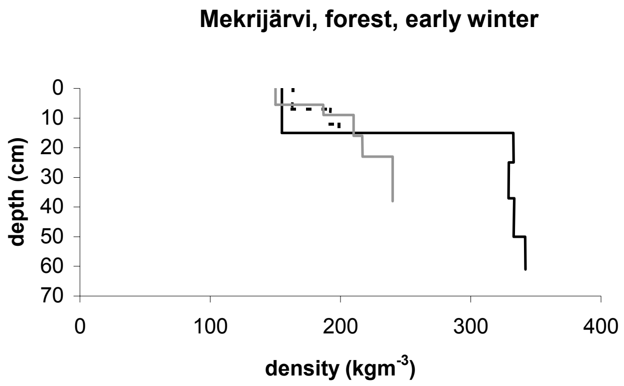

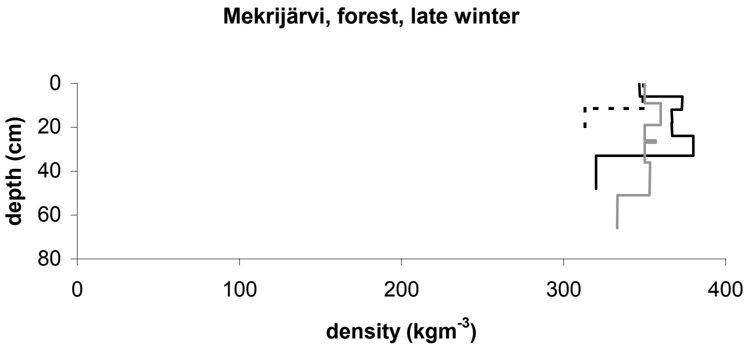

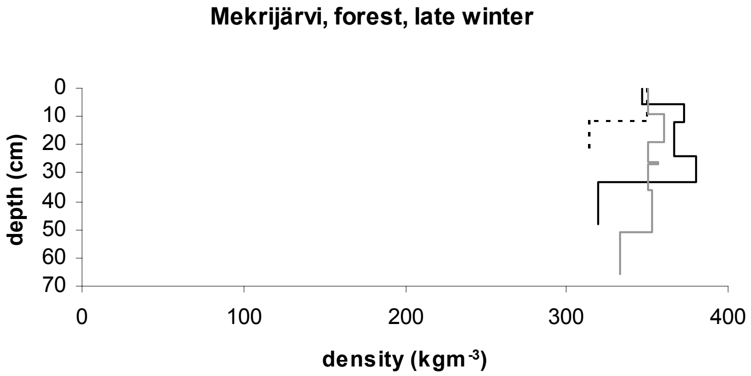

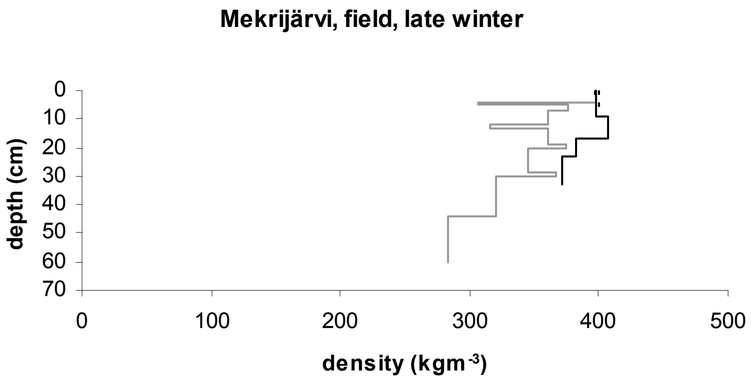

Figure series 3.29, continued. Average density profiles during different winters.

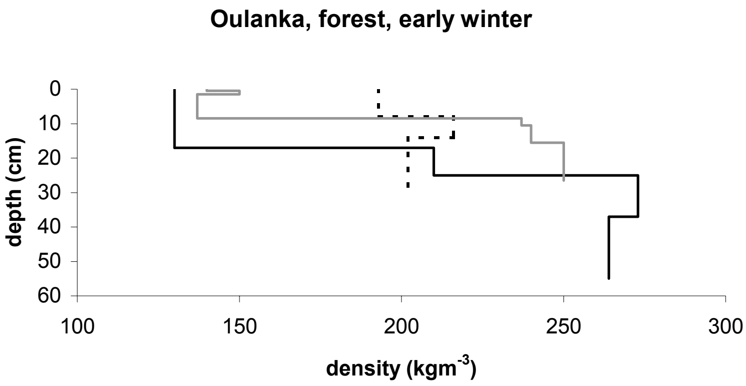

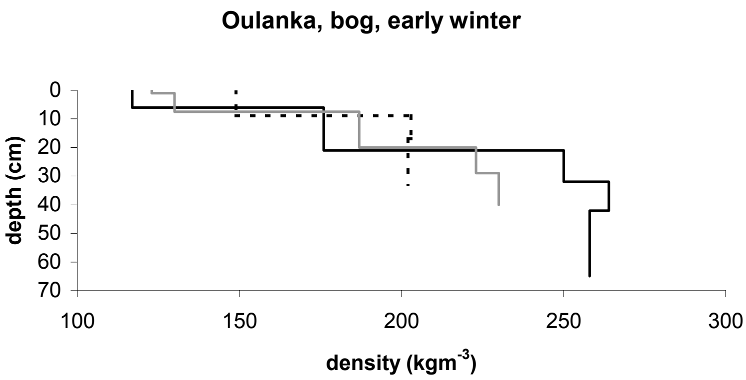

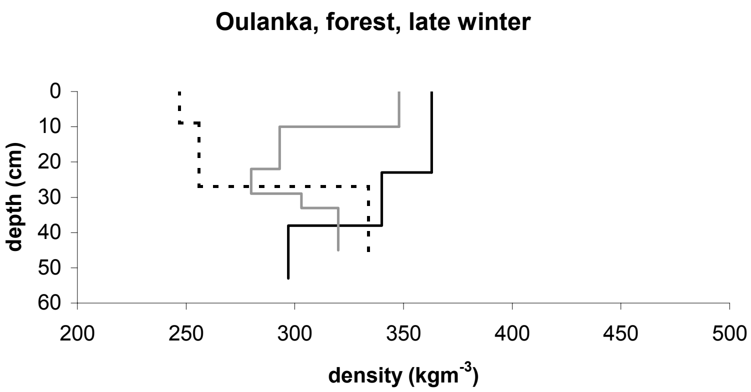

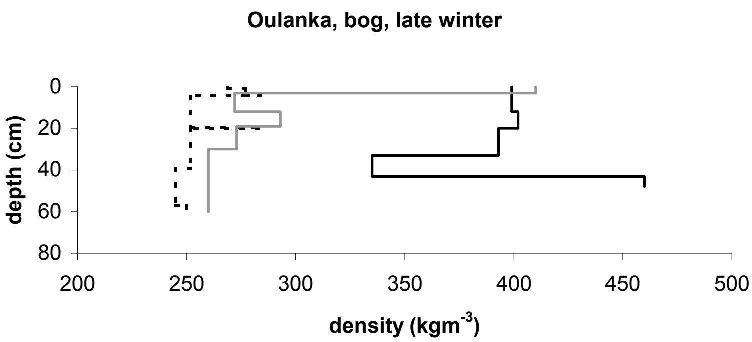

Figure series 3.29, continued. Average density profiles during different winters.

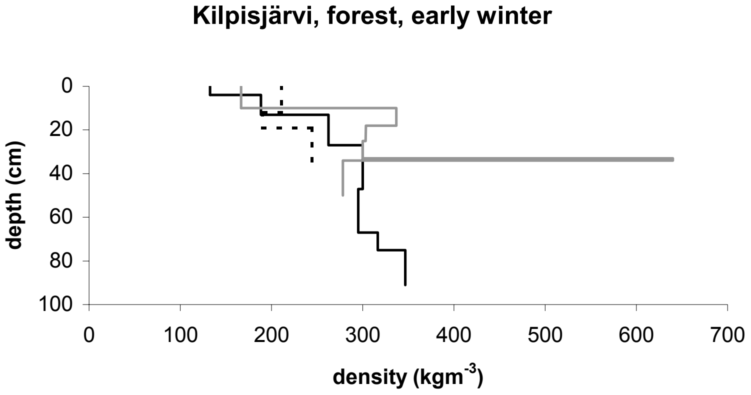

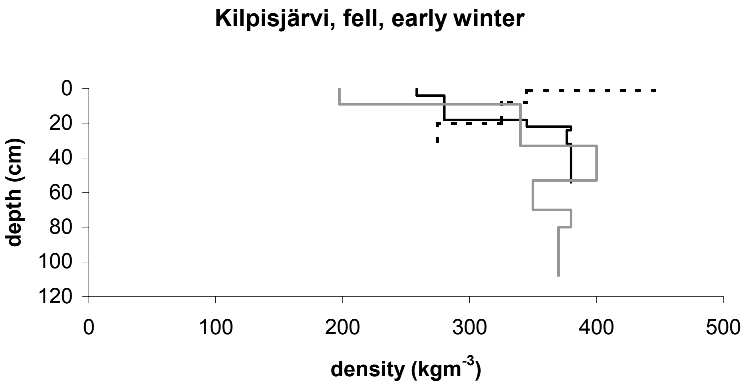

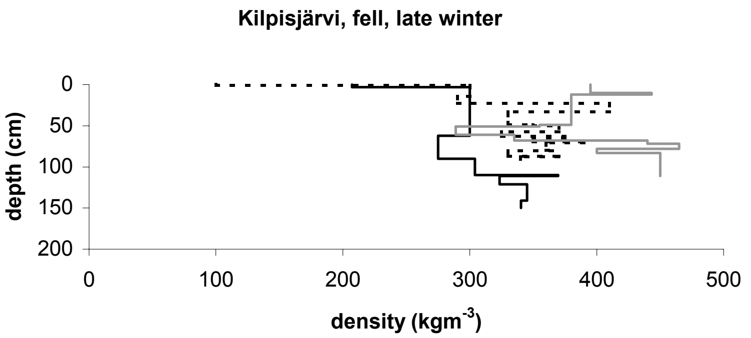

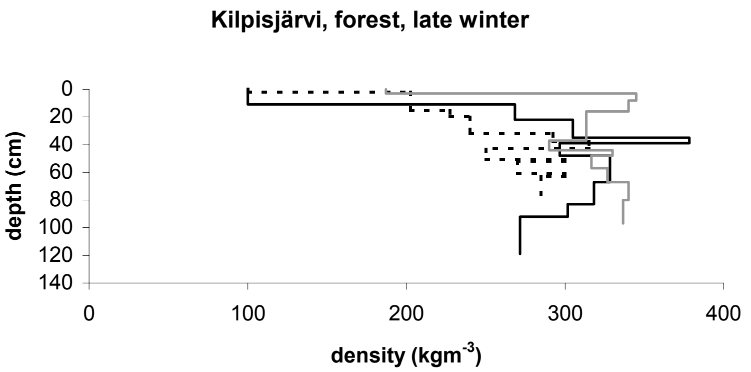

Figure series 3.29, continued. Average density profiles during different winters.

The grain size profiles in Lammi show no significant variation, except in late winter field case, where one of the profiles is totally different from the other two. Also variation between forest and field is small. Generally the grain size is increasing with depth, but during the late winter some maximas are observed near or at the snow surface, indicating melt and/or refreezing. Clear increase in grain size is seen when going towards late winter, especially near the bottom of the snow cover.

In Mekrijärvi the winter time increase in grain size is not seen. The reason for this may be that the depth hoar growth is seen already in the early winter profiles, and also that the early melting during the late winter has changed the large depth hoar crystals into somewhat smaller melt grains. Variation is quite large in the profiles observed in Mekrijärvi, variation between the biotypes is not that clear. The grain size gradually grows with depth in the early winter profiles, together with depth hoar crystals. During the spring time the profiles are more homogenous. In early winter also some surface hoar with large grain size is seen in the field.

In Oulanka the profiles look very much like the ones observed in Mekrijärvi during the early winter. No clear change is seen in grain size when going towards the late winter, also no great difference is seen between the biotypes. More variation is seen inside the forest and the bog observations separately. Every grain size profile shows increase with depth.

Rather variable grain size profiles are seen in Kilpisjärvi in figure series 3.30. Mostly the grain size is increasing with depth, but also some layers with exceptional grain sizes are seen in the middle part of the snow cover. Variation between shape and placement of some of the profiles is considerable, indicating large variation in general snow conditions in tundra zone. Variation is also quite large between the biotypes, especially during late winter. Some grain size growth is observed when going towards the late winter.

Hardness

In the graph series 3.31 examples of the hardness profiles observed during the winter 1999/2000 are shown, once again Santala left out. The forest and field are treated separately, as well as early and late winter cases. The different colours represent different observed profiles.

The variation in observed hardness profiles is small in Lammi, except in early winter forest where one of the profiles differed greatly from the others. In early winter cases the hardness increases with depth; during late winter there is a hard layer observed also on the snow surface. Variation of hardness is great with depth, ranging between almost zero and several thousands Nm^{-2}. The hardness range widens when going towards late winter. No significant difference is seen between forest and field.

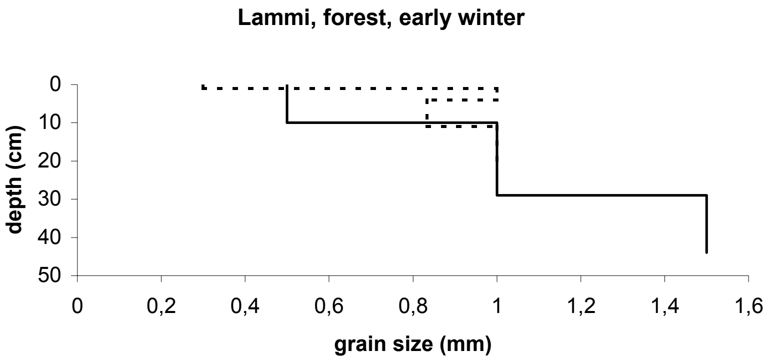

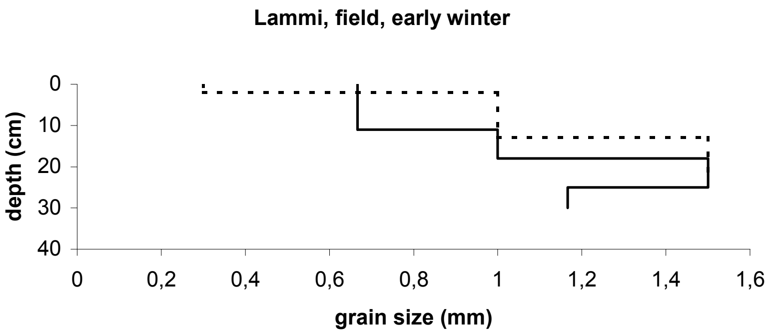

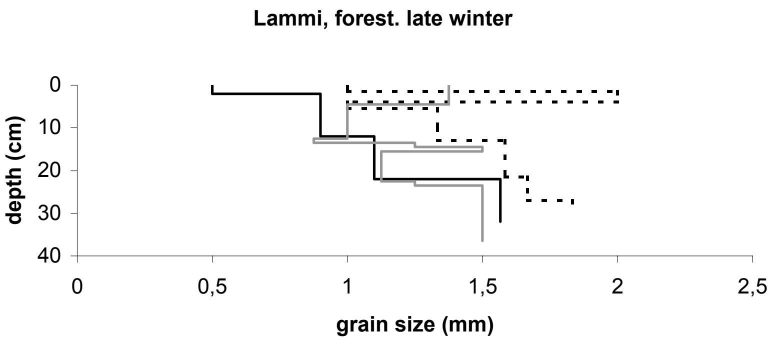

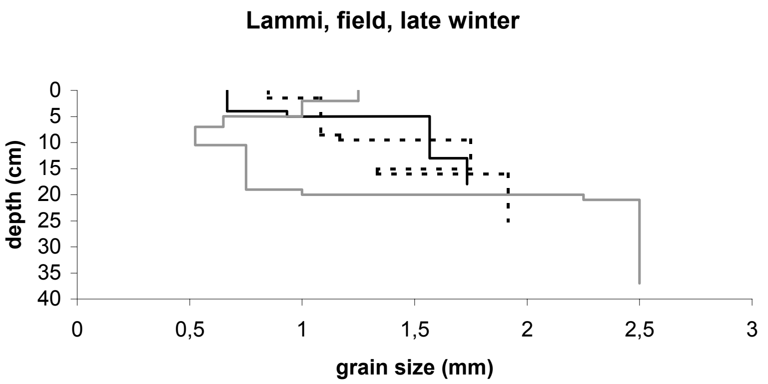

Figure series 3.30. Average grain size profiles during different winters. The black line refers to 1999/2000, the dotted line to 2000/2001 and the grey line to 2001/2002.

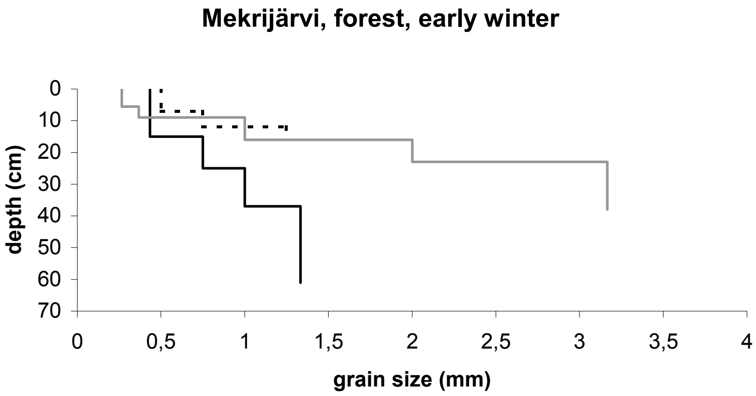

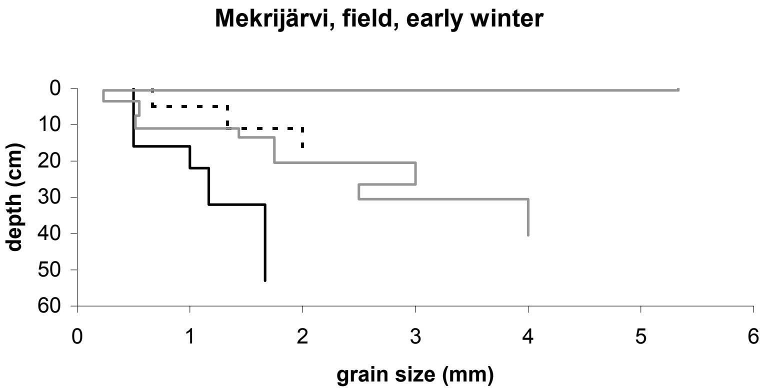

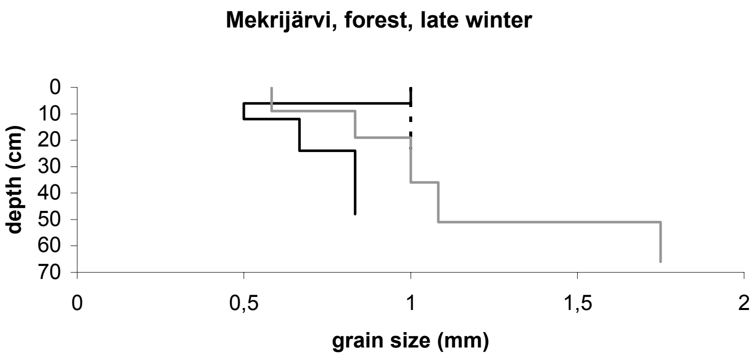

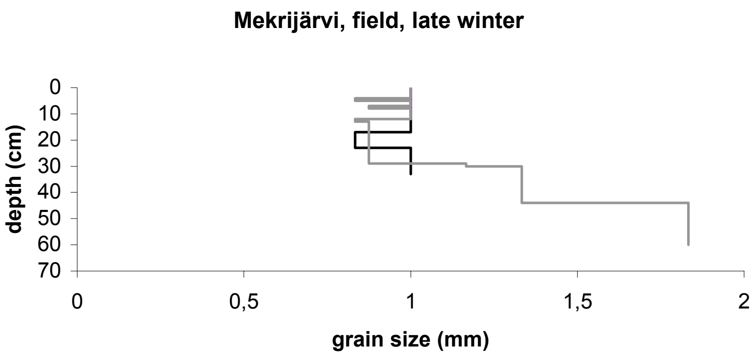

Figure series 3.30, continued. Average grain size profiles during different winters.

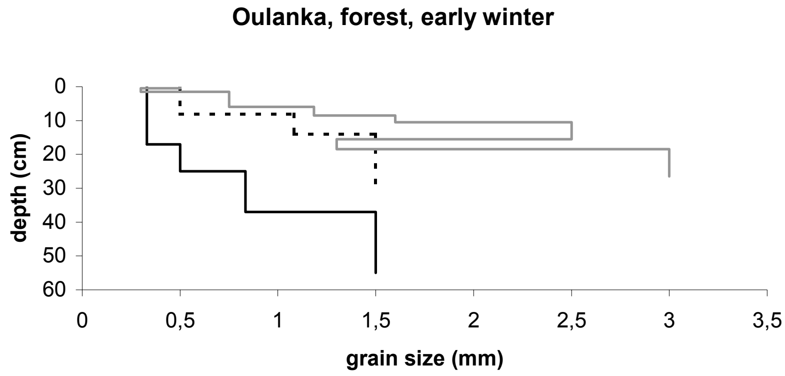

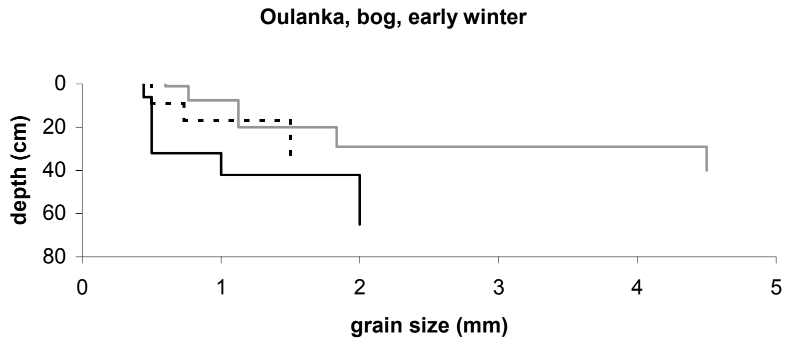

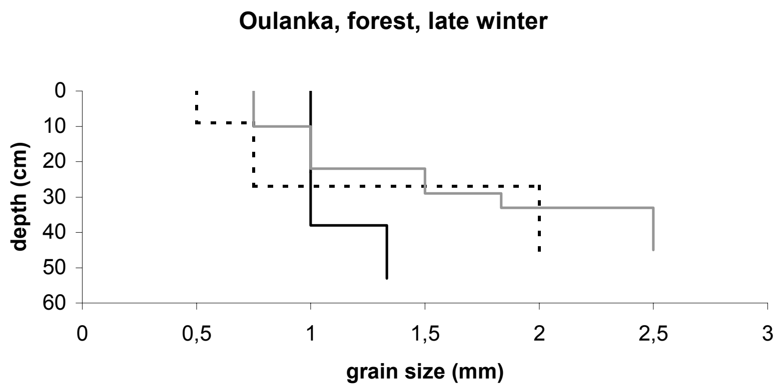

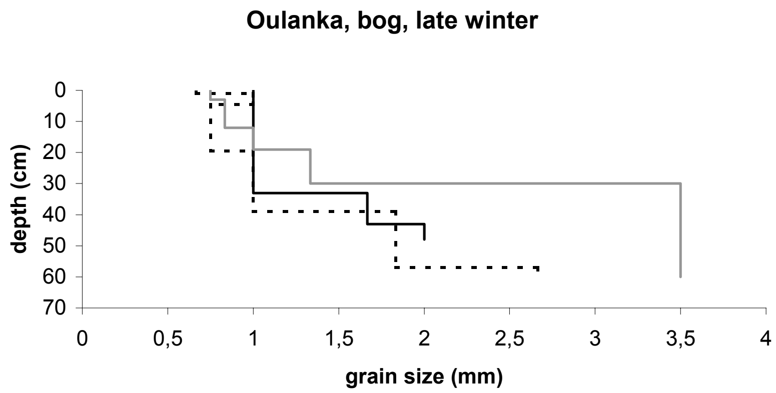

Figure series 3.30, continued. Average grain size profiles during different winters.

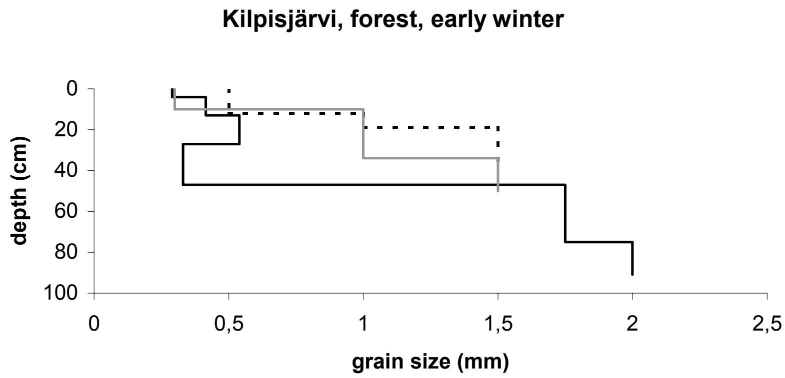

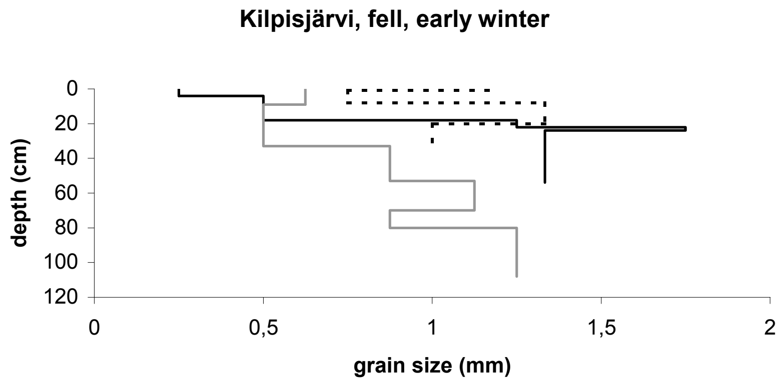

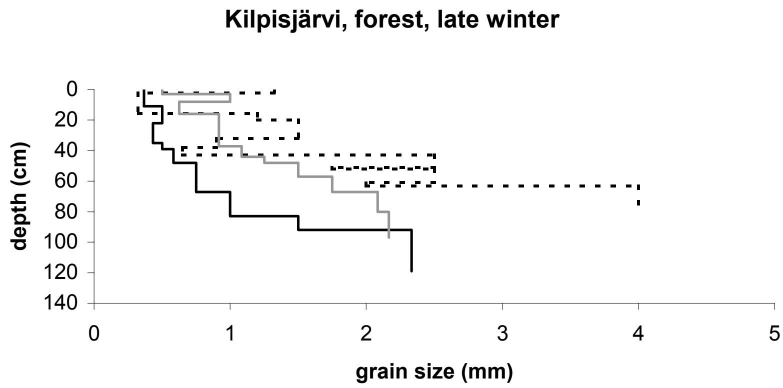

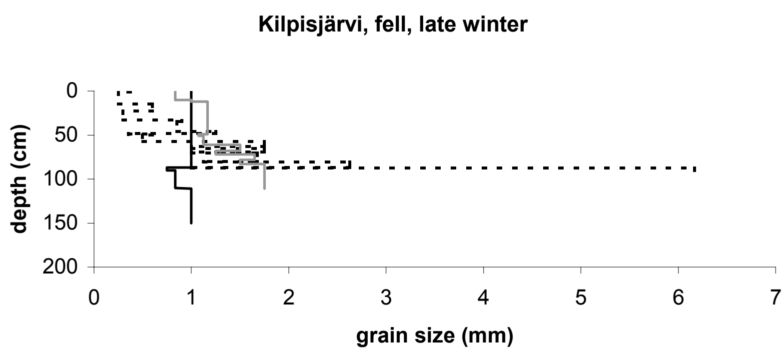

Figure series 3.30, continued. Average grain size profiles during different winters.

More stratigraphy is seen in Mekrijärvi hardness profiles when comparing to the Lammi ones. There is little variation in early winter profiles, but the variation increases when going towards late winter. In any case, the hardness range is relatively small here, between near zero and several hundreds of Nm^{-2}. Only in early winter forest the range is wider because of some icy layers. This is also the only occasion, when there is large difference between forest and field cases. In Mekrijärvi hardness is increasing with depth, although especially in late winter some layers stand out as significantly harder than the neighbouring ones.

In Oulanka the observed hardness range is between near zero and 100 Nm^{-2} in early winter and near zero and between 300 Nm^{-2} in late winter. No significant variation is seen between the profiles; in bog, one of the late winter profiles has greater hardnesses than others. Also differences between forest and bog are small, at least in early winter case: hardness increases with depth with some harder layers in the middle of the snow cover. In late winter the difference is bigger. In forest decreasing trend with depth is observed, while as the bog profiles are quite homogenous indicating wet snow cover.

In Kilpisjärvi hardnesses are generally small, but some wind slabs or icy layers may have hardnesses exceeding 8000 Nm^{-2}. These layers are not always seen in all profiles, which causes rather large variation between the profiles. Variation between the biotypes is not very large. Variation is largest in late winter fell case: different snow depths and variation between deflation surfaces and snow beds cause large variation also to hardness there. More, and harder layers are observed during the late winter.

The hardness profiles were not observed in such detail during all the winters, therefore it was chosen not to do more averaging between the winters.

<u>Temperature</u>

In the graph series 3.32 examples of the temperature profiles observed during the winter 1999/2000 are shown, once again Santala left out. The forest and field are treated separately, as well as early and late winter cases. The different colours represent different observed profiles.

In Lammi, during the early winter, the different temperature profiles from each biotope follow each other very closely. Even the forest and field profiles are close together, the field snow being a bit warmer than the forest snow. Clear temperature gradient is seen in the profiles. During the late winter the variation of profiles is much higher, partly because of many measurers. The snow is warmer than in the early winter case, but there is a colder part below the surface under which the normal temperature gradient prevails.

In Mekrijärvi forest and field profiles are very close together in both of the biotypes, but further away from each other than in Lammi. This kind of variation mainly reflects conditions during and just before the measurement times, especially when it is seen that the temperatures near the bottom of the snow cover are close together in both of the biotypes. In forest temperature gradually increases with depth; in field there is temperature minimum in the middle of the snow cover. During the late winter measurements all of the snow pack was in melting temperature and no variation was seen between the biotypes.

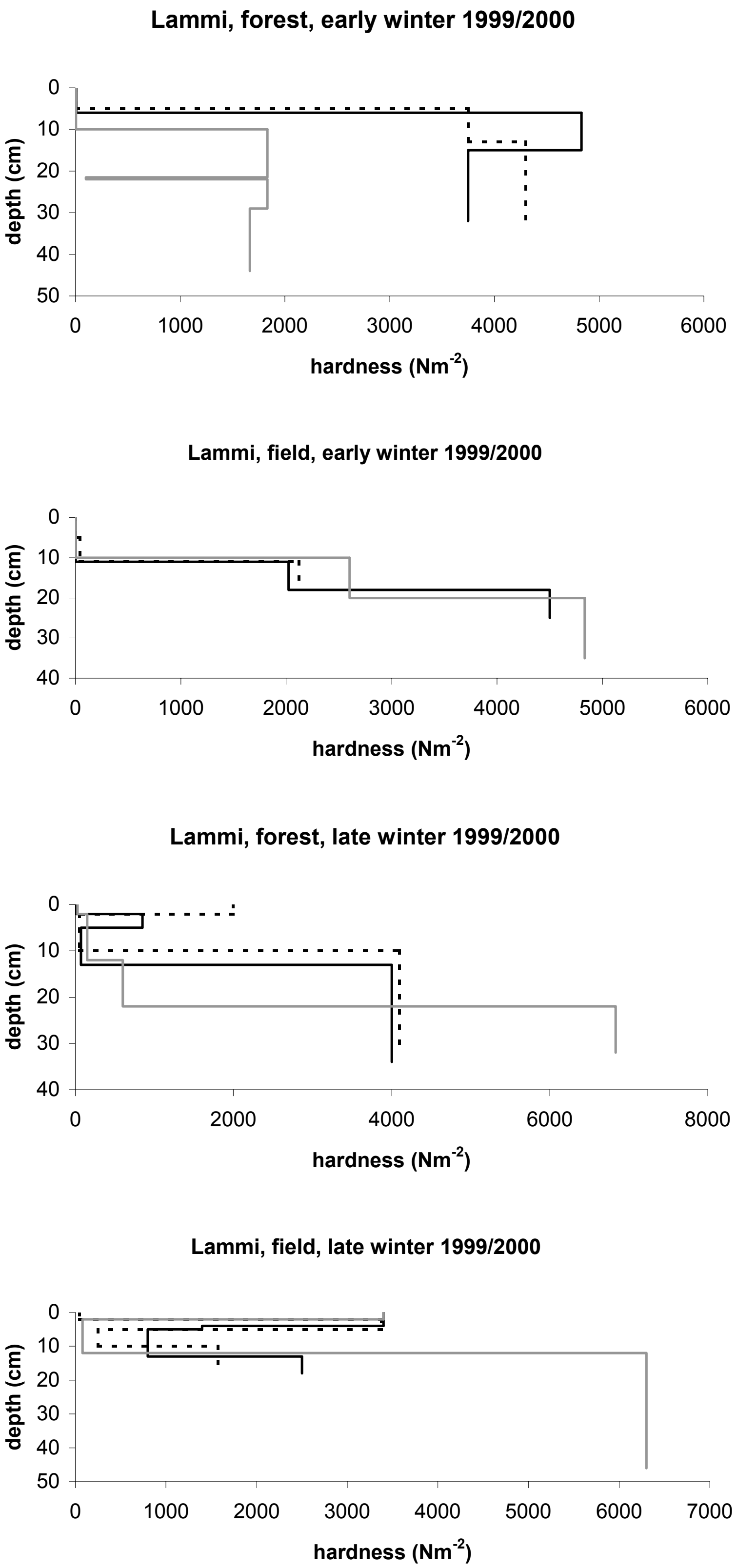

Figure series 3.31. Examples of the hardness profiles observed during the 1999/2000 winter. Different shading refers to different observed profiles.

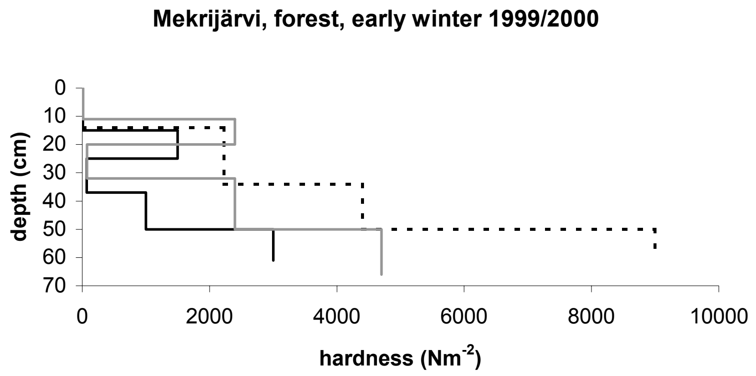

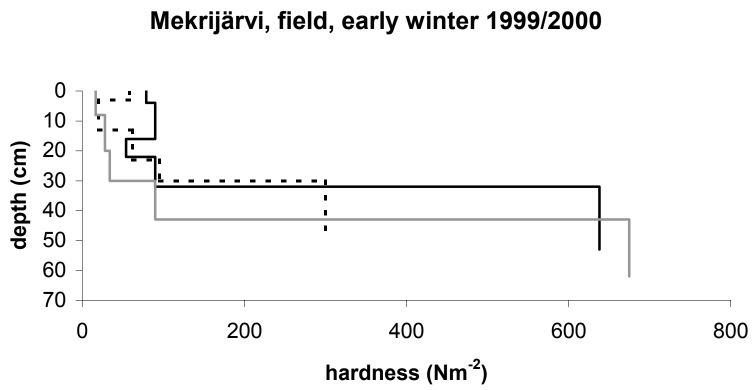

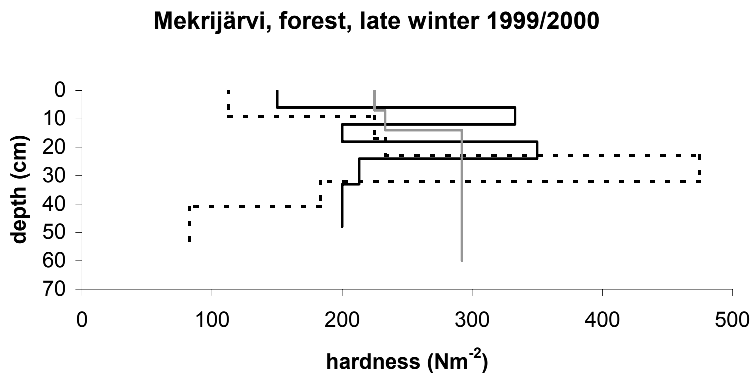

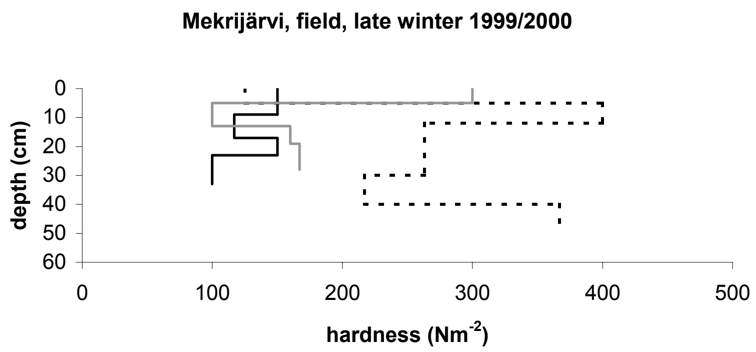

Figure series 3.31, continued. Examples of the hardness profiles observed during the 1999/2000 winter.

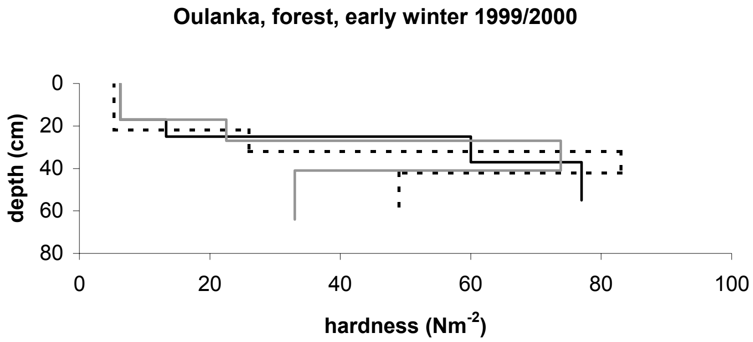

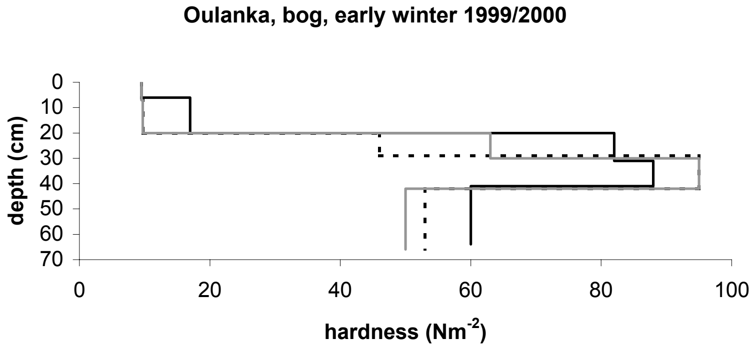

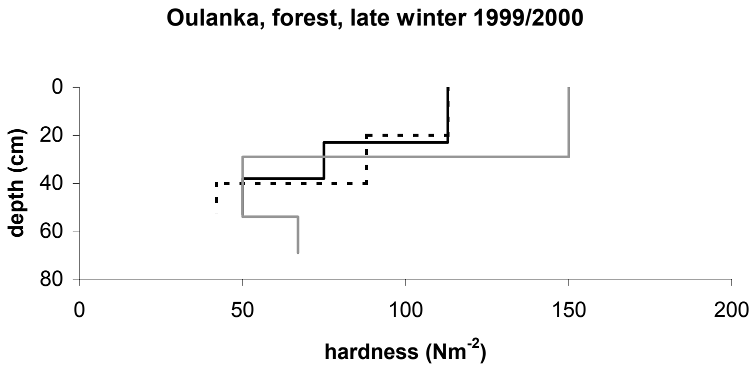

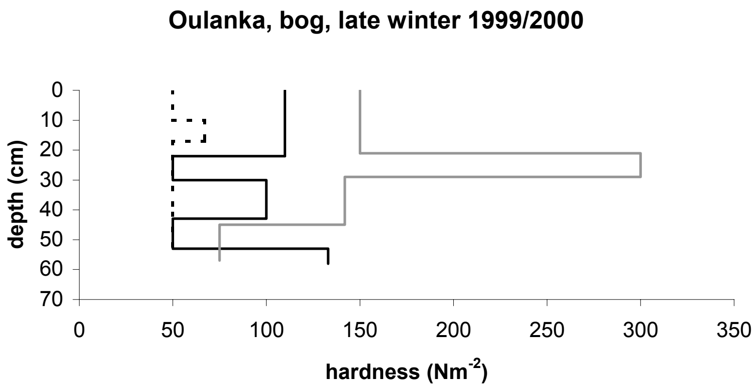

Figure series 3.31, continued. Examples of the hardness profiles observed during the 1999/2000 winter.

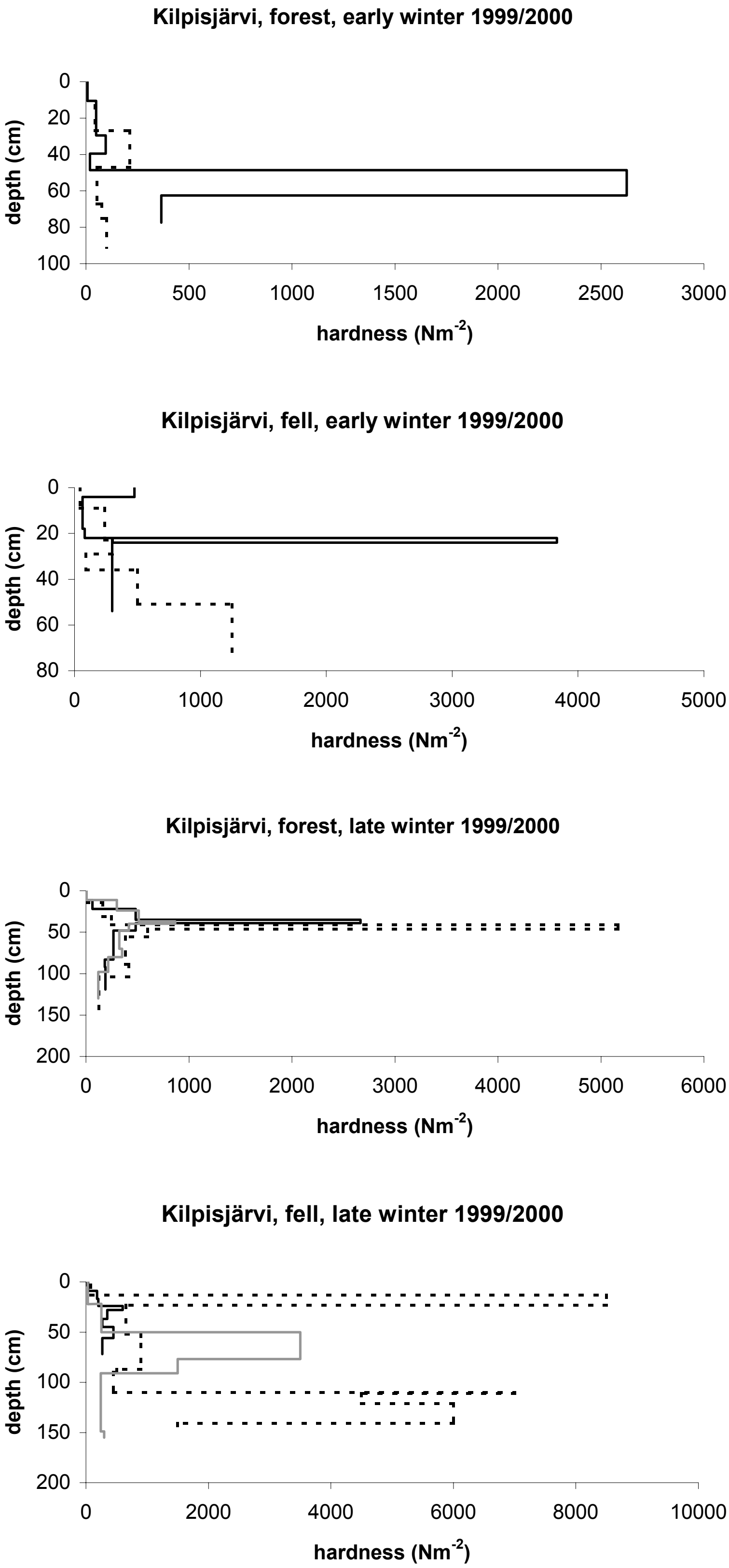

Figure series 3.31, continued. Examples of the hardness profiles observed during the 1999/2000 winter.

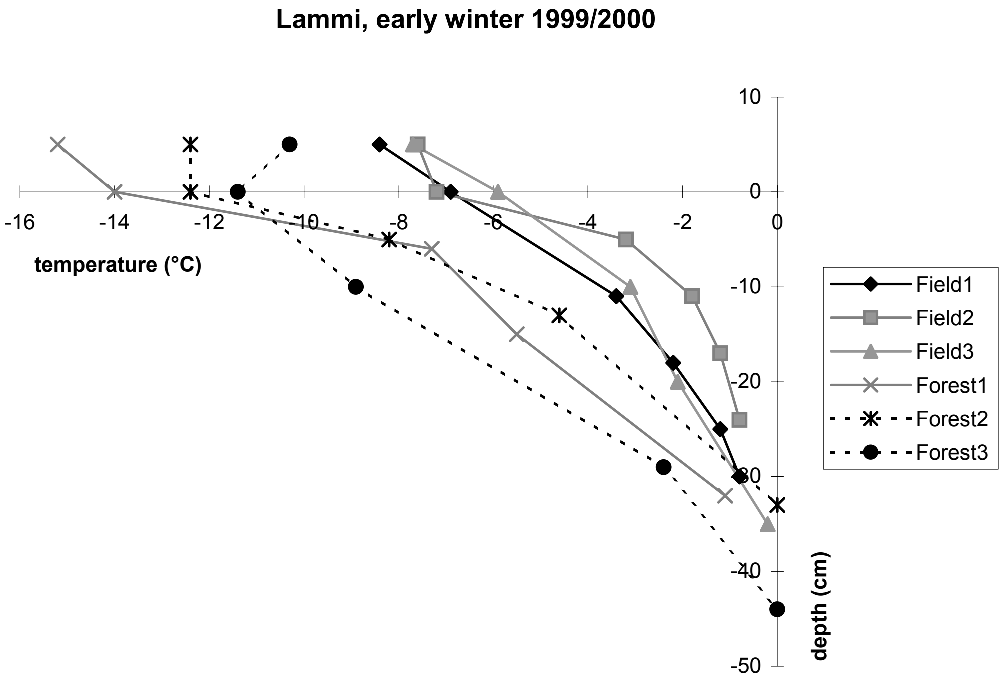

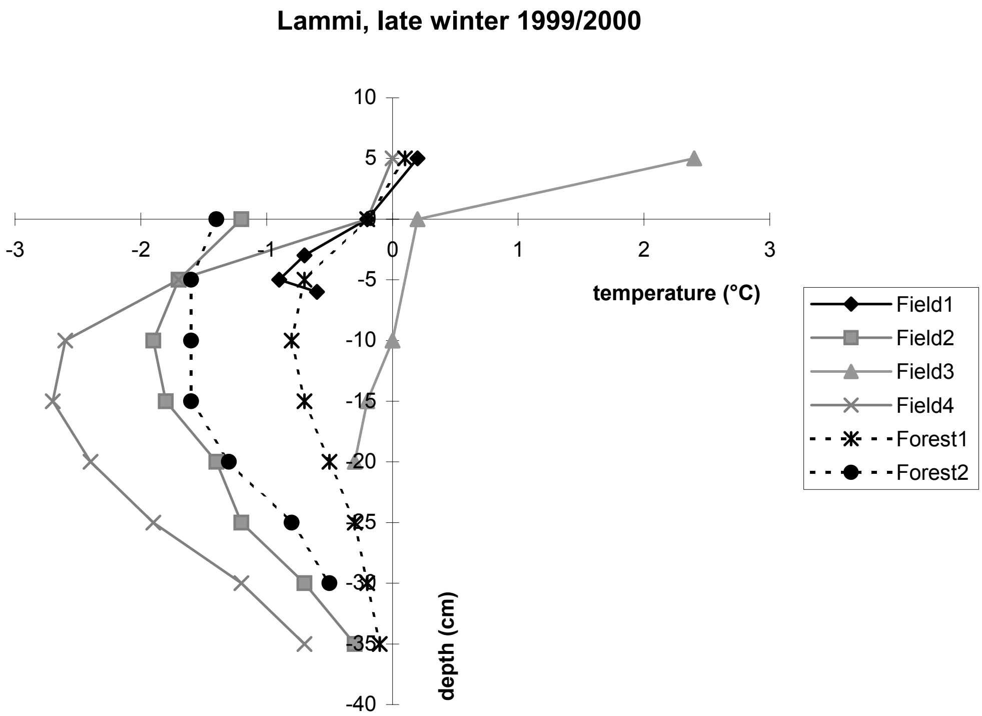

Figure series 3.32. Examples of the temperature profiles observed during the 1999/2000 winter.

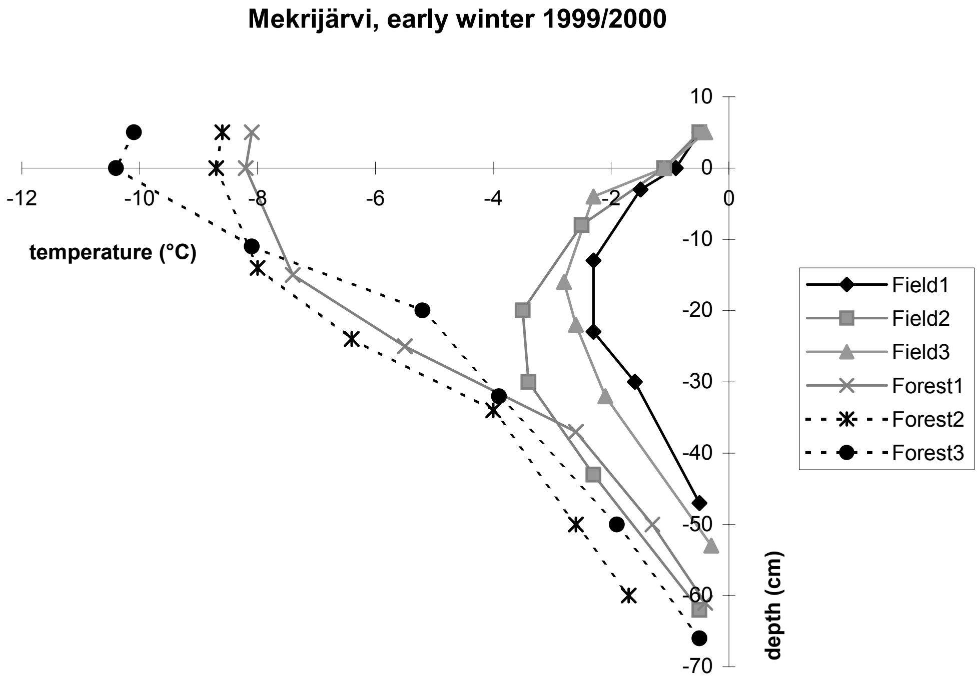

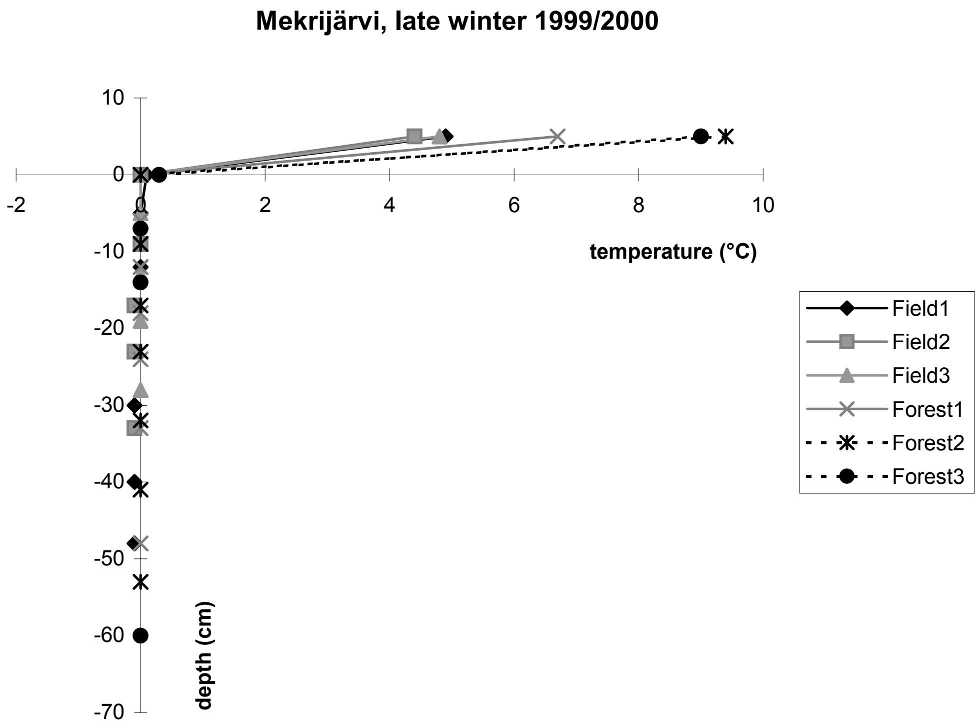

Figure series 3.32, continued. Examples of the temperature profiles observed during the 1999/2000 winter.

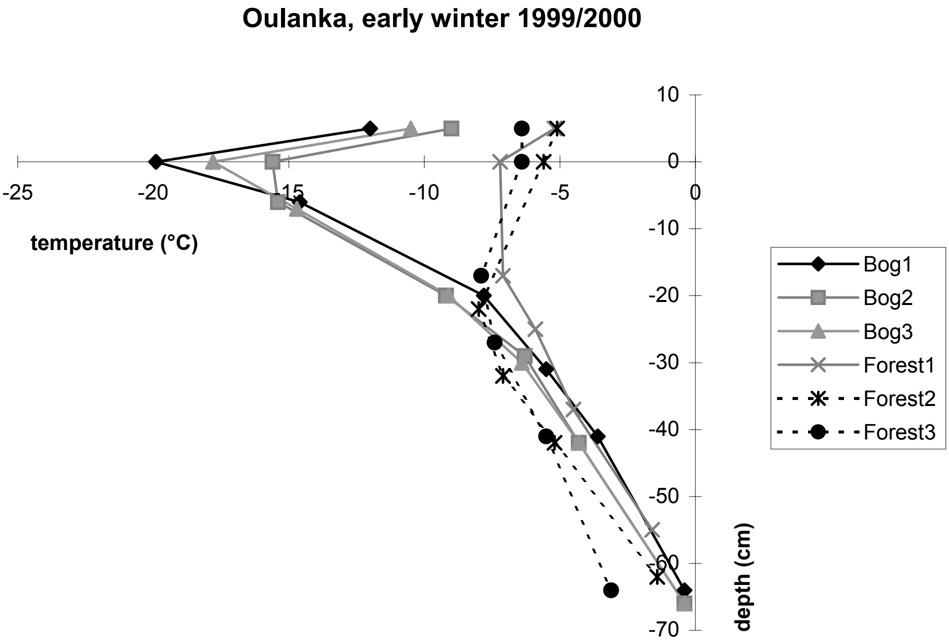

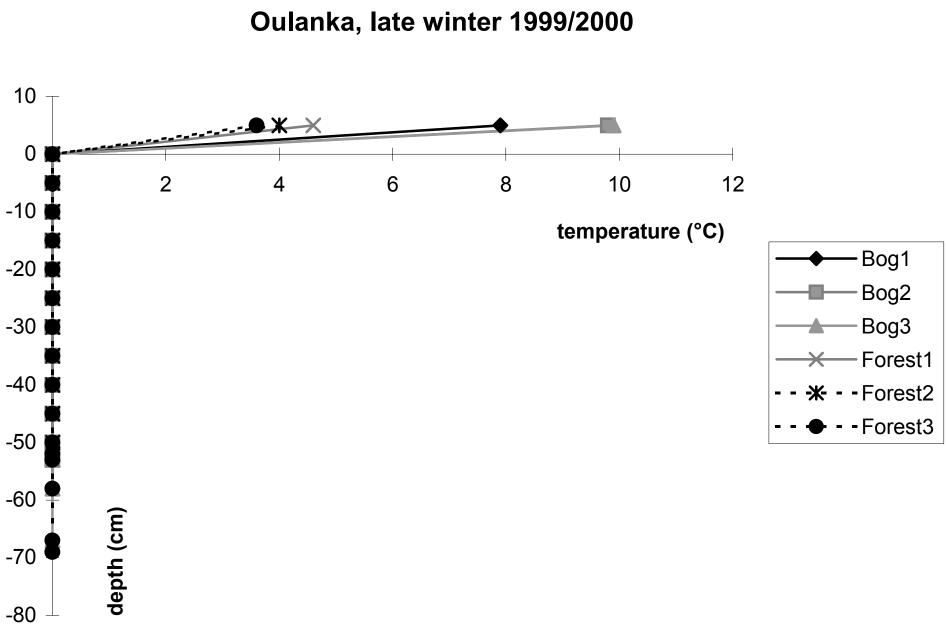

Figure series 3.32, continued. Examples of the temperature profiles observed during the 1999/2000 winter.

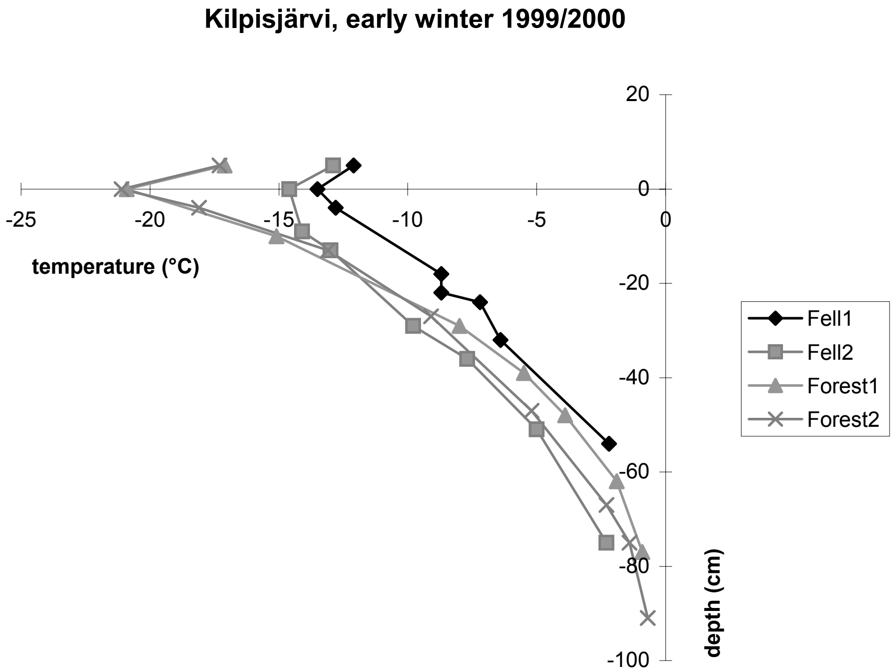

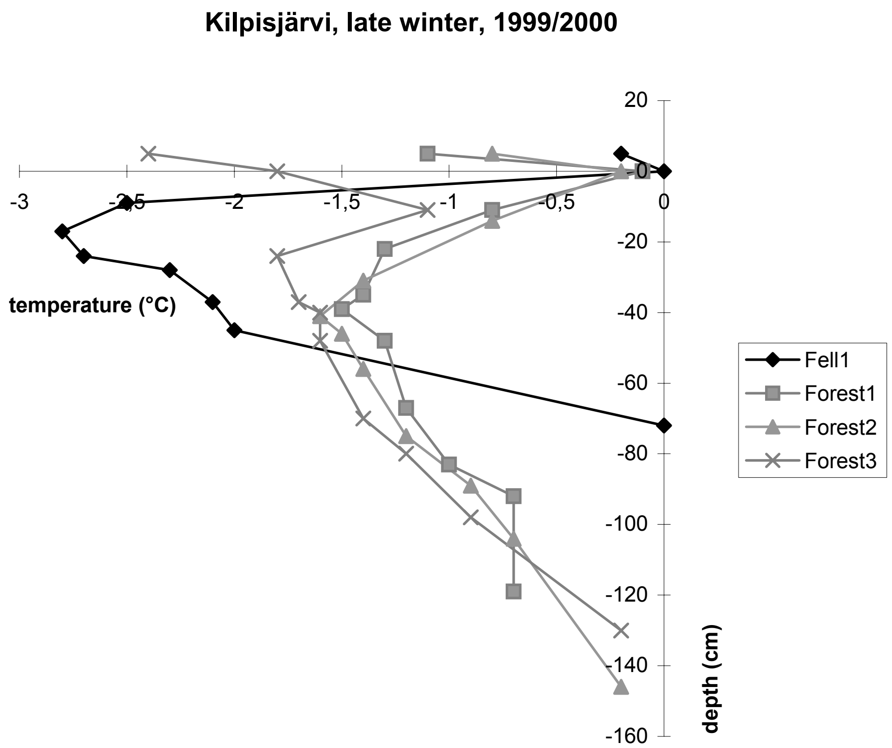

Figure series 3.32, continued. Examples of the temperature profiles observed during the 1999/2000 winter.

In Oulanka, the early winter situation was similar to that in Mekrijärvi. Bottom temperatures were similar in both of the biotypes, but near surface temperatures in the bog were much lower than the ones in the forest. In the forest not very significant temperature minimum was observed in the middle of the snow cover. Like in Mekrijärvi, also here during the late winter measurements all of the snow pack was in melting temperature and no variation was seen between the biotypes.

In Kilpisjärvi, observed temperature profiles in early winter were close together in both of the biotypes, only the surface parts of the profiles were warmer in open fell. All of the profiles show gradual increase of temperature with depth. During the late winter variation is higher. Notice that only one fell profile is shown in the figure series 3.32. There is a temperature minimum below the surface in the fell profile, and after this steep gradient when going towards the bottom. In the forest the shape of the profiles is the same, but the gradients are more gentle. The profiles in the forest are close together. The snow cover is remarkably warmer than in the early winter case, but not in the melting temperature.

The variability seen in the temperature profiles is largely caused by changes in the weather at the measurement moment. The effect of the time of the day was tried to be kept small by doing measurements same time of the day every time; it is still seen in the temperature profiles observed. Also only few measurements were available and some of the temperature profile observations are missing. Because of all these reasons it was chosen not to do more averaging between the winters, and not to analyse the local variability of the temperature profiles very closely.

3.2.3. Average snow conditions

The following table series 3.6 includes averages for certain snow parameters as observed in different locations, separately for field and forest cases and early and late winter. All three profiles observed during the three winters are used in averaging, so on average nine profiles have been used to get the average values. This data can possibly be used when needing an “average” snow profile for certain area of our country. It is important to notice in any case that these average conditions are based only on three winters’ measurements. Also the values for snow depth and WE depend on the measurement date, and are not average maximums for the locations. The snowless situations in Santala and in Mekrijärvi have been taken into account only in snow depth averaging.

Snow depth is gradually increasing, as expected, when going from ephemeral Santala towards the north, which is seen in the tables when going from left to right. The same trend is seen both in the forest and in the open area, during early and late winter. Very little difference is seen between the forest and the open area during the early winter; during the late winter there is more snow in the forest than in the open area in most of the locations.

Table series 3.6. Averages of certain snow parameters as observed in different locations, separately for field and forest cases and early and late winter.

Early winter; forest:

	Santala	*Lammi*	*Mekrijärvi*	*Oulanka*	*Kilpisjärvi*
Depth	6	26	39	40	49
Layers	1.2	3.5	4.2	3.8	5.3
WE	23	70	97	84	127
Density	260	270	228	210	252
Hardness	400	370 / 2700	50 / 2100	43	200
Temperature	-4	-3.9	-7.4	-4.3	-9.7
Grain size	1.8 / 6.3	1.0	1.2	1.3	1.1
Rounded%	42	28	38	40	34
Hoar%	0	0	55	60	63
Ice %	58	72	7	0	3

Early winter; field:

	Santala	*Lammi*	*Mekrijärvi*	*Oulanka*	*Kilpisjärvi*
Depth	6	26	38	45	47
Layers	1.3	3.2	5.3	4.1	5.4
WE	26	70	94	92	162
Density	290	269	228	201	329
Hardness	400	490 / 1900	30 / 230	42	370
Temperature	-4.4	-4.7	-5.9	-3.6	-7.5
Grain size	0.8 / 5.7	1.1	1.5	1.4	1.0
Rounded%	47	24	33	41	33
Hoar%	0	0	67	59	51
Ice %	53	76	0	0	16

Late winter; forest:

	Santala	*Lammi*	*Mekrijärvi*	*Oulanka*	*Kilpisjärvi*
Depth	4.2	30	46	49	105
Layers	1	6.1	4.6	3.3	9.1
WE	22	92	159	151	307
Density	358	297	342	306	292
Hardness	315	2600	41 / 240	56	214
Temperature	0	-1.4	-0.3	-0.3	-2.2
Grain size	1 / 5	1.4	0.98	1.3	1.4
Rounded%	0	29	9	2	35
Hoar%	0	23	16	11	61
Ice %	100	48	75	87	4

Late winter, field:

	Santala	*Lammi*	*Mekrijärvi*	*Oulanka*	*Kilpisjärvi*
Depth	2.4	29	35	58	97
Layers	1	5	5.9	5.4	9.1
WE	31	89	136	174	360
Density	422	309	358	306	361
Hardness	293	2450	192	65	630
Temperature	0	-0.5	-0.6	-0.4	-1.4
Grain size	1 / 5	1.5	1.2	1.6	1.5
Rounded%	0	33	12	16	38
Hoar%	0	20	16	15	54
Ice %	100	47	72	69	8

The water equivalent increases accordingly when going towards the north. The only difference is that most of the time the WE in Mekrijärvi exceeds the one in Oulanka. Some difference is seen between WE in open area and in the forest, but quite small and random except in Kilpisjärvi. In Kilpisjärvi WE observed in open fell is much higher than the one observed in the forest. WE values grow, in some places even to double amounts, when going towards late winter and when the amount of snow increases. During the same time snow is densified and the amount of liquid water increases.

The behaviour of the amount of layers is quite similar to the one of WE. In any case, less layers are regularly observed in Oulanka than in Mekrijärvi. This implies to less frequent but more intense snowfall events in Oulanka; on the other hand melting and refreezing may add the layer amount in Mekrijärvi. There is some, but little, variation between the layer amount in the forest and the open area, in many cases more layers were observed in the open field. In most of the places there were more layers observed during the late winter, but only in Kilpisjärvi the increase was remarkable with four layers more during the late winter case.

Bulk density values do not snow large variation around the country, varying between 200 and 330 kgm^{-3} during the early winter and 290 and 420 kgm^{-3} during the late winter. The largest densities are most often seen in ephemeral zone and in tundra; lower values are observed in maritime and taiga zones. The density values grow when going towards spring. In many places the bulk density is higher in the open area than in the forest; in some places the difference is not observed.

In some locations two values for bulk hardness of snow are given in the tables. The reason for this is the large temporal variation in hardness. During one year the hardness may be a hundred times larger than during the other two, whereas the values may be close together during these two winters. It does not seem reasonable to combine all these observed values to a single number. The maritime zone locations, Lammi and Mekrijärvi, seem to have the most variable hardness conditions. Most variation is seen during the early winter. This is due to the variation in occurrence of melt-freeze periods during the different winters. Beside this variation, the hardest snow is found in Santala and in Kilpisjärvi, the former due to the refrozen and the latter due to the wind-blown snow. Lowest hardness values are found in Oulanka. The same pattern is seen both in early and late winter, but especially in late winter case the hardnesses observed in Lammi are much higher, although variable, than in other locations. Kilpisjärvi is the only location, where hardness in open area is clearly larger than in the forest. In tundra condition wind slab formation explains this. In other locations snow in the forest, especially during the late winter, consists partly of ice snow lumps fallen from the trees and refrozen melt water from the trees. This makes measurement of the snow hardness more difficult, and increases the snow hardness.

Observed bulk temperature depends so strongly on the recent weather in the measurement location and on the measurement time, that the temperature values in the table series 3.6 cannot be generalised at all. It is common to find snow packs very close or at melting temperature during the late winter. On the other hand snow covers are rather cold during the early winter period.

In Santala two values are given also for the bulk grain size of the snow cover. This is because in this location snow cover consisted mainly of one layer only, and this surface layer was most often formed of melted and refrozen polycrystals. Smaller value gives the average diameter of the single grains, larger the average diameter of the polycrystals. If concentrating on the single grains, the grain size is with some exceptions growing when going towards the north. In Kilpisjärvi however, the early winter grain sizes are rather small. This may be due to the more efficient wind breaking of the crystals. Increase in grain size when going towards colder and more stable conditions may be explained by prolonged periods of faceted grain and depth hoar growth. As shown in the section 3.2.5, the faceted grains are on average bigger than other crystal types, this is why increase in fraction of faceted grains in the snow cover also leads to the increase in bulk grain size. Small differences are seen between the grain size in the forest and in the open area: most often the field grain size is a bit larger than the forest one. A slight growth of the grain size is observed in most of the locations when moving from early winter to late winter case. At least two processes may be working here: increase in fraction of faceted grains, and melt-freeze cycles occurring more often.

Fraction of rounded grain snow does not show large variation around Finland, at least not in the early winter case. The amount of rounded grain snow is mainly affected by the amount of falling new snow, because this is counted also to this category and also because normally this is firstly changing into rounded and sintered snow by equilibrium growth metamorphosis, and only after this to faceted grains by kinetic growth metamorphosis. During the late winter case the variation between the locations is much larger, but it can be still explained by temporal and areal variation of snowfalls. No new snow has fallen in Santala during and just before the measurement periods in spring times, and very little also in Mekrijärvi and in Oulanka. In Lammi and especially in Kilpisjärvi, where real winter weather lasts longer than in other locations, more new snow has been accumulated. In Kilpisjärvi the fraction of rounded grain snow has stayed quite constant all through the winter, in other locations the fraction is remarkably smaller during the late winter. Only a little difference is observed between field and forest fractions of rounded grain snow. The difference is bigger in the late winter, when larger fractions of rounded grain snow is found in the open field than in the forest.

Occurrence of faceted grain snow and depth hoar is not seen at all in ephemeral and thin maritime locations during the early winter. In more stable conditions in northern locations the fraction is quite similar in all of the locations, around 60 per cents. In late winter case the faceted grain snow is seen in all the locations except ephemeral Santala, but the fractions are smaller, below or around 20 per cents. The only exception is Kilpisjärvi, where snow cover still is real winter snow cover, and the fraction of faceted grain snow has remained around 60 per cents all through the winter. The difference between forest and open area cases is random and small.

Only small fractions of melting snow or icy snow is seen in Mekrijärvi, Oulanka and Kilpisjärvi during the early part of the winter; in open fell the fraction of icy snow is somewhat larger. During the late winter two special cases are seen in the tables: in ephemeral Santala all of the snow cover is formed of icy or melting snow, but in Kilpisjärvi still only a few per cent of the snow cover is formed of icy or melting snow. In other locations the fraction does not show very large variation. The weather during the measurement winters has a great effect also on this quantity. No big differences are seen between forest and open area. Only in Kilpisjärvi the fraction of icy snow is remarkably bigger in the open fell in the early winter case; in some occasions forest values are higher in maritime and taiga locations indicating perhaps some icy lumps and refrozen melt water observed under the canopy. Naturally, in almost all of the locations the fraction of melting and refrozen snow increases greatly when going towards late winter and spring melt. In Kilpisjärvi this phenomenon does not appear, and quite surprisingly neither in Lammi.

The fraction of faceted grain snow and on the other hand that of icy or melting snow, as observed during the early winter or winter before spring time melting, divide Finland into two areas. In the first, southern area, where Santala and Lammi are located, no faceted grain snow or depth hoar is observed, but fractions of icy snow are quite large. In the northern area, where Mekrijärvi, Oulanka and Kilpisjärvi are located, the situation is reversed: only small fractions of icy and melting snow are seen, often not at all, but fractions of faceted grain snow and depth hoar are large. No marked differences are seen inside these areas that comes to the fractions discussed above. It may be possible to define very simple two-class snow zonation for Finland, zones being depth hoar zone (including perhaps maritime, taiga and tundra zones from the zonation shown in figure 3.6) and melt zone (including perhaps thin maritime, ephemeral and transition zone from the same zonation). Naturally more study locations and more winters are needed before this conclusion can be drawn. Also this division breaks up during the late winter.

Some of these results (snow depth, amount of layers, bulk density and snow type fractions) have also been discussed in the section 3.2.1, when validating the placement of a certain location in a certain snow zone.

3.2.4. Surface values for certain quantities; ground temperature

In the following table series 3.7 the observed surface values for density, hardness and grain size are listed in the same manner like it was done for the bulk properties in the section above. Also the difference between observed snow surface temperature and simultaneously measured air temperature is found in the table. Whenever this difference is negative, the surface is colder than the air above it; when it is positive, the surface is warmer. Weather and vegetation have great effect to the sign of this quantity. The average snow surface values may be of use in interpreting the satellite images of the snow cover and in other remote sensing work of the snow.

Also one ground value is added into the table: that is temperature on the ground surface. The ground surface temperature in Jokioinen (situated quite close to Hyytiälä) varies normally in November-March period between zero and –7°C, based on observations in 1957-1970. The monthly mean ground surface temperature is close to –1°C during all these months. The observed minimas around snow depth maxim (48 cm) are close to –3°C. (Finnish meteorological Institute, 1979)

In Sodankylä (situated quite close to Oulanka) the ground surface temperature varies between –1 or –2°C and –11°C in November-March period. The monthly mean ground surface temperature varies between –2 and –5°C during these months. The observed minimas around snow depth maxim (82 cm) are close to –6°C. In Kevo (situated in northern Lapland) the situation is close to that in Sodankylä. (Finnish meteorological Institute, 1979)

Table series 3.7. The observed surface values for density, hardness and grain size, as well as the difference between observed snow surface temperature and simultaneously measured air temperature.

Early winter; forest:

	Santala	*Lammi*	*Mekrijärvi*	*Oulanka*	*Kilpisjärvi*
Tsnow-Tair	-1.2	-0.03	0.3	-1.2	-3.0
Tground	-1.2	-0.4	-2.8	-2.9	-
Surface density	250	135	156	153	175
Surface hardness	180	8 / 260	16	6	33
Surface grain size	0.8 / 6.3	0.4	0.4	0.4	0.4

Early winter; field:

	Santala	*Lammi*	*Mekrijärvi*	*Oulanka*	*Kilpisjärvi*
Tsnow-Tair	-5.1	-0.6	0.3	-3.2	-0.1
Tground	-0.9	-1.3	-0.7	-0.5	-
Surface density	280	113	167	132	312
Surface hardness	221	2.2 / 200	78	8	540
Surface grain size	0.8 / 5.7	0.5	0.5	0.5	0.71

Late winter; forest:

	Santala	*Lammi*	*Mekrijärvi*	*Oulanka*	*Kilpisjärvi*
Tsnow-Tair	-2.6	-1.1	-4.8	-2.6	-0.4
Tground	0	-0.5	0	-0.1	-0.3
Surface density	358	224	349	319	174
Surface hardness	361	1200	280	62 / 520	6 / 3090
Surface grain size	1 / 5	0.97	0.86 / 8	0.75 / 3	0.4

Late winter; field:

	Santala	*Lammi*	*Mekrijärvi*	*Oulanka*	*Kilpisjärvi*
Tsnow-Tair	-3.2	-0.8	-3.9	-5.0	-2.9
Tground	0	-0.4	0	0	-1.3
Surface density	422	256	407	359	335
Surface hardness	296	3170	155 / 4920	181	320
Surface grain size	1 / 5	0.87	0.92 / 7	0.86 / 5	0.71 / 3

In the Santala area the ground remains unfrozen during 5 to 10 winters out of 100. In the Lammi region the corresponding number is between 10 and 15, in the Mekrijärvi region it exceeds 15. Winters with unfrozen soil occur slightly more frequently in forests than in open fields. (Solantie, 1998) In any case it is safe to assume that the ground is frozen during most of the winters in the measurement locations.

The relationship of surface density to bulk density of the snow pack depends on the nature of the snow surface during the measurement periods. In most of the cases during the early winter period there existed new or recent snow on top of the snow cover during the measurement campaign; because of this many of the surface density values are lower than the bulk density values. However, in late winter in most of the cases the surface temperature was equal or exceeded the bulk density. This tells about wet snow cover, or about refrozen or melting surface layer. During the early winter the surface density values were highest in ephemeral snow zone and quite low elsewhere, the

Kilpisjärvi fell being an exception. In the late winter case ephemeral zone still had the highest values, but also other locations had high surface densities.

Surface hardness follows the same zonal pattern than the surface density. The surface hardness of the snow is difficult to measure, especially if there is a thin layer of new snow on top of the older one, because it is difficult to tell which layer you are measuring with your device. Because of this in some locations two alternative values for surface hardness is given. Basically values below 20 Nm^{-2} tell about new or recent snow, values of several hundreds of Nm^{-2} about rounded or melting snow and values of several thousands of Nm^{-2} about refrozen snow or ice layers, sometimes also about wind crust. The highest values are found during late winter indicating the work of melt-freeze cycles in the surface layers. In most of the cases the surface hardness is higher in the open field than in the forest.

The surface grain size, which refers to maximum grain diameter, varies between 0.4 and 1 mm, or even to 8 mm. These values are visual estimates, and somewhat bigger than assumed grain sizes in many modelling or remote sensing applications. In many cases two alternative grain size values are given in the tables. This means that the surface layer is formed of partly melted or refrozen polycrystals, and the smaller value gives the average diameter of single grains and bigger the average diameter of polycrystals. In most of the cases the grain size is found to be bigger in the open field than in forest. During the late winter this might tell more about efficient melting and refreezing in the open areas, but during the early winter the difference is not that easy to explain. The ephemeral snow shows biggest, polycrystal grain sizes also during the early winter. In other locations the variation of grain size is very small. The increase of grain size is observed when going towards the late winter.

The weather at the measurement moment has a great effect on the difference between snow surface and air temperature. Still, this value is negative except in early winter Mekrijärvi measurements, and here also very close to zero. The difference ranges between 0.3 and – 5.1°C, and in many places the difference is bigger during the warm late winter days than during the early winter. In most of the places the difference is bigger in the open field than in the forest, meaning that snow surface is warmer under the canopy, probably because of dampened energy exchange at the snow surface.

The lowest average ground surface temperature observed was warmer than –3 °C. In most of the cases temperature was between 0 and –1°C, at least during the late winter. Temperatures seem to be a bit colder in the forest than in the open field during the early winter; no significant difference is noted during the late winter. It could be said based on the observations during the three study winters that the ground temperature is near zero all through the winter in Finland. Naturally the measured ground surface temperature depends strongly on the weather at the measurement moment and recent past. Referring to the earlier measurements (Finnish Meteorological Institute, 1979) this conclusion can be said to be incorrect.

In most of the cases the averages are based on three winter observations, and on three snow pits for each winter. This means that the sample size is too small to draw any far-reaching conclusions. When ground surface temperature was not measured every early winter in Kilpisjärvi, it was not suitable to list this value there.

3.2.5. Values for different grain types

In the table 3.8 some statistics of snow density have been shown separately for different grain types; the same is done for snow hardness in table 3.9. Observations from all locations and from all the winters have been combined in these tables, so that the sample size is more than 200 observations for each grain type. Rounded grains include here both rounding precipitation particles and rounded grains (all equilibrium growth forms) and hoar all kinetic growth forms. Mixed forms have been left out from this analysis. Melt-freeze forms and melting snow have also been separated.

Table 3.8. Statistics of snow density.

	Rounded	*Hoar*	*Melt-freeze*	*Melting*
Min	30	210	175	250
Max	335	408	500	435
Ave	177.1	289.1	325.7	359.9
StDev	74.7	41.1	61.0	40.0
Var	0.42	0.14	0.19	0.11

The average density of snow increases when going from rounded grain snow (this means new snow and snow going through equilibrium metamorphosis) towards melting snow via hoar (snow going through kinetic growth metamorphosis) and melt-freeze snow. The average density of melting snow is greater than that of melt-freeze snow, most likely because of a large liquid water content of melting snow; on the other hand maximum density values are higher for melt-freeze snow because of ice lenses falling into this group. Density values are well grouped in hoar and melting snow cases, which is seen also in small coefficients of variation. Rounded grain snow shows here largest variation.

Table 3.9. Statistics of observed snow hardness.

	Rounded	*Hoar*	*Melt-freeze*	*Melting*
Min	1.1	9.4	65	42
Max	600	417	6833	475
Ave	70.7	138.4	2454.7	187.4
StDev	133.6	116.3	1936.2	108.5
Var	1.89	0.84	0.79	0.58

The variation in hardness is far larger than in density, but values of coefficient of variation show similar pattern than in the density case. The largest variation is found in rounded types of snow, smallest in melting snow. The variation is very large also in hoar and melt-freeze types of snow. Minimas are small for rounded grain snow and hoar, and large for melt-freeze snow and melting snow. The largest maximas are found in melt-freeze snow, once again because of the ice layers. The average hardness pattern differs slightly from the average density pattern; the largest average hardnesses are also found in melt-freeze snow. This difference can be explained, because adding liquid water into the snow cover increases the snow density, but decreases the cohesion of the snow particles together. Melting snow shows not only more homogenous hardness conditions than other snow types but also decrease in cohesion compared to icy melt-freeze snow.

Statistics on snow grain size have been shown in table 3.10, once again separately for different grain types. Ice includes here both melt-freeze snow and melting snow. Combining some classes makes the table more easy to read, but it also increases variation inside the classes. For example in class rounded grains the biggest sizes are from precipitation particle observations and in class ice from observations of large polycrystals; average grain sizes differ greatly from these values.

Table 3.10. Statistics of observed grain size for different snow types.

	Rounded	*Hoar*	*Ice*
Min	0.1	0.5	0.5
Max	2.5	7	10
Ave	0.66	1.66	1.24
StDev	0.38	1.07	0.83
Var	0.58	0.64	0.67

Both minimum and maximum grain sizes increase from rounded snow via hoar to melt-freeze snow. It is clear that recrystallized depth hoar crystals are larger than rounded grains, as well as it is clear that melted and refrozen polycrystals reach large values for grain size. In any case the average grain size is larger for hoar than for melt-freeze type. This would imply that very large grains are more rare in melting or refrozen snow than in depth hoar. Coefficients of variation do not show much variation here; slight tendency of increase is seen when going towards melt-freeze types of snow.

Here no discrimination between melting snow and melt-freeze snow has been made. Some uncertainty may exist in discrimination of single snow crystals to a certain type category and this has also possibly affected to the grain size distribution presented here.

3.2.6. Snow zonation testing

In the section 3.2.1 the placing of measurement location of the different snow zones was discussed on the basis of snow pack structure. As one of the ways to divide areas into different snow zones is to study the time-density curves (described in section 3.1.2), this has also been done. Two methods for zonation validation are described in this section, and they have been tried for the measurement locations.

Firstly, the evolution of snow pack bulk density in the measurement locations was studied during all three winters. The bulk density values were calculated averaging all of the bulk density observations from the location and the study period. The values from early and late winter were used to calculate the slope of the time-density curve. To have the values comparable with Sturm and others (1995) the time is days from 27.10. The results for different years are collected in the table 3.11. Values with good agreement with Sturm and Holmgren (1998) data are marked with darker shades of grey; values very close to the assumed range but falling slightly outside are marked with lighter shades of grey.

Please notice that some data from the year 2002 are not available for calculations. Notice also that reference data is available only from maritime, taiga and tundra zones by Sturm and Holmgren (1998). For this reason the comparison between observations in the thin maritime zone is made also with reference data from the maritime zone.

Table 3.11. Slopes of the density versus time curves (kgm^{-3}d^{-1}) as calculated from the observations in the study sites during different winters. The ranges and averages of the curves from Sturm and Holmgren (1998) are also shown. The intercept is taken from t=-65, that is October 27., when t=0 is January 1.

Zone	*2000*	*2001*	*2002*	*Sturm et al. (1998)*	*Average of Sturm et al.(1998)*
Ephemeral	5.4	0.83	-		
Thin maritime	1.32	0.15	-		
Maritime	1.25	2.28	1.16	1.31	1.03-2.04
Taiga	0.69	0.83	0.78	0.57	0.43-0.72
Tundra	0.19	0.28	0.89	0.24	0.10-0.53

For all of the winters agreement between observations and reference data is reasonably good in maritime and in taiga zones, in tundra zone year 2002 gives too high slope values. Variation is high in this maritime zone, as well as in ephemeral zone. The problem here is that only two measurements of the bulk density were available for the slope calculations, and this adds randomness into the analysis. Not very much can be said on the basis of this study about the suitability of the zonation or placement of the locations.

The other method tried was to collect all the snow survey data collected by the Finnish Environment Institute during a single winter, 1998/1999, which was quite close to the 30-year average that comes to the snow conditions in Finland. This way 3-8 bulk density measurements per winter were collected, from altogether 125 locations around Finland. Snow surveys including snow depth, snow bulk density and snow water equivalent measurements from the main biotypes of the locations are made every 16th day of the month. In addition to this, results from “small surveys” (less measurements on the last, and sometimes on 15th day of each month) from 50 locations were collected. The slopes and initial values were calculated from the lines linearly fitted to the time-density curves based on combined bulk density observations from each survey, not dividing the surveys into different biotopes. After this the locations were sorted on the basis of the slopes of the linear fittings to the time-density curves. Different colours were used for the assumed slope values (see table 3.11) for different snow zones, and the sorted slope value tables were marked with these colours. Only good and excellent fits ($R^2 > 0.8$) were used in the sorting. The sorted table is shown in Appendix II. The snow survey locations marked in capital letters are from “small surveys”.

Total 63 fittings were used in the sorting, and 32 of them fell into the assumed snow zone. This means that only a bit more than 50 % of the assumed placements were correct. For taiga zone 60 % of the placements were correct and for maritime zones 45 %. It is good to remember that borders between the zones are not precise after so very few winters of research, and they are changing from winter to winter. In any case this result from one winter gives some reason to suspect that perhaps the snow zonation described in section 3.1.2 is not suitable in Finland; on the other hand the method described here is not necessarily very reliable to base a snow zonation on.

It is interesting to see that no slopes indicating transition or ephemeral zone time-density curves (curves with the slope higher than 2.04 $kgm^{-3}d^{-1}$) were observed in this analysis. Some explanations could be given to this absence of proof of very effective densification: fitting can be poor or very poor and because of this it does not show in the final sorting; there are only a few snow survey locations especially in ephemeral zone; only a few measurements were done during the winter in these locations. Also the very flat curves indicating tundra conditions are missing; one very good reason for this is the lack of the snow surveys above the tree line. The only measurements, which were assumed to fall into the tundra category were from Iittovuoma.

What comes to the measurement locations, only Kilpisjärvi (represented by Iittovuoma 2-4), Oulanka (represented by Kuusamo) and Mekrijärvi (represented by Ilomantsi and Ilomantsi, Naarva) are shown in the final sortings. All of the Iittovuoma measurement locations fall into taiga category, which is a good representation of the Kilpisjärvi conditions below the tree line. The other locations are found in the maritime category. This is assumed to be correct for Mekrijärvi, but the time-density curve shows too efficient densification in Kuusamo, at least in the winter 1998/1999. More study winters are needed before the usefulness of this method in snow zonation work can be discussed further.

3.2.7. Hardness measurements

Simultaneous snow surface density and hardness measurements, 237 pairs altogether, were collected during the measurement winters from all over Finland. The first intention was to find an overall equation combining the snow hardness measured by penetrometers to snow density. This was found out to be very difficult, perhaps impossible, and after this the different snow types were treated separately.

The pairs were divided on the basis of grain type. Of the pairs 59 fell into the category of equilibrium metamorphosis snow (new or recent snow going through rounding and sintering, as well as rounded grain snow) and 34 pairs into the category of kinetic growth metamorphosis (faceted grain snow or depth hoar). Of the pairs 46 were of melt-freeze snow and 62 pairs of melting snow. In addition 36 pairs were of mixed type of snow (icy hoar, rounding faceted grains or faceting rounded grains), but because of the great diversity inside this category, the results of these measurements are not used here.

The snow hardness has been measured during decades by Rammsond, plate penetrometers and cone penetrometers. It has been said that it is impossible to give a hardness value, which is independent of the measurement device. Measurement techniques have remained surprisingly unchanged for more than half a century. Recently some small digital cone penetrometers have been developed in Japan. Plate penetrometers are not widely used tools to measure snow hardness nowadays, but they were used already in the 1950s in snow mechanical studies. The penetrometers were used to study the different deformation behaviour of snow samples of the same density but different degree of bonding (Shapiro et al. , 1997). Quervain (1950) wrote an early article about snow hardness measurements by penetrometers, and already he stated that "measurement of this type is subjective, and it it is difficult to distinguish the "real" snow structure break-down from the viscous behaviour of the snow and from several consequent break-downs". The only snow type where a connection between density and hardness has ever been found is rounded grain snow. In different sources exponential equations have been suggested for this connection. The problem here is that the equations are device-dependent.

In this study Canadian type penetrometers with different sized plates and a spring balance were used to measure the snow hardness; or more precisely the pressure the snow structure can stand before breaking. Most of the observations are about surface hardness, not about vertical hardness of other snow layers. It was decided to use this method in spite of its shortcomings; at least it gives a value of a physical quantity as a result, and this way differs from Rammsond, which is normally used to get an index of snow cover total hardness. The observed pressures could be used for example to calculate animal sinking depths for animals with different weights and hoof sizes.

In the figures 3.33-3.36 the distribution of measured density-hardness pairs are shown for each snow type separately.

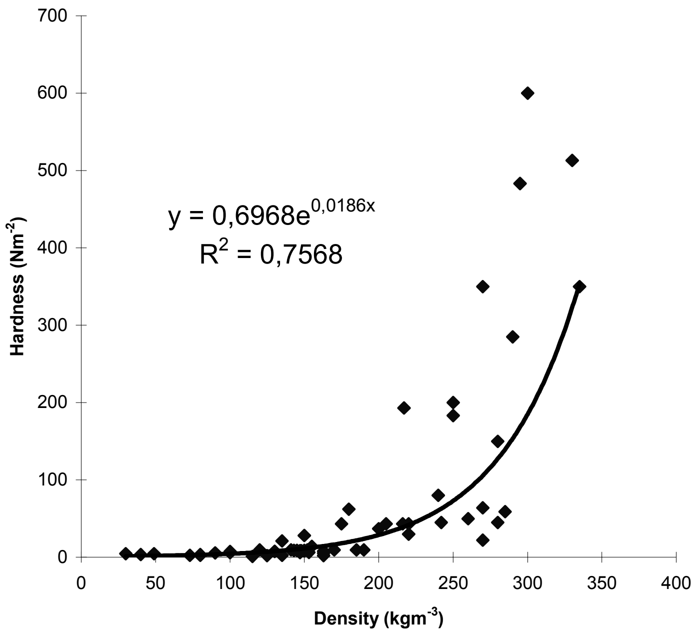

Figure 3.33. The distribution of measured density-hardness pairs for new, recent or rounded snow.

In figure 3.33 the distribution of density-hardness pairs of new, recent or rounded snow is shown. This is the snow type, for which some hardness equations have been developed. Here it is easily seen that the exponential curve would be too steep for this data set and the device that has been used. A logarithmic equation has been fitted to the data set here, which in turn seems to be sloping a bit too gently. The density of this type of snow ranges between 30 and 335 kgm^{-3}, and hardness between 1.1 and 600 Nm^{-2}, so the variation is big depending on the age and microstructural stage of the snow.

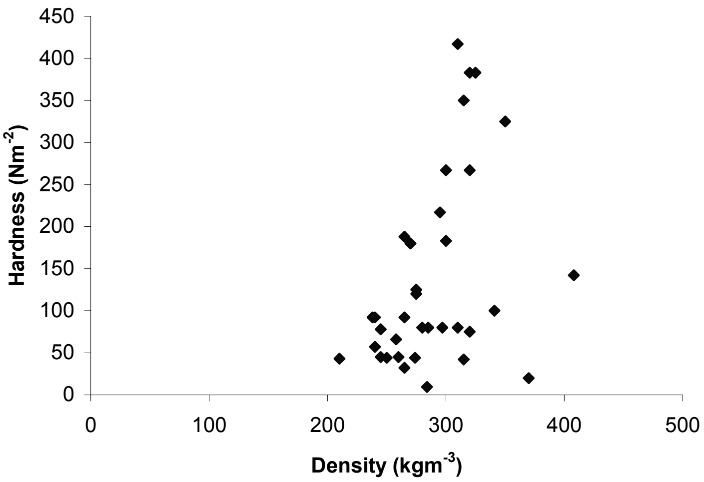

Figure 3.34. The distribution of measured density-hardness pairs for faceted grain snow and depth hoar.

In figure 3.34 the distribution of the pairs is shown for faceted grain snow and depth hoar. The distribution of density is remarkably smaller than in the previous figure, but the distribution of hardness remains big. Also, no correlation seems to be found between density and harness in this data set.

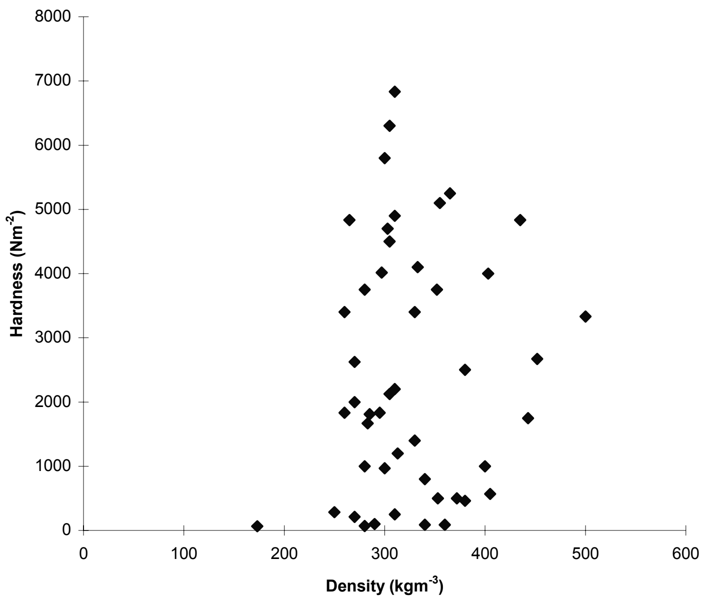

Figure 3.35. The distribution of measured density-hardness pairs for melt-freeze type snow.

The distribution remains almost similar in figure 3.35, where the distribution of pairs is shown for melt-freeze type of snow. But the distribution is even more random than in the previous picture, and the distribution of hardness is much wider, reaching almost

7000 Nm^{-2}. The hardness of melt-freeze snow depends of course on the stage of the metamorphic cycle, and because the snow type can vary between icy but porous crusts to impermeable ice lenses, the distribution is understandable.

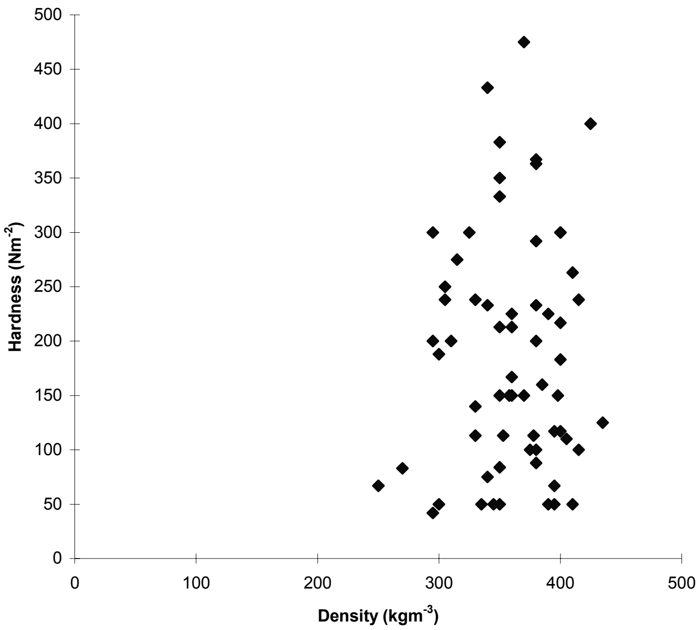

Figure 3.36. The distribution of measured density-hardness pairs for melting snow.

Figure 3.36 shows the distribution of pairs for melting snow. Here some interesting changes are seen when compared to the previous figure: firstly the hardness drops dramatically when compared to the melt-freeze snow. Introducing liquid water into the snow pack weakens the bonding between the snow grains efficiently, and this is seen also in the decrease in hardness. Also the distribution of density grows narrower, and so does the one of hardness. In fact, the narrowest distribution of hardness is found for snow going through kinetic growth metamorphosis, and for melting snow. This tells that these snow types are more homogenous than the other snow types studied.

The only result of this work is the assumed correlation between density and hardness for rounding or rounded snow. For all other types of snow only distribution of data, no correlation, can be given. These distributions have already been discussed in section 3.2.5. The relation between snow hardness and temperature could be found, because temperature relates to the liquid water amount in the snow, which in turn affects the viscous behaviour of the snow, notable during the warm days in the melting periods.

It would be possible to develop equations of hardness based not only on snow density, but also on the age of the snow and snow type. However, it seems that the most important snow quantity affecting to hardness is the snow microstructure (grain type and size, bonding between the grains, bond size), which in turn affects to the density, and to which the age of the snow affects.

3.3. Variation of snow cover in Finland

Variation of snow pack structure based on visual observation of snow pits is discussed in section 3.2.1. In the section 3.3.1 the variation of snow depth is dealt with statistically. As there are only a few snow pit observations to work with on each location, it was chosen not to use the snow pack structure observations for any statistical analysis. Analysis including agreement scores (see chapters 4 and 5) is tried instead.

3.3.1. Variation of snow depth

In this section variation of snow depth inside and between the forest and open areas in different locations is discussed. The data used here is from the snow line measurements including on average 180 depth measurements in each biotype. Because of the large sample size statistical measures can be used in this analysis. For other observed quantities this was not possible because of the small sample size.

In the tables 3.12 – 3.16 the averages, standard deviations and coefficients of variation are listed for all of the locations separately. The observations are divided into early and late winter cases as well as into forest and field parts. The average depth listed here may differ from the ones in section 3.2.3., because the depths used in that section are from the average depths of the snow pits. The statistical measures are not given for every single measurement period, because during some of them not enough snow depth data was collected.

Table 3.12. The averages, standard deviations and coefficients of variation for snow depth in Santala.

		Averages		*Standard deviations*		*Coefficients of variation*	
		Forest	*Open*	*Forest*	*Open*	*Forest*	*Open*
2000	*Early*	7.8	8.7	3.7	2.0	0.48	0.23
	Late	3.2	6.2	2.8	2.5	0.87	0.41
2001	*Early*	8.0	8.0	3.7	2.1	0.46	0.26
	Late	0.9	0	2.4	0	2.80	0
2002	*Early*	-	-	-	-	-	-
	Late	-	-	-	-	-	-

Table 3.13. The averages, standard deviations and coefficients of variation for snow depth in Lammi.

		Averages		*Standard deviations*		*Coefficients of variation*	
		Forest	*Open*	*Forest*	*Open*	*Forest*	*Open*
2000	*Early*	29.5	28.7	11.2	8.5	0.38	0.30
	Late	29.5	26.8	12.9	12.8	0.44	0.48
2001	*Early*	17.8	22.4	5.4	5.5	0.30	0.25
	Late	23.0	25.8	6.7	6.0	0.29	0.23
2002	*Early*	-	-	-	-	-	-
	Late	-	29.3	-	8.7	-	0.30

Table 3.14. The averages, standard deviations and coefficients of variation for snow depth in Mekrijärvi.

		Averages		*Standard deviations*		*Coefficients of variation*	
		Forest	*Open*	*Forest*	*Open*	*Forest*	*Open*
2000	*Early*	57.9	53.2	11.9	11.2	0.21	0.21
	Late	56.4	32.7	10.1	9.4	0.18	0.29
2001	*Early*	19.1	19.1	3.6	2.0	0.19	0.10
	Late	16.3	4.4	8.4	6.9	0.52	1.58
2002	*Early*	41.9	40.3	5.4	5.6	0.13	0.14
	Late	66.4	61.8	7.6	9.2	0.11	0.15

Table 3.15. The averages, standard deviations and coefficients of variation for snow depth in Oulanka.

		Averages		*Standard deviations*		*Coefficients of variation*	
		Forest	*Open*	*Forest*	*Open*	*Forest*	*Open*
2000	*Early*	63.1	66.9	8.1	3.3	0.13	0.05
	Late	54.4	56.5	11.2	7.2	0.21	0.13
2001	*Early*	33.7	33.6	6.2	3.4	0.18	0.10
	Late	55.9	57.5	11.7	6.2	0.21	0.11
2002	*Early*	27.3	36.1	4.1	3.2	0.15	0.09
	Late	42.6	64.3	7.6	3.5	0.18	0.05

Table 3.16. The averages, standard deviations and coefficients of variation for snow depth in Kilpisjärvi.

		Averages		*Standard deviations*		*Coefficients of variation*	
		Forest	*Open*	*Forest*	*Open*	*Forest*	*Open*
2000	*Early*	83.8	55.1	10.3	36.0	0.12	0.65
	Late	130.9	98.7	13.2	58.1	0.10	0.59
2001	*Early*	34.2	31.7	3.5	18.7	0.10	0.59
	Late	83.7	59.2	8.3	36.8	0.10	0.62
2002	*Early*	43.1	-	5.5	-	0.13	-
	Late	102.1	72.4	9.9	25.7	0.10	0.36

The average snow depth naturally varies a lot between different winters in each of the location. This is seen clearly when looking at snow depth during winter 2000/2001 and early winter 2001/2002 in almost all of the locations. The variability of snow depth is reflected also in the variability of standard deviation. The dimensionless coefficient of variation on the other hand shows relative variation in the snow depth, and seems to be more stable between different years in most of the locations. In Santala even this quantity shows huge variation, reflecting the differing conditions of the ephemeral site: during one time the snow conditions may be homogenous, and during the next, highly variable. For this reason conditions in Santala are not discussed here any further.

In Lammi the coefficient of variation ranges between 0.29 and 0.44 in the forest and between 0.23 and 0.48 in the open area. The open area variation is normally lower than the one in the forest.

In Mekrijärvi the ranges are 0.11-0.21 in the forest and 0.10-0.29 in the open area. Late winter 2000/2001 is left out from the examination here, because uneven melting and patchy snow cover lead to very high coefficients of variation. Normally the variation in the forest and in the open area are close together, only during melting the variability in the open field increase compared to the forest case. The increase of variability is also seen between early and late winter cases in the open field; in the forest the snow WE seems to get more homogenous when going towards late winter.

The range of coefficient of variation in Oulanka forest is 0.13-0.21, and in the open area only 0.05-0.13. In the forest the early winter coefficients are regularly lower, between 0.13 and 0.18, than the late winter coefficients, which range between 0.18 and 0.21. In the open area the late winter coefficients are also higher in most of the cases.

In Kilpisjärvi's forest the range is narrowest of all of the locations: between 0.10 and 0.13. In two thirds of all the cases the coefficient of variation of WE is 0.10. In the open fell, on the other hand, the range is largest: between 0.36 and 0.65, during most of the cases around 0.60. So the difference in variation between the two biotypes is also largest in Kilpisjärvi. This is naturally due to the special snow conditions in the open fell. Not much difference is seen between the values of coefficient during the early and late winter cases. In figure 3.37 the diagram of location of the ranges discussed above is shown.

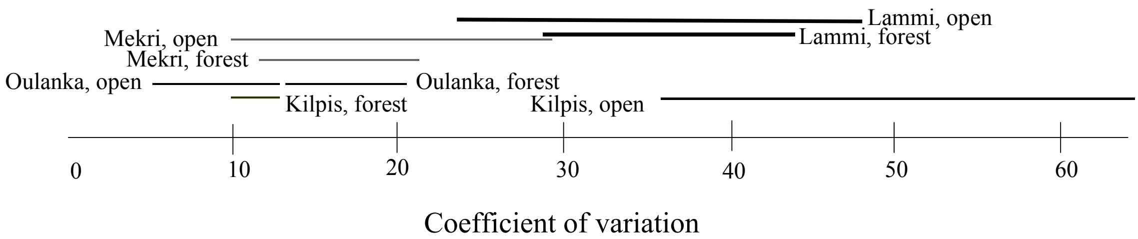

Figure 3.37. The ranges of coefficients of variation in snow depth in different locations.

It is seen in the figure that even though some of the ranges are overlapping, also some distinct coefficient of variation ranges exist. Lammi, for example, stands out with its "own" range. When looking only at the forested area coefficients, the differences are more clear: first comes Kilpisjärvi, then together Oulanka and Mekrijärvi, and after this Lammi. If Santala were taken into account, coefficient of variation in snow depth in the forest there would follow the Lammi forest range beginning from 0.46. In the open area case the ranking is different, and depends a lot on the type of the open area: small bog in Oulanka comes first, after this fields in Mekrijärvi and Lammi, and Kilpisjärvi fell comes last. Other things seen in the figure is that normally the open area variation range is wider than the one for the forest.

What if it could be proved that the standard deviation is very close to constant at one of the locations, and would clearly differ from the ones at the other locations? How about if the same was true for the coefficient of variation? If the first assumption were correct, it would mean that the variation in depth decreases with increasing depth and vice versa. If the second assumption were true, the deviation in the snow depth increases when the depth increases and vice versa. Both of the assumptions cannot be correct at the same time. In the figure 3.38 the case a illustrates roughly the situation in the first assumption, and case b in the second.

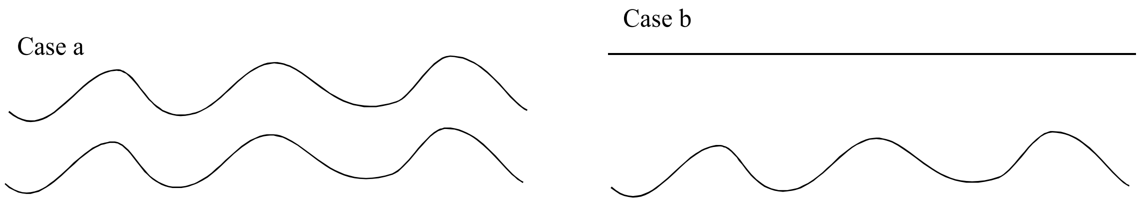

Figure 3.38. Case a: the standard deviation of the snow depth is constant. Case b: the coefficient of variation of the snow depth is constant.

It can be seen from the figure that, in most of the cases, the case b is correct from our own experience in the snowy nature. The unevenness of the terrain is hidden under the even-looking snow cover. If the theory presented here was correct, it would be possible to find coefficients of variation close to constant in different locations. Based on figure 3.37 this also seems to be the case. Separate ranges for the coefficient can be found for different locations from one winter to the other. Naturally the data series is too short to make any serious conclusions about this. More data should be collected. It seems worthwhile to study, if this larger data set could be used to distinguish the snow zones based on the differences in variation of snow depth.

The observations of coefficients of variation are earlier reported by Solantie (2000). In his study the coefficients for Lammi area were around 0.56 in the forest and 0.61 in the open field. In the Mekrijärvi area the coefficient for forest was around 0.23, and in Oulanka area around 0.22. The values are calculated based on a long time series, and the locations for snow depth measurements, as well as the measurement times during each winter, do not match with the ones used in this study. When taking all this into account, the results of these studies are fairly close together. Lammi values are high, but Mekrijärvi and Oulanka values are very close to the maximas observed in this study. Also the ranking of the locations is similar.

In the table 3.17 the observed snow depth in the forest is compared to the one in the open area. The values listed in the table show how many percentages the snow depth in the forest has been of the snow depth in the open field, bog or fell.

Table 3.17. The observed snow depth in the forest compared to the one in the open area.

		2000	*2001*	*2002*
Santala	*Early*	1.00	0.90	-
	Late	-	0.52	-
Lammi	*Early*	1.03	0.79	-
	Late	1.10	0.89	-
Mekrijärvi	*Early*	1.09	1.00	1.04
	Late	1.72	3.76	1.07
Oulanka	*Early*	0.94	1.00	0.76
	Late	0.96	0.97	0.66
Kilpisjärvi	*Early*	1.52	1.08	-
	Late	1.33	1.41	1.41

The table shows that in Mekrijärvi and in Kilpisjärvi the open area snow cover is regularly thinner than in the forest. In Kilpisjärvi the fell snow depth is highly variable, and in the forest the snow cover is homogeneously deep. Also the snow interception is very small in the birch forest. In Mekrijärvi the difference is small during the early winter, which refers to small snow interception, but larger during the late winter. This can be explained by the more efficient melting in the open field. In Oulanka on the other hand the snow depth in the forest is regularly a little bit less than the one in the open area. This may be explained by the snow interception, and also by the small size of the open area, bog, studied. The wind effect there is very small, and the snow depth there very likely represents the local snow depth maximum. In Lammi the situation is different during different winters, unluckily not enough data is available in winter 2001/2002. During winter 1999/2000 there was a little bit more snow in the forest than in the open field; during winter 2000/2001 there was a little bit less snow. In Santala the field and forest snow depths are quite similar; during the only available late winter case only half of the snow depth measured in the open area was observed in the forest.

3.3.2. Variation of water equivalent and bulk density

The snow water equivalent data together with data about snow bulk density were collected during the snow surveys in winter 2000/2001. In the tables 3.18 and 3.19 the coefficients of variations based on the observations are shown. There were enough late winter observations available only in Lammi.

Table 3.18. The coefficients of variation for snow water equivalent during winter 2000/2001.

		Coefficients of variation	
		Forest	*Field*
Lammi	*Early*	0.38	0.20
	Late	0.29	0.24
Mekrijärvi	*Early*	0.26	0.11
	Late	-	-
Oulanka	*Early*	0.24	0.12
	Late	-	-
Kilpisjärvi	*Early*	0.10	0.30
	Late	-	-

The water equivalent shows rather large spatial variation, ranging between 0.10 and 0.38. When both the forest and open area are taken into account in the calculations, the range narrows to 0.20 and 0.36. Here Lammi shows the largest variability, whereas values for other locations are close together.

Only in Kilpisjärvi the WE in the open area shows larger variability - three times larger - than in the forest. The minimum value for coefficient of variation is found in the Kilpisjärvi birch forest. In other locations the variability in the forest is larger than in the open field. In Mekrijärvi and in Oulanka the coefficients are very small in the open field cases. The coefficients of variation show more narrow ranges in the WE than in the snow depth case, and also the ranges are more closely together in the different locations.

Table 3.19. The coefficients of variation for snow water equivalent during winter 2000/2001. The observations from forest and from open area are combined here.

		Coefficients of variation
Lammi	*Early*	0.36
	Late	0.30
Mekrijärvi	*Early*	0.20
	Late	-
Oulanka	*Early*	0.20
	Late	-
Kilpisjärvi	*Early*	0.23
	Late	-

The averages, standard deviations and coefficients of variation of snow bulk density, measured during winter 2000/2001, are given in the tables 3.20 and 3.21.

Table 3.20. The averages, standard deviations and coefficients of variation for bulk snow density during winter 2000/2001.

		Averages		*Standard deviations*		*Coefficients of variation*	
		Forest	*Field*	*Forest*	*Field*	*Forest*	*Field*
Lammi	*Early*	231.2	269.4	26.7	35.4	0.12	0.13
	Late	234.1	261.5	28.8	33.6	0.12	0.13
Mekrijärvi	*Early*	152.6	158.9	25.8	15.2	0.17	0.10
	Late	-	-	-	-	-	-
Oulanka	*Early*	188.8	170.2	29.7	15.4	0.16	0.09
	Late	-	-	-	-	-	-
Kilpisjärvi	*Early*	209.3	266.0	16.6	39.5	0.08	0.15
	Late	-	-	-	-	-	-

Table 3.21. The averages, standard deviations and coefficients of variation for bulk snow density during winter 2000/2001. The observations from forest and open area are combined here.

		Averages	*Standard deviations*	*Coefficients of variation*
Lammi	*Early*	250.0	36.5	0.15
	Late	246.5	33.6	0.14
Mekrijärvi	*Early*	155.7	21.3	0.14
	Late	-	-	-
Oulanka	*Early*	181.3	25.7	0.14
	Late	-	-	-
Kilpisjärvi	*Early*	235.4	40.7	0.17
	Late	-	-	-

The bulk densities listed here may differ somewhat from the ones found in section 3.2.3, because the values listed earlier are from combined layer density measurements and these listed above are from Korhonen-Relander snow tube measurements. In the tables more interest should be paid to standard deviations and especially to coefficients of variation in the different locations. In most of the cases not enough data were available during the late winter case.

The variability of standard deviations depends also on the average snow density. The dimensionless coefficient of variation on the other hand tells the relative variation of the snow density. It is noted that in Lammi the coefficient is very near constant during early and late winter and in the forest and in the field. In Oulanka and in Mekrijärvi the variation in the forest is much larger than in the open field. In Kilpisjärvi the situation is the reverse, open fell showing almost double variation when comparing to the forest. In the Kilpisjärvi forest the coefficient of variation of bulk density is smallest.

The combined coefficients in table 3.21 are a little bit larger than the ones calculated separately for forest and field cases. They are very close together all through the country, ranging only between 0.14 and 0.17. The values for coefficients of variation are much lower for the bulk density than for the WE, and the ranges observed are much more narrow. The same is true with the ranges in the snow depth, the values are of the same order or a bit lower. So, the WE shows larger variation together with snow depth, and bulk density lower variation, as assumed. The sample size for both WE and density cases is around 30.

3.3.3. Variation based on agreement scores

As not enough data were collected to allow statistical analysis of snow pack structure variation, and because visual intercomparison discussed in section 3.2.1 is a rather subjective method of studying the variation, an agreement score between different snow profiles was used.

Calculation of agreement scores between different snow profiles of each studied snow pack structure quantity, and overall agreement score, is discussed later in this work in chapters 4 and 5. The method is introduced in details in the Appendix IV. Shortly, in this method the modeled snow profile is first stretched to match the height of the observed snow profile, and after this the mapping of the layers is performed to find the matching layers. Scores describing agreement between observed and modeled layer properties are calculated for each property separately, and finally these scores are combined to the overall agreement score using certain weighing factors for each property. The weighing factors for all of the studied properties are here kept as 1. Properties studied here are temperature, density, grain size and grain type.

In chapter 5 the agreement scores have been calculated between simulated and observed snow profiles, as well as between different simulated profiles. Here a new method of studying the local snow pack structure variability is introduced: agreement scores are calculated between different observed snow profile, both inside a certain biotype, as well as between the field and the forest.

Agreement scores between different measurements were calculated separately for certain locations and for certain measurement periods. For three snow pit observations per biotype three agreement scores needed to be calculated: between pits 1 and 2, between pits 1 and 3 and between pits 2 and 3. The average agreement score was calculated after this for the whole biotype. The average agreement score for the whole location was also calculated, here averaging is done for 15 different agreement scores between different pit pairs. Naturally more snow pits would be needed also in this method.

The calculating of agreement scores is a method developed by the Swiss Federal Institute for Snow and Avalanche Research, and it is meant to be used together with the SNOWPACK –model. (Lehning and others, 2001) Before calculating the agreement scores the snow pit observations have to be processed to the following format:

JULLAY	H	T	RHO	WC	GrSz	Class
2	0.20	271.85	270	0	1	330
1	0.10	271.05	300	0	2	550

Where JULLAY is the layer by age order, H the height of the layer surface from the ground (m), T temperature at the layer surface (K), RHO layer density (kgm^{-3}), WC the liquid water content of the layer (not used), GrSz the average grain diameter in the layer (mm) and Class grain type in three number code (first indicating major type, second minor type and third possible melt-freeze).

Agreements core values range between 0 (no agreement between the two snow profiles) and 1 (perfect agreement). Not only differences in the measured temperature profiles and in layer density, grain size and type have effect on the agreement score; also differences in snow depths at the snow pit locations affect the value of the score through density. So, when the snow depth is highly variable in some location, this makes the agreement scores lower even if the snow pack structure is homogenous.

In the tables 3.22-3.26 the average agreement scores between the observed snow pits are listed separately for different locations. The tables show agreement scores for grain type, grain size, temperature and density, as well as overall agreement scores. Different winters, as well as different times of the winters are treated separately. Agreement scores are given first for the forest and field separately, after this also combined agreement scores for the whole location are given. The closer the agreement scores are 1 in certain location, the smaller is the variation in the snow pack structure. On the other hand, if the scores are very low, the variation is high.

In the following, agreement score results are gone through in different locations.

Santala

Only a two year data set is available in Santala. Agreement scores show great variability here between the winters, times of the winter and the different quantities. So the variation may be large for a certain time and for a certain quantity, but small for some others. The overall level of the agreement scores is low, and even scores close to zero are often seen in the table, indicating a very high variability in this location.

In winter 2000/2001 very high agreement scores are found for grain type, grain size and temperature in Santala, and on the other hand very low for density. This must be due to the high variation in snow depth. During the winter 1999/2000 highest values are found for grain size and temperature – during many occasions the snow in Santala was at melting temperature. There is no clear tendency of increase or decrease in the agreement scores between early and late winter, neither between field and forest cases.

Table 3.22. Agreement scores between different observed snow profiles in Santala.

	Overall	*Grain type*	*Grain size*	*Temperature*	*Density*
Santala					
1999/2000					
Forest					
Early winter	0.51	0.30	0.75	1	0
Late winter	0.83	1	1	1	0.33
Field					
Early winter	0.59	0.53	0.83	0.67	0.31
Late winter	0.25	0	0	0	1
Combined					
Early winter	0.53	0.40	0.79	0.84	0.12
Late winter	0	0	0	0	0
2000/2001					
Forest					
Early winter	0.75	1	1	1	0
Late winter	0.75	1	1	1	0
Field					
Early winter	0.56	0.67	0.67	0.83	0.077
Late winter	0.75	1	1	1	0
Combined					
Early winter	0.64	0.78	0.78	1	0
Late winter	0.75	1	1	1	0

Lammi

From Lammi, only late winter agreement scores are available for the winter 2001/2002. The overall tendency during the years seems to be that the agreement scores are a bit lower during the late winter. This might be true, or the student measurers doing the snow pack structure observations may have some effect on this. The overall agreement scores are quite close to each other during all of the winters, ranging between 0.61 and 0.75 for the early winter and 0.54 and 0.66 for the late winter case. Higher values are seen for the early winter 1999/2000 and for the late winter 2000/2001.

In some of the cases the overall agreement scores are lower in the open field than in the forest. The situation may be reversed for some of the quantities. Grain size and temperature generally have the highest agreement scores, grain type the lowest.

Table 3.23. Agreement scores between different observed snow profiles in Lammi.

	Overall	*Grain type*	*Grain size*	*Temperature*	*Density*
Lammi					
1999/2000					
Forest					
Early winter	0.75	0.74	0.81	0.69	0.78
Late winter	0.65	0.49	0.72	0.66	0.73
Field					
Early winter	0.75	0.80	0.69	0.81	0.68
Late winter	0.54	0.63	0.69	0.50	0.35
Combined					
Early winter	0.69	0.62	0.80	0.69	0.67
Late winter	0.59	0.56	0.76	0.63	0.44
Lammi					
2000/2001					
Forest					
Early winter	0.61	0.40	0.69	0.79	0.58
Late winter	0.57	0.42	0.76	0.81	0.28
Field					
Early winter	0.63	0.48	0.62	0.67	0.73
Late winter	0.66	0.38	0.72	0.89	0.63
Combined					
Early winter	0.63	0.52	0.72	0.62	0.68
Late winter	0.60	0.38	0.81	0.71	0.49
Lammi					
2001/2002					
Forest					
Early winter					
Late winter	0.6	0.47	0.78	0.62	0.53
Field					
Early winter					
Late winter	0.57	0.24	0.82	0.83	0.41
Combined					
Early winter					
Late winter	0.51	0.37	0.64	0.49	0.54

<u>Mekrijärvi</u>

The level of overall agreement scores in Mekrijärvi are high. Ranging between 0.76 and 0.86 in early winter and 0.64 and 0.77 in later winter cases. Exceptional low values are seen in the field, late winter 2000/2001, when the snow cover was patchy and snow depth extremely variable. Otherwise, no large variation between the winters is seen, but the late winter scores are somewhat lower than the early winter ones.

The scores are quite high for all of the quantities; low values are seen for grain type and density more often than for grain size and temperature; so these values seem to be the most variable ones in Mekrijärvi.

Table 3.24. Agreement scores between different observed snow profiles in Mekrijärvi.

	Overall	*Grain type*	*Grain size*	*Temperature*	*Density*
Mekrijärvi					
1999/2000					
Forest					
Early winter	0.76	0.57	0.69	0.87	0.90
Late winter	0.77	1	0.67	0.94	0.48
Field					
Early winter	0.77	0.67	0.86	0.80	0.75
Late winter	0.71	1	0.97	0.61	0.28
Combined					
Early winter	0.64	0.51	0.84	0.56	0.64
Late winter	0.68	0.94	0.69	0.76	0.33
Mekrijärvi					
2000/2001					
Forest					
Early winter	0.78	0.75	0.75	0.90	0.73
Late winter	0.64	0.83	0.83	0.67	0.22
Field					
Early winter	0.81	0.87	0.90	0.78	0.69
Late winter	0.18	0.33	0.22	0.11	0.24
Combined					
Early winter	0.72	0.86	0.78	0.59	0.65
Late winter	0.50	0.67	0.67	0.5	0.16
Mekrijärvi					
2001/2002					
Forest					
Early winter	0.86	0.88	0.87	0.83	0.8
Late winter	0.64	0.42	0.74	0.79	0.61
Field					
Early winter	0.78	0.76	0.78	0.90	0.70
Late winter	0.68	0.45	0.83	0.80	0.65
Combined					
Early winter	0.76	0.71	0.76	0.88	0.68
Late winter	0.60	0.42	0.80	0.65	0.52

<u>Oulanka</u>

In Oulanka the level of overall agreement score is a bit lower than in Mekrijärvi during most of the measurement periods, which means that the variation in the snow pack structure is higher. Still the level is high, around 0.7 and 0.8. Agreement scores are lowest in early winter forest cases. In most of the cases the agreement scores rise towards late winter, so the structure variation decreases towards spring in this location.

Almost every time the agreement score is higher in the open area than in the forest; the variation in the snow pack structure is much lower in quite homogenous bog, where the open area measurements were conducted. Like in Mekrijärvi, all of the quantities show quite high agreement scores. Lower values are most often seen in grain type.

Table 3.25. Agreement scores between different observed snow profiles in Oulanka.

	Overall	*Grain type*	*Grain size*	*Temperature*	*Density*
Oulanka					
1999/2000					
Forest					
Early winter	0.74	0.67	0.73	0.77	0.81
Late winter	0.77	0.89	0.72	0.89	0.60
Field					
Early winter	0.85	0.73	0.89	0.85	0.93
Late winter	0.67	0.76	0.63	0.77	0.53
Combined					
Early winter	0.72	0.67	0.76	0.69	0.77
Late winter	0.79	0.85	0.72	1	0.58
Oulanka					
2000/2001					
Forest					
Early winter	0.55	0.47	0.62	0.61	0.51
Late winter	0.65	0.76	0.62	0.67	0.56
Field					
Early winter	0.70	0.51	0.85	0.67	0.77
Late winter	0.72	0.52	0.83	0.88	0.64
Combined					
Early winter	0.60	0.44	0.69	0.80	0.49
Late winter	0.59	0.47	0.58	0.93	0.40
Oulanka					
2001/2002					
Forest					
Early winter	0.56	0.51	0.56	0.62	0.56
Late winter	0.67	0.76	0.73	0.75	0.43
Field					
Early winter	0.70	0.63	0.66	0.77	0.74
Late winter	0.82	0.85	0.83	0.80	0.80
Combined					
Early winter	0.65	0.66	0.66	0.62	0.66
Late winter	0.66	0.74	0.76	0.71	0.42

Kilpisjärvi

In Kilpisjärvi the agreement scores once again reach quite high values. During one early winter case the score is 0.57, but otherwise the overall score ranges between 0.65 and 0.76 in early winter and between 0.67 and 0.85 in late winter cases. The agreement score is regularly higher in the forest than in the open area, which tells about the great variability of the tundra snow. Also the late winter cases have regularly higher agreement score values than the early winter values.

The different quantities have once again quite high agreement score values, and the same pattern than in most other locations is seen: grain size and temperature show lower values than grain type and density. Especially density has lower values in the open fell than in the forest, indicating variability of the snow depth there.

Table 3.26. Agreement scores between different observed snow profiles in Kilpisjärvi.

	Overall	*Grain type*	*Grain size*	*Temperature*	*Density*
Kilpisjärvi					
1999/2000					
Forest					
Early winter	0.73	0.53	0.72	0.90	0.77
Late winter	0.83	0.77	0.88	0.80	0.87
Field					
Early winter	0.65	0.69	0.74	0.78	0.40
Late winter	0.68	0.51	0.87	0.83	0.52
Combined					
Early winter	0.74	0.72	0.78	0.81	0.64
Late winter	0.61	0.53	0.47	0.77	0.67
Kilpisjärvi					
2000/2001					
Forest					
Early winter	0.71	0.92	0.73	0.67	0.54
Late winter	0.85	0.79	0.83	0.89	0.90
Field					
Early winter	0.66	0.66	0.85	0.67	0.46
Late winter	0.67	0.51	0.74	0.91	0.51
Combined					
Early winter	0.53	0.69	0.67	0.49	0.28
Late winter	0.68	0.53	0.76	0.80	0.64
Kilpisjärvi					
2001/2002					
Forest					
Early winter	0.76	0.63	0.91	0.76	0.73
Late winter	0.78	0.77	0.86	0.82	0.70
Field					
Early winter	0.57	0.67	0.83	0.59	0.20
Late winter	0.72	0.84	0.79	0.97	0.29
Combined					
Early winter	0.59	0.48	0.80	0.63	0.44
Late winter	0.59	0.44	0.79	0.75	0.38

In the table 3.27 overall agreement scores have been combined from different years for all of the locations. Early and late winter cases are separated, but also both have been used to get an extremely averaged overall agreement score to describe variation inside and between the biotypes in these locations.

With only a few exceptions the agreement scores are relatively high all through Finland. In Santala values below or close to 0.5 are seen, but in most of the locations score values range around 0.6 and 0.7. So the variation in the studied biotypes are not very high.

Table 3.27. Combined overall agreement scores for the measurement locations.

	Santala	*Lammi*	*Mekrijärvi*	*Oulanka*	*Kilpisjärvi*
Early					
Forest	0.63	0.68	0.80	0.62	0.73
Field	0.58	0.69	0.79	0.75	0.63
Combined	0.59	0.66	0.71	0.66	0.62
Late					
Forest	0.79	0.61	0.68	0.70	0.82
Field	0.50	0.59	0.52	0.74	0.69
Combined	0.38	0.57	0.59	0.68	0.63
Both					
Forest	0.71	0.65	0.74	0.66	0.78
Field	0.54	0.64	0.66	0.75	0.66
Combined	0.49	0.62	0.65	0.67	0.63

During early winter the values increase when going towards the north; in Oulanka the agreement score is however a bit lower, and the maximum is reached in Mekrijärvi. This is seen both in the forest and open field case. The open area score in Kilpisjärvi is low, indicating high variation in tundra conditions.

In most of the cases agreement score values are lower during the late winter case, thus the variation increases when going towards spring melt period. In most locations the difference between forest and open area increases when going towards late winter measurements. This indicates increase in differences between forest and open area conditions during the melt period. The same tendency of increase in agreement scores when going towards the north is seen also in late winter case. In the Kilpisjärvi forest the late winter snow pack structure seems to show very little variation, but the variation in the open fell is high. Surprisingly also Santala shows high agreement scores for forest cases. In most of the locations and measurement times the combined agreement is lower than the one for a single biotype, which was also expected.

The agreement score calculated using both early and late winter values is naturally lower than the ones calculated separately. The same tendency of growing agreement score values towards the north is still seen; the only exceptions are in the forest case Santala (high score) and Oulanka (low score), in the field case Kilpisjärvi shows lower agreement score values than the location south from it, Oulanka. The same is true for the combined agreement score on the last row of table 3.27.

To conclude: variation in the snow pack structure seems to be decreasing when going towards northern and more stable snow zones, excluding the open fell sites. In the open field variation is larger than in the forest. Based on this data, it is not possible to say how this agreement score relates to for example coefficient of variation of a single snow pack quantity.

4. SNOWPACK –model

4.1. Snow pack structure modelling

Several snow cover models have been developed for different purposes: temperature index models, energy balance models as well as models including snow pack structure. It has been shown that the simple models may perform even better than the more sophisticated snow pack structure models, at least when estimating snow melt and melt water runoff (Vehviläinen, 1992), but in this study the most attention is paid to the snow pack structure during the winter before melt period. This is why a short overview of only snow pack structure models is given here. Also the SNOWPACK –model is handled in this overview; after this in the latter sections of this chapter the SNOWPACK –model is gone through in detail.

Modelling of snow pack structure using numerical mass and energy balance models started in 1970's. These models were originally developed for hydrological use. The problem to be solved in all of the snow pack structure models is estimating the snow stratigraphy (amount, height and properties of the layers – mostly temperature, density and possibly also grain form and size and some mechanical quantities) at a certain point, and also its evolution during the winter. Depending on the model the number of output quantities may be smaller. Definition of the exact problem depends on the aims of the modelling – for example in avalanche forecasting exact knowledge about snow layering and metamorphoses is needed.

A point energy and mass balance model of a snow cover

First modern snow pack structure model is "A point energy and mass balance model of a snow cover" published by Anderson (1976). The energy exchange between the snow surface and the atmosphere is described in the model, as well as heat conduction in the snow and through the snow/ground interface. Also snowfall, settlement of snow cover, water percolation, phase changes and snow metamorphoses are included as processes in the model. Most of the processes are however not defined physically, but they affect through parameters. For example metamorphoses are included in snow settlement coefficients. Equations about the development of snow density during different metamorphic processes are experimental. The minimum input for the model is air temperature, water vapour pressure, wind velocity and incoming short wave radiation. The optional input includes reflected short wave radiation, incoming long wave radiation, precipitation and ground surface temperature. The model gives data about snow water equivalent, snow depth, bulk density, surface snow density, snow temperature and melt water runoff. (Anderson, 1976)

SNTHERM

SNTHERM is a one-dimensional snow pack structure model, primarily developed to calculate temperatures within the snow pack and at the surface. It was developed in Cold Regions Research and Engineering Laboratory (CRREL) in USA, and it has been widely used, mostly to model snowmelt hydrology. The model is based on the mass, energy and momentum balance in each grid point. The model includes different phases of precipitation, melt-freeze –cycles and variation between bare and snow covered ground. Transport of liquid water and water vapour are included in the heat balance.

The model takes into account snow accumulation, melting, packing and metamorphoses, as well as the effects these have on the properties (heat conductivity, optics) of snow. Snow and soil are described as ice or soil particle skeleton, with air, liquid water or ice in the pores. All of the phases are assumed to be in thermal equilibrium. The thermal conductivity is calculated as average conductivity of snow. Like in the work by Anderson (1976), the packing of snow is divided into new and old snow regimes. An experimental equation is used for the packing of new snow, and the packing of old snow is calculated by using the weight of overlying snow layers. Input of the model includes air temperature, relative humidity, wind speed, incoming short wave radiation, outgoing short wave radiation, and incoming long wave radiation. As an output the model gives snow depth and water equivalent, temperature and density profiles of the snow cover, liquid water content and grain size of snow, and some soil parameters. (Jordan, 1991)

SNOMOD

SNOMOD combines some of the sophistication of the layer structure models to the simplicity of the temperature index models. The aim of the model is to simulate accumulation, melting, density profiles and temperature profiles in slopes with varying aspects and directions by using simple laws of energy and mass conservation. The average snow surface temperature is assumed to follow the average air temperature, and ground surface temperature is set to 0°C. Snow pack internal temperature gradient is calculated not taking near surface variation into account. The model adds new layers to the snow pack with the snow falls and calculates melt by a degree day method if needed. Water vapour pressure gradient is calculated, and using this and temperature in different parts of the snow pack, the ongoing metamorphoses are defined. Snow densification is calculated by using the weight of overlying layers when equilibrium growth metamorphism dominates; when kinetic growth metamorphism dominates an experimental equation is used. When melt-freeze is going on, melting layers are removed from the snow pack, melt water fills the snow layers below one by one, and part of it may be freed as runoff. Input needed includes air temperature, new snow depth and new snow density. (Dexter, 1987)

DAISY

DAISY is one of the first ”new generation” snow pack structure models. DAISY is a physically based snow cover distribution model, which estimated the mass, energy and momentum transfer between snow and the atmosphere. The model handles ice, water, water vapour and air separately. For example heat capacities of all of the phases are found in the equation of heat conductivity. Snow pack is assumed to consist of layers with homogenous physical properties. The model calculates packing, or densification, of the snow by assuming that snow behaves like a simple viscous material. The model does not deal with mass transport through phase changes, neither with water vapour transfer in the snow pack. This means that depth hoar is not possible to simulate. DAISY needs air temperature, air humidity, wind speed, short and long wave radiation and new snow amount as input. It calculates temperature distribution inside the snow pack, as well as energy and mass fluxes in the layered snow pack. As boundary conditions and energy source terms are used energy absorbed at the snow surface, energy absorbed inside the snow cover, temperature at the snow surface and heat conductivity. (Bader, 1992; Morris, 1994)

Yamazaki model

A model by Yamazaki (1993) is a bit more sophisticated than most of the runoff models. It takes snow metamorphoses into account and calculates temperature profile in the snow pack. On the other hand the most important use of the model is the estimation of the water equivalent of snow and runoff from the snow melt. The model estimates snow temperature, liquid water content, dry snow density and density of the solid impurities. These are used to calculate other quantities: albedo, heat conductivity, liquid water flux, snow depth, water equivalent and melt water runoff. Heat capacity is parameterised using porosity dependent on snow density, and packing of snow is defined using viscosity dependent on liquid water content. Input needed includes incoming radiation, air temperature, relative humidity, wind speed and precipitation. (Yamazaki, 1993).

The most advanced snow pack structure models of today – French CROCUS and Swiss SNOWPACK – are built on the foundation of the previously presented models and on the theories and observations described in Chapter 2. One of the biggest differences between the ”new” and ”old” models is the internal microstructure of snow included in the ”new” models. Including the microstructure makes the models more consistent with the reality, and it enables simulating of more quantities than before. It also makes simulations more reliable.

CROCUS

Crocus is part of the chain of three physically based models, which is used to estimate avalanche hazard in certain mountain massifs, in different aspects and elevations. The SAFRAN-CROCUS-MEPRA chain has been developed in Centre d'études de la neige in France, and it has been in operational use in France since 1992. (Durand 1999)

The first model, SAFRAN, estimates values of the meteorological quantities of importance to snow pack evolution. It is needed because there are no observations from all of the elevations and aspects of the slopes. SAFRAN uses meteorological observations from automatic stations, snow and weather observation network, irregular observations, synoptic observations and upper atmosphere sondings. It combines the data available, and estimates the values of the needed parameters in the locations of interest using methods of weather forecasting. The parameters are used as input of CROCUS model and they include air temperature, wind speed, air humidity, cloudiness, snowfall and rain, long wave radiation as well as direct and diffuse short wave radiation. (Durand, 1999)

The second part of the chain, CROCUS, is a numerical model, which simulates snow pack internal processes and evolution of the snow pack structure. CROCUS calculates evolution of the snow pack energy and mass balance. It uses output from SAFRAN and simulates snow depth, temperature, density, liquid water content, bottom runoff and snow stratigraphy. The model is able to describe realistically the snow metamorphoses, because of snow microstructure included. Snow metamorphism laws are from the works by Colbeck (e.g. 1982), as well as results of the Japanese and French laboratory measurements. The model takes into account the grain size and grain type by estimating the sphericity and dendricity of the grains. For example albedo is a function of grain size and type in the model. It is also possible to calculate compressivity of the snow using grain size and type. This allows realistic simulation of the snow density, which in turn affects the important quantities like heat conductivity. Crocus does not use any initial information about the snow cover. It is assumed that the ground is snow free in the beginning of August, and the winter snow cover is developed using only information from SAFRAN. (Brun, 1994; Durand, 1999)

The last model in the chain, MEPRA, is a model of avalanche hazard. It calculates mechanical indexes of the strength for the snow packs simulated by CROCUS. The model classifies the profiles, and gives a risk of natural and human triggered slab avalanching. MEPRA does not give risk in a certain point; estimates for slopes with different degrees of risk are given.(Durand, 1999)

The strength of the model chain is that it needs only daily meteorological observations as input, or alternatively forecast of a weather model with good resolution. Models are used for certain mountain massifs, where properties of the slopes with the same aspects, directions and elevations are assumed to be constant. This is why the models do not give information about the local conditions, like wind erosion. The chain gives average snow pack structures in different mountain conditions, and also the corresponding avalanche risks. This means that the model chain is used in different ways and for different purposes compared to the model SNOWPACK, which is a point model.

SNOWPACK

SNOWPACK is a one dimensional snow pack structure model, which has been developed at the Swiss Federal Institute for Snow and Avalanche Research (SLF) for avalanche warning purposes. The model is a point model, and it provides information about the state of the snow pack including amounts of new snow and possible surface hoar formation for the avalanche forecasters. Model is used operationally for avalanche forecasting in Switzerland. Model uses input data from 50 weather and snow stations: wind, air temperature, relative humidity, snow depth, surface temperature, ground temperature, reflected short wave radiation and three temperatures inside the snow cover. Stations send the data every hour, and snow pack state is calculated in the station location: new snow amount, settling rate, formation of surface hoar, temperature and density profiles and metamorphic development in the layers. Also water equivalent, melt and runoff are modelled. The SNOWPACK –model can be set to calculate the snow pack structure development for a certain period of a winter by giving the snow pack structure in the beginning of the period as input. Simulation can as well be started from the bare ground. (Lehning et al., 1998)

SNOWPACK is a predictive model that uses finite elements to solve the partial differential equations governing the mass, energy and momentum conservation within the snow pack. The model is physically based: energy balance, mass balance, phase changes, water and water vapour movement and wind transportation are included, and most of the calculations are based on snow microstructure (crystal size and form, bond size, number of bonds per crystal). Snow is modelled as porous medium including ice, water and air in SNOWPACK. (Lehning et al., 1998)

Special numerical procedures have been introduced to treat new snowfall, which add finite elements to the existing grid. Finite elements can also be added or subtracted from the grid to model the snow drift. Mass can be removed also by melt water runoff or water vapour sublimation. To determine the densification rate, which is of special importance for avalanche forecasting, snow is treated as a viscoelastic material. The layering of the snow pack is modelled; layers are defined by their sizes, macroscopic properties like bulk density, mean stress or temperature as well as by microscopic properties like grain size and shape and bond size. It is also possible to follow the microstructural properties of the ice lattice over time, while the snow goes through metamorphoses. All of these properties are especially useful in avalanche forecasting. (Bartelt and Lehning, 2002)

In the on-going project SNOWMIP more than 20 snow cover models with different complexities are compared using input data from several different climatic zones. The models are developed in ten different countries for varying purposes. Three snow pack structure models take part into intercomparison: CROCUS, SNOWPACK and SNTHERM. The differences between the models as listed in Essery and Yang (2001) are:

- The ablation and deposition of snow by wind is represented only in SNOWPACK.

- In SNTHERM the albedo is calculated separately for direct and diffuse radiation.

- The influence of atmospheric stability is treated differently in the models: in CROCUS and SNTHERM the sensible heat flux is maintained also during very low wind speeds by windless exchange coefficients, while the effect of wind pumping on surface transfer is introduced in the SNOWPACK.

- CROCUS and SNOWPACK simulate snow microstructure. SNOWPACK also uses microstructural properties, not bulk density, to calculate thermal conductivity of the snow.

SNOWPACK model has been validated in different snow zones in Finland in this work. The overall performance of the model is tested in five locations, and several sub-models have been tested, as well as sensitivity tests made in Hyytiälä in Southern Finland.

SNOWPACK has never before been used in climate change studies. Here a method to combine output from regional climate scenario and SNOWPACK model has been presented, as well as possible snow conditions in future winters as simulated by the model.

4.2. Main principles of the SNOWPACK -model

SNOWPACK -model calculates the physical properties of the snow pack at some time t as function of depth z (z=0 at the ground surface and z=h at the snow surface). It is assumed that all the slope parallel velocities are zero, and all lateral gradients are zero also. Each snow layer is described by volumetric fractions of the three constituents: ice, water and moist air θ_i, θ_w and θ_a, respectively. The volumetric fractions are between 0 and 1 and

$$\theta_i+\theta_w+\theta_a = 1 \tag{4.1}$$

The constants are defined per unit constituent volume, for example ice density ρ_i , and they are used to define all macroscopic variables, like snow density:

$$\rho_s=\rho_i\theta_i+\rho_w\theta_w\rho_a\theta_a \qquad (4.2)$$

It is assumed that at any given time t all the constituents have the same temperature, snow or bulk temperature T_s. (Bartelt and Lehning, 2002)

All melt water phase changes and water vapour transport processes are energy and mass conserving. When the ice phase melts or melt water refreezes, the energy sink or source terms, proportional to the constituent mass changes, are placed into the bulk energy equation. These energies keep the temperature field to the melting/refreezing temperature. Also water vapour mass is either deposited onto the solid ice phase or sublimated so that the snow vapour pressure $p_a(z,t)$ is never greater than the fully saturated vapour pressure $p_s(z,t)$. The mass changes in the form of crystal growth and energy needed to keep the constraint $p_a(z,t)=p_s(z,t)$ are calculated. The vapour pressure distribution is governed by the vapour diffusion equation. (Bartelt and Lehning, 2002)

The self-weight of the snow pack is assumed to be carried by the solid ice lattice. The air or water does not directly resist motion. Snow strength is related to water content and bulk temperature, as well as to the coordination number and the air content. Only a single momentum conservation equation for the solid ice lattice is required. The influence of air and water is treated in constitutive equations for snow elasticity and viscosity. (Bartelt and Lehning, 2002)

In the model a Lagrangian coordinate system that moves with the ice matrix is employed, not Eulerian coordinates with a stationary computational grid. This choice has several advantages: the mass continuity equation of the ice phase is automatically fulfilled, so only two mass conservation equations are needed; discontinuities in layer density are possible; the position of the top snow pack surface is known exactly, so the treatment of thermal and mass boundary conditions is easier; the history of the material is known, and it is possible to formulate constitutive laws which are based on snow microstructure. (Bartelt and Lehning, 2002)

A volumetric constitutive relation governs the settling of the snow, that is the height changes of the elements. For non-dendritic snow the microstructural parameters are used in the relation. The macroscopic stress is related to the stress in the bonds between the grains. For large stresses the deformation is non-linear. Also the effective thermal conductivity is formulated as a function of the snow microstructure. (Lehning et al., 1998)

The model includes ten interrelated functions or segments (See figure 4.1). Meteorological input and snow pack status at the time t=0 are given to the segment 0. The water vapour pressure gradients and temperatures are calculated in different parts of the snow pack in this segment; depending on these the different parts are processed further in the segments 1, 2 or 3, where mean grain radius and mean bond radius are calculated using known temperatures, densities and grain properties. In the segment 1 grains of the melting snow are processed, and further processing is done either in segment 4 or 5 depending if the snow is saturated by liquid water or not. If not, the change in grain radius will be calculated using volumetric fractions of ice and water; if yes, the changes in grain and bond radii will not be calculated. In the segment 2 changes in grain and bond radii are calculated in case of small temperature gradient; in the segment 3 changes in grain radius in case of large temperature gradient. In the segment 6 changes in the grain sphericity and dendricity are calculated using snow temperature and temperature gradient. Results from segments 2, 3, 4 and 5 are processed further in the segment 7. Here the sintering (change in bond radius) is calculated from grain radius, bond radius, temperature, stress and coordination number. In the segment 8 the values for microstructural parameters are updated taking into account the calculated changes. In the segment 9 mechanical properties of the snow cover are defined. In the segment 10 the effective thermal conductivity of the snow is determined. Also the results are directed back to segment 0 as snow pack status input for the next calculation time step. (Bartelt and Lehning, 2002)

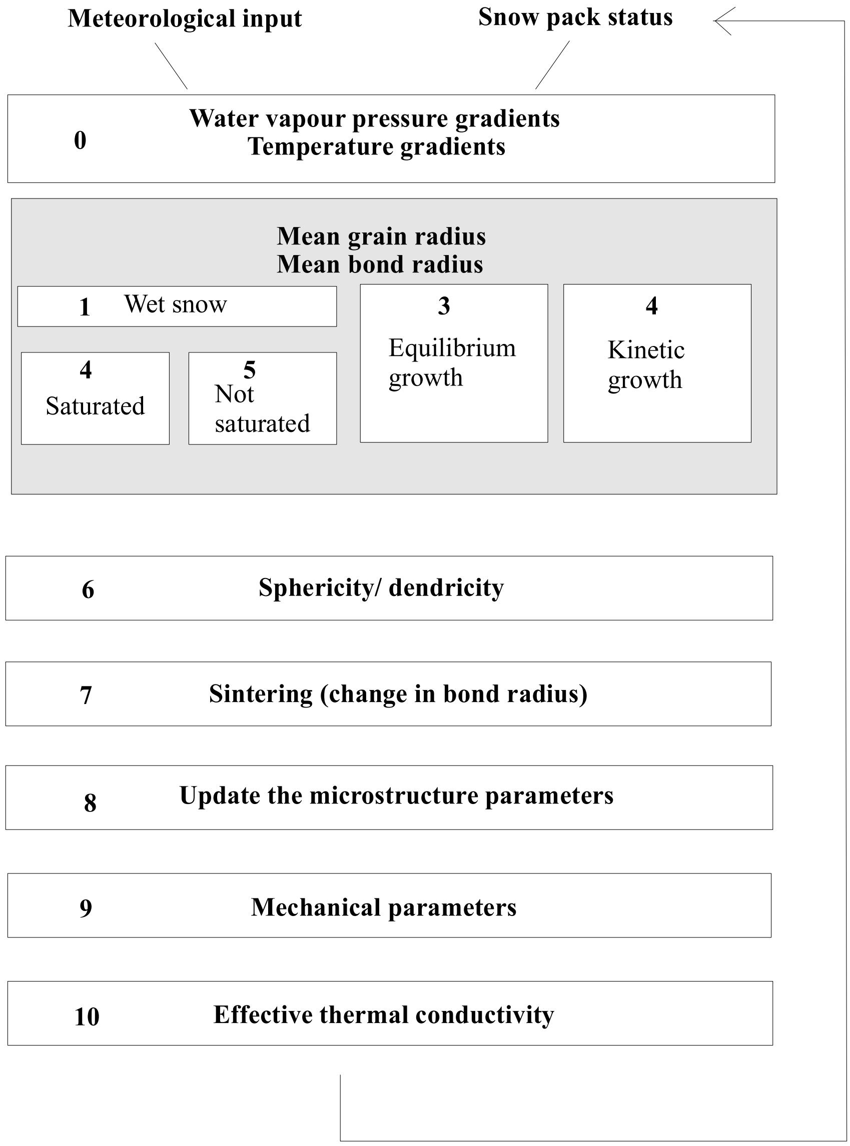

Figure 4.1. Flow chart of the model SNOWPACK. Calculations carried out during one time step.

In the SNOWPACK principles of mass, energy and momentum conservation for all of the constituents are applied, but because of the assumptions listed above only four differential equations are required:

- One energy equation, because the three constituents are in the same temperature, heat transport is described by an effective conductivity and surface energy exchanges by bulk heat fluxes (Combination of equations 2.1 and 2.2).

- A single momentum equation governs snow cover settlement, because the ice lattice carries the entire self-weight of the snow pack (Equation 2.7).

- Two mass conservation equations for the vapour (Equation 2.9) and water phases (Equation 2.10). The mass conservation for the ice phase is automatically fulfilled because of the Lagrangian coordination system. (Bartelt and Lehning, 2002)

The different terms in the equations listed above are gone through in detail in Appendix III of this work, as well as the model parameterisation.

Modelling the snow microstructure is one of the most important parts in the SNOWPACK -model. There are two ways to introduce texture-related quantities into snow cover model. One is to introduce shape-related parameters like in CROCUS, but in this method the direct link to texture does not exist; the other is microstructure-based formalism including grain and bond size, coordination number, bond neck length etc. The snow microstructural texture is more important than grain shape to snow cover properties, and this is why the latter is used in the SNOWPACK model. In any case, new snow and decomposing particles are treated according to the shape parameters. (Fierz and Lehning, 2001)

SNOWPACK uses four independent microstructure parameters: sphericity, dendricity, grain size and bond size. Bond size has not been considered before in the snow cover modelling. Also the three dimensional coordination number is important, it tells the number of bonds per grain and determines the interconnectivity of the ice matrix. (See figure 2.2 and table 2.2 for snow microstructure definitions.) Differentiation between bonds and necks are important, because stresses within the material are greatest within the necks, and the necks begin yielding and flowing much more readily than the ice grains. (Brown et al., 2001)

The empirical equations for sphericity and dendricity changes are based on the formulation described in Brun et al. (1992) and adjusted to the new experimental data. As long as dendricity is larger than zero the grains are not growing. Grain growth is governed by the water vapour flux resulting from the temperature gradient. (Fierz and Baunach, 2000) The microstructural changes are treated separately in the SNOWPACK –model for the equilibrium growth metamorphism, kinetic growth metamorphism and wet snow metamorphism. The equations governing the changes in size and shape of the snow grains in SNOWPACK are presented in Appendix III.

4.3. Input data

The quality of the simulations depends on the choice and availability of input quantities, as well as the quality of the surface energy and mass exchange models (Lehning et al., 2002b) . In operational avalanche warning system in Switzerland the SNOWPACK -model is used together with high Alpine automatic weather and snow stations (IMIS). The IMIS stations measure wind velocity and direction, air temperature, relative humidity, snow depth, surface temperature, ground surface temperature, reflected short wave radiation and three temperatures within the snow cover. Time resolution of the IMIS stations is 30 minutes, which is also an ideal time resolution for the SNOWPACK model. (Lehning et al., 1998)

The list above is also the ideal set of input parameters for the SNOWPACK -model. When considering synoptic weather data or climate model outputs as input data it is clear that not all of the listed parameters are always possible to obtain. There are several ways to overcome the input data problems, and these will be discussed later in the chapter 5. The model itself has been developed so that snow depth can be replaced with new snow water equivalents obtained from precipitation measurements and reflected short wave radiation with incoming short wave radiation. Surface temperature can be replaced with incoming long wave radiation, and if this is also missing the model can give a reasonable estimate. Temperatures within the snow cover are not necessarily needed, and ground surface temperature can, at least in central Europe, be assumed to be close to 0 °C. (Lehning et al., 1998) The input parameters can be provided as a simple ASCII file.

Below there is an example of the input SNOWPACK file. The first row includes information about amount of rows in the file, and in other rows are listed after letter M: date, time, Julian day beginning from 1.1.1900, air temperature (°C), relative humidity (0-100), wind velocity (m/s), wind direction (°), incoming long wave radiation (Wm^{-2}), incoming short wave radiation (Wm^{-2}), surface temperature (°C), ground temperature (°C), precipitation (mm in water equivalent) and snow depth (cm). As seen in the example below, some of the columns include only zero, because the model estimates the parameters or the parameter is not used in the calculations.

```
MTO <OperationalData> 10176
M  10.1.00  0:15:00  36796.90511  9.41  84.58  0.64  218.54  0  2.46  9.41  0  0  0
M  10.1.00  0:45:00  36796.92596  9.26  85.25  0.78  218.4   0  2.62  9.26  0  0  0
M  10.1.00  1:15:00  36796.94682  9.07  87.22  0.86  222.09  0  2.5   9.07  0  0  0
…
End
```

Possible gaps in snow depth data were filled by linear interpolation in this work. Gaps in other parameter columns are filled with value –999, and SNOWPACK data control algorithms make the necessary corrections. (Grönholm, 2003) Because of the occasional measurement errors and gaps, it is necessary to control and correct the input data before using it as input for the model calculations. All measured input parameters have to be within reasonable physical limits. All measured time series are checked for outliers, and gaps are filled with linear interpolation. The control algorithm for snow depth includes check for absolute upper and lower bonds, the elimination of outliers and spikes and a maximum increase and decrease in snow height. (Lehning et al., 2002b)

There are some choices the user has to make before a SNOWPACK run depending on the input data quality:

- Surface boundary conditions: are the measured surface temperatures used (Dirilect boundary conditions) or will the model calculate total energy balance at the snow surface (Neumann boundary conditions)
- Is the new snow depth calculated from the measured snow depths or is the precipitation observed
- Is the measured short wave radiation incoming or reflected
- Are there measurements on incoming long wave radiation or does it need to be estimated by the model
- Are there measurements on temperature inside the snow cover and from what depths
- What is the height of the meteorological measurements
- What kind of model is used for the new snow density
- What is the time resolution of the input data

Additionally there are several model parameters, some of them can be changed by the user, some are based on laboratory work and should not be changed without a good reason:

- Water percolation parameters (residual water content, saturated water content, residual water content for water transport routines)
- Parameters associated with element compression (minimum element length, condense interval, condense tolerances: ice, water, sphericity, grain size, maximum length for condensating)
- Input data control parameters (smoothing, maximum height change, exponent of non-linear increase, maximum spike width, new snowfall warning)
- The parameters for new snow density models
- The parameters for the albedo models
- Limits for the snowfall (maximum incoming short wave radiation 200-250 Wm^{-2}, relative humidity over 50-70%, air temperature less than 1.1°C; ranges are due to the different model versions)
- Parameters for minimum snow layer thicknesses (element thickness, onset of melt, minimum thickness for a melted layer)
- Surface hoar properties (minimum thickness of the layer, maximum for the relative humidity, maximum amount of hoar layers, surface hoar density 100 kgm^{-2})
- Parameters for drifting snow (minimum and maximum transport, average length of the slope)
- New snow properties (albedo 0.9, grain radius 0.15, bond radius 0.25*grain radius, marker 0, stability 0, interface stability 0.)
- Parameters for grain size growth (growth rate maximum, limit for bond radius)
- Wind pumping parameterisation (advective flux attenuation, displacement coefficient, ratio of porosity to tortuosity)
- Sensible and latent heat wind factors
- Parameters for the settling and bond growth and conductivity (bare soil roughness length, wind speed geometrical factor, factors controlling settling and bond growth and ice to ice conduction)

4.4. Initial and boundary conditions

Initial conditions

The SNOWPACK –model does not preferably use the measured precipitation rate in the calculations, mainly because of problems and errors in such measurements (precipitation measurements typically underestimate the snowfall considerably). It determines the amount of new snow from the measured snow depth and the settling rate estimated by the model. The measured snow depth is compared to the snow depth predicted by the model for the theoretical case that no snowfall has been taking place. The difference is taken as a new snow depth. (Bartelt and Lehning, 2002)

Initial conditions mean the specification of a new snow properties. The new snowfall mass can be expressed using new snowfall height Δh_n and new snowfall density ρ_n, when the snowfall begins at time t_n. The new snow height is discretized into finite elements, and they are added to the existing grid. (Bartelt and Lehning, 2002) The elements are added if relative humidity is higher than 50-70% and reflected short wave radiation is lower than 200-250 Wm^{-2}, depending on the model version. During the settlement period when the depth is decreasing, the model predicts depth independent of the measurements, so a good description of the snow pack mass balance is obtained only if a good estimation of the snow pack settling rate and new snow density is possible. (Lehning et al., 1998)

The procedure sets the model snow height to the measured one during periods of snowfall. So the estimation of the initial snow density is important to model the mass balance of the snow cover correctly. The relationship between new snow density and meteorological parameters is derived statistically from long term measurements in the Swiss Alps. The density prediction is limited to a range between 30 – 150 kgm^{-3}. The regression is valid for 30-60 minutes time interval. (Lehning et al., 2002b). The new snow density parameterisation is discussed further in Chapter 5.

Knowing the density, the volumetric contents can be defined. Normally it is assumed that new snow is dry (θ_w=0). The initial temperature of the new snow is air temperature.

The initial vapour pressure is determined by assuming that moist air within the new snow is at the fully saturated vapour pressure, which is the function of the temperature:

$$p_a(t_n, z)=p_s(T_n) \tag{4.3}$$

New snow falls in an undeformed state:

$$U_i(t_n, z)=0 \tag{4.4}$$

The initial strains are all zero. The initial stress is determined from the overburden pressure. The microstructure of new snow is described as follows. New snow has dendricity of 1 and sphericity of 0.5. New snow grain and bond radii can be changed; originally they are assumed to be 0.15 mm and 0.0375 mm respectively. (Bartelt and Lehning, 2002)

Boundary conditions

In SNOWPACK there are two possibilities for the boundary conditions for the energy exchange on the snow pack surface. The first is Neumann boundary conditions, where surface heat flux is determined using the meteorological parameters (taking into account net long-wave radiation energy, sensible heat exchange, latent heat exchange and heat flux from rain).

It is also possible to use the Dirilecht boundary conditions:

$$T_{ss}(z=h, t)=T_h(t) \tag{4.5}$$

and

$$T(z=0, t)=T_g(t) \tag{4.6}$$

where T_{ss} is the measured surface temperature and T_g is the measured ground temperature.

Displacement at the ground surface is always zero:

$$U_i(z=0, t)=0. \tag{4.7}$$

Two Neumann boundary conditions are specified for the vapour diffusion equation:

$$D\frac{\partial p_a}{\partial z} = q_h \tag{4.8}$$

and

$$D\frac{\partial p_a}{\partial z} = 0 \tag{4.9}$$

where q_h is the vapour mass flux at the snow pack surface (Bartelt and Lehning, 2002).

Processes included in the boundary conditions modelling are snowfall, rain, short wave and long wave radiation, sensible and latent heat exchange (surface hoar formation, sublimation), snow drift and wind pumping. The surface heat fluxes are parameterised assuming a neutral atmospheric surface layer, which is justified over snow in presence of moderate to high wind speeds in complex terrain in Alpine conditions. Slightly stable conditions may be present at low wind speeds. The Monin-Obukhov similarity theory is used, and the theory takes into account the effect of changing the height of the measurement sensors from the snow surface. (Lehning et al., 2002b) Mass and energy exchange models in SNOWPACK are most suitable for alpine conditions. The reliability of the models has to be validated in flatlands, and the models have to be changed when using in forested conditions. (Lehning et al., 2002b)

To deal with wind pumping the SNOWPACK –model has a wind speed description analogous to canopy flow: the wind speed does not vanish at the snow surface. This is a new principle in the snow cover modelling. Snow surface albedo is calculated by statistical model, so either reflected or incoming short wave radiation can be given. The albedo parameterisation is discussed further in Section 5.4. of this work. If neither incoming long wave radiation nor atmospheric emissivity is obtained, SNOWPACK estimates the atmospheric emissivity and calculates the incoming long wave radiation. (Lehning et al., 2002b) The parameterisation of the initial and boundary conditions are presented in detail in Appendix III.

4. 5. Numerical solutions

The four governing differential equations are solved with the finite-element method. The finite element approximation leads to the matrix system:

$$[C]\{\dot{S}\}+[K]\{T\}=\{Q\} \tag{4.10}$$

where $\{\mathbf{S}\}^{\mathbf{T}}$ is the vector of unknown field variables, which are defined at the *N* finite-element nodes.

$$\{S\}^T=\{T_s,\theta_w,u_i,P_v\} \tag{4.11}$$

The matrix [C] includes the specific heat, water vapour and water capacity matrices, and matrix [K] the finite-element heat conductivity, vapour diffusion and stiffness matrices. The right-hand side vector contains the energy sink and source terms, the mass of melt water produced or refrozen, the self-weight of the snow pack and the water vapour mass due to the sublimation or deposition onto the ice matrix. The system is only loosely coupled via the constitutive relations and vector {Q}. Each equation of the matrix system is solved independently using a block Gauss-Seidel method. Typical time steps for the implicit time integration are of the order of 15 minutes. (Bartelt and Lehning, 2002)

4.6. Model output, model versions and development

The SNOWPACK –model has been written using C programming language, and it can be used in any Unix environment with only minor alterations. Use in Linux and Windows environments is also possible. The most recent model version is operational version 7.4.1. This version includes also simple soil model. It is combined to a Java based graphical user interface SN_GUI. The model version used in this work is operational version 5.0, which corresponds to research version 1.0. The version was planned to be used together with graphical software IDL, where the graphical output could be studied.

In IDL the following model input time series can be studied:

- Air temperature
- Relative humidity
- Wind speed and direction

- Short wave radiation (in/out)
- Long wave radiation (in/out)
- Ground temperature
- Surface temperature
- Snow pack height
- Rain rate

The following time series are derived from the model input, can be studied from IDL graphics and are used in the SNOWPACK simulations:

- Absorbed short wave radiation
- Albedo
- Net long wave radiation
- Long wave radiation emissivity
- Surface energy exchange
- Sensible heat flux
- Latent heat flux
- Vapour pressure in air and in snow
- Temperatures in depths of 25, 50 and 100 cm
- Dew point difference

Model output includes graphical time series of the following snow pack quantities:

- Snow pack mass and water equivalent
- Surface melt water runoff
- Mass change from runoff
- Height of new snow and change in water content in 3, 6 and 24 hours
- Temperature
- Temperature gradient
- Density
- Number of grains and bonds
- Volumetric contents of ice, water and air
- Grain dendricity and sphericity
- Grain and bond size
- Coordination number
- Viscosity
- Thermal conductivity
- Strain
- Strain rate
- Surface hoar
- Interface stability
- Displacement
- Stress
- Depth hoar index
- Drift index

Evolution of some of the quantities through the winter, like temperature and density profiles, can be animated.

It is also possible to get numerical output of the snow pack profiles during different times of the winter with selected time step. The profile output includes layer by layer:

- Julian day of the formation date
- Height from the ground surface
- Temperature
- Density
- Liquid water content
- Grain diameter
- Grain class in three number code including major grain type, minor grain type and indication of melt

At the moment the SNOWPACK –model has been used in central Europe, North America, Scandinavia, Japan and Greenland. The model use has also been planned in Antarctica. Different conditions naturally cause problems in the model use, and force to continue the model development.

Formulations for sensible and latent heat fluxes are valid for neutral atmospheric conditions. An extension to stable stratification on larger flat areas like Greenland, is in preparation. A more detailed treatment of the short wave radiation penetration is also in preparation, as well as a model component that describes the interaction of radiation with vegetation in the snow cover. A link to the probability of avalanche formation in certain snow cover is a next step in the SNOWPACK development. The SNOWPACK model development will focus on dynamics of thin critical layers like surface hoar, melt-freeze crusts and ice lenses. The comparison algorithm (agreement score calculations, see Appendix IV) will also be altered to include these layers. (Lehning et al., 2002b) Parts of the one dimensional model are planned to be extended to two or three dimensions. (Bartelt and Lehning, 2002)

Areas needing improvement in SNOWPACK –model are especially surface hoar formation and wet snow metamorphism processes. (Lundy et al. 2001) More work has to be done also on the initial stage of snow metamorphism, meaning the change from precipitation particles into small rounded or faceted particles. (Fierz and Lehning, 2001)

4.7. Recent model validation

The first validation study of the SNOWPACK –model was made by Lehning (1998). A very good agreement between measured and modelled snow depth in Klosters, Switzerland, indicated that the settling rates were well predicted. The ablation was somewhat underestimated. The deduced precipitation rates seem to be more reliable than the standard precipitation gauge measurements. (Lehning, 1998)

A thorough validation of the SNOWPACK model has been made by Lundy and others (2001) in mountainous part of Montana. To obtain an objective validation of the model the measurements and observations were not only compared visually, but statistical means were used. Problems here are differences in simulated and measured parameters, different formats and resolutions used. The level of agreement was evaluated using statistical measures for temperature, density, grain size and grain type. The agreement score method is described in detail in Appendix IV of this work. (Lundy et al. 2001)

The different statistical descriptors were used for the output parameters to evaluate the model's ability to match the observations: The mean bias indicating the direction of the expected model error; the root mean square error estimating the expected magnitude of error; Pearson's correlation coefficient indicating linear correlation; Nash-Suttcliffe coefficient of efficiency and index of agreement by Willmott and Wicks. Because grain type is not a numeric parameter but measured on a categorical scale, two Chi-Square based statistics, Cramer's Phi and Sakoda's adjusted contingency coefficient, were used to check the degree of association between the observed and modelled grain types. (Lundy et al. 2001)

The model predicted the snow cover temperature well. Model accuracy decreased slightly near the snow pack surface, and with colder temperatures. Slight difficulties arose when temperatures approached 0°C. Early in the winter SNOWPACK predicted the settlement quite accurately, but in the springtime it underestimated the snow pack densification. There was also a consistent underestimation of the measured density for the densities greater than 250 kgm^{-3}. (Lundy et al. 2001)

The comparison of predicted and observed grain size was problematic, and very little can be said about the accuracy of the model in this sense. However, the agreement was found to be rather poor. There are problems both in the modelling (adjusted new snow grain size; limitations in the grain growth) and in the observations (subjective grain size estimate, estimation based to the grain shape). Relationships between observed and modeled grain types were not strong either, partly due to similar problems than with grain type. A common classification system does not exist between the model (sphericity and dendricity) and observers. (Lundy et al. 2001)

Lehning and others (2001) have made a model validation during winter 1999/2000 in the Swiss Alps. The agreement scores (See Appendix IV) were calculated through the winter for density, temperature, grain type and grain size. The individual scores were also combined to get an overall agreement score for the match of measured and simulated profiles.

During the measurement period in March the agreement score for the grain size was around 0.8. The model failed to reproduce a low density layer, and this dropped the agreement score for density to 0.7. The temperature had a high score of 0.9, in the uppermost layers the agreement was not that good. Only an agreement of 0.3 was reached for the grain type. The measurers observed several layers of rounded faceted crystals, which were not included into model version first used. The model metamorphism and classification codes were altered and this grain type included; after this the agreement score for grain type rose to 0.7. The overall agreement score rose also from 0.65 to 0.77 after the change. The overall agreement score was around 0.8 all through the winter for the two stations used, as well as the scores for density. (Lehning et al., 2001)

From the results of the study by Lehning and others (2001), the energy balance processes at the beginning of the melt season were noted to need improvement. The scores for liquid water content and temperature fall when melt-freeze dynamics start to take place. The scores rose again with the spring ripening of the snow pack. (Lehning et al., 2001)

In a study by Bartelt and others (2002) the comparison between simulated and measured snow profiles in the Swiss Alps during avalanche winter 1999 showed good general agreement. For example growth of faceted crystals at the base of the snow pack was modelled, as well as the time it takes to break down the dendritic structure of the new snow. The model correctly predicted the temperature variations in the snow pack, including the isothermal snow packs in the spring and minor melt periods during the winter. (Bartelt et al., 2002)

The calculated and measured snow heights were in good agreement, but there was a small systematic underestimation of snow ablation. The overall performance of the model is best checked by evaluating the mass balance of the seasonal snow pack, because it depends both on the dry snow mass balance (snowfall, wind drift) and also on the energy balance (melting, sublimation, rain). Modelled water equivalents agreed very well to the sum of the daily new snow water equivalents for the accumulation period with a small systematic overestimation of modelled ones. The melting period was also captured by the model, but a systematic underestimation of the melt rate existed during the final stage of the melt season. (Bartelt et al. 2002)

The agreement between modelled and measured snow surface albedo had been very good in the Swiss Alps. Deviations are seen in the high frequency variability, but this is not thought to be important for the overall energy balance. SNOWPACK is noted to give a realistic picture of the layered snow cover structure, also of critical thin layers like surface hoar and melt-freeze crusts. (Lehning et al., 2002b)

The validation of the model was once again done in the Swiss Alps by Lehning and others (2002b) using the agreement scores. The overall score was on average above 0.8 with a small scatter between the years. It was slightly higher than for the two stations analysed by Lehning and others (2001) due to improvements in this more recent model version, which now includes a parameterisation of wind pumping and an improved turbulent flux parameterisation. (Lehning et al., 2002b)

The temperature was predicted best, followed by density, while on average grain size and grain type showed more scatter and a lower score. The partly empirical formulations governing grain growth and metamorphism were less accurate than the formulations for the mass and energy balance. Some of the scatter is also due to subjective observations. (Lehning et al., 2002b)

A preliminary validation of the SNOWPACK –model in Finnish conditions has been made by Grönholm (2003). This work concentrated on model performance in grain type simulation during one winter in Hyytiälä, in Southern Finland. In this work the agreement scores for grain type varied between 0.7 and 0.95. The following chapter in this work, chapter 5, deals with a thorough validation of the SNOWPACK –model in Finland.

5. Validation of the SNOWPACK –model in Finland

In this chapter SNOWPACK -model validation carried out in Finland is described. The earlier SNOWPACK model validation includes for example studies by Lundy and others (2001), and Fierz and others. The study by Lundy and others (2001) includes detailed statistical validation of the model, but all the other studies concentrate on visual intercomparison of the model output and observations, as well as use of the agreement scores (see Appendix IV). Normally studies have concentrated on few locations with similar snow climatology. No study of the model sensitivity to the input data has been conducted.

For these reasons the model validation in Finland was done in five different snow zones to allow a better understanding of the model's ability in different snow climates. No model fitting has been performed on the basis of the results of a single location or year, but the model performance and its differences have been looked at five locations and during two years in each location.

Overall performance of the model has been studied using the visual comparison, comparison between observed and modelled snow cover evolution, and agreement scores. In addition to this, one location was selected for detailed model sensitivity testing site. Several test runs were made to see the model's reactions to different input data and boundary conditions. Sensitivity tests including systematic changes to different input quantities were also performed.

In the validation a bit old model version (Operational version 5.0) has been used, despite the fact that the more recent version would have been available during the validation. Choice to use the version 5.0 was based on the use of this version also by Grönholm (2003), who started the model validation work in Hyytiälä during the year 2000/2001, as well as in the climate change work described in Chapter 6.

5.1 Data

5.1.1. Snow data

Overall performance of the SNOWPACK model has been studied during two winters (1999/2000 and 2000/2001) in four different locations in Finland: Santala, Mekrijärvi, Oulanka and Kilpisjärvi. The locations and their descriptions are in table 3.2. During the winter 2000/2001 an intensive model verification campaign was also carried out in Hyytiälä, and other during melt period in 2002/2003. Hyytiälä (61°51' N; 24°17' E) is located in thin maritime snow zone, and the main biotypes in the area are coniferous, mainly pine, forests and fields.

The comparison was made between model output and snow pit studies including measurements of snow pack layering, layer depth, temperature, density, grain size and grain type. Traditional methods were used especially in the measurements (see section 3.1.5.). Several snow pits were dug both in open areas and in the forest in each location. In the model testing only representative open area snow pack structure in flat land is taken into account. Several snow depth and water equivalent observations were also made on study locations. Data of snow depth was also collected from the Finnish

Meteorological Institute (FMI), and snow water equivalent from the Finnish Environment Institute. In this way continuous time series of these quantities could be gathered; in other locations than Hyytiälä snow stratigraphy were studied only twice a winter.

The snow depth and water equivalent measurements are standard measurements, and they are of good quality. The snow depth is however measured only from one point near the FMI weather station, and it does not necessarily tell the average open area snow depth. The water equivalent measurements have a poor time resolution. Quality of the snow pack structure data is variable. Several different measurers have been gathering the data and this must have had an effect to the data quality. The winters in question were rather different from each other. Detailed description of the locations, measurement methods and the winter weather is in Chapter 3.

5.1.2. Meteorological data

For all of the locations synoptic data with either 3 hour (Mekrijärvi and Kilpisjärvi) or 6 hour (Santala, Hyytiälä and Oulanka) time resolution have been used as an input for SNOWPACK model. The used meteorological parameters were measured from 2 m height and they are listed in table 5.1.

Table 5.1. FMI data used for the validation simulations, height of the measurements is 2 m.

Parameter	*Unit*
Air temperature	°C
Relative humidity	0-100
Wind velocity	m/s
Wind direction	°
Cloudiness	1-8
Snow depth	Cm
Precipitation	mm in WE

As the set of input parameters required by SNOWPACK are little bit different, the meteorological data had to be handled before running the model. The incoming short wave radiation was estimated using a method described first by Iqbal (1983), with alterations made by Venäläinen (1994). Laevastu (1960) cloud correction scheme was also used with this method. Niemelä et al. (2001) have validated the methods and concluded that they give very reliable results for Finnish conditions. This method is described in detail in Grönholm (2003).

The snow surface temperature was set to air temperature. The ground surface temperature was set to 0°C. Setting air temperature as snow surface temperature is rather a rough estimate, when in many cases especially in clear conditions snow surface may be several degrees colder than overlaying air. For example the measurements in Finnish Arctic showed that the mean difference between snow surface and 2 m air temperature was 3.2°C (Koivusalo et al., 2001). The colder snow surfaces were also observed in this work, see section 3.2.4. Naturally the snow surface temperature cannot exceed 0°C. The ground temperatures measured in this work (see section 3.2.4.) were near zero all through the winter.

Incoming long wave radiation was estimated by the model. In the test runs described later also incoming long wave radiation was parameterized using a method differing from the one used in SNOWPACK –model. This method includes cloudiness, and it is described in Omstedt (1990).

The quality of the FMI data is good, but the poor time resolution could make it unreliable input for the snow cover modeling. The weather stations are situated in flat, open areas, in most cases small forest openings allowing good comparison to measured snow pack structure. In Santala and Mekrijärvi the distance between the measurement site and the weather station was 10-20 km, in other locations the weather station was situated close to the measurement site.

In Hyytiälä also meteorological data from the SMEAR II Station (Station for Measuring Forest Ecosystem-Atmosphere Relations) have been used. The station is located at the Hyytiälä forest station of the University of Helsinki, in the community of Juupajoki. (Vesala et al. 1998) The data gathered from SMEAR II station are listed in the table 5.2.

Table 5.2. SMEAR II data used for the validation simulations.

Parameter	*Unit*	*Device*	*Height*
Air temperature	°C	Pt-100 sensors, Ventilated and shielded	4 m
Relative humidity	0-100	Calculated from temperature and Air water content (Teflon pipes and gas analyzer URAS 4)	4 m
Wind velocity	M/s	Vector cup anemometer	4m
Wind direction	°	Vector vane	Above canopy
Shortwave radiation	Wm^{-2}	Reeman pyranometer	Above canopy

SMEAR II data are of good quality. All measurements in Hyytiälä are half an hour averages calculated from 1-minute data. Unphysical or disturbed data are rejected before calculation. (Grönholm, 2003) FMI measurements of snow depth and precipitation are used together with the SMEAR II data in Hyytiälä.

5.2. Model validation in different locations

5.2.1. Snow cover evolution

The following quantities of snow cover evolution were studied from both the simulated and real winters from all of the locations: snow cover formation, melt and duration (in days), date of maximum snow depth, maximum depth (in cm) and water equivalent of the snow cover (in mm). The results are listed in tables 5.3 and 5.4. Hyytiälä is given a table on its own, because of different measurement winters there.

Table 5.3. Observed and simulated snow cover evolution in different locations.

Santala	*1999/2000*		*2000/2001*	
	Observed	*Simulated*	*Observed*	*Simulated*
Formation	19.12.	19.12.	29.12.	28.12.
Melt	19.3.	31.3.	12.3.	19.3.
Max date	30.12.	31.12.	26.1.	25.1.
Duration	92	104	75	83
Max depth	9	7	14	13
Max WE	20	15	30	23
Mekrijärvi	*1999/2000*		*2000/2001*	
	Observed	*Simulated*	*Observed*	*Simulated*
Formation	5.11.	5.11.	14.11.	14.11.
Melt	26.4.	9.5.	21.4.	22.4.
Max date	17.3.	20.3.	5.3.	4.3.
Duration	173	186	159	160
Max depth	111	110	59	58
Max WE	260	340	130	157
Oulanka	*1999/2000*		*2000/2001*	
	Observed	*Simulated*	*Observed*	*Simulated*
Formation	11.11.	10.11.	20.11.	23.11.
Melt	7.5.	10.6.	2.5.	1.5.
Max date	10.3.	10.3.	5.4.	4.4.
Duration	179	214	165	161
Max depth	106	105	75	75
Max WE	256	325	180	190
Kilpisjärvi	*1999/2000*		*2000/2001*	
	Observed	*Simulated*	*Observed*	*Simulated*
Formation	9.10.	9.10.	30.10.	31.10.
Melt	1.6.	16.6.	13.5.	1.6.
Max date	29.3.	30.3.	12.4.	12.4.
Duration	236	251	196	214
Max depth	124	123	74	73
Max WE	309	380	245	205

Table 5.4. Observed and simulated snow cover evolution in Hyytiälä.

Hyytiälä	*2000/2001*		*2002/2003*	
	Observed	*Simulated*	*Observed*	*Simulated*
Formation	17.12.	24.12.	1.11.	24.10.
Melt	23.4.	26.4.	22.4.	23.4.
Max date	23.3.	22.3.	2.2.	8.2.
Duration	127	123	172	181
Max depth	43	42	49	49
Max WE	95	117	100	125

Rather large differences are seen between observations on different years in the table, but the overall tendency of increasing duration, maximum depth and water equivalent when going towards north is clear. During snowy winters the snow depth and water equivalent in maritime Mekrijärvi may also exceed the ones in Oulanka in the taiga zone.

It is easily seen from the table that SNOWPACK uses the measured snow depth during the accumulation periods: observed and simulated snow cover formation, the date of the maximum depth and maximum depth follow each other closely. Melt is however in most of the cases prolonged, and this increases simulated snow cover duration to unrealistic values, on average by 7%.

Observed maximum water equivalent may differ greatly from the real maximum water equivalent of the site because of the poor measurement resolution both in time and space. The differences between observations and simulations for this quantity may for these reasons be unrealistic. SNOWPACK tends to give too high a maximum water equivalent values, which means too high densities when the snow depth is correct. The difference between observed and simulated water equivalents was on average 20%. The difference was bigger during the snowy winters. In Santala the model gave exceptionally low values. No clear trend can be seen for the agreements when going towards north.

The date of first complete wetting of the snow cover was also checked from the simulations, but there is lack of the comparison data.

5.2.2. Snow depth and water equivalent

In the figure series 5.1-5.3 the measured and simulated snow depths are presented for each location and winter separately. For the accumulation periods the SNOWPACK model uses the measured snow depth in the calculations, but during the winter time blowing snow and settlement periods the snow depth is calculated by the model. Also during the melt period the snow depth is calculated independently from the measured one. In the figures most attention should be paid to these ablation periods and the agreement between simulations and reality during them.

The SNOWPACK has certain problems in representing the snow depth changes in Santala for both of the winters, but the overall variability of the snow depth typical for ephemeral snow zone is seen. An interesting feature in Hyytiälä simulation is the model's inability to melt all the snow away, when the snow cover forms and melts several times before the build-up of the winter snow cover. In Mekrijärvi, Oulanka and in Kilpisjärvi the winter time snow depth is very well simulated, also the ablation periods with only a couple of exceptions. These exceptional periods are melt periods, not dry snow settling or blowing snow periods. In the spring time the modelled snow depth is typically overestimated for these sites, as the melting is too slow in the model.

Because of a lack of the surface temperature measurements the air temperature was used as a snow surface temperature. A test run was made replacing this temperature with constant 0°C for the melting period in Hyytiälä 2000/2001. This made the snow melting even slower, and when the Neumann boundary conditions were replaced with Dirilecht boundary conditions the snow melt was practically stopped.

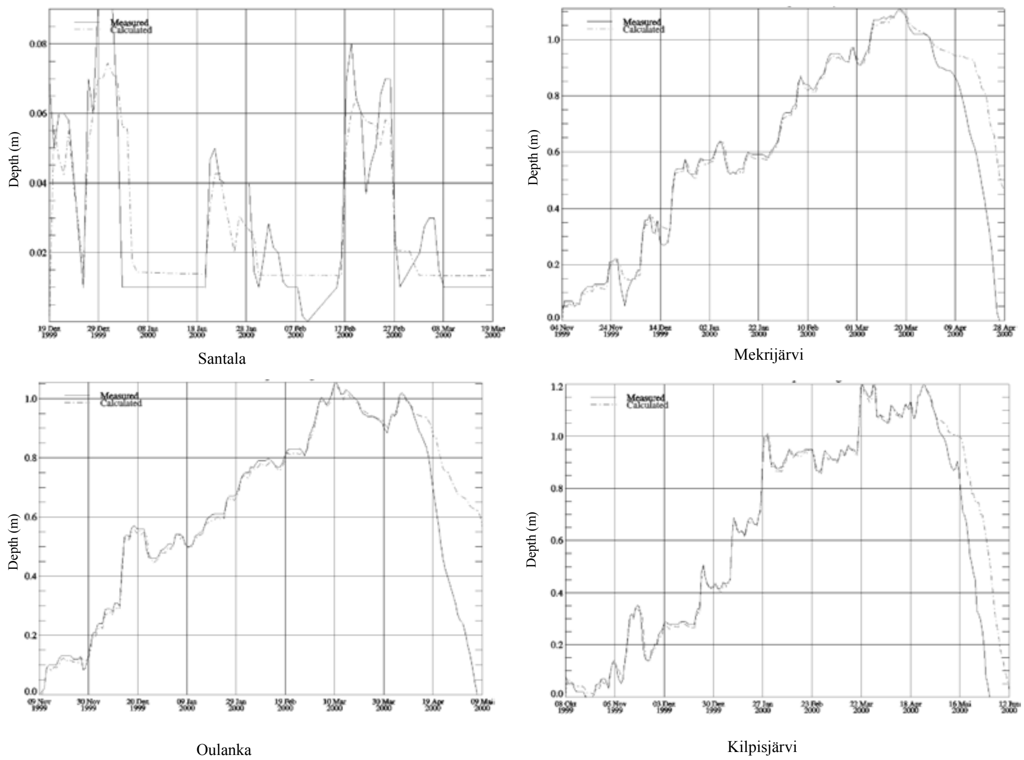

Figure series 5.1. The measured and simulated snow depths in Santala, Mekrijärvi, Oulanka and Kilpisjärvi during winter 1999/2000. Snow depth data by FMI.

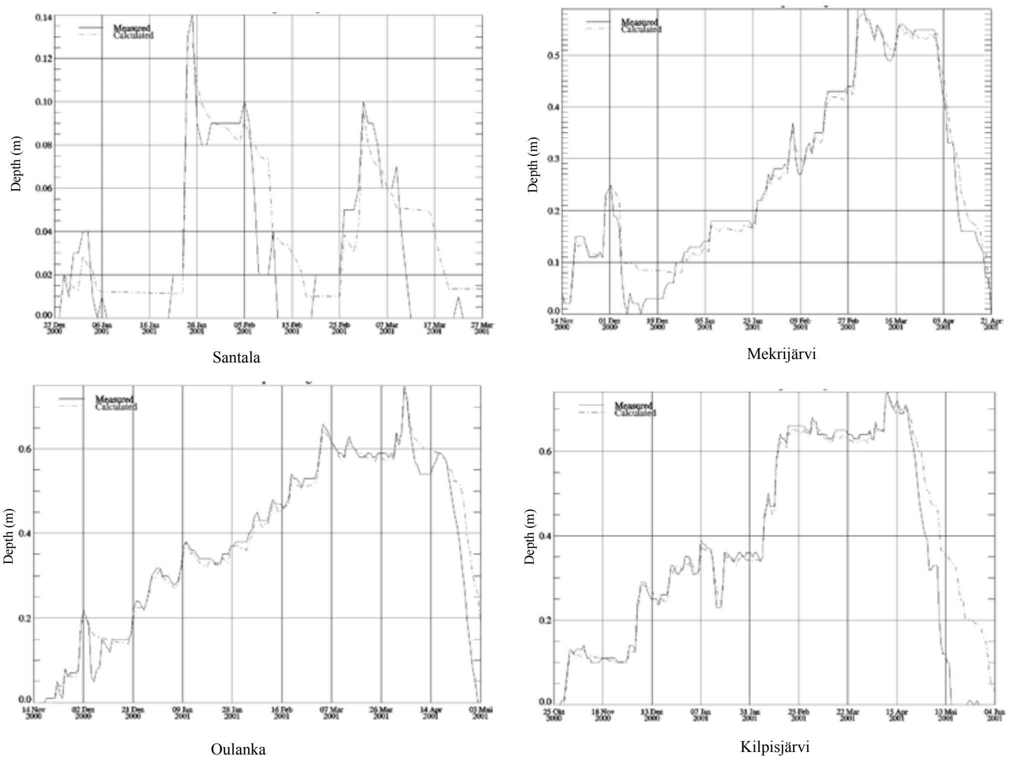

Figure series 5.2. The measured and simulated snow depths in Santala, Mekrijärvi, Oulanka and Kilpisjärvi during winter 2000/2001. Snow depth data by FMI.

Unfortunately data available of the water equivalent of snow were so sparse in time and space that no reliable validation of the model could be done. In most of the cases water equivalent measured during these measurement campaigns or by the Finnish

Environment Institute was markedly lower than the simulated ones. Only one example showing both the simulated and measured water equivalents (latter showing also the spatial variability) is included in the figure series 5.3, Hyytiälä 2000/2001. The black bars show the observed minimum and maximum water equivalents in the location (10 measurements), and the grey bars are based on data from the Finnish Environment Institute (50 depth and 10 density measurements), whose measurements were made in Orivesi, 20 km from Hyytiälä. Reasonable overall agreement between measurements and simulations is shown between the measurements from the site and simulations. The model overestimates the water equivalent greatly during the spring time when comparing to the Finnish Environment Institute data. The distance between the measurement and simulation location of course makes the comparison difficult.

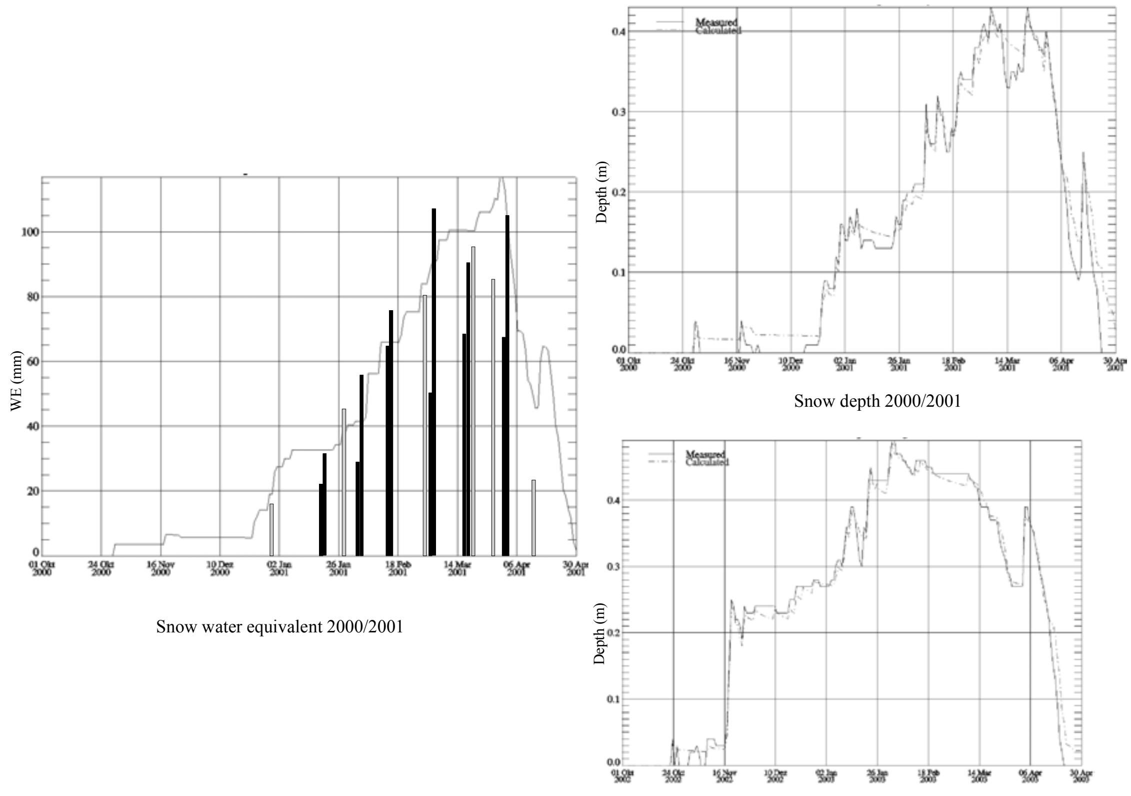

Snow water equivalent 2000/2001

Snow depth 2000/2001

Snow depth 2002/2003

Figure series 5.3. The measured and simulated snow depths in Hyytiälä during winters 2000/2001 and 2002/2003; measured and simulated snow water equivalents in Hyytiälä during winter 2000/2001. Snow depth data by FMI. Black bars are based on the measurements from the location, grey bars on the data from Finnish Environment Centre from Orivesi.

5.2.3. Visual comparison

In figures 5.4-5.8 the modelled snow pack structure evolution during the two winters as well as some observed snow pack structure profiles are presented for the different locations. The main interest in these figures is placed onto the snow microstructure, and especially onto the grain type of the snow. The shading code differs from the one in the figures in the section 3.2. This is because outputs of the SNOWPACK –model are used in figures 5.4-5.8, and observed profiles wanted to be kept comparable to the shading used in these. The code is shown in figure 5.4 to help to distinguish between different grain types; the grain type code is also marked in the figures. In the figures evolution of the stratigraphy is easily seen, as well as temporal continuity of the layers.

It is important to notice the differences between observed snow depth and snow pack structure evolution between different locations and different winters. Perhaps the most remarkable difference between winters 1999/2000 and 2000/2001 is the difference between the amounts of snow in most of the snow zones studied. In maritime, taiga and in the tundra zones the maximum snow depth during winter 2000/2001 was not much more than half of the one during 1999/2000. Also the snow cover formed later and melted earlier during the winter 2000/2001. The difference between winters 2000/2001 and 2002/2003 was not that pronounced in Hyytiälä. There was more snow in Santala during 2000/2001 than during 1999/2000, but both of the winters showed continuous snow cover formation and melt typical for ephemeral snow zone.

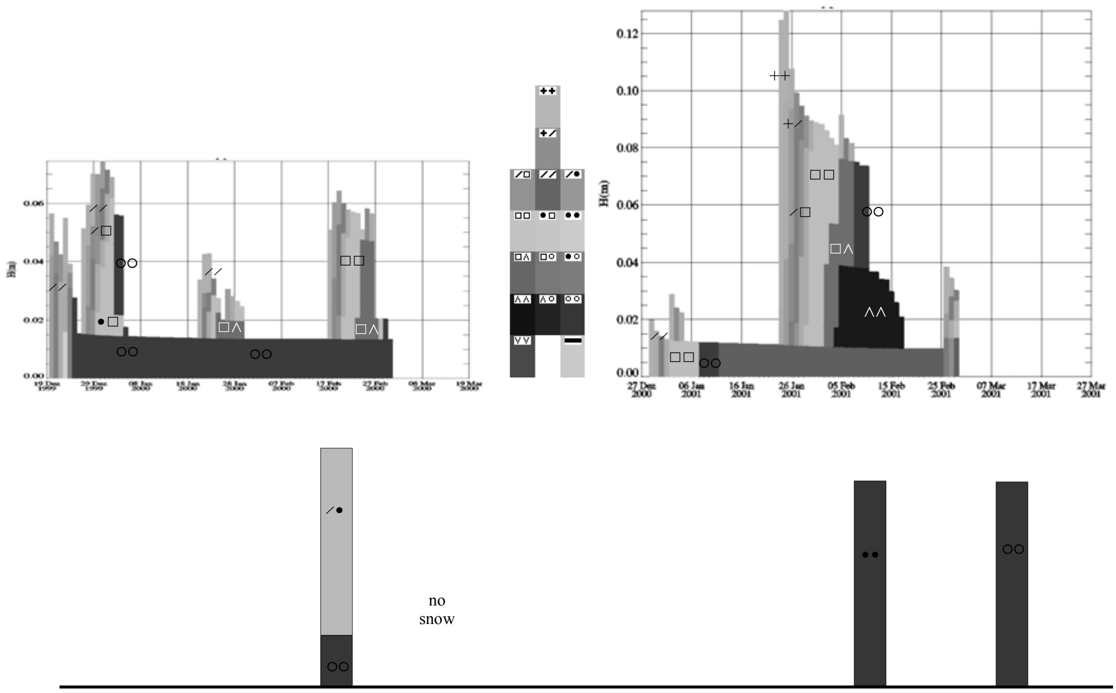

Figure 5.4. The modelled snow pack structure evolution in Santala during winters 1999/2000 and 2000/2001, as well as snow pit observations from the location.

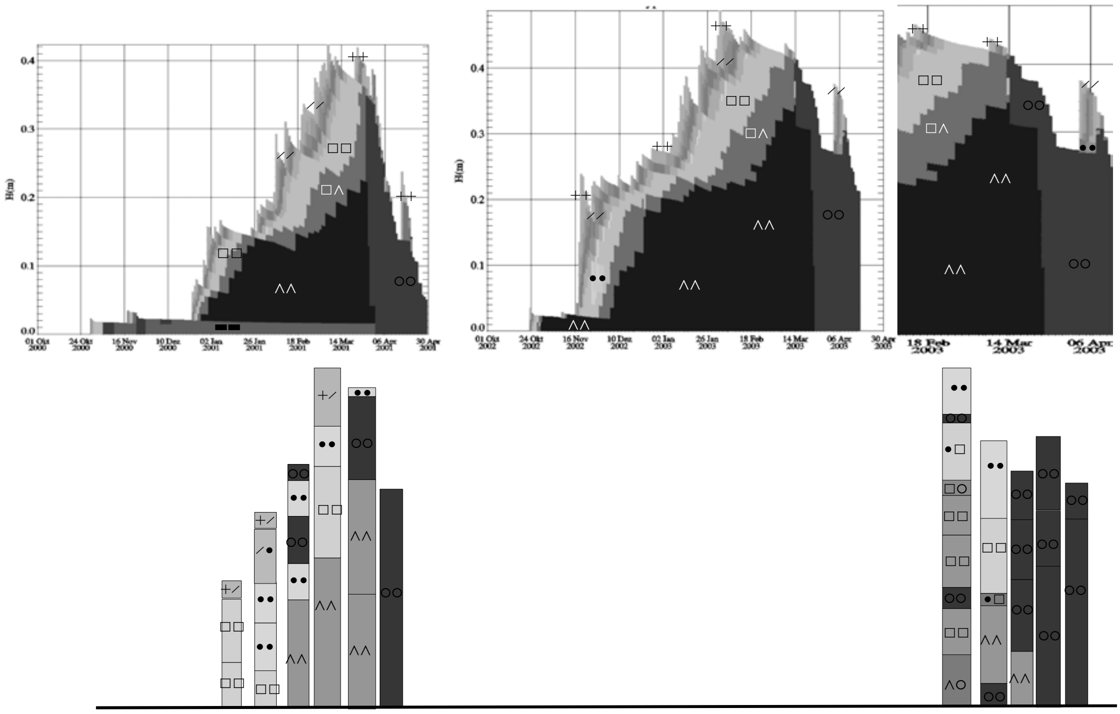

Figure 5.5. The modelled snow pack structure evolution in Hyytiälä during winters 1999/2000 and 2000/2001, as well as snow pit observations from the location.

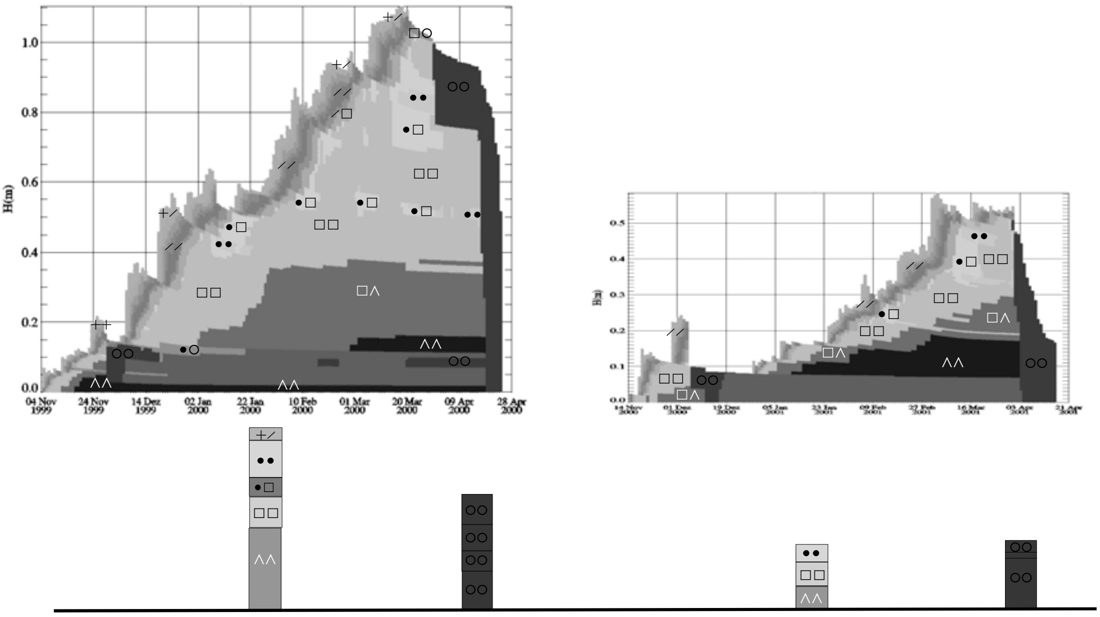

Figure 5.6. The modelled snow pack structure evolution in Mekrijärvi during winters 1999/2000 and 2000/2001, as well as snow pit observations from the location.

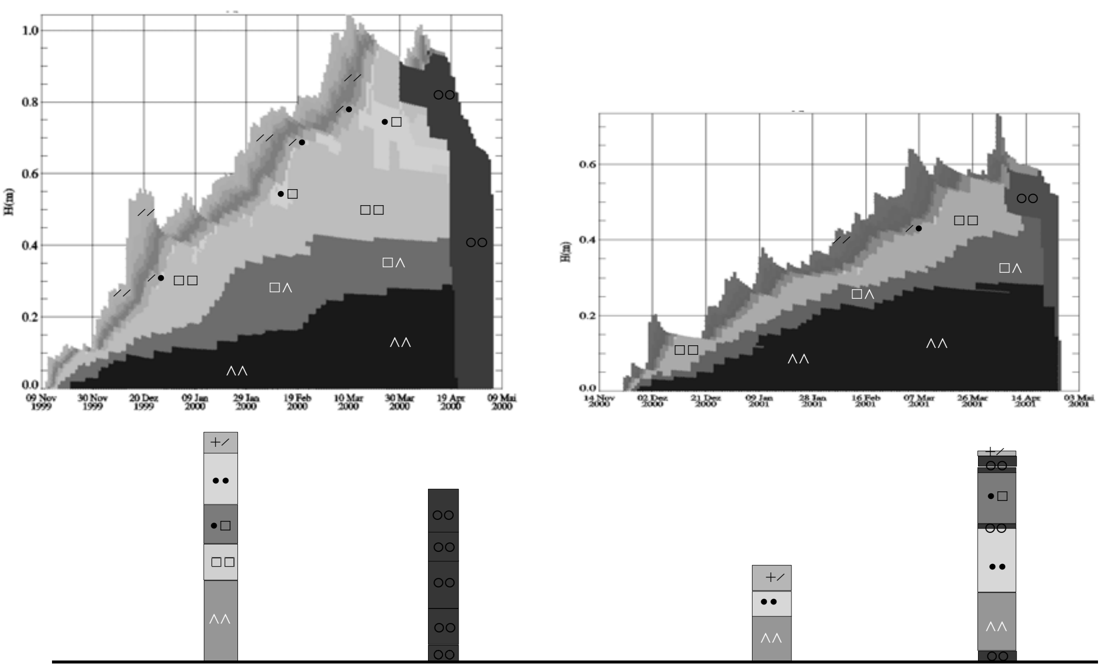

Figure 5.7. The modelled snow pack structure evolution in Oulanka during winters 1999/2000 and 2000/2001, as well as snow pit observations from the location.

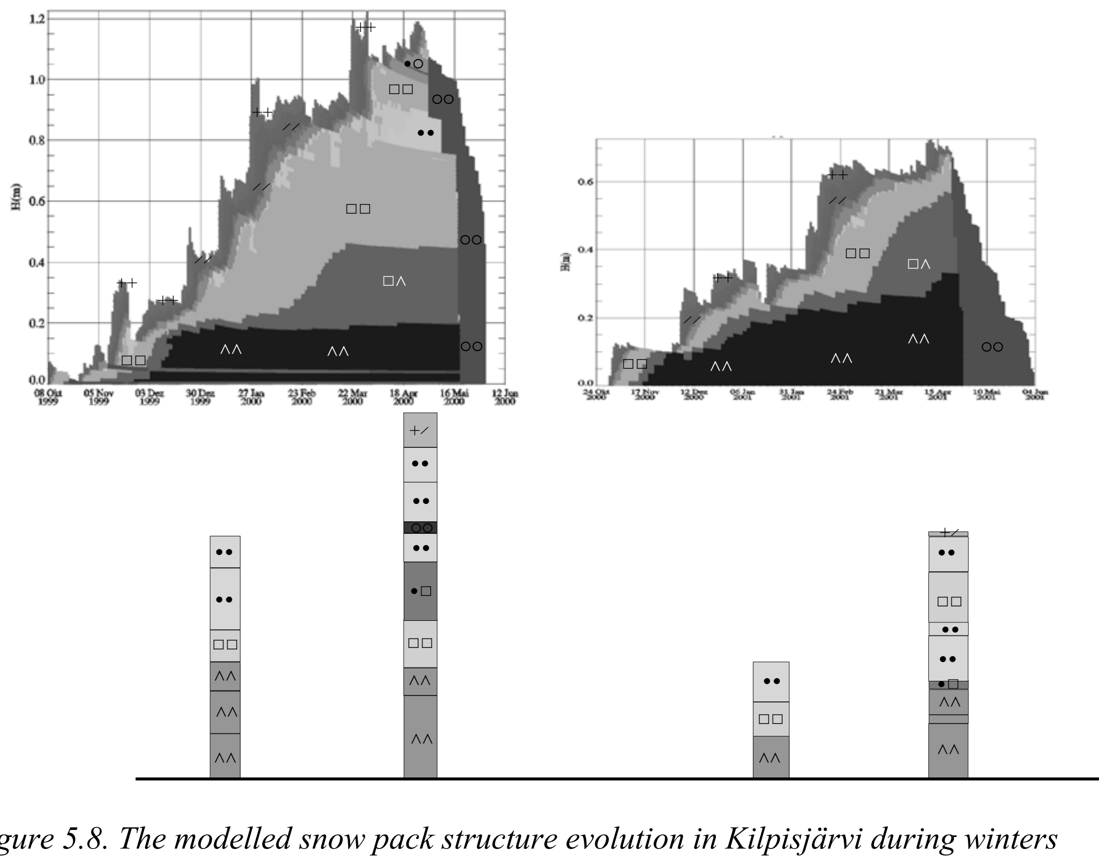

Figure 5.8. The modelled snow pack structure evolution in Kilpisjärvi during winters 1999/2000 and 2000/2001, as well as snow pit observations from the location.

As to the differences in snow pack structure between the two winters, no marked differences are seen. In both of the winters the simulated snow pack structure shows typical stratigraphies and grain type evolutions for the snow zone in question. In Santala the forming of either dry or wet snow cover and soon after this melt or melt-freeze of the snow is seen. In Hyytiälä and in Mekrijärvi the maritime snow cover is formed; in Hyytiälä the snow depth was lower, because this site is situated in a thin part of the snow zone. The structure in Mekrijärvi fits more closely to the description of the maritime snow: melt features are present in the snow cover, as well as quite a large fraction of rounded grains. The snow cover simulated in Hyytiälä seems to be too cold to be realistic. The snow pack structures simulated in Oulanka and Kilpisjärvi are very similar, as expected, because the input data in Kilpisjärvi are from below the tree line. Both of the locations show cold and dry snow packs mainly consisting of new snow and faceted grains. During 1999/2000 also some melt features not typical for the Kilpisjärvi region are shown in the simulations.

The simulated snow covers could be divided into two classes; wet and dry snow covers, which were separated by existence of the melt features in the snow cover. Locations in the ephemeral and maritime snow zones belong to the first, the ones in taiga and tundra zone to the latter. The taiga and tundra zone snow packs could not be separated from each other on the basis of simulations, and in not all the time the simulated maritime snow covers showed maritime features.

The overall agreement between measured and simulated snow pack structure varied from place to place. Only a few measurements were available to perform the comparison, so no far reaching conclusions can be made on the basis of this; the Hyytiälä situation was best because of the regular snow pit measurements during 2000/2001 and melt period in 2003. Results of the visual comparison are given below in the table 5.5 for different locations and winters.

In this comparison the differences in snow depth between simulation and measurements are not dealt with. The distance between snow pit measurement site and FMI snow depth measurement site may be several kilometers, and the local variability of the snow depth makes the comparison difficult, even if the snow pit locations have been tried to be chosen as representative for the location as possible.

Another problem in the comparison is the different description of the grain types by an observer and the model; also no two observers give identical snow pit observations. Consequently, no attention is paid for the slight differences in grain types. New or rounded snow, faceted snow and wet or refrozen snow have been chosen as main categories for the grain types.

During the winter 2000/2001 also some runs were made replacing the measured snow depth with precipitation data. For some locations (Kilpisjärvi and Mekrijärvi) the model was not able to complete the calculations, most probably because of the large amounts of liquid precipitation during the melt season. In figures 5.9-5.10 the snow pack structure evolution calculated using precipitation data is presented for Santala, Hyytiälä and Oulanka.

Table 5.5. Results of the visual comparison between modelled and observed snow pack structures for the different locations and winters.

Location	*Year*	*Agreement*
Santala	99/00	Good
Santala	00/01	Early winter: Reasonably, no faceted crystals observed
		Late winter: Poor, no snow on the ground
Hyytiälä	00/01	Early winter: Reasonable, more rounded grains and less melt layers observed
		Middle winter: Reasonable, more rounded grains and different melt layers observed
		Late winter: Good
Hyytiälä	02/03	Early period: Reasonable, more rounded grains and melt layers observed
		Late period: Good
Mekrijärvi	99/00	Early winter: Good, but no refrozen layer observed everywhere
		Late winter: Very good
Mekrijärvi	00/01	Early winter: Good, but no refrozen layer observed everywhere
		Late winter: Very good
Oulanka	99/00	Good
Oulanka	00/01	Early winter: Reasonable, more rounded grains observed
		Late winter: Reasonable, more rounded grains and melt layers observed
Kilpisjärvi	99/00	Early winter: Good, but no melt layers observed everywhere
		Late winter: Reasonable, some rounded grain and melt layers shifted
Kilpisjärvi	00/01	Early winter: Good
		Late winter: Reasonable, more rounded grains observed

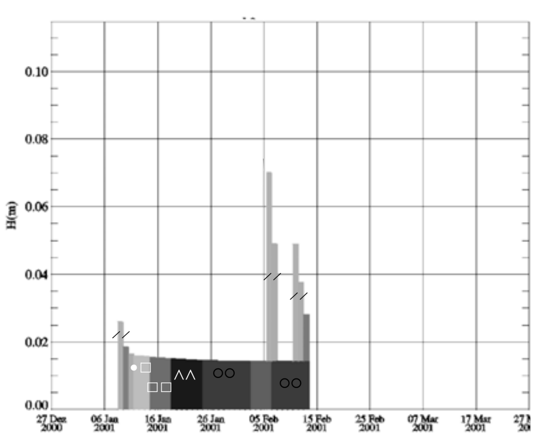
Santala 2000/2001

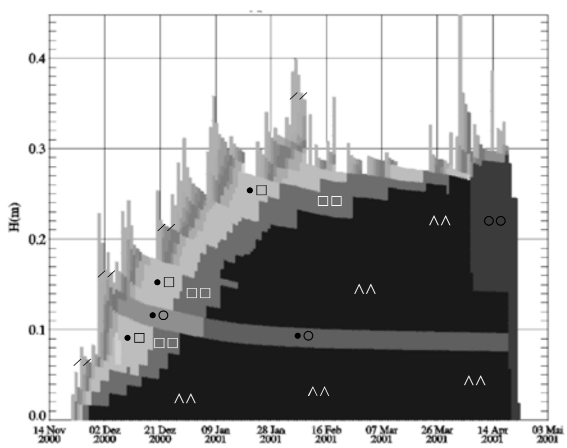
Oulanka 2000/2001

Figure 5.9. The modelled snow pack structure evolution calculated using precipitation data in Santala and Oulanka during winter 2000/2001.

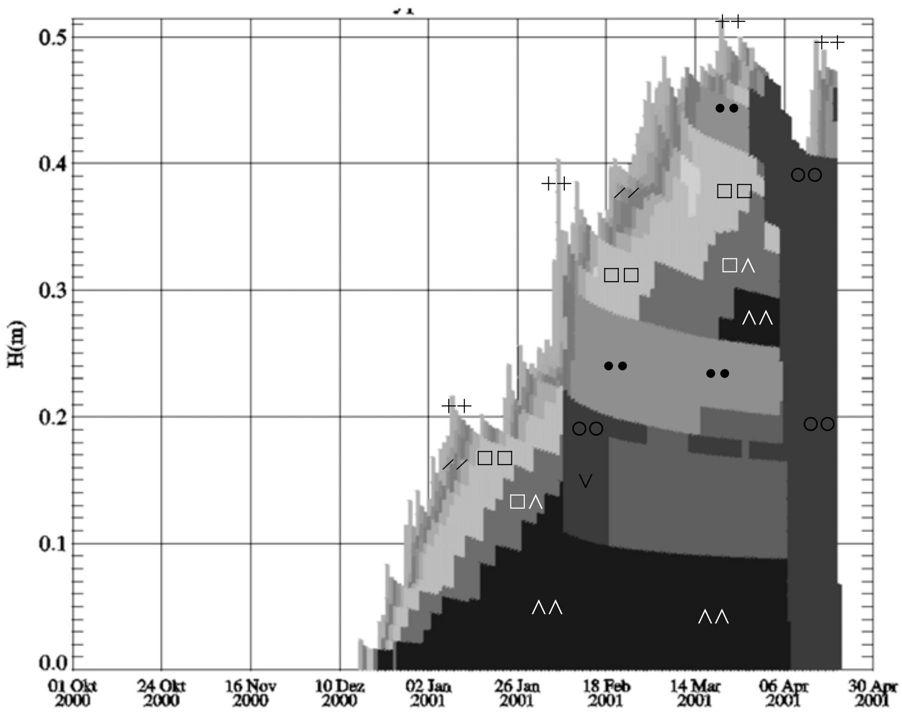

Figure 5.10. The modelled snow pack structure evolution calculated using precipitation data in Hyytiälä during winter 2000/2001.

In Santala the model fails to reproduce the correct evolution with these boundary conditions. In Oulanka the beginning of the winter is reasonably well simulated, but later the amount of snow is largely underestimated. Also there are marked differences in the snow pack structure between these runs; the most significant feature is melt-freeze layer seen in the precipitation run output. This layer can also be found from the late winter measurements, but not from the ones from early winter. In Hyytiälä the formation of the snow cover is more realistic using the precipitation data, but the snow depth is too high, and the melting too rapid. The snow pack stratigraphy is more realistically modeled using the precipitation data, the only exception for this is a period in the middle of the winter.

The solid precipitation error varies between 13% to 66% including error by wind, wetting and evaporation. The error due to an unsuitable position is linked with the wind error. (Koivusalo et al., 2001) The precipitation data were also corrected using a method described by Solantie and Junila (1995) for Tretjakov type precipitation gauges. This method takes into account the effect of the wind and fastening of snow to the gauge. The results were not better when using this corrected precipitation data in the calculations.

The differentiation between the solid and liquid precipitation in the SNOWPACK – model should not cause error in the estimation of the amount of the snowfall. When the air temperature is below +1.1°C, the precipitation is assumed to be solid. According to the study by Koivusalo and others (2001), 25 % of the precipitation is solid in Finland when the air temperature is +1.3°C; 50 % in +0.9°C; 75% in 0°C and 90% in –1.2°C.

In the model the irreducible water content (the volumetric fraction of liquid water, after which the water begins to drain) is called residual water content. It is possible that rather a small value for residual water content, 0.05, has something to do with the failing of the model in some cases. In more recent model versions the value of 0.08 is being used. In a study by Koivusalo and others (2001) the value was most often observed to be between 0.16 and 0.05 in Finland. On the other hand, in Kuusisto (1973) the value was observed to be between 0.02 and 0.05 in Finland.

5.2.4. Agreement scores

Not only visual comparisons between the simulated and observed snow pack stratigraphies were made, but also an objective comparison method was used. This means the calculation of agreement score (see also Lehning and others, 2001) between simulations and observations of each studied snow pack structure quantity, and overall agreement score. In this method the modeled snow profile is first stretched to match the height of the observed snow profile, and after this the mapping of the layers is performed to find the matching layers. Scores describing agreement between observed and modeled layer properties are calculated for each property separately, and finally these scores are combined as an overall agreement score using certain weighing factors for each property. Agreement score ranges between 0 (no agreement) and 1 (perfect agreement). Properties studied are temperature, density, liquid water content, grain size and grain type. The method is described in detail in Appendix IV.

For the purposes of this study minor changes were made to the procedure described in Lehning and others (2001). Liquid water content was not taken into account in calculations, because of the lack of field measurements. Weighing factors for all of the studied properties were kept as 1, and so all of the properties were treated equally important.

In figure 5.11 the evolution of the agreement scores during the winter 2000/2001 in Hyytiälä is shown. It is easy to see that overall agreement between observations and simulations is quite high through the winter. The agreement score drops when melting starts, although the agreement score for temperature reaches 1 when the snow cover is isothermal. Scores for temperature and grain size are high through the winter, whereas grain type and density go through more changes.

In figure 5.12 the agreement score evolution is shown for the melt period 2003. No dramatic drop for the agreement score is seen here, unlike to the figure 12. Here the score for grain type shows great variability, and also the score for the temperature is much more variable. For both winters the average overall agreement score was around 0.6, which is a reasonably good agreement between the simulations and observations.

In table 5.6 the agreement scores for all of the locations except Hyytiälä are listed. The scores could be calculated only twice a winter because of the lack of snow pit observations. The snow profiles shown in figures 5.4-5.8 are used as observed snow profiles here.

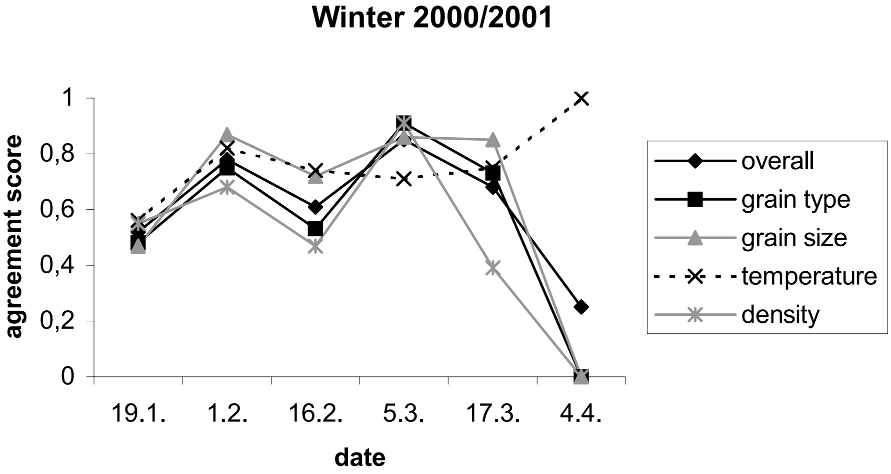

Figure 5.11. The evolution of the agreement scores during the winter 2000/2001 in Hyytiälä.

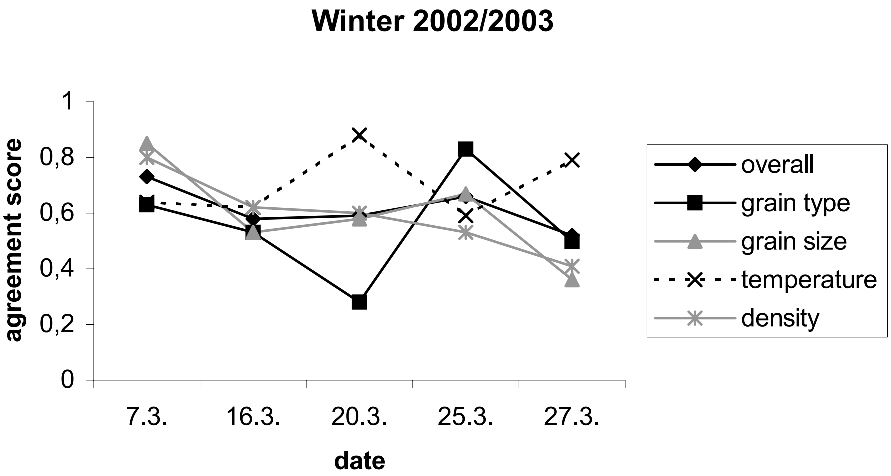

Figure 5.12. The evolution of the agreement scores during the melt period 2003 in Hyytiälä.

The same trends like in Hyytiälä's case can be found here: the scores are relatively high especially in the early winter cases and with the exception of ephemeral Santala; temperature and grain size have normally higher scores than grain type and density.

The conditions during the especially good (overall agreement score more than 0.80) and poor agreement (overall agreement score less than 0.30) were studied. Also the Hyytiälä scores were taken into account here. Some common features were found from the snow conditions and weather conditions during the good agreement scores: the snow depth was quite homogenous in the area, the snow was relatively soft and porous and consisted of "winter snow", meaning in most of the cases dry rounded and faceted snow in turns. The weather was cold and dry. Also during poor agreement scores some common features could be found: in most of the cases the snow was isothermal, dense, hard and wet or melting. The snow depth was not homogenous; maybe there were bare plots on the ground already. The weather was warm.

Table 5.6. The agreement scores for different locations during early and late winters 1999/2000 and 2000/2001.

1999/2000	*Overall*	*Grain type*	*Grain size*	*Temperature*	*Density*
Santala					
Early winter	**0.25**	0	0	1	0
Late winter	**0.48**	0.13	0.80	1	0
Mekrijärvi					
Early winter	**0.67**	0.70	0.77	0.69	0.50
Late winter	**0.60**	0.67	0.58	0.67	0.49
Oulanka					
Early winter	**0.65**	0.78	0.54	0.63	0.63
Late winter	**0.76**	0.57	0.83	1	0.64
Kilpisjärvi					
Early winter	**0.65**	0.43	0.89	0.67	0.61
Late winter	**0.88**	0.92	0.82	0.86	0.93
2000/2001	*Overall*	*Grain type*	*Grain size*	*Temperature*	*Density*
Santala					
Early winter	**0.54**	0.50	0.50	0.52	0.65
Late winter	**0**	0	0	0	0
Mekrijärvi					
Early winter	**0.76**	0.67	0.78	0.58	0.82
Late winter	**0.28**	0.05	0.35	0.63	0.07
Oulanka					
Early winter	**0.88**	0.85	0.89	0.90	0.88
Late winter	**0.51**	0.37	0.50	1	0.17
Kilpisjärvi					
Early winter	**0.77**	0.77	0.68	0.81	0.83
Late winter	**0.81**	0.81	0.91	0.68	0.86

Also the quality of the measurements naturally affects the agreement scores: replacing the measured grain sizes and densities with estimates, differing grain type definitions and snow pit depth deviating from the local average all worsened the agreement scores slightly.

5.3. Model sensitivity

5.3.1. Test and sensitivity simulations

To test the sensitivity of the model output to changes in model input or boundary conditions several test runs were made. Sensitivity tests aimed at two goals: to see which output quantities are most sensitive to the changes in input, and on the other hand to see which input quantities have the greatest effect on the modelled snow pack structure.

Sensitivity testing was done using SMEAR II data from Hyytiälä Forest station. The control run, which was used as a baseline to which all the other run outputs were compared, consists of measured air temperature, relative humidity, wind speed, wind direction and incoming solar radiation with 30 min time resolution. In addition the snow depth observations from FMI were used. Snow surface temperature was set to air temperature and ground surface temperature to 0 °C. Cloudiness observations from FMI were used when incoming short wave and long wave radiations were calculated; precipitation data comes also from FMI. Neumann boundary conditions have been used in the control run simulation. In table 5.7 all the other runs made in the sensitivity testing are listed, as well as changes in input compared to the control run.

From the model output of each run the following quantities were studied:

1: Date of snow cover formation
2: Date of snow melt
3: Date of maximum snow depth
4: Date of first complete wetting of the snow pack
5: Maximum snow depth
6: Maximum snow water equivalent
7. Snow cover duration

In addition, from the modelled snow profiles for March 15 (the average date for present day maximum snow depth), the following quantities were calculated:

8: Snow depth
9: Snow water equivalent
10: Bulk density
11: Bulk temperature
12: Bulk grain size
13: Fraction of new or rounded grain snow
14: Fraction of faceted grain or depth hoar snow
15: Fraction of icy or melting snow

5.3.2. The most sensitive snow parameters

The absolute changes in percentages for all of the studied quantities were calculated between each test run and control run. For quantities 1-4 including dates the percentile differences were calculated by comparing differences in dates to snow cover duration; temperature was handled in degrees of centigrade; quantities 13-15, which already are fractions calculated in percentages, simple subtraction of the control and sensitivity run outputs was carried out. The changes for different quantities were after this arranged by different runs. The quantities most often seen in the top 5 of the sorted tables were looked for, because these were the quantities most sensitive to the changes in input or boundary conditions of the runs. Thirteen different quantities could be found in top 5 ranges of the 31 runs, so for most of the runs the same quantities are the most sensitive ones. The results are listed in the table 5.8.

In class “grain form” the changes in fractions of faceted snow, rounded grain snow and wet or icy snow are combined; in class “WE” the same has been done to maximum water equivalent of the snow cover and water equivalent on March 15; and in the class “Depth” for maximum snow depth and depth on March 15.

Table 5.7. The runs made in the sensitivity testing of the SNOWPACK –model and the changes in input in these runs compared to the control run.

Run	*Differences*
Control	-
Dirilecht	Run made with Dirilecht, not with Neumann boundary conditions
Iqbal	Short wave radiation calculated using Iqbal parameterisation
Longwave	Long wave radiation calculated using parameterisation by Omstedt
Precipitation	Snow depth replaced with precipitation data
FMIsnow	6 hour synoptic data, Iqbal parameterisation in short wave radiation, snow depth
FMIprecipitation	6 hour synoptic data, Iqbal parameterisation in short wave radiation, precipitation
Water	Residual water content set to 0.04 (original 0.05)
ConstantAlbedo	Albedo model output replaced by constant albedo 0.78
Alb_old	Old albedo model (SLF1) used
Albmodel3	Most recent albedo model (SLF3) used
New_alb	New snow albedo set to 0.78 (original 0.90)
New_grsz	New snow grain radius set to 0.2 mm (original 0.15)
Dens_old	Old model for new snow density used
Density	New snow density model output replaced by constant 100 kgm^{-3}
AddTair	20 % added to air temperature
AddRH	20 % added to relative humidity
AddWS	20 % added to wind speed
AddRad	20 % added to short wave radiation
AddTsnow	20 % added to surface temperature
AddTGround	20 % added to bottom temperature
AddDepth	20 % added to snow depth
DimTair	20 % reduction to air temperature
DimRH	20 % reduction to relative humidity
DimWS	20 % reduction to wind speed
DimRad	20 % reduction to short wave radiation
DimTsnow	20 % reduction to surface temperature
DimTGround	20 % reduction to bottom temperature
DimDepth	20 % reduction to snow depth
AddTsnowDIR	20 % added to surface temperature, Dirilecht boundary conditions
DimTsnowDIR	20 % reduction to surface temperature, Dirilecht boundary conditions
3h	Control run time resolution changed to 3hours
6h	Control run time resolution changed to 6 hours
Tsnow0	Surface temperature set to 0 for melting period
Tsnow0DIR	Surface temperature set to 0 for melting period, Dirilecht boundary conditions
Ta3Ts0	Surface temperature set to 0 and air temperature to 3-8 °C for melting period
Ta3Ts0DIR	Surface temperature set to 0 and air temperature to 3-8°C for melting period, Dirilecht boundary conditions

Table 5.8. The most sensitive snow cover quantities in SNOWPACK –model based on the sensitivity test.

Quantity	*Times in top 5*
WE	35
Bulk temperature 15.3.	19
Grain form 15.3.	19
Bulk grain size 15.3.	16
Depth	15
Melt	12
Bulk density 15.3.	7
Duration	6
Wetting	6

The amount of snow seems to be most sensitive (combining WE and depth), after this the snow pack structural characteristics (bulk temperature, grain form and size, density), and after this the snow cover evolution characteristics (melt, duration, wetting).

Some runs could be found, which had small or zero effect on all of the studied quantities. These were runs with added ground temperature, altered new snow albedo, constant albedo and altered residual water content. For most of the cases the changes were large (more than 10%) for only few of the quantities. For runs with precipitation used as input, the changes were larger than for other runs.

In many cases input data for the modelling has poor time resolution (6h), the incoming solar radiation has to be estimated (for example Iqbal –parameterization) and snow depth data have to be replaced with precipitation data. The maximum changes, or errors, found in these analyses were 8%, 21% and 41%, respectively, for the most sensitive quantities for this kind of runs compared to the control run cases. Changes for most of the quantities ranged between 0-4%; between 3-28% for precipitation used as input.

5.3.3. The runs with largest effects

The other possible way to study the model sensitivity is to turn around the sorting method described above. Now the changes caused by different runs were arranged by different snow quantities studied. The runs most often seen in the top 5 of the sorted tables were looked for, because these were the runs having the greatest effects on changes in modelled snow conditions. 15 different runs could be found in top 5 ranges of the 15 quantities, so the scattering here is larger than for the most sensitive quantities case. The results are listed in table 5.9. Like in the section above, the bottom 5 values were not analysed because the zero or very small effects were common.

Most of the runs with large effects can be classified either as runs having changed amount of snow (39 times in top 5) or as runs having changed radiation scheme (24 times in to 5). Runs with changes in relative humidity, time resolution or new snow parameterization had minor effect on one or few quantities.

Table 5.9. The sensitivity test runs with largest effect on SNOWPACK –model outputs.

Run	*Times in top 5*
Precipitation	12
FMIprecipitation	11
Dirilecht	7
Iqbal	6
FMIsnow	6
DimDepth	6
Alb_old	5
AddDepth	4
6h	3
Longwave	3
DimRad	2
Constant_albedo	2
AddRh	2
Density	1
New_grsz	1

The precipitation/snow depth runs were most important for snow cover formation, depth and water equivalent and changes in radiation for snow melt and snow cover duration. For other quantities the effects were not so easily classified. Runs with changed snow surface temperature were made using the Dirilecht boundary conditions also; these runs appeared to have effect on grain size on March 15 as well as for snow bulk density and water equivalent on March 15. For most of the quantities, not all of the runs had any effect; in many cases only one or two thirds of the runs affected the model outputs.

5.3.4. Sensitivity using box plots

The differences in percentages described above were also used to draw box plots, which is a more descriptive way to study the model sensitivity. A box plot displays the locations of the basic features of the distribution of the data. The median of the data is represented by a horizontal line segment within the rectangle and the top and bottom areas show the upper and lower quartiles. Outer fences of the box plot indicate the extent of the data beyond the quartiles. Possible outliers are shown by dots. A box plot also shows a rough shape of the distribution of the data (symmetricity).

In the box plots shown in figures 5.13-5.15 the numbers on x-axis refer to the numbering of the studied snow cover quantities listed in section 5.3.1. The y-axis shows the differences between control run and test runs in percentages. Each of the boxes shows the distribution of the differences for all of the quantities separately. So in these plots information about the effect of a single test run is lost; all we see is the distribution of differences for example for date of the snow melt when outputs from all of the test runs are combined. The smaller the box, the less sensitive the snow cover parameter is to the changes in input or boundary conditions. Looking at the shapes and the locations of the boxes also the tendency to over- or underestimations and shape of the distribution is shown.

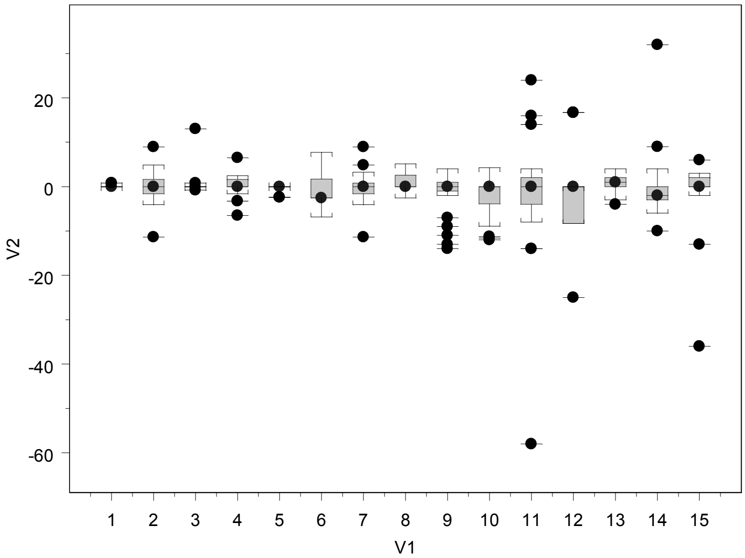

Figure 5.13. Box plots showing the distribution of all the test run outputs for different snow pack quantities. The numbers on the x-axis refer to the numbering of the studied snow cover quantities listed in section 5.3.1. The y-axis shows the differences between the control run and the test runs in percentages.

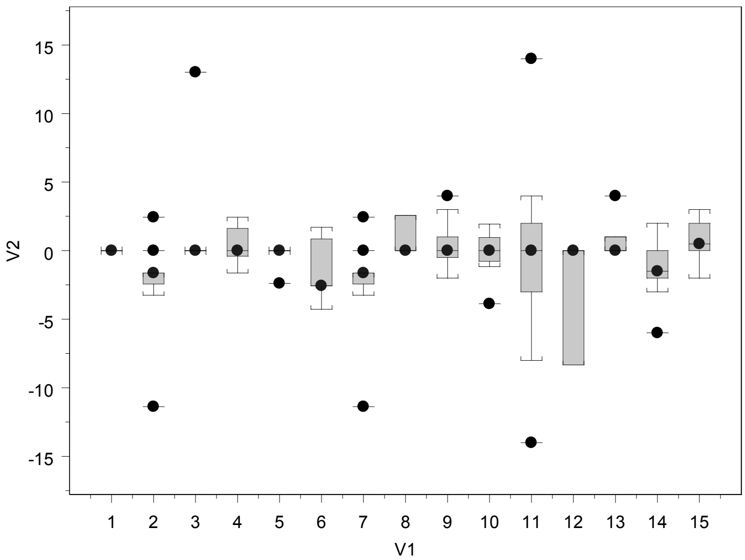

Figure 5.14. Box plots showing the distribution of the sensitivity run (only increases and decreases in the input file columns are taken into account) outputs for the different snow pack quantities. The numbers on the x-axis refer to the numbering of the studied snow cover quantities listed in section 5.3.1. The y-axis shows the differences between the control run and the test runs in percentages.

In the figure 5.13 all of the runs listed in table 5.7 are taken into account. In figure 5.14 only sensitivity test runs are used, which means only increases and decreases to the input file columns are taken into account. In figure 5.15 all the rest test simulations are used, and these include mainly runs with changed boundary conditions (new snow properties, albedo models, estimated short wave or long wave radiation).

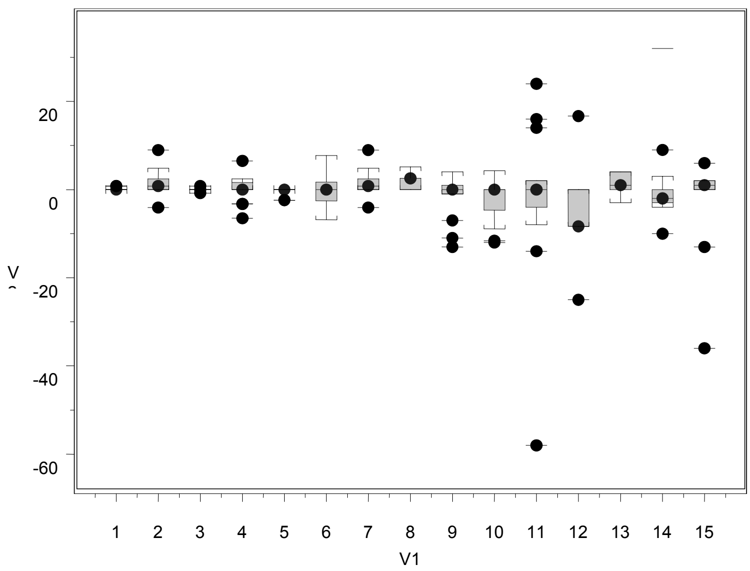

Figure 5.15. Box plots showing the distribution of the test run outputs for the different snow pack quantities. The sensitivity runs were not taken into account. Runs with changed boundary conditions (new snow properties, albedo models, precipitation data, estimated short wave or long wave radiation) are mainly dealt with here. The numbers on the x-axis refer to the numbering of the studied snow cover quantities listed in section 5.3.1. The y-axis shows the differences between the control run and the test runs in percentages.

From all of the figures the runs including changes in snow depth as well as runs using precipitation, not snow depth, are left out. Taking these into account increased the amount of outliers especially in snow depth and water equivalent cases, but did not change the overall pattern of the box plots greatly. It is reasonable to say that the use of precipitation data and changes in snow depth are very important for snow model outputs as was seen in section 5.3.3., but leaving them out from here makes the figures easier to read. Data set in these figures consists approximately of 30 runs, half of which sensitivity runs and half other test runs.

When looking at the figure 5.13, parameter 11, bulk temperature on March 15 is the only snow parameter clearly more sensitive than others. The situation is the same in figure 5.15. In figure 5.14 the temperature does not stand out so clearly, but also melt date, maximum water equivalent, snow cover duration and bulk grain size on March 15 have wide distributions.

Formation date, date of the maximum snow depth, maximum snow depth, snow depth on 15.3. and fraction of the rounded grains show a narrow distribution in all of the figures 5.13-5.15. This implies that they are the snow parameters not sensitive to the changes in model input. In reality, most of the listed quantities are strongly linked to the measured snow depth used by model snow depth during the accumulation periods, and their narrow distribution does not tell very much about the snow cover sensitivity. In figure 5.14, the sensitivity runs, also the water equivalent and bulk density on March 15 show relatively narrow distributions. Also the date of the first wetting and other snow type fractions (faceted and wet or icy snow) do not seem to be very sensitive.

When comparing these results with the ones in table 5.8, it can be seen that all of the snow parameters showing wide distribution in box plots are also found in the table 5.8 among the most sensitive parameters.

5.3.5. Comparison between test runs and observations

Overall agreement scores were calculated between observations in Hyytiälä 2000/2001 and all the different test runs listed in table 5.7. The resulting agreement scores can be found from the Appendix V. The average agreement scores, agreement scores between observations and control run and standard deviation of the agreement scores are shown in table 5.10 for every measurement date separately.

Table 5.10. The average agreement scores calculated from the ones between observations and test runs, agreement scores between observations and control run and standard deviation of the agreement scores for every measurement date separately.

	19.1.	*1.2.*	*16.2.*	*5.3.*	*17.3.*	*4.4.*
Ctrl-obs	0.52	0.78	0.61	0.85	0.68	0.25
Average	0.52	0.74	0.61	0.81	0.64	0.43
StDev	0.04	0.05	0.02	0.05	0.06	0.18
Variation	0.08	0.07	0.03	0.06	0.09	0.42

In all of the cases, except melting season 4.4., the overall agreement score between the control run and observations was as high or higher than the average for all of the test runs. This confirms the choices made for the use of selected input data from all the different possibilities. On the other hand, the standard deviations and coefficients of variation are relatively small all through the winter, which tells that the model overall output is not very sensitive to the changes in the input or boundary conditions. During melt period also the standard deviation and coefficient of variation are more than three times the ones during the winter season. This means that the model sensitivity grows towards the melting period, and also choices for the input data and boundary conditions become more important.

Many high values were found for agreement score on March 5, and many low values on April 4. Many of the test runs gave better agreement scores compared to the control run on January 19, February 16 and April 4, which were all relatively warm days, some with wet snow. None or only a few runs gave better agreement scores on February 1, March 5 and March 17, which in turn were cold and dry days. So the model sensitivity seems to be increasing with the more wet and warm snow and warmer weather conditions.

In table 5.11 the runs which have made the overall agreement score clearly better than the one using the control run are looked at. The same is done for the runs, which have worsened the overall agreement score remarkably.

Among the runs making the overall agreement score better were many times found Dirilecht boundary conditions and runs using precipitation data. This is somewhat surprising, because the Neumann boundary conditions were considered better because of the lack of the surface temperature data, and the precipitation runs shown in figures

Table 5.11. The runs which made the overall agreement score clearly better than the one using the control run; the runs which made the overall agreement score clearly worse than the one using the control run. Different days are treated separately.

	Runs with better agreement	*Runs with worse agreement*
19.1.	Dirilecht FMIprecipitation AddWS AddDepth DimTsnow Density Alb_old	Longwave DimDepth
1.2.	AddDepth	AddTair AddRH DimWS DimTG DimDepth Dens_old 6h resolution
16.2.	Dirilecht Iqbal Precipitation	AddTair AddRH DimWS
5.3.	-	Precipitation AddRH AddDepth DimDepth 3h resolution
17.3.	Dirilecht Precipitation	Longwave AddRad DimRH DimDepth New_grsz Albedo 3h resolution
4.4.	Dirilecht Precipitation FMIPrecipitation AddRH AddWS AddRad AddTsnow DimRH DimRad DimTsnow DimTG DimDepth Dens_old Alb_old Water	-

5.9 and 5.10 did not show too good agreement with observed snow cover evolution. It may be safe to conclude that the assumption that surface temperature equals air temperature is not very bad at least in Hyytiälä's case. Several more random runs are also seen in the table, especially in the beginning of the winter and during the melt season.

Changes in air temperature, relative humidity, wind speed and snow depth appeared several times among the runs with worse agreement scores. In addition to this also some more random runs were found in the table, as well as runs with worse time resolution than in the control run. This was expected, but the changes between control run and 3h and 6h time resolution run agreement scores is not big. Many of the runs found in the table 5.11 are also found in the table 5.9 with the runs with the largest effect to snow model outputs.

The melt season should be dealt separately because of the differences in wet snow behaviour compared to the one of dry snow. All of the test runs gave better or same agreement score with the observations than the control run. Among the runs were also some of the runs normally found among the runs making agreement score worse. It seems that slight changes in input or boundary conditions cause big changes in the output; the model sensitivity grows towards the melt period. The collection of runs seems more or less random.

Use of the most recent albedo model gave better agreements in half of the cases, especially during the melt period. Snow density, which also reflects the differences between observed and modelled snow depth, stays a problematic parameter also here.

5.3.6. Sensitivity using agreement scores

The last method used for the model sensitivity tests was to study the agreement scores between several different model runs. Here once again the control run was used as a baseline, to which all the other runs (29) were compared. To remind the reader, the closer to 1 the agreement score between the two runs is, the closer to each other the two studied snow profiles are. Here once again Hyytiälä 2000/2001 with 6 measurement periods are studied.

The average for overall agreement scores was close to constant ranging between 0.89 and 0.92. Smaller scores were found in the beginning and in the end of the winter. The averages for the agreement scores of the different snow parameters (temperature, density, grain size and grain type) were also calculated, and the average agreement scores on each measurement period were arranged by parameters. The bigger the agreement score for a certain parameter, the less deviation there is between different runs and the less sensitive the parameter is. From the sorted lists temperature was most often found in the top 2 of the lists; grain type only once. From the bottom 2 the temperature could not be found at all, grain type 5 times. Grain size and density were found equally often from the top and bottom parts of the lists. No differences were found between the early, middle or late winter. So with this method the temperature was found to be the least sensitive of these parameters, and grain type the most sensitive.

When comparing these results to the table 5.8, it is noticable that they are somewhat reversed. It is difficult to guess what causes this difference; the method is little bit different and here attention is paid to several snow profiles while as the results for table 6 are from study of a single snow profile and snow cover overall evolution. One would in any case assume to find the same properties to be the most sensitive ones.

Same method like in the sections 5.3.2 and 5.3.3 was used to study the sensitivity of the snow parameters and the runs with the largest effects, except that now the agreement scores described above were sorted. Four different tests were made. They are described below, and the results are collected in the tables 5.12 and 5.13.

Test 1: The sorting was done by different runs taking into account all the snow parameters. After this it was calculated how many times certain run was found from the top or bottom 5 of the sorted lists on each measurement date, and if the time of the winter had any effect.

Test 2: The sorting was done by different runs, like the test 1, but now all the dates were taken into account and the top and bottom 5 ratings were counted separately for all the snow parameters. Attention was paid if certain runs had more effect on certain parameters.

Test 3: The sorting was done by snow parameters taking into account all of the runs. The top and bottom 2 ratings were counted every measurement date like in test 1.

Test 4: The sorting was done by different snow parameters, like in test 3, but all of the dates were taken into account and top and bottom 2 ratings were counted separately for all the test runs. Sensitivity runs were left out from this analysis.

Tests 1 and 2 tell about the effect of the runs to snow cover modelling, while as the tests 3 and 4 can be used to check once again the sensitivity of the snow parameters to changes in input or boundary conditions.

Results of the tests 1 and 2 are listed in the table 5.12. Only the runs gathering more than 10 ratings have been included in the table.

The runs with most bottom 5 ratings have had lowest agreement scores with the control run, which means the largest deviations from the control run output snow profiles and bigger effect to the snow cover modelling. The results in table 5.12 confirm the ones listed in table 5.9: use of the precipitation or Dirilecht boundary conditions and changes in long wave parameterisation, snow depth or time resolution have the largest effects on SNOWPACK output.

As the runs with least effects were not studied before in the section 5.3.3, the top 5 ratings here give some new information. Albedo parameterisation and changes in short wave radiation, and especially changes in ground temperature do not seem to be very important for the SNOWPACK output. This is good news that comes to the estimating ground surface temperature and incoming solar radiation.

Table 5.12. The effect of the runs on snow cover modelling. Bottom ratings show large deviation from the control run output and large effect; top ratings show minor deviation and minor effect.

	Test 1		Test 2	
	Top 5 ratings	Bottom 5 ratings	Top 5 ratings	Bottom 5 ratings
AddTG	26		27	
New_alb	21		23	
DimRad	18		18	
Albedo	11		11	
AddRad	10		11	
FMIprecipitation		20		14
Precipitation		18		12
Dirilecht		15		12
Longwave		13		
6h resolution		12		10
DimDepth		12		

The effects of some of the runs were changing through the winter: increase in the snow depth and use of the Dirilecht boundary conditions had more effect in the beginning of the winter, while as the effect of time resolution increased towards the melt period. On the basis of test 2 results it can be said that only very few of the runs have a large effect on all of the snow parameters. Relatively few runs had any effect on the snow density, but the effect of these runs was large and intensive. Use of long wave parameterisation had a large effect only on grain size, use of precipitation on grain type and density and time resolution on grain type and size. Other runs having large effects on density were changes in the snow depth and use of the Dirilecht boundary conditions. These runs did not have large effects on other snow parameters.

The results of the tests 3 and 4 are listed in table 5.13. Only the runs gathering more than 100 ratings for test 3 and 50 ratings for test 4 have been included in the table. No sensitivity runs have been taken into account in test 4; the results should be in agreement with the results of test 2, this being a sort of transpose of the test.

Table 5.13. Sensitivity of the snow parameters to changes in input or boundary conditions using the agreement score tests, described in text. Top ratings show less variation between the runs; bottom ratings show large variation between the runs

.

	Test 3		Test 4	
	Top 2 ratings	Bottom 2 ratings	Top 2 ratings	Bottom 2 ratings
Temperature	120		67	
Density	107		54	
Grain size		118		54
Grain type		116		63

Of the four snow parameters studied here the temperature and density show the closest agreement with the control run for most of the test runs made. This implies once again that of these parameters temperature and density are least sensitive to changes in input and boundary conditions. Grain size and grain type are most sensitive to the changes, and it seems that the sensitivity runs with systematic changes in input are more important to the grain size; while as the test runs concentrating mainly on changes in boundary conditions have larger effect on grain type. Looking at the table 5.8 it is clearly seen that also there density is the least sensitive of the parameters studied here, and temperature, grain size and grain form have almost equal sensitivity. But, as was said already before, the insensitivity of the modelled temperature seems to be in contrast with the earlier results reported in this study.

The sensitivity of some of the snow parameters appeared to change during the winter. The sensitivity of the temperature was largest in the beginning of the winter, and of grain size in the melting period. The sensitivity of the density was almost constant through the winter, but the one of the grain type was relatively small during the beginning of the winter and melt period.

5.4. Testing the albedo sub-models

There is a sub-model for suface albedo calculations included in the SNOWPACK – model. Model is statistical, and it has been derived and evaluated against measurements from high Alpine sites in the Swiss Alps. It is a reliable and a stable model for those sites (Lehning et al., 2002b). In this section applicability of the model in Finland is discussed.

In SNOWPACK the user can choose from different albedo models. The first one (here SLF-1) includes only meteorological parameters, while the second (here SLF-2 and SLF-3, most recent version) includes also modelled or measured snow parameters.

The models have the form:

$$\alpha = 0.8 + \ln(1 + x)\,. \tag{5.1}$$

For SLF-1, x is a linear function of the meteorological parameters:

$$x = \beta VW + \gamma T_A + \delta T_{SS} + \eta RSWR + \kappa T_A T_{SS} + \lambda T_A RSWR \tag{5.2}$$

For SLF-2 x is a function of both meteorological and snow parameters:

$$x = \beta VW + \gamma T_A + \delta T_{SS} + \eta RSWR + \kappa T_A T_{SS} + \lambda\rho + \mu\theta_w + \nu RB + o DN + \pi SP + \theta FR \tag{5.3}$$

Here VW is wind speed (ms^{-1}), T_A air temperature (K), T_{SS} surface temperature (K), RSWR reflected short wave radiation (Wm^{-2}), ρ snow density (kgm^{-3}), θ_w liquid water content (0-0.08), RB crystal bond radius (mm), DN dendricity of snow crystals (0-1), SP sphericity of snow crystals (0-1) and FR categorical variable indicating previous melt and refreeze (0 or 1).

The SLF-3 model has the form

$$\alpha = 0.8047 + \ln(1.005 + x) \tag{5.4}$$

and

$$x = \beta VW + \gamma T_A + \delta T_{SS} + \eta RSWR + \lambda\rho + \mu\theta_w + \nu RB + o DN + \pi SP + \sigma RH + \varpi n + \upsilon RG \tag{5.5}$$

Here RH is air relative humidity (0-1), n days from the latest snow fall and RG crystal radius (mm). All of the models are limited to a minimum of 0.15 and a maximum of 0.95. (Lehning et al., 2002b) The parameter values for different albedo models are listed in table 5.14.

Table 5.14. Parameter values for different albedo models.

Parameter	*SLF-1*	*SLF-2*	*SLF-3*
α_0	0.8	0.8	0.8047
β	0.0053	0.0056	0.005784
γ	-0.041	-0.0052	-0.0002487
δ	0.016	0.0084	-0.0001659
η	-0.0015	$-6.8 * 10^{-5}$	$-1.803 * 10^{-5}$
κ	$-4.2 * 10^{-5}$	$-1.1 * 10^{-5}$	-
λ	$-5.3 * 10^{-6}$	-0.0003	$-4.692 * 10^{-5}$
μ	-	-3	-2.149
ν	-	0.06	-0.3057
ο	-	0.017	-0.07602
π	-	0.021	0.009639
θ	-	-0.032	-
σ	-	-	0.1287
τ	-	-	$-1.575 * 10^{-4}$
υ	-	-	0.1074

The measurements on snow surface albedo, snow properties and meteorological parameters were collected during two observation campaigns, one 24.4.-1.5.2002 (period 1) and other 23.4.-30.4.2003 (period 2) in Kilpisjärvi, Finland. April 2002 was relatively warm in Kilpisjärvi. In table 5.15 some comparison between long term average and the situation in 2002 is presented. In figure 5.16 mean daily air temperature and snow depth during the measurement period are presented. The end of April 2002 was warm: mean daily air temperatures were above zero for all the measurement period, and in the end of the month there was only half of the normal amount of snow on the ground.

Measurements were carried out near Kilpisjärvi Biological Station (69°03' N; 20°48' E). Elevation there is approximately 500 m above sea level, but the highest peaks in the area reach over 1000 m above sea level. Kilpisjärvi is situated in the tundra snow zone, where the snow cover is assumed to be relatively thin, dense and consisting mainly of wind packed layers and depth hoar. This is valid for snow on the lake ice and on fjell plateau above the tree line, but in the birch forest area snow is more like the taiga zone snow: relatively thick and homogenous and consisting mainly of rounded crystals and depth hoar. (Sturm et al., 1995) The variation of the snow depth in the tundra snow area is also notable in Kilpisjärvi: extreme cases are snowless deflation areas and snowbeds which can endure even many summers without melting totally.

Table 5.15. Average monthly values for some meteorological quantities in April in Kilpisjärvi (Finnish Meteorological Institute, 1991), and monthly values in April 2002 (FMI) for some quantities.

	Mean	*2002*
Average air temperature	-4.8°C	-1.4°C
Maximum temperature	+8°C	+10.4°C
Minimum temperature	-33°C	-21.9°C
Average cloudiness	61 %	74 %
Average snow depth 15.4.	91 cm	89 cm
Average snow depth 30.4.	79 cm	40 cm

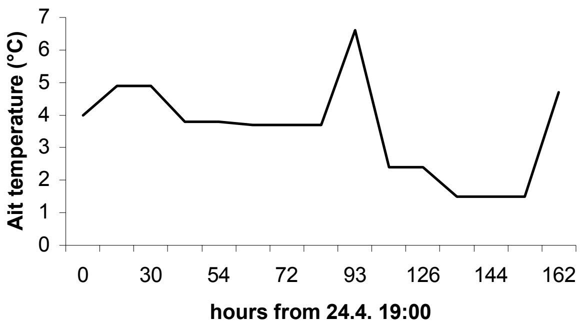

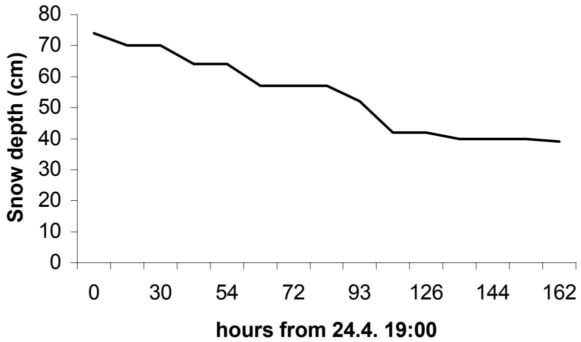

Figure 5.16. Weather conditions (FMI) in Kilpisjärvi during the measurement period 24.4.-1.5.2002: above mean daily air temperature, below snow depth.

A Middleton EP-16 pyranoalbedometer system was used to make albedo measurements. This system measured downwelling and upwelling irradiances from 300 to 3000 nm. The instrument is a modified thermopile pyranometer with an additional inverted sensor assembly. The dual sensors have been matched for response and sensitivity and their collector surfaces are parallel. The instrument was mounted on the end of a pole, which was clamped onto a tripod. This set-up placed the sensor head 1 m above the ground. A spirit level, which was built into the sensor assembly, was used to level the instrument. The EP-16 pyranoalbedometer was connected to a Gantner IDL-100 datalogger, which was set to scan at 10-second intervals, and record an average of 3 scans. This produced a dataset of upwelling and downwelling irradiance and total albedo with a temporal resolution of 30 seconds. The accuracy of the EP-16 pyranometers is 3%. Other sources of error include instrument tilt. The instrument was levelled with a spirit level located on the instrument housing so the tilt error is approximately 1%. Shading of the instrument is a problem especially in the forest where the sun can be totally shaded by a tree or a branch but the snow surface reflects the unshaded sunlight causing the albedo values to go over 1. As the sun moves in the sky, different branches and trees shadow the instrument causing spikes to become vivible in the time series measurement. (Rasmus, K. et al., 2003)

The snow depth and the depth of wet snow (on the lake ice) were observed near the albedometer two or three times a day. Surface values of the density, temperature, crystal size, crystal form and liquid water content were measured using standard methods (see Colbeck et al., 1990). Crystal size and form was studied, not only by estimating visually in the field, but also using digital image processing of crystal photos taken every time snow observations were made.

Albedos for the snow measurement moments were calculated taking continuous albedo measurements half an hour before and also half an hour after the measurement moment, and averaging albedo over this period. In the same manner also the average level of the reflected short wave radiation needed in the calculations was checked, and the effect of the changing cloudiness diminished. Observations by Finnish Meteorological Institute of air temperature, wind velocity, relative humidity, precipitation and cloudiness were available during the measurement period.

During period 1 measurements were carried out on the lake ice and in the sparse birch forest. In the beginning of the measurement period the ice on lake Kilpisjärvi was covered by dry snow. During four warm days snow turned into slush that froze from the surface during the night, and in the end the ice was covered by water. In the birch forest change was not that dramatic. Crystal form, crystal size and liquid water content of snow varied depending on the time of the day: the surface melted during daytime and refroze during the night. Crystal size increased steadily during the four days. Crystal type was the same all through the measurement period: depending on the time of the day snow surface consisted of clustered single rounded crystals with liquid water at the crystal boundaries or polycrystalline particles after the daily melt-freeze cycle.

In table 5.16 changes in measured snow parameters during period 1 are collected. Crystal size in the table is an average diameter of single surface crystals obtained by image processing. Snow observation times are hours from April 24 at 19:00, when the albedometer started continuous measurements.

The snow crystal structure is an important parameter affecting snow albedo. During the 2002 measurement campaign, as crystal type remained the same, crystal size is assumed to be one of the most important factors. This is a very difficult parameter to measure objectively. In the field conditions one tends to decide maximum crystal diameter to be the average crystal diameter. For this reason also crystal photographs were taken using field camera developed and built at the Department of Physical Sciences, University of Helsinki. Photos were digitalized and averages of minimum and maximum diameters and areas were obtained using ImageJ software for both single crystals and also for crystal clusters. This was done to find out which of the listed quantities are most important for the snow albedo. Example of the snow microstructure during the measurement period is shown in figure 5.17. The figure is a crystal photograph of the surface snow from the forest sampled 30.4.2002. Notice crystal clusters with several single rounded crystals, and also liquid water between the clusters.

Table 5.16. Changes in measured snow parameters during the measurement period 1. Numbers in Italics describe measurements in the birch forest.

Hours from 24.4. 19:00	Snow depth (cm)	Snow density (kgm^{-3})	Grain size (mm)	Water content (%)
0	36			
26	9	440		11
50	5	500		
64			1,33	
72			1,40	
90	*52*	*360*	*0,99*	*11*
112			*1,02*	
121	*39*	*380*	*1,03*	*6*
134	*39*	*380*	*0,91*	*8*
140	*33*	*380*	*0,92*	*11*
146	*26*	*390*	*0,93*	*3*
159	*30*	*360*	*0,95*	*11*

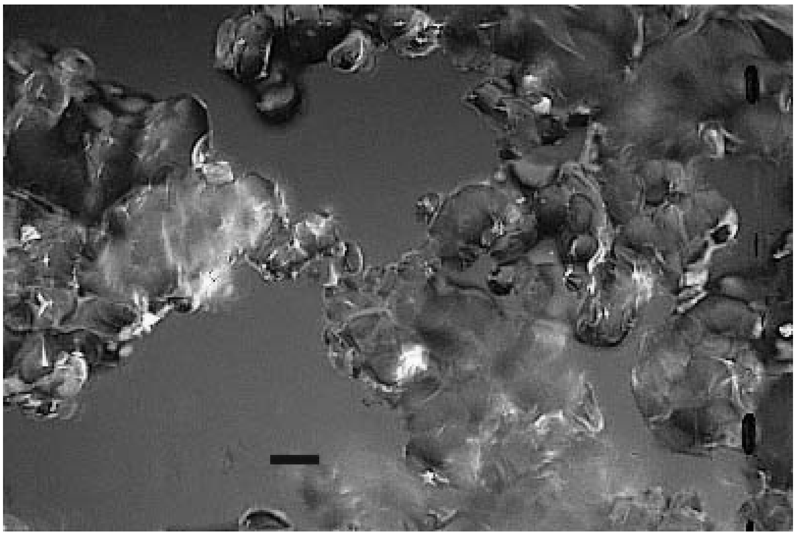

Figure 5.17. Snow microstructure 30.4.2002. Bar is 1 mm scale.

Comparisons between visual estimation and image prosessing results are presented in table 5.17. Hours in the column on the left are counted from April 24 at 19:00, when the albedometer started continuous measurements. Please notice that also image processing was slightly subjective, because crystal boundaries were unclear and they had to be marked manually.

Table 5.17. Comparisons between visual estimation and image processing results for different crystal dimensions in millimetres. Numbers in Italics describe measurements in the birch forest.

Hours From 24.4. 19:00	Single grain				Grain cluster			
	Maximum diameter	OBS	Minimum diameter	Average area	Maximum Diameter	OBS	Minimum diameter	Average area
64	1,33	1	0,94	1,44	4,39	4	2,45	9,97
72	1,40	1	0,99	1,27	4,83	4	2,54	10,74
90	*0,99*	*1*	*0,66*	*0,48*	*4,09*	*4*	*2,36*	*8,29*
97	*0,97*	*1*	*0,65*	*0,63*	*5,25*	*4*	*2,67*	*12,74*
112	*1,02*	*1*	*0,70*	*0,80*	*5,93*	*4*	*2,77*	*13,77*
121	*1,04*	*1*	*0,72*	*0,70*	*6,31*	*4*	*2,86*	*17,10*
134	*0,91*	*1*	*0,56*	*0,60*	*5,30*	*4*	*2,26*	*11,40*
140	*0,92*	*1*	*0,66*	*0,65*	*5,75*	*4*	*3,12*	*14,78*
146	*0,93*	*1*	*0,62*	*0,63*	*6,83*	*4*	*2,73*	*17,17*
159	*0,95*	*1*	*0,68*	*0,60*	*5,96*	*3*	*2,42*	*12,91*

During period 2 measurements were made on the fell plateau and once again in the sparse birch forest. As the visual estimate of the mean grain diameter and the image processing result of the maximum diameter were found to be very close to each other, during 2003 it was decided to trust the visual estimates of the mean grain diameter and use this in the calculations.

For SLF models the following assumptions were made: crystal radius is the average maximum radius of the crystals, bond radius is one fourth of the crystal radius, and liquid water content is constant 0.08 – a residual water content in the most recent SNOWPACK version. For liquid water content the limiting values from Colbeck and others (1990) have been used. New snow dendricity was set to 1 and sphericity to 0.5; for rounded grains dendricity was 0 and sphericity 1.

In table 5.18, minimas, maximas, averages, standard deviations and coefficients of variation for different albedo datasets are listed. Datasets are observed as well as outputs from albedo models SLF-1- SLF-3.

In table 5.19 the correlations between observed and measured snow surface albedo and several model parameters are listed. Weak correlation means correlation around 0.3-0.4, strong between 0.5-0.6 and very strong correlation around 0.8. The data set used in this study is rather limited, results from only 30 albedo measurements together with needed meteorological and snow surface measurements were collected. The results should not be seen as a final truth in this question, but giving some hint of the important parameters in albedo modelling.

Table 5.18 Minimums, maximums, averages, standard deviations and coefficients of variations for the observed albedo dataset and the ones simulated with different albedo models.

	Obs	*Model1*	*Model2*	*Model3*
2002:				
Min	0.38	0.15	0.35	0.60
Max	0.73	0.87	0.44	0.67
Average	0.57	0.51	0.40	0.64
Stdev	0.094	0.29	0.030	0.023
CV	0.16	0.57	0.077	0.036
2003:				
Min	0.60	0.15	0.73	0.63
Max	0.90	0.93	0.87	0.76
Average	0.83	0.61	0.81	0.70
Stdev	0.068	0.32	0.043	0.035
CV	0.081	0.53	0.052	0.049

Table 5.19. Correlations between absolute error (measured - modelled albedo) and model parameter values for different albedo models.

Parameter	*SLF-1*	*SLF-2*	*SLF-3*
Wind	-	-	-
T air	-	Weak positive	Weak negative
T surface	-	Weak positive	Weak negative
Radiation	Strong positive	-	-
Density		Strong positive	Strong negative
Liquid water		Weak positive	Strong negative
Bond size		Weak positive	Weak negative
Dendricity		Weak negative	Strong positive
Sphericity		Weak positive	Strong negative
Melt-freeze		Weak positive	
Humidity			-
Age			Very strong negative
Grain size			Weak negative

There are also several sources of error in the observations, which are used to drive the albedo models as well as in albedo measurements, as listed above. For a few occasion during measurement period in 2003 the reflected short wave radiation had to be estimated from normal conditions and cloud coverage, because of the problems in measurements. For the same reason for some time intervals the albedo is assumed to be constant 0.85, as the same value was measured in the beginning and in the end of the measurements.

From table 5.19 it is easily seen that different albedo models are sensitive to different input parameters. When looking at some of the parameters as a group it can be noted that model SLF-2 seems to be more sensitive to conditions prevailing in wet or melt-freeze snow: high temperatures, densities and liquid water contents, grains are rounded and have gone through a melt-freeze cycle. Reaction of the SLF-3 on the other hand is reversed: the model is sensitive to low temperatures, densities and liquid water contents and small grains that are dendritic new snow. The error of the model decreases when the snow surface is aging.

This leads to the conclusion that the model version 2 should be used in new or cold and porous snow cases, while the new model version 3 performs better in wet and old, frozen snow case. Models could certainly be fitted to the observations, but this was not done because of the limited data set available.

In figure 5.18 the observed and modelled albedo data sets are shown, separately for both of the years. Error bars of 5% are added to the observed albedos. During the observation period 2003 the model SLF-2 otputs fit reasonably well in the error range; during the period in 2002 neither of the models fit that well in spite of the fact that model SLF-3 performs better. Low correlations were found between the observations and modelled albedos for all of the models for both periods.

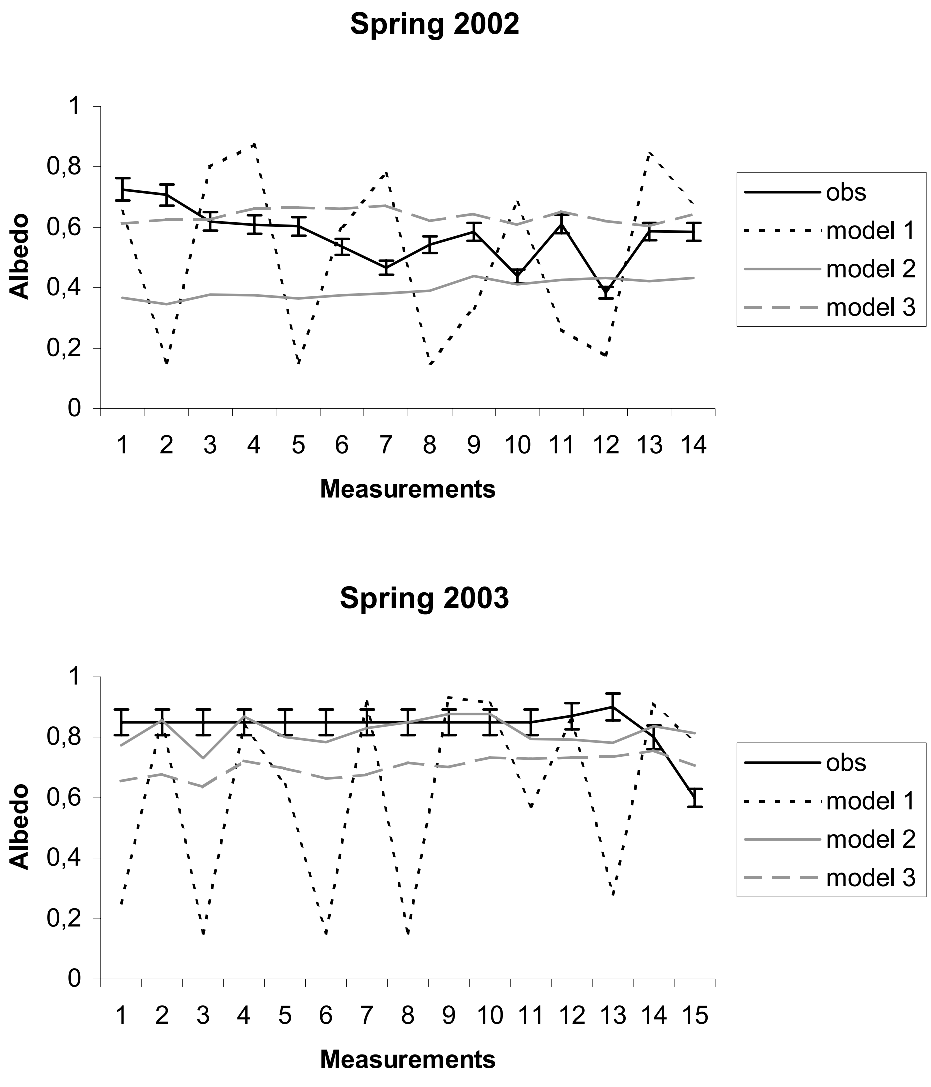

Figure 5.18. Observed and modelled albedo data sets in Kilpisjärvi.

Models SLF-2 and SLF-3 have far better overall performance compared to model SLF-1 only having meteorological parameters included. The relative error compared to measurements ranges between 1.5 - 82% for SLF-1 average being 35%. For SLF-2 the values are 0-43% and 17%; for SLF-3 1-62% and 18%.

In figure 5.19 the comparison between certain crystal size assumptions are made. Here model SLF-3 has been used with the following crystal sizes as input: average maximum single crystal radius, average minimum single crystal radius, average maximum polycrystalline particle radius and average minimum polycrystalline particle radius. One may ask if the size of a single crystal is more crucial to the snow albedo, or if the sizes of the melted and refrozen polycrystalline particles are more important to the behavior of the solar radiation. It seems that in most cases it is better to use single crystal values. This suggests that smaller particles have more significance for the snow albedo, as well as crystal boundaries have significance even when they are part of a polycrystalline particle.

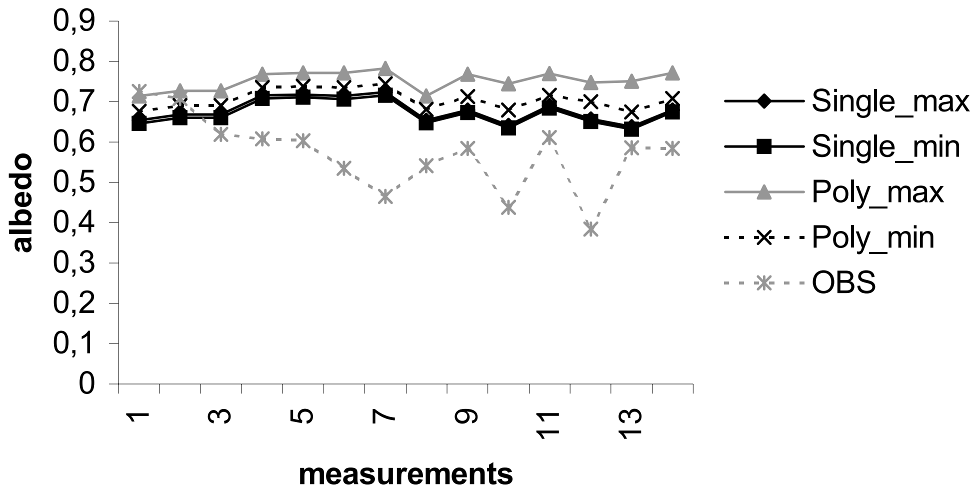

Figure 5.19. Effect of different crystal size assumptions to the performance of the SLF-3 albedo model.

5.5. Testing the new snow density sub-models

There are two new snow density sub-models available in the SNOWPACK model at the moment. The models are also statistical and developed using meteorological and snow measurements in the Swiss Alps. Both of the models use measured air temperature, surface temperature, relative humidity and wind velocity to calculate new snow densities. New snow density is limited between 30-150 kgm^{-3} in the model outputs. (Lehning et al., 2002b)

The new snow density ρ_n is estimated by the equation 5.6 in the SNOWPACK version used (new model):

$$\rho_n = \alpha + \beta T_A + \gamma T_{SS} + \delta RH + \eta VW + \phi T_A T_{SS} + \mu T_A VW + \nu RHVW + o T_A T_{SS} RH \qquad (5.6)$$

In the older model versions also following relation has been used (old model):

$$\rho_n = \alpha + \beta T_A + \gamma T_{SS} + \delta RH + \eta VW + \phi T_A T_{SS} + \mu T_A VW + \nu RHVW \qquad (5.7)$$

In these equations T_A is air temperature (°C), T_{SS} surface temperature (°C), RH relative humidity (%) and VW wind speed (ms^{-1}). In table 5.20 the parameters for the new snow density models in the SNOWPACK –model are listed.

Table 5.20. Parameters for the new snow density models in the SNOWPACK –model

Parameter	*New model*	*Old model*
α	70	70
β	6.5	30
γ	7.5	10
δ	0.26	0.4
η	13	30
ϕ	-4.5	6
μ	-0.65	-3
ν	-0.17	-0.5
o	0.06	-

For testing purposes a data set consisting of new snow density measurements and data about age and type of the snow, air temperature, surface temperature, relative humidity and wind velocity were collected during winter 2002/2003 in Hyytiälä and in Oulanka. 10 new snowfalls were recorded in Oulanka between 19.12.2002 and 12.3.2003, mostly during the standard snow measurements. In Hyytiälä 14 snowfalls between 18.12.2002 and 5.4.2003 were measured. In Hyytiälä new snow density was measured from more than one location to ensure the correct value for the density. Snow densities were measured in sparse forest or in open areas.

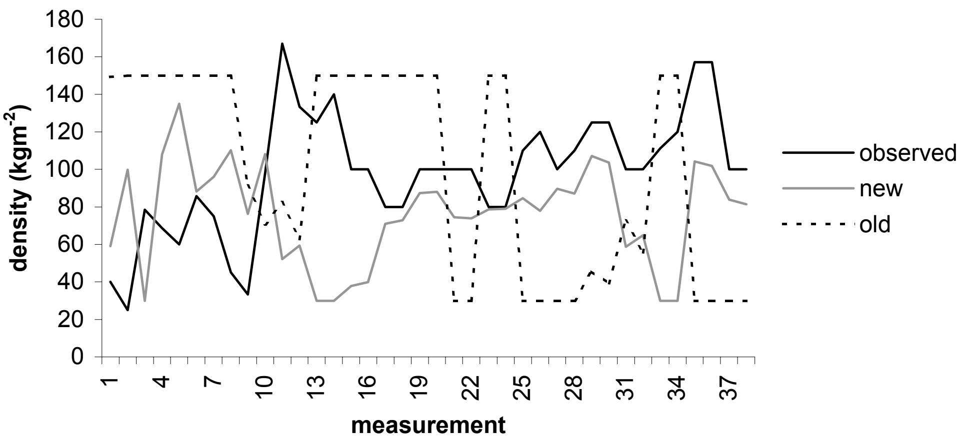

Figure 5.20. Observed and modelled new snow densities. Data points 1-10 are from Oulanka, data points after that are from Hyytiälä.

In figure 5.20 both observed and modelled new snow densities are shown for the new and old model. Data points 1-10 are from Oulanka, data points after that from Hyytiälä. The new model is performing better in both places; Oulanka seems to be more problematic for both of the models. This might be due to the taiga climate that is further from Alpine climate than the maritime climate in Southern Finland. Low correlations were found between the observations and modelled densities for both of the models.

In the figure 5.21 the distribution of the new snow densities is shown. The data sets are divided into three parts: light (0-50 kgm^{-3}), medium (50-100 kgm^{-3}) and dense (more than100 kgm^{-3}) new snow. From both the table and also the figures it is seen that new model statistics and distribution are more close to the ones of observed data set.

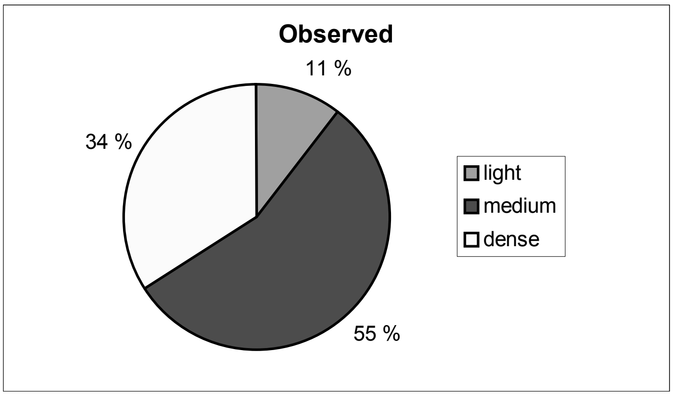

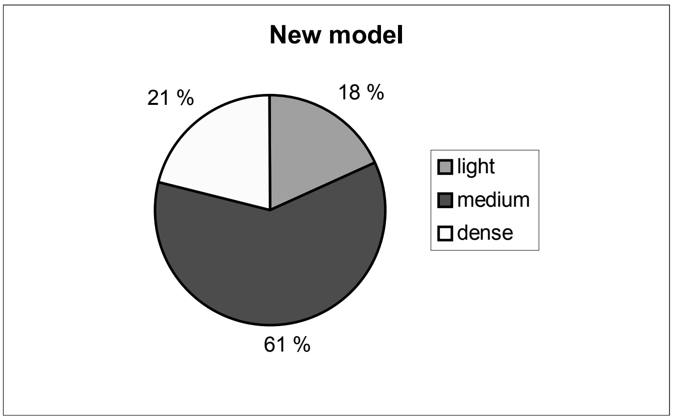

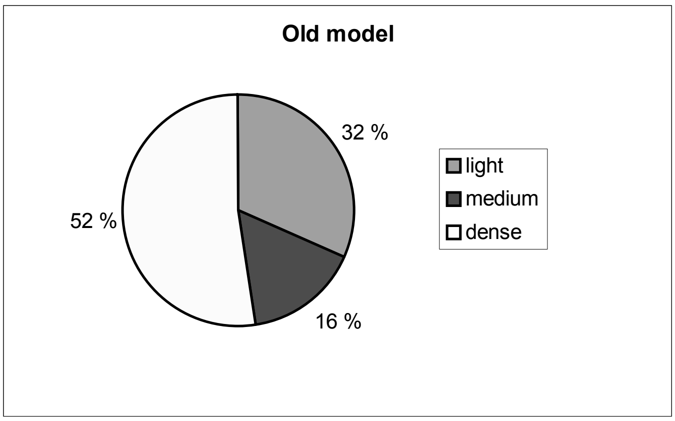

Figure 5.21. The distribution of new snow densities for observed and modelled data sets. The data sets are divided into light (0-50 kgm^{-3}), medium (50-100 kgm^{-3}) and dense (more than 100 kgm^{-3}) new snow.

Unfortunately it was not possible to develop a new snow density model for Finland with such a limited data set during this study. In table 5.21 minimas, maximas, averages, standard deviations and coefficients of variation are listed for the observed and modelled, with old and new model, data sets.

Table 5.21. Minimums, maximums, averages, standard deviations and coefficients of variation for the observed and modelled new snow density data sets, using both old and new model.

	Obs	*Old*	*New*
Min	25	30	30
Max	167	150	135
Average	98	101	76
Stdev	32	55	27
CV	0.33	0.54	0.35

5.6. Reliability and the use of the SNOWPACK –model in Finland

SNOWPACK simulates snow amount and snow pack structure evolution satisfactorily in Finnish conditions. Only in ephemeral snow zone the model has serious difficulties. Most of the problems with the SNOWPACK –model encountered during this study have been solved in the more recent versions of the model.

In the spring time the modelled snow depth is typically overestimated by the SNOWPACK -model, and the melting is too slow. There are several possible reasons for this model behaviour. The Iqbal parameterisation for incoming short wave radiation may be underestimating the radiation, or the albedo scheme of the SNOWPACK model is not good for the melting period in Finland. The latter may have significance: some runs were made using the most recent SLF-3 albedo model in the SNOWPACK, which seems to be more suitable for melting snow albedo calculations. In these simulations slight improvement of melting season snow depth was seen, but it did not totally solve the problem. The measured and Iqbal parameterised short wave radiation fluxes in Hyytiälä in winter 2000/2001 melting period were studied closely. The overall agreement between these two is excellent, and it is shown also in some statistics of the two radiation data sets: measured radiation ranged between 0 and 743 Wm^{-2}, and calculated between 0 and 655 Wm^{-2}. Averages and standard deviations were 116 and 160 Wm^{-2} for measured and 127 and 151 Wm^{-2} for calculated values, respectively. The only possible reason for marked difference between these data sets is the cut-off of the maximum radiation periods in the calculated case, which can of course be important for the snow pack energy balance.

An other possibility is the error in energy input, because liquid precipitation could not be taken into account when the snow depth was used as input for the model. Large amounts of heat is transported to the snow cover by rain during the melt period. When comparing the melting of the snow in figures 5.4-5.8 (snow depth used as input) and in figures 5.9-5.10 (precipitation used as input) it is really seen that melting is more rapid and more realistic in the precipitation cases. On the other hand quite severe problems are seen in the middle winter snow depth in Santala and in Oulanka, when using precipitation as input. This might be due to some combined effect of weather during the measurement winters and model behaviour. Not necessarily enough of the observed precipitation has been used by the model to increase the snow depth, because of large fraction of the liquid precipitation, and perhaps the real snow precipitation exceeds greatly the observed one. The correction of the precipitation should be done knowing all the details on wind patterns, liquid/solid partition of the precipitation and the situation of the precipitation gauge.

Grain type agreement scores were calculated by Grönholm (2003) for all of the locations for winter 2000/2001. The values ranged between 0.7 and 0.95 in Hyytiälä, 0.3 and 0.7 in Santala, 0.3 and 0.8 in Mekrijärvi, 0.9 and 0.93 in Oulanka and between 0.78 and 0.92 in Kilpisjärvi. These results were somewhat higher than the results of this study. Small changes may be due to different classification for grain types and layering typical for any two measurers. Please note that agreement score should not be mixed up with the correlation coefficient R^2. The usable values of agreement score range between 0 and 1, and also small values give knowledge about agreement or disagreement between two profiles. Values around 0.6 and 0.7 show very reasonable agreement between two profiles.

Some small problems seem to be found in the agreement score calculations. The perfectly similar profiles do not all the time give agreement score 1 for all of the properties, but the overall agreement score lies between 0.97 and 0.99. Especially during the melting period the agreement score for some of the properties is zero, which is of course acceptable. When the observed and simulated snow height differ a lot from each other, the stretching of the profiles makes the agreement for the density unrealistically poor. For some of the observed snow profiles some values for grain size or density had to be interpolated or “guessed” afterwards because of too sparse measurements. The surface hoar layers do not compress realistically in the model, and because of this surface hoar grain size stays unrealistically large once the layer has formed. This might have an effect to difference between observed and modelled bulk grain sizes. One thing that might have had a small effect to calculation results was the choice of a Unix system. The system used was SGI Origin 2000 used by CSC (Scientific Computing Ltd) in Espoo, Finland.

The results of this study are in good agreement with the earlier ones. Comparisons between simulated and measured snow profiles in the Swiss Alps have shown good general agreement. The overall agreement score of 0.8 all through the winter was found in the study by Lehning and others (2001). The score was highest for the temperature, whereas grain type and grain size reach lower scores. A small systematic overestimation of modelled water equivalents have been noted, as well as a systematic underestimation of the melt rate during the final stage of the melt season. (Bartelt et al. 2002)

The validation tells about the SNOWPACK model sensitivity to changes, not natural snow cover sensitivity. In any case, by assuming that the model represents the natural snow cover reasonably well, the results can be used to estimate the possible changes in snow conditions under changing climate. The most possible changes in a hundred year time scale are increases in air temperature, precipitation, wind speed and relative humidity. Using the results of the sensitivity tests, small to moderate changes (around 2-30%) can be expected. The most sensitive quantities would appear to be snow water equivalent, snow temperature, grain size, snow depth, date of snow maximum and grain form.

In this study observed snow pack characteristics were also compared to the observed snow surface albedo. Sophisticated models with snow parameters as input could handle the difficult data set better than a simple model. A problem with this kind of snow albedo models is that the user seldom has all needed input data. Models SLF-2 and SLF-3 including weather and snow parameters worked better than SLF-1 with only weather parameters as input. It also seems that the model version 2 should be used in new or cold and porous snow cases, while new model version 3 performs better in wet and old, frozen snow case.

The choice of the crystal size estimate (whether to use for example single crystal radius or polycrystalline particle radius) seems to have some significance in the albedo modelling. Using average single crystal radius gave the best agreement between the model and the observations – choice between maximum, minimum or average radius does not seem to play a big role at least in the rounded grain case.

There is a temptation in this kind of study to start fitting model parameters using the observation data. Even if the albedo data set may give some help in parameterizing albedo during difficult melting season events, this data set is too short and perhaps too extreme to be used in the parameterizing of the models.

The new snow density models of the SNOWPACK –model work reasonably well also in Finland. “New” model statistics and distribution are closer to the ones of observed data set than the ones of “Old”. Unfortunately it was not possible to develop a new snow density model for Finland with only a very limited data set during this study.

Some additional comments and recommendations can be given about the input data and parameterization of the model used:

- Use of the air temperature as snow surface temperature may cause errors in SNOWPACK simulations, but based on the sensitivity tests the effect of the error seems to be small. The same can be said of the 0°C ground temperature assumption. Naturally it would be ideal to have observations also of these quantities as input.
- Time resolution of 3 or even 6 hours did not affect very much the model output.
- In most of the conditions in Finland, the use of snow depth instead of precipitation is recommended.
- Attention should be paid to the accuracy of the snow depth and radiation input, as these seem to have the largest effects on the model output. This is especially true during the melt period.
- It is recommended to use higher value than 0.05 to residual water content
- The most recent parameterization for new snow density is recommended for use, as well as model versions 2 or 3 for albedo. Version 2 is recommended for use in cold, version 3 in wet conditions.

No modifications of the SNOWPACK -model were done during this study. The suitability of the model in Finnish conditions was studied without fitting the model or any of the parameters. The effects of the changes in parameterization was studied in section 5.3.5. In most of the cases the control run without any modifications seemed to be working better than the ones with changes.

It is clear that the parameterization of the initial and boundary condition equations should be validated and modified when starting the model use in forested conditions in Finland. Wind speed, affecting the sensible and latent heat fluxes has to be estimated and transfer coefficients of the fluxes changed, long wave emissivity of the canopy has to be taken into account as well as snow interception and short wave radiation extinction in the canopy. The snow surface temperatures are normally higher in the forest than in the open area, so the difference between air and surface temperature is decreased in the forest. Changes in air temperature and wind speed have an effect on new snow density; albedo may be affected by the litter on the surface. Falling snow may have different properties in the forested conditions compared to the snow falling in the open areas.

6. Possible future snow conditions in Finland

As the concentrations of carbon dioxide and other atmospheric greenhouse gases keep increasing, the global mean temperature is expected to rise (Houghton et al. 2001). The warming will likely be accompanied by changes in other aspects of the climate, such as precipitation and cloudiness. Several global changes may affect to the greenhouse gas balance of the Earth. A northward migration of the Arctic tree line, permafrost degradation, climatic change effects to carbon fluxes from wetlands are among these changes (Kuhry et al., 2002). Although climate change projections are still associated with large quantitative uncertainty, the consequences of climate change for natural and human systems need to be studied.

The snow cover has large effects on global and local climate, the hydrological cycle and ecology. Snow cover duration, snow depth and snow pack structure all depend on prevailing weather. It is expected that the amount of snow and snow cover duration will decrease in the future.

The atmospheric circulation pattern referred to as the North Atlantic Oscillation (NAO) regulates winter climate in the North Atlantic-European region. In years with positive NAO-index, warm air masses from the Atlantic produce milder and wetter winters, while negative NAO-index winters are characterised by more severe and dryer winters. The evidence from lake sediments suggest that warming by a few degrees during a positive NAO-index winter causes considerably shortening or even a disappearance of the persistent snow cover. (Saarnisto et al., 2002)

The annual mean temperatures have increased about 0.7°C during the 20th century in Finland, with the greatest warming in spring. Mean daily minimum temperatures have risen more than maximum temperatures, possibly because of increase in cloudiness. The winters and springs were exceptionally mild during the 1990s. There has also been tendency towards a shorter snow cover season and reduced amounts of snow during recent decades in Southern Finland. (Carter et al., 2002)

To get estimates of the future snow winters, estimates of the future winter climate are needed first. Different global atmosphere-ocean general circulation models (GCM) show encouraging agreement on the direction of climate changes (in particular on an overall increase in temperature and high-latitude precipitation), but the variation between models is significant (Houghton et al. 2001;
Räisänen 2001). In addition, the regional details of climate are difficult to model with GCMs having a grid size of several hundred kilometers. Regional climate models (RCMs) are run with higher (e.g., 50 km) horizontal resolution than GCMs. This enables a more detailed and potentially more realistic description of local climates, partly because the effects of smaller-scale topography and water bodies like the Baltic Sea can be taken into account much better than it is possible in GCMs. However, such high-resolution models can only be run in a limited domain and they need GCM boundary data that describe climate evolution outside their own area. (Rasmus, S. et al., 2005)

In this chapter possible future snow conditions are studied using meteorological data simulated by the Rossby Centre regional climate model RCAO (Räisänen et al. 2003). This model has been run using boundary data from two state-of-the-art GCMs

(HadAM3H and ECHAM4/OPYC3), and for each of these, two scenarios of future greenhouse gas and aerosol emissions (IPCC SRES A2 and B2) have been used. Through the four climate change scenarios obtained in this way it is hoped to get some indication of the certainties and uncertainties associated with future snow properties.

The RCAO simulations are used to drive the SNOWPACK –model. Climate models also give estimates on snow cover formation, melt and snow water equivalent, but snow models included in GCMs and RCMs are very rough. In particular, they give no information on the snow pack structure. Many of the ecologically, climatically and hydrologically important effects of snow cover are due to the combined properties of single snow layers.

In this chapter snow cover scenario calculations are presented for the 2080s (2080-2089) in Finland. Climate change scenarios for that time are more stable than those for the next few decades, because the signal is stronger and therefore easier to discern from natural variability (Räisänen, 2001). The results for this future period are compared with simulated conditions for the years 1980-1989. The mentioned two decades were selected from the 30-year RCAO control (1961-1990) and scenario runs (2071-2100) as the ones in which the simulated winter climate conditions in Finland are, as a whole, closest to the respective 30-year means. Most of the world's snow zones can be found in Finland. It is possible that trends shown here may be representative also for other parts of the world with similar climate change, even if the snow depths and water equivalents differ greatly between for example maritime snow zones in Finland and in Northern America.

6.1. Rossby Centre regional climate scenarios

The Rossby Centre regional climate model RCAO (Räisänen et al. 2003) was run at 49 km horizontal resolution in an area covering Europe and the eastern North Atlantic Ocean. Two series of three 30-year RCAO simulations were made, one with boundary data from the Hadley Centre HadAM3H GCM (Gordon et al. 2000) and the other with boundary data from the Max Planck Institute for Meteorology ECHAM4/OPYC3 GCM (Roeckner et al. 1999). For each driving GCM, a control run representing the period 1961-1990 and two scenario runs representing the period 2071-2100 were made. The latter two were based on the IPCC SRES A2 and B2 emission scenarios, respectively, the A2 scenario assuming larger greenhouse gas emissions than B2 (Nakićenović et al. 2000). In the following, the HadAM3H-driven simulations are referred to as RCAO-H and the ECHAM4/OPYC3-driven simulations as RCAO-E. (Rasmus, S. et al., 2005)

The IPCC storylines, A1, A2, B1 and B2 describe the relationships between the forces driving greenhouse gas and aerosol emissions and their evolution for large world regions and globally. The A-type world implies strong economic growth accompanied by rapid increase in CO_2 –concentration and climate warming. The B-type world shows milder changes. (Carter et al., 2002)

The RCAO control run climates and the simulated climate changes from 1961-1990 to 2071-2100 are documented in Räisänen et al. (2003). Briefly, the RCAO-H and RCAO-E control climates are of similar quality, both giving a reasonable simulation of climate in northern Europe. In comparison with the observed conditions in 1961-1990, however, the winters are slightly too mild in Finland, especially in the north. Precipitation is larger than observed, especially in winter and spring, but biases in the measurement of (especially) solid precipitation complicate the interpretation. The global mean warming from 1961-1990 to 2071-2100 varies in the driving GCMs from 2.3°C in the HadAM3H B2 scenario to 3.4°C in the ECHAM4/OPYC3 A2 scenario. These values are in the midrange of the recent IPCC estimates (Houghton et al. 2001). (Rasmus S. et al., 2005)

These values can be compared with the new climate change scenarios, developed for Finland in a project FINSKEN using five different coupled atmosphere-ocean general circulation models and four different scenarios. All scenarios show increases in temperature (from 1.8 to 5.2 °C) and precipitation (from 1 to 28 %) over Finland by the 2050s compared to 1961-1990 period. Changes range from 2.4 to 7.4 °C and from 6 to 37 % by the 2080s. Changes are greater in winter. For time slice 2070-99 the temperature changes for scenario A2 vary between 4.4 and 5.9 °C and for B2 between 3 and 5 °C. The precipitation changes vary between 8 and 29 % (A2) and between 6 and 28 % (B2). (Carter et al., 2002)

To drive the SNOWPACK-model, single (but as far as possible, representative) decades of the RCAO control (1980-1989) and scenario simulations (2080-2089) were selected. The scenario periods are characterised by much warmer conditions than the control simulations, in particular during the winter half-year. The average simulated warming in Finland from the 1980s to the 2080s during the November-March period is from 3.7°C in the RCAO-H B2 scenario to 5.1°C in the RCAO-H A2 scenario. A considerable increase in November-March precipitation (from 18% to 49%) also occurs in all four scenario simulations.

The SNOWPACK –model was driven with six-hourly RCAO output, using at each of the selected study locations (Santala located in the ephemeral snow zone, Lammi in thin maritime, Mekrijärvi in maritime, Hyytiälä in transition zone and Oulanka in taiga zone) data from the nearest RCAO grid box. In Kilpisjärvi there were problems with input data, and the location was left out of this study.

6.2. Estimating the future snow conditions

6.2.1. Method for the estimation of future snow conditions

Ten-year time series of RCAO-data were taken for each location for the years 1980-1989 and 2080-2089. Input data included air temperature (°C), relative humidity, wind speed (ms^{-1}) and direction (deg), precipitation (mm), incoming short wave radiation and incoming long wave radiation (Wm^{-2}) with 6 hour time resolution. For most of the locations only the RCAO-H control and A2 data were used. For the Hyytiälä simulations, the other four RCAO runs (RCAO-H B2 and RCAO-E control, A2 and B2) were also included to have a sensitivity range for the results. The SNOWPACK model uses the temperature between snow and soil as the lower Dirilecht boundary condition. This temperature has been set to 0 °C.

The snow cover evolution has been calculated during ten selected winters using the SNOWPACK model. The following aspects of the model results were studied:

- dates of snow cover formation and snow melting
- date of maximum water equivalent
- maximum of water equivalent and snow depth

For March 15 (the average date for present day maximum snow depth) in addition the following quantities were analysed:

- Bulk density, temperature and grain size
- Fraction of icy or melting snow
- Fraction of new or rounded grain snow
- Fraction of faceted grain or depth hoar snow

Averages and standard deviations were calculated for both decades for all of the listed quantities and the results of the control and scenario runs were compared.

6.2.2 Observed and modelled present day snow conditions

To allow a comparison between observed and modelled present day snow winter characteristics both long-term observed and modelled present day (RCAO-H control run) snow winter characteristics are shown in table 6.1. The dates for snow cover formation, snow melt and maximum snow depth, as well as maximum snow water equivalent and snow depth are presented for different locations.

In all cases model simulations show too shallow snow covers with too low water equivalents, in unstable ephemeral conditions as low as one fifth of the observed mean WE. This is probably due to the slightly too warm winter air temperatures and too high, possibly liquid, precipitation in the RCAO control runs. The use of precipitation, not snow depth, as input for SNOWPACK –model may also cause some deviations to the snow depth and the water equivalent, as discussed in section 5.3. Also in some locations snow cover formation is too early in the modelled case as well as the date for the maximum water equivalent. In most of the cases the "shape" and time evolution of the snow cover is realistic. The agreement between observed and modelled mean states seems to get better when going towards the north, to the more stable snow conditions and less melting periods and liquid precipitation events during the winter. The results suggest that the snow cover in the south is much more susceptible to warming trends than the snow cover in the north. The smaller errors in the climate control run simulation from the south have a larger impact on the snow cover than the larger errors in the north. The uncertainties and large spatial variance in the snow cover observations have also to be taken into account when interpreting these results.

Table 6.1. Means and standard deviations for some snow winter characteristics at different locations as observed; present day conditions in simulated RCAO-H control run winters 1980 – 1989 and future conditions in simulated RCAO-H A2 scenario run winters 2080-2089. In the middle columns mean differences between "future" and "present day" cases are given for all of the characteristics. Snow cover duration observations are from 1960/61-1989/90 (Solantie, 1996; Finnish Meteorological Institute, 1991) and water equivalent observations from 1952-1984 (Perälä and Reuna, 1990).

	1960-1989, observed		*1980-1989, modelled*		*Change*		*2080-2089 modeled,*	
	Mean	*Std Dev.*	*Mean*	*Std dev.*	*To observed*	*To modelled*	*Mean*	*Std dev.*
Santala:								
Formation (date)	02.01.	30	26.11.	13	-15	+22	18.12.	20
Melt (date)	25.3.	35	09.04.	14	-3	-17	22.03.	15
Max (date)	16.3.	10-20	16.02.	34	-32	-3	12.02.	25
Max WE (mm)	100	30-40	19	7	-77	+4	23	11
Max depth (cm)	23	5	9	3	-13	+1	10	3
Hyytiälä:								
Formation (date)	03.12.	25	31.10.	9	-5	+28	28.11.	13
Melt (date)	17.04.	20	26.04.	10	-10	-19	07.04.	13
Max (date)	26.03.	10-20	25.03.	15	-33	-34	21.02.	27
Max WE (mm)	120	30-40	104	31	-43	-27	77	35
Max depth (cm)	55	10	36	8	-28	-9	27	9
Lammi:								
Formation (date)	03.12.	25	07.11.	13	-4	+22	29.11.	15
Melt (date)	17.04.	20	20.04.	10	-16	-19	01.04.	16
Max (date)	26.03.	10-20	15.03.	23	-49	-41	05.02.	34
Max WE (mm)	120	30-40	81	34	-75	-36	45	18
Max depth (cm)	42	10	29	9	-25	-12	17	5
Mekrijärvi:								
Formation (date)	18.11.	15	27.10.	11	+1	+23	19.11.	10
Melt (date)	02.05.	10	27.04.	13	-18	-13	14.04.	10
Max (date)	01.04.	10-20	26.03.	19	-25	-18	07.03.	15
Max WE (mm)	180	30-40	117	28	-82	-19	98	37
Max depth (cm)	63	10	40	7	-30	-7	33	10
Oulanka:								
Formation (date)	29.10.	15	26.10.	18	+10	+13	08.11.	12
Melt (date)	17.05.	5	05.05.	11	-27	-15	20.04.	10
Max (date)	16.04.	10-20	24.03.	32	-20	+2	27.03.	18
Max WE (mm)	200	30-40	140	40	-80	-20	120	41
Max depth (cm)	68	10	48	12	-28	-8	40	11

In figure 6.1 examples of the snow pack crystal structure evolution for typical snow winters for different locations are shown based on RCAO-H control run calculations. At all locations, the most representative winter development, i.e. the one closest to the climatological mean is shown. Snow cover formation and melt at different snow zones, as well as different snow pack structure evolution, are clearly seen in this figure. The shading code is the same as in the figures in the section 5.2; the code is shown in the figure to help distinguish between different grain types.

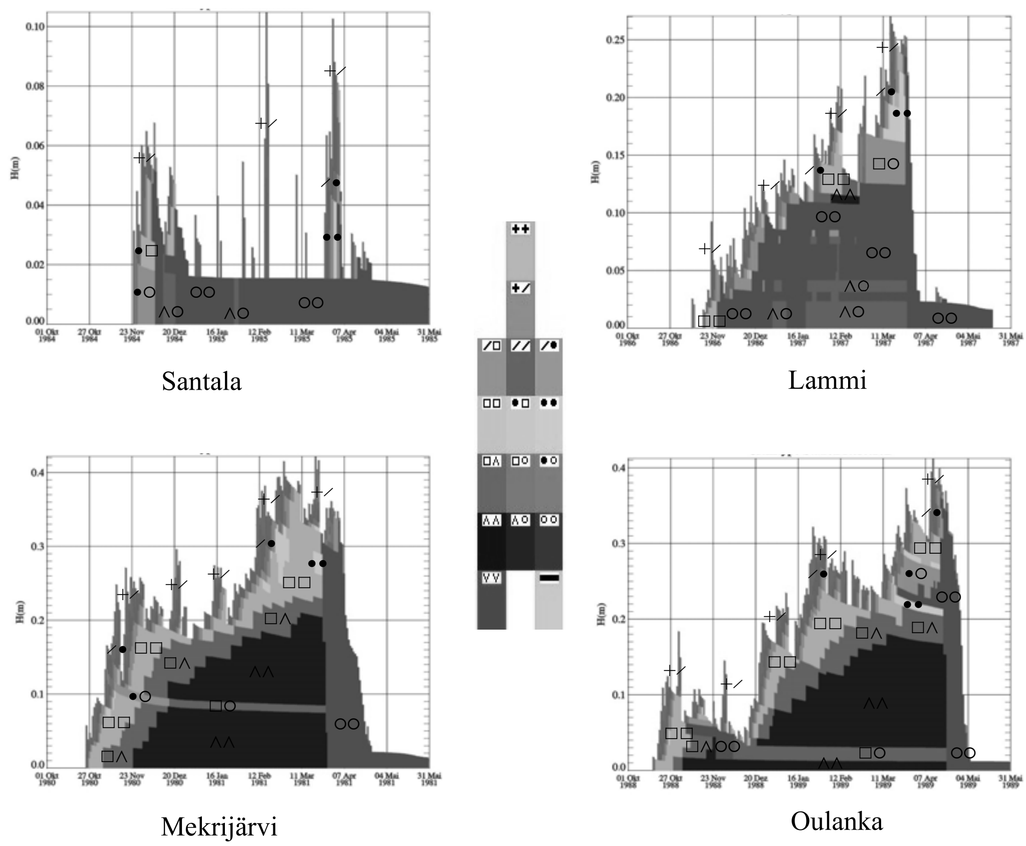

Figure 6.1. Examples of typical snow winter crystal structure evolution in the study locations using RCAO-H control runs (compares to the present day situation).

6.2.3. Estimated future snow conditions

In table 6.1 also values for period 2080-2089 (RCAO-H A2 scenario run) are given, as well as changes between present day observations and scenario run, and control run and scenario run. In table 6.2, the respective snow pack structure characteristics for March 15 are analysed.

From the simulations, a clear trend is visible: around 2090 snow pack formation happens later (13-18 days) than nowadays, while melting occurs earlier (13-19 days). The date of the maximum water equivalent is also earlier than nowadays. The maximum water equivalents and snow depths decrease approximately by one fifth of the present day mean values, although with some variation between the individual sites. An noteworthy exception is Santala, where due to higher winter precipitation slightly higher maximum snow depth and maximum water equivalent are observed.

Changes are homogenous in all of the snow zones (except ephemeral). The results confirm the earlier observation based on the control run that the snow cover in the southern part of the country will undergo more severe changes. Assuming that the future climate simulation has a comparable systematic error as the present day scenario, the magnitude of the changes in snow characteristics are given by the comparison

Table 6.2. Means and standard deviations for some snow pack structure characteristics in 15.3. at different locations in simulation winters 1980 – 1989 and 2080 – 2089. Only RCAO-H control runs and A2 scenario runs were used here. In the middle column mean difference between "future" and "present day" cases are given for all of the characteristics.

	"1980"		*Change*	*"2080"*	
	Mean	*Std dev.*		*Mean*	*Std dev.*
Santala:					
Depth (cm)	3	2	0	3	4
WE (mm)	9	5	+1	10	10
Density (kgm^{-2})	395	149	- 23	372	150
Temp (°C)	-0.3	0.6	+0.3	0	0
Size (mm)	2	1.3	0	2	0.9
Hoar (%)	25	35	-22	3	11
Rounded (%)	22	23	-12	10	29
Ice (%)	53	39	+34	87	30
Hyytiälä:					
Depth (cm)	29	9	-11	18	12
WE (mm)	87	29	-28	59	41
Density (kgm^{-2})	300	25	+35	335	44
Temp (°C)	-1.7	1.6	+1.1	-0.6	0.9
Size (mm)	1.2	0.3	+0.2	1.4	0.5
Hoar (%)	66	29	-48	18	27
Rounded (%)	13	14	-2	11	17
Ice (%)	21	23	+50	71	31
Lammi:					
Depth (cm)	23	8	-15	8	8
WE (mm)	67	23	-42	25	25
Density (kgm^{-2})	297	30	+60	357	159
Temp (°C)	-1.5	1.5	+1	-0.5	1.2
Size (mm)	1.2	0.3	+0.7	1.9	0.9
Hoar (%)	52	39	-45	7	12
Rounded (%)	15	17	-5	10	16
Ice (%)	33	37	+50	83	24
Mekrijärvi:					
Depth (cm)	33	7	-7	26	11
WE (mm)	97	19	-13	84	41
Density (kgm^{-2})	298	21	+19	317	39
Temp (°C)	-2.1	2	+1.1	-1	1.6
Size (mm)	1.3	0.2	-0.1	1.2	0.3
Hoar (%)	78	24	-33	45	33
Rounded (%)	10	8	+2	12	16
Ice (%)	12	23	+31	43	30
Oulanka:					
Depth (cm)	40	14	-7	33	11
WE (mm)	118	43	-16	102	39
Density (kgm^{-2})	291	9	+18	309	29
Temp (°C)	-2.5	0.9	+1.3	-1.2	1
Size (mm)	1.3	0.1	-0.2	1.1	0.2
Hoar (%)	95	5	-29	66	31
Rounded (%)	5	5	+7	12	5
Ice (%)	0	0	+22	22	31

between modelled present day and modelled future case. Therefore, comparison between observed present day and modelled future snow pack structure is not interpreted. Also, the limited number of point observations appears to be a small data basis to represent present day snow pack structure conditions in Finland. However, one cannot be sure if the assumption of non-changing systematic error is justified.

Analysing the results for March 15, the same decreasing trend can be seen in the snow depth and water equivalent at all locations except Santala. The following changes are also seen in most of the cases: increase in snow bulk temperature towards the melting point, which reflects higher air temperatures; increase in density and in grain size, which can be explained by more frequent melt-freeze cycles in the snow pack. The most pronounced changes can be seen in the fractions of differently metamorphosed snow. There is a large increase in melt forms and melt-freeze crusts by several tens of percent units. The occurrence of these forms increased mainly by reducing the occurrence of faceted crystals. A smaller decrease is also observed for rounded crystals.

In figure 6.2, typical examples of a snow winter crystal structure evolution in different locations in the 2080s are shown, using RCAO-H A2 data. Also here, different winters were chosen at different locations to find as close a match as possible to mean conditions during the 10-winter time slice at each location. As in figure 6.1, also here the differences between different snow zones are seen. When comparing the figure 6.1 to figure 6.2, changes in snow depth, snow cover formation and melt, and snow pack structure can be seen between the two decades analyzed.

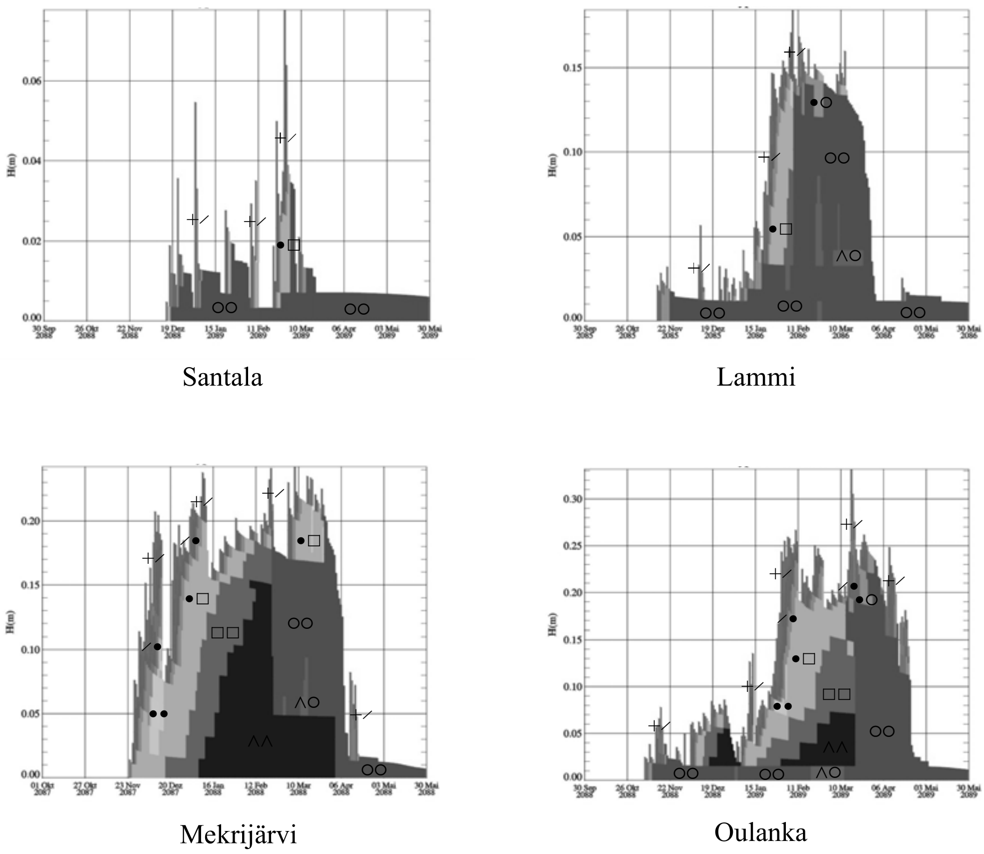

Figure 6.2. Examples of typical snow winter crystal structure evolution in the study locations around 2080 using RCA-H A2 scenarios.

To conclude: in a climate represented by the RCAO scenario runs, snow cover thickness and duration are likely to decrease. The decrease in the snow depth is connected both to the average winter air temperature and to the change in it, which is also shown in the present day observation in the Table 3.4 (Chapter 3). Even if the mean monthly air temperature is several degrees higher than long-term mean, thicker than average snow cover can build up because of larger amounts of precipitation if the air temperature stays long periods below 0°C.

Snow quality is also likely to change:

- Snow will be denser and closer to the melting point even in the midwinter, grains will be bigger
- Fraction of depth hoar in the snow pack will decrease
- Fraction of icy or wet snow in the snow cover will increase

These changes will have certain effects on for example hydrology (winter runoff increases), building (snow loads on the roofs might increase even when the snow depth stays the same or decreases) and ecology. Many plants and animals especially in the boreal and arctic zones are adapted to the shelter of the snow against cold and dry winter conditions. For example a doubling of density, caused perhaps by a midwinter rain fall, would reduce the thermal resistivity by a factor of eight (Pomeroy and Brun, 2001). Some animals also need to have some faceted grain snow to move and nest in the snow. Some of these species may have severe problems if snow winter characteristics change too quickly and "present day" winters are too rare.

6.3. Comparison between different RCAO scenarios

In table 6.3, mean air temperature as well as mean daily precipitation for November-March period in Hyytiälä during the studied decades are given for RCAO-H and RCAO-E control runs. These results are compared to the long term observations from Hyytiälä between 1960/61 – 1989/90. Both RCAO runs give slightly too high mean temperatures and daily precipitations.

Table 6.3. Mean air temperatures as well as mean daily precipitation values for November-March period in Hyytiälä for different RCAO control and scenario runs. Observations are from 1960/61 – 1989/90 (Finnish Meteorological Institute, 1991).

	Temperature (°C)			*Precipitation (mm/d)*		
	OBS	*RCAO-H*	*RCAO-E*	*OBS*	*RCAO-H*	*RCAO-E*
CTRL	-5.94	-5.6	-5.5	1.59	2.01	1.99
A2		-1.0	-0.2		2.42	2.87
B2		-1.7	-1.0		2.38	2.75
A2-CTRL		4.6	5.2		20%	44%
B2-CTRL		3.8	4.5		19%	38%

In table 6.3, also different RCAO scenario runs are compared. As expected, changes in B2 runs are smaller than in A2 runs when compared to the control run situation. Also increases in temperature and in precipitation are greater in the RCAO-E cases than in the RCAO-H cases. The increase in precipitation is remarkably high for the RCAO case – this is mostly due to the increase in liquid precipitation.

In table 6.4 “present day” snow winter characteristics in Hyytiälä as simulated with RCAO-H and RCAO-E control run data are compared. Simulated winters are surprisingly similar between the two cases. Table 6.4 also compares the results for Hyytiälä in the 2080s between the four different simulations (RCAO-H A2, RCAO-H B2, RCAO-E A2, RCAO-E B2). The simulations based on the RCAO-E results give shallower snow covers than those based on the RCAO-H results. The snow packs are also denser and warmer, and they consist of larger grains. The fractions of icy/melting snow and faceted grain snow give an idea of warmer winters with more melt-freeze cycles than in the RCAO-H cases. Differences between the A2 and B2 scenarios are more pronounced for the RCAO-E than the RCAO-H results. In figure 6.3 the examples of typical snow winter crystal structure evolution in Hyytiälä around 2080 for different scenarios (RCAO-H A2 and B2, and RCAO-E A2 and B2) are shown.

Table 6.4. “Present day” and “future” snow winter characteristics in Hyytiälä as presented in RCAO-H and RCAO-E control runs and scenario runs RCAO-H A2 and B2, as well as RCAO-E A2 and B2.

	1980-1989		2080-2089			
	RCAO-H	RCAO-E	RCAO-H A2	RCAO-H B2	RCAO-E A2	RCAO-E B2
Formation	31.10.	5.11.	28.11.	19.11.	23.11.	13.11.
Melt	26.04.	27.04.	07.04.	07.04.	27.03.	15.04.
Max date	25.03.	10.03.	21.02.	25.02.	25.01.	06.02.
Max depth (cm)	36	35	27	24	18	21
Max WE (mm)	104	102	77	69	45	55
15.3.:						
Depth (cm)	29	27	18	14	5	9
WE (mm)	87	85	59	45	20	30
Density (kgm^{-2})	300	311	335	348	391	346
Temp (°C)	-1.7	-2.6	-0.6	-0.9	0	-0.8
Size (mm)	1.2	1.3	1.4	1.5	2.9	1.4
Hoar (%)	66	64	18	39	0	17
Rounded (%)	13	10	11	10	16	15
Ice (%)	21	26	71	51	84	68

6.4 Reliability of the estimation method

The SNOWPACK mass balance has been shown to be accurate for high Alpine locations (Lehning et al., 2002b) as well as temperate climates (Etchevers et al., 2002) with a small bias towards underestimation of melt and overestimation of snow accumulation. Therefore, the observed discrepancy between data and the control run in southern Finland is interpreted as being due to a bias in the meteorological input data. But the control run already serves as a sensitivity case and demonstrates that the temperate snow covers in southern Finland might react stronger on climate change than the more stable snow covers in the north. (Rasmus, S. et al., 2005) Some significant problems have also been reported with the use of GCMs and also with the use of RCMs on the regional scale (Christensen, 1999).

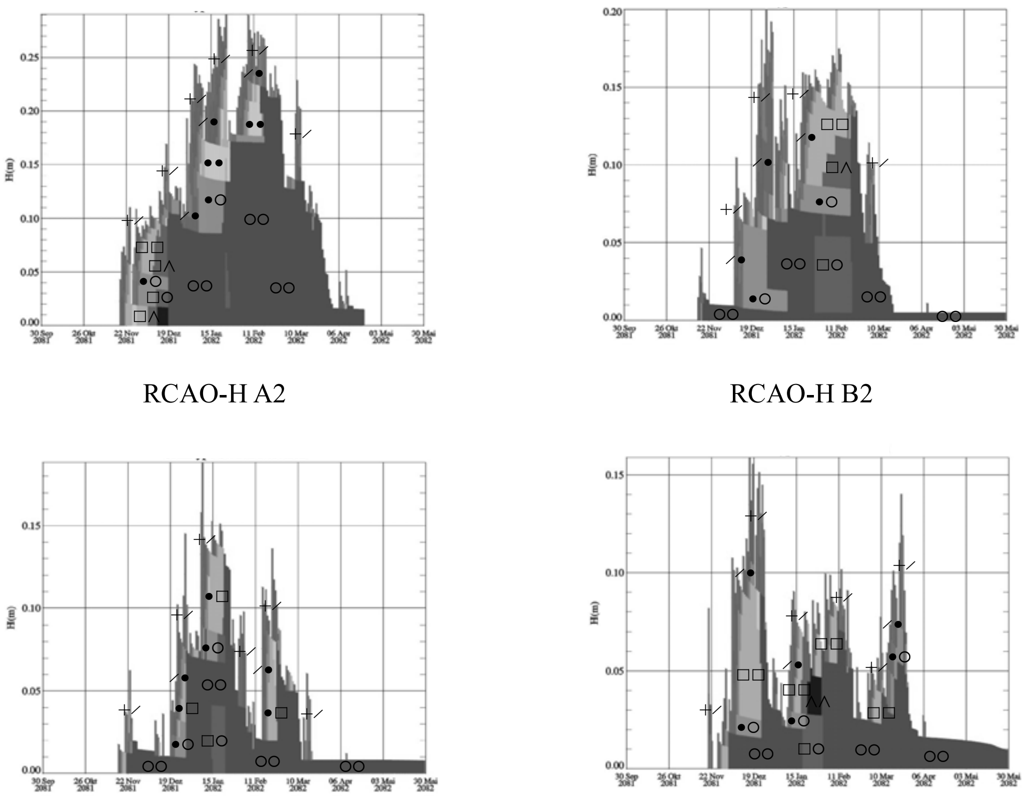

RCAO-H A2 RCAO-H B2

RCAO-E A2 RCAO-E B2

Figure 6.3. Examples of typical snow winter crystal structure evloution in Hyytiälä around 2080 using different scenarios (RCAO-H A2 and B2, as well as RCAO-E A2 and B2).

It has been said that the model invalidation should be as a relevant a goal as a model validation, if the model appears to perform inadequately against past observations, or if the model operation is limited to present-day conditions. (Hulme and Carter, 1999) Based on the validation of the SNOWPACK –model described in the chapter 5, the model can be said to perform satisfactorily against present day observations. It is on the other hand impossible to say if the model operation can be extended to future conditions also.

Uncertainty is always present in the modelling work, and its existence should never be suppressed when estimating the reliability of the results. Uncertainty suppression is done when scenarios and impacts are based on one climate model only or when scenarios and impacts are based on one forcing function only (for example GCM experiments forced only with 1 % per annum growth in concentrations) (Hulme and Carter, 1999). In this sense uncertainty is taken into account only by the intercomparison described in section 6.3; model runs with different scenarios should be done in other locations also. Sources of uncertainty include measurement error, natural variability and model structure. (Katz, 1999) There are uncertainties in forcing scenarios, global climate change, regional climate change, baseline climate, natural climate variability and in the snow model. (Jones et al., 1999) Model uncertainties should be compared to the uncertainties attributable to future climate. (Hulme and Carter, 1999)

The study presented shows qualitative trends and quantitative estimates for snow changes are to be expected. The different scenarios calculated give a first assessment of variability. They show differences between different climate model outputs. The presented simulations are not sufficient to calculate statistical trends and to separate interannual variability from the variability between the model scenarios. More model runs are needed at many locations with several GCM outputs and probably longer time series to make a statistical analysis.

This study is concentrating on the mean state of the snow pack – the detailed interannual variations of snow conditions in the 2080s are, of course, unpredictable. If the climate will change as in the model scenario run, the average snow conditions in different snow zones in Finland are expected to change.

Extremities in the climate are very difficult to model, and there are always some surprises in the climatic system, which are impossible to model. In any case, extremes and surprises should be accounted for somehow (Katz, 1999). This has not been done in this study. One interesting result is the increase in the standard deviations for many of the studied quantities at many of the locations in this study. This suggests that interannual variation of both snow winters and also snow pack structure characteristics could be larger in the future. This could lead to more frequent extreme events also in snow winters. Of course it needs to be once again pointed out that a 10-year sample is too small to make a statistical trend analysis.

Impacts and their uncertainties can be estimated using six alternative methods: expert judgement, experiment, impact model uncertainties, response surfaces (to run impact models for the present-day observed climate and then to apply arbitrary adjustments to the observed climate), impact model intercomparison and accounting for non-climatic scenarios and adaptation. Non-climatic factors need to be accounted for if impact assessments are to provide a realistic representation of future conditions with and without climate change. (Hulme and Carter, 1999) It is crucially important to understand that this study of the climate change impact on the snow conditions is based on modelling work. In this study the model has been compared with observed data and also some long-term observations are presented so that the reader might be able to judge the uncertainties associated with the study. The results are mainly based on a comparison between a control run for the present climate and scenario runs for the future. Therefore, model bias errors are avoided, if the bias is not changing over time.

7. Conclusions

In this study the snow pack structure characteristics in Finland have been studied, using both field measurements and modelling as tools. Chapter 1 of this work gave an introduction to the subject; in chapter 2 theoretical background of the subject has been collected; modelling of snow pack structure and the SNOWPACK –model were discussed in chapter 4. Chapters 3, 5 and 6 consist of new findings. In chapter 3 the results of the measurements of the snow pack structure in different snow zones in Finland have been presented, new knowledge of the variation in time and space being the most important result of the chapter. The snow pack structure model SNOWPACK has been validated in Finnish conditions in chapter 5; in chapter 6 the possibility of using the combination of regional climate model outputs and SNOWPACK model to get an estimate of future snow conditions has been discussed. The conclusions of the results have been listed in this chapter separately for the chapters 3, 5 and 6.

Observed snow pack structure:

1. The study locations fell in most of the cases into expected snow zones. In Lammi and in Mekrijärvi also some taiga snow properties were observed. Mekrijärvi could be said to switch from the taiga properties during the early winter to maritime properties during the late winter. In Kilpisjärvi taiga snow was found below the tree line, tundra snow above the tree line. Snow zonation testing based on the snow densification did not give clear answer to the question if the zonation by Sturm et al. (1995) is correct for Finland or not.

2. The variation of snow depth and snow pack structure was observed to be small inside single biotypes. More variation was seen between the forest and open area; normally effects of more efficient metamorphic processes in the open area were seen.

3. Snow depth as well as water equivalent was observed to increase when going towards north, in maritime Mekrijärvi the water equivalent might exceed the one in Oulanka in taiga zone. During late winter a little bit more snow was observed in the forest than in open area.

4. The largest bulk densities were observed in ephemeral and tundra zones. Density reached higher values in open areas. Snow was hardest in the ephemeral and tundra zones. In the maritime zone the snow hardness showed large variability. Snow was generally harder in the forest. Bulk grain size increased when going towards north. Grains were a bit larger in the open area.

5. The fraction of faceted grain snow and that of icy or melting snow during the early and mid-winter divided Finland into two areas. In the first, southern area, where Santala and Lammi are located, no faceted grain snow or depth hoar was observed, but fractions of icy snow were quite large. In the northern area, where Mekrijärvi, Oulanka and Kilpisjärvi are located, the situation was reversed: no or only small fractions of icy and melting snow were seen, but fractions of faceted grain snow and depth hoar were large. Not much variation was seen in the fraction of new or rounded grain snow between the locations.

6. The difference between snow surface temperature and air temperature was almost always negative and ranged between 0.3 and – 5.1°C. In most of the places the difference was bigger in the open field than in the forest. The ground temperature was near zero during the measurement periods; in most of the cases between 0 and –1°C. Temperatures were a bit colder in the forest than in the open field during the early winter.

7. The average density of snow increased when going from rounded grain snow (this means new snow and snow going through equilibrium metamorphosis) towards melting snow via hoar (snow going through kinetic growth metamorphosis) and melt-freeze snow. The average density of melting snow was greater than that of melt-freeze snow. Variation in hardness was large: largest variation was found in rounded type of snow, smallest in melting snow. The largest average hardnesses were found in melt-freeze snow. Both minimum and maximum grain sizes increased from rounded snow via hoar to melt-freeze snow. The average grain size was larger for hoar than for melt-freeze type.

8. No correlation was found between snow hardness and density for other snow types than new or rounded grain snow.

9. Distinguished coefficient of variation ranges were found for the snow depth in different locations, especially in the forested conditions. Kilpisjärvi had the lowest coefficient of variation, then Oulanka and Mekrijärvi, and after this Lammi and Santala. Normally the open area variation range was wider than the one for the forest. Coefficients of variation for snow depth and bulk density were lower than the ones for snow water equivalent.

10. Based on the agreement scores between the observed snow profiles inside single biotypes it could be said that the highest agreement scores and lowest variability were seen in grain size and temperature. The lowest agreement scores and highest variability were seen in density and grain type. In Lammi and in Mekrijärvi the agreement scores were lower (variability higher) in the late winter cases; in Oulanka and in Kilpisjärvi higher (variability lower).

11. Based on the combined agreement scores between the observations from the forested and open areas it can be said that with only a few exceptions the agreement scores are relatively high (around 0.6 and 0.7) all through Finland. During early winter values increase when going towards north; in Oulanka agreement score is however a bit lower, and maximum is reached in Mekrijärvi. This is seen both in the forest and open field case. The open area score in Kilpisjärvi is low, indicating high variation in tundra conditions. In most locations the difference between forest and open area cases increases when going towards late winter measurements.

Validation of the SNOWPACK –model:

1. Measured and simulated snow depth agreed very well during the accumulation periods, as well as during the dry snow settling and blowing snow periods. During the melt the snow depth was overestimated, and snow melt was prolonged by an average of 7 %.

2. Modelled snow water equivalent was most often overestimated. This might be due to too high a snow pack settling rates and because of this to too high a density.

3. Visual agreement between the snow pack structure observations and simulations was reasonably good throughout the country. There were problems with modelling of snow depth when using precipitation as input; on the other hand the melt period and snow pack structure were better simulated in some cases.

4. Agreement scores between the observed and simulated snow profiles were highest for temperature and grain size, and lower for grain type and density. Agreement scores were generally high during the early and middle winter and dropped during the melting period. Agreement scores reached higher values when going towards the north and towards more stable snow zones in Finland. In the ephemeral zone scores were low and very variable.

5. The most sensitive snow parameters in this study were snow water equivalent, temperature, grain form and size, snow depth and timing of the snow melt.

6. In this study the runs using precipitation instead of snow depth, different boundary conditions, different short wave radiation scheme and slightly changed snow depth had the largest effects on the model outputs. Model sensitivity test based on the agreement scores between the control run and the different test runs confirmed the result of the runs with the largest effects on the model outputs, but did not confirm the result of the most sensitive snow parameters.

7. The model sensitivity grew towards the melting period, and also the choices of the input data and boundary conditions became more important.

8. The most recent version of the new snow density model included in the SNOWPACK –model worked reasonably well in Finnish conditions. The SLF-2 albedo model worked better in cold and dry snow conditions; the most recent albedo model version SLF-3 in wet and warm snow conditions.

Even if the SNOWPACK -model works reasonably well in Finnish conditions, modifications should be made before it could be taken in extensive use in Finland. Wet snow metamorphism and water transport routines should be checked, together with the albedo and new snow parameterisation using Finnish observations. User often has only synoptic meteorological observations as input data to the model. It would be good to take this into account also in model development. Interface program estimating snow surface temperature, ground surface temperature as well as incoming long wave and short wave radiation should be possible to develop using a long time series of observations on these and synoptic meteorological observations on for example air temperature, wind speed and cloudiness. Measured precipitation could also be corrected by this program using knowledge of local conditions.

As discussed in Section 5.6, the adding of forest layer between the atmosphere and snow cover is very important for use of the SNOWPACK -model in a forested county like Finland. In a forest layer changes would be made to wind speed, incoming short wave and long wave radiation, measured in open area, as function of forest properties.

Forest affects also new snow density and albedo; also interception and changes in transfer coefficients of the sensible and latent heat fluxes should be taken into account. After this areal snow cover properties could be studied knowing the fractions of different forests and open area in a study location.

Estimating future snow conditions:

1. In a climate represented by the RCAO scenario runs around 2080s, snow cover thickness is likely to decrease by one sixth to one third compared to the present day snow depth; duration is likely to decrease by 3-5 weeks.

2. Snow quality is also likely to change:
- Snow will be denser and closer to the melting point even in the midwinter, grains will be bigger
- Fraction of depth hoar in the snow pack will decrease
- Fraction of icy or wet snow in the snow cover will increase

3. The standard deviations for many of the studied quantities at many of the locations will also increase in 2080s when compared to the present day case.

Several interesting factors affecting the snow pack structure had to be left out from the study. Especially the effect of the forest on the local meteorology, snow pack structure evolution and snow pack structure modelling are very important subjects for future studies. Another important study field is snow ecology, that is the study of interdependencies between snow cover and living things, and the role of snow cover in an ecosystem.

References

Adams, E.A. and Sato, A. 1993. Model for effective thermal conductivity of a dry snow cover composed of uniform ice spheres. *Annals of Glaciology*. Vol. 18. 300-304.

Adams, W. P. 1976. Areal differentiation of snow cover in East Central Ontario. *Water Resources Research*. Vol. 12. No. 6. 1226-1234.

Ahti, T., Hämet-Ahti, L. and Jalas, J. 1968. Vegetation zones and their sections in northwestern Europe. *Ann. Bot. Fennici*. 5.

Anderson, E. 1976. A point energy and mass balance model of a snow cover. *NOAA Technical Report NWS*. No. 19.

Angervo, J. M.1952. Lumitutkimuksesta. *Terra*. Vol. 64. No. 4.

Bader, H. et. al. 1939. Der Schnee und seine Metamorphose*. Beiträge zur Geologie der Schweitz. Geotechnische Serie*. Hydrologie, Lief 3.

Bader, H.-P. and Weilenmann, P. 1992. Modeling temperature distribution, energy and mass flow in a (phase-changing) snowpack. I. Model and case studies. *Cold Regions Science and Technology*. Vol. 20.

Bartelt, P. and Von Moos, M. 2000. Triaxial tests to determine a microstructure-based snow viscosity law. *Annals of Glaciology*. Vol. 32. 457-462.

Bartelt, P. and Lehning, M. 2002. A physical SNOWPACK model for the Swiss avalanche warning: Part I. Numerical model. *Cold Reg. Sci. Technol*., Vol. 35. No. 3. 123-145.

Baunach, T., Fierz, C., Satyawali, P.K. and Schneebeli, M. 2001. A model for kinetic grain growth. *Annals of Glaciology*. Vol. 32. 1-6.

Benson, C.S. and Sturm, M. 1993. Structure and wind transport of seasonal snow on the Arctic slope of Alaska. *Annals of Glaciology*. Vol. 18.

Bentley, W. A. and Humphreys, W. J. 1931. *Snow Crystals*. McGraw-Hill Book Company, Inc.

Brown, R.L., Edens, M.Q. and Sato, A. 1994. Metamorphism of fine-grained snow due to surface curvature differences. *Annals of Glaciology*. Vol. 19. 69-76.

Brown, R.L., Barber, M., Edens, M.Q. and Sato, A. 1997. Equitemperature metamorphism of snow. In Izumi, Nakamura and Sack (Eds). *Snow engineering: Recent Advances*. Rotterdam.

Brown, R.L., Satyawali, P.K., Lehning, M. and Bartelt, P. 2001. Modeling the changes in microstructure of snow during metamorphism. *Cold Regions Science and Technology*. Vol. 33. 91-101.

Brun, E., David, P., Sudal, M. and Brunot, G. 1992. A numerical model to simulate snow-cover stratigraphy for operational avalanche forecasting. *Journal of Glaciology*. Vol. 38. No. 128. 13-22.

Brun, E., Durand, Y. and Martin, E. 1994. Snow modelling as an efficient tool to simulate snow cover evolution at different spatial scales. *IAHS Publications*. No. 223.

Brutsaert, W. 1975. On a derivable formula for long-wave radiation from clear skies. *J. Water Resour. Res*. Vol. 11. No. 5. 742-744.

Carter, T. R. and 19 others. 2002. The FINSKEN global change scenarios. In Käyhkö, J and Talve, L. (eds.) *Understanding the Global System. The Finnish Perspective*. Figare 1999-2002. Turku 2002.

Christensen, J. H. 1999. Climate projections: Scale-related uncertainties. In Carter, T. R., Hulme, M. and Viner, D. (eds*) Representing Uncertainty in Climate Change Scenarios and Impact Studies*. ECLAT-2 Report No.1. Helsinki Workshop, 14-16 April, 1999. CRU, Norwich, UK

Colbeck, S.C. 1982. An Overview of Seasonal Snow Metamorphism*. Reviews of Geophysics and space physics*. Vol. 20, No. 1. 45-61.

Colbeck, S.C. 1982b. Growth of faceted crystals in a snow cover. *CRREL Report* 82-29.

Colbeck, S.C. 1983. Snow particle morphology in the seasonal snow cover. *Bulletin American Meteorological Society*. Vol. 64. No. 6. 602-609.

Colbeck, S. C. 1987. History of snow-cover research. *J. Glaciol*. Special Issue 1987. 60-65.

Colbeck, S.C. and 7 others (edt.). 1990. *The international classification for seasonal snow on the ground*. Wallingford, Oxfordshire, International Association of Scientific Hydrology. International Commision on Snow and Ice.

Colbeck, S.C. 1997. A review of sintering in seasonal snow cover. *CRREL Report* 97-10.

Dexter, L. 1987. A simple snowpack structure model and its application to mountain snowpack. *IAHS Publications*. No. 166.

Donald, J. R., Soulis, E. D., Kouwen, N. And Pietroniro, A. 1995. A land cover –based snow cover representation for distributed hydrologic models. *Water Resources Research*. Vol. 31. No. 4. 995-1009.

Durand, Y., Giraud, G., Brun, E., Merindol, L. and Martin, E. 1999. A computer-based system simulating snowpack structures as a tool for regional avalanche forecasting. *Journal of Glaciology*. Vol. 45. No. 151. 469-484.

Edens, M. Q., and Brown, R. L. 1995. Measurements of microstructure of snow from surface sections. *Def. Sci. J*. 45. 107-116.

Essery, R. and Yang, Z. 2001. An overview of models participating in the snow model intercomparison project (SNOWMIP). *8th Scientific Assembly of IAMAS*. Innsbruck 2001.

Etchevers, P. *and 21 others*. 2002. SnowMIP, an intercomparison of snow-cover models: first results. *In* Stevens, J.R., *ed. International Snow Science Workshop 2002, 29 September--4 October 2002, Pentiction, British Columbia. Proceedings.* Victoria, B.C., B.C. Ministry of Transportation. Snow Avalanche Programs, 353-360.

Eugster, H. P. 1952. Beitrag zu einer Gefugeanalyse des Schnees. *Beitr. Geol. Schweiz, Geotech. Ser. Hydrologie*, Kummerly u. Frey, Bern.

Eurola, S., Kyllönen, H. and Laine, K. 1980. Lumen ekologisesta merkityksestä kasvillisuudelle Kilpisjärven alueella. *Luonnon Tutkija*. 84. 43-48.

Fierz, C. and Baunach, T. 2000. Quantifying grain-shape changes in snow subjected to large temperature gradients. *Annals of Glaciology*. Vol. 32. 439-444.

Fierz, C., P. Etchevers, R. Jordan, M. Lehning, Y. Lejeune, E. Martin. SnowMIP, an intercomparison of snow models: Comparison of detailed snow-cover simulations. *Annals of Glaciology*. Vol. 38. (in press).

Fierz, C. and Lehning, M. 2001. Assessment of the microstructure-based snow-cover model SNOWPACK: thermal and mechanical properties. *Cold Regions Science and Technology*. Vol. 33. 123-131.

Finnish Environment Institute.1999. *Monthly hydrological reports; Hydrological Review* 1999. Finnish Environment Institute, Helsinki.

Finnish Environment Institute.2000. *Monthly hydrological reports; Hydrological Review* 2000. Finnish Environment Institute, Helsinki.

Finnish Environment Institute.2001. *Monthly hydrological reports; Hydrological Review* 2001. Finnish Environment Institute, Helsinki.

Finnish Environment Institute.2002. *Monthly hydrological reports; Hydrological Review* 2002. Finnish Environment Institute, Helsinki.

Finnish Meteorological Institute. 1979. Results of soil temperature measurements in Finland, 1961-1970. *Soil temperature measurements*. No. 3. Finnish Meteorological Institute, Helsinki.

Finnish Meteorological Institute. 1991. Climatological statistics in Finland 1961-1990. *In Meteorological Yearbook of Finland*, *1990.* (Supplement 1-1990). Finnish Meteorological Institute, Helsinki.

Finnish Meteorological Institute. 1999. *Climate Review*. December 1999. Finnish Meteorological Institute, Helsinki.

Finnish Meteorological Institute. 2000. *Climate Review*. December 2000. Finnish Meteorological Institute, Helsinki.

Finnish Meteorological Institute. 2001. *Climate Review*. December 2001. Finnish Meteorological Institute, Helsinki.

Finnish Meteorological Institute. 2002. *Climate Review*. December 2002. Finnish Meteorological Institute, Helsinki.

Formozov, A. N. 1946. *Snow cover as an environmental factor and its importance in the life of mammals and birds.* Moscow Society of Naturalists, materials for the Study of Fauna and Flora USSR, Zoology Section, N.S. 5. 141 pp.

Fukuzawa, T. ja Akitaya, E. 1993. Depth-hoar crystal growth in the surface layer under high temperature gradient. *Annals of Glaciology*. Vol. 18, 39-45.

Gjaerevoll, 0. 1956. The plant communities of Scandinavian alpine snow-beds. *Kongel. Norske Videnskabers Selsk*. Skr. 1956 (1) 1-405.

Gobulev, V.N. and Frolov, A.D. 2000. Model of structure and mechanical properties of dry granular snow. *Annals of Glaciology*. Vol. 32. 434-438.

Golding, D. L. and Swansson, R. H. 1986. Snow distribution patterns in celarings and adjacent forest. *Water Resources Research*. Vol. 22. No. 13. 1931-1940

Gordon, C. *and 7 others*. 2000. The simulation of SST, sea ice extents and ocean heat transports in a version of the Hadley Centre coupled model without flux adjustments. *Climate Dyn.*, Vol. 16. No.2-3. 147-168.

Granberg, H. B. 1998. Snow cover on sea ice. In Leppäranta, M. (edt.) *Physics of ice-covered seas.* Vol. 2. IAPSO Sea Ice Commission. University of Helsinki.

Grönholm, T. 2003. *Lumipeitteen rakenteen SNOWPACK mallin toimivuus Suomen lumivyöhykkeillä*. Master's Thesis. University of Helsinki.

Hallikainen, M., Jääskeläinen, V. And Van Oijen, J. 1990. Effects of land cover categories to microwave remote sensing of snow. IGARSS '90. *10th Int. Geosc. And Remote Sensing Symp.* Washington, USA.

Helle, T. 1984. Foraging behaviour of semi-domesticated reindeer (Rangifer tarandus tarandus) in relation to Snow in Finnish Lapland. *Reports from the Kevo Subarctic Research Station.* 19. 35-47.

Helle, T., Kojola, I. and Timonen, M. 2001. Lumipeitteen vaikutus Käsivarren porolukuihin: mikä on Pohjois-Atlantin säävaihtelun (NAO) merkitys? *Suomen Riista.* 47. 75-85.

Hiltunen, R. 1980. Tuulenpienksämän ja lumenviipymän lämpötila- ja lumioloista Pikku-Mallalla. *Luonnon Tutkija*. 84. 11-14.

Houghton, J.T. and 7 others (Edt.). 2001. *Climate change 2001: the scientific basis.* Cambridge, etc., Cambridge University Press. Intergovernmental Panel on Climate Change. (Contribution of Working Group I to the Third Assessment Report.)

Hulme, M. and Carter, T. R. 1999. Representing Uncertainty in Climate Change Scenarios and Impact Studies. In Carter, T. R., Hulme, M. and Viner, D. (eds*) Representing Uncertainty in Climate Change Scenarios and Impact Studies*. ECLAT-2 Report No.1. Helsinki Workshop, 14-16 April, 1999. CRU, Norwich, UK.

Iqbal, M. 1983. *An introduction to Solar Radiation*. Academic Press. Canada, Ontario. 390 p.

Jones, R. N. and 9 others. Representing uncertainties in water resource impact assessments. In Carter, T. R., Hulme, M. and Viner, D. (eds*) Representing Uncertainty in Climate Change Scenarios and Impact Studies*. ECLAT-2 Report No.1. Helsinki Workshop, 14-16 April, 1999. CRU, Norwich, UK

Jordan. R. 1991. A one-dimensional temperature model for a snow cover. *CRREL Special Report*
91-16.

Katz, R. W. 1999. Techniques for Estimating Uncertainty in Climate Change Scenarios and Impact Studies. In Carter, T. R., Hulme, M. and Viner, D. (eds*) Representing Uncertainty in Climate Change Scenarios and Impact Studies*. ECLAT-2 Report No.1. Helsinki Workshop, 14-16 April, 1999. CRU, Norwich, UK.

Koivusalo, H., Heikinheimo, M. and Karvonen, T. 2001. Test of a simple two-layer parameterisation to simulate the energy balance and temperature of a snow pack. *Theor. Appl. Climatol*. Vol. 70. 65-79.

Korhonen, V. 1917. Lumisateista Suomessa. *Suomalaisen tiedeakatemian esitelmät ja pöytäkirjat*. Helsinki. 43 p.

Kuhry, P. and 14 others. 2002. Arctic feedbacks to global warming. In Käyhkö, J and Talve, L. (edt.) *Understanding the Global System. The Finnish Perspective*. Figare 1999-2002. Turku 2002.

Kuusisto, E. 1973. Lumen sulamisesta ja sulamiskauden vesitaseesta Lammin Pääjärvellä 1970-72. *Vesihallituksen tiedotus.* 46.

Kuusisto, E. 1984. Snow accumulation and snow melt in Finland. *Publications of the Water Research Institute*. 55.

Körner, C (edt.). 2003. *Alpine Plant Life*. Springer Verlag.

Laevastu, T. 1960. Factors affecting the temperature of the surface layer of the sea. *Commentat. Phys. Math*., 25.

Lavila, T. O. 1949. Lumisademäärän alueellinen jakautuminen Suomessa. *Turun yliopiston julkaisuja*, Sarja A, osa VII:2.

Lehmusjärvi, R. 2001. *Lumen vesiarvon mittaaminen ja tulokset eri menetelmillä*. Candidate of Science thesis. University of Helsinki.

Lehning, M., Bartelt, P., Brown, B., Russi, T., Stöckli, U. and Zimmerli, M. 1998. SNOWPACK moldel calculations for avalanche warning based upon a network of weather and snow stations. *Cold Regions Science and Technology*. Vol. 30. 145-157.

Lehning, M., Doorschot, J. and Bartelt, P. 2000. A snowdrift index based on SNOWPACK calculations. *Annals of Glaciology*. 31. 382-386.

Lehning, M., Fierz, C. and Lundy, C. 2001. An objective snow profile comparison method and its application to SNOWPACK. *Cold Regions Science and Technology*. Vol. 33. 253-261.

Lehning, M., P. Bartelt, B. Brown, C. Fierz and P. Satyawali. 2002a. A physical SNOWPACK model for the Swiss avalanche warning. Part II. Snow microstructure, *Cold Reg. Sci. Technol*., Vol. 35. No. 3. 147-167.

Lehning, M., P. Bartelt, B. Brown and C. Fierz. 2002b. A physical SNOWPACK model for the Swiss avalanche warning service. Part III. Meteorological forcing, thin layer formation and evaluation, *Cold Reg. Sci. Technol.,* Vol. 35. No. 3., 169-184.

Lemmelä, R. 1970. *Lumen sulamisesta, sulamisesta aiheutuvasta valunnasta sekä pohjaveden muodostumisesta hiekkaperäisellä alueella*. Licenciate Thesis. University of Helsinki.

Leppäranta, M. 1995. *Lumen ja jään geofysiikka*. University of Helsinki

Lind, D. ja Sanders, S. P. 1996. *The physics of skiing*. AIP Press.

Liston, G. E. and Sturm, M. 1998. A snow-transport model for complex terrain. *Journal of Glaciology*. Vol. 44. No. 148. 498-516.

Lundy, C., R.L. Brown, E.E. Adams, K.W. Birkeland and M. Lehning. 2001. A statistical validation of the SNOWPACK model in a Montana climate. *Cold Reg. Sci. Technol*., **33**(2-3). 237-246.

Maanmittaushallitus. 1964. Peruskartta no. 4613 03, Oulanka.

Maanmittaushallitus. 1965. Peruskartta no. 2134 04, Lammi.

Maanmittaushallitus. 1974. Peruskartta no. 4244 05, Lehtovaara.

Maanmittaushallitus. 1987. *Suomen kartasto*. Vihko 131: Ilmasto. Maanmittaushallitus,Suomen maantieteellinen seura.

Maanmittaushallitus. 1998. Ulkoilukartta, Kilpisjärvi.

Maanmittaushallitus. 1999. Peruskartta no. 2011 09, Horsön.

Mahajan, P. and Brown, R. 1993. A microstructure-based constitutive law for snow. *Annals of Glaciology*. Vol. 18. 287-294.

Marbouty, D. 1980. An experimental study of temperature-gradient metamorphism. *Journal of Glaciology*. Vol. 26. No. 94. 303-312.

Marsh, P. 1987. Grain growth in a wet arctic snow cover. *Cold Regions Science and Technology*. Vol. 14. 23-31.

McKay, G.A. and Gray, D.M. 1981. The distribution of snowcover. In Gray, D.M. and Male, D.H. (Eds). *Handbook of Snow*. Pergamon Press. Canada. 153-190.

Morris, E.M. and 4 others. 1994. Modelling mass and energy exchange over polar snow using DAISY model. *IAHS Publications*. No. 223.

Mustonen, S. 1965. Ilmasto- ja maastotekijöiden vaikutuksesta lumen vesiarvoon ja roudan syvyyteen. *Acta Forestalia Fennica* 79.

Nakićenović, N. and 27 others. 2000. *Climate Change 2001*: *the scientific basis*. Cambridge, etc., Cambridge University Press. Intergovernmental Panel on Climate Change. (A Special Report of Working Group III.)

Niemelä, S., Räisänen, P. and Savijärvi, H. 2001. Comparison of surface radiative flux parameterizations. Part II. Shortwave radiation. *Atmospheric Research*. 58. 141-154.

Nordiska ministerrådet. 1984. *Vegetationstyper i Norden*. Berlings, Arlöv.

Nordlund, A. 1999. *Sääpäiväkirja*. Otava, Keuruu.

North Atlantic Oscillation (NAO) Indices Information. 2004. NCAR. Climate Analysis Section. Climate and Global Dynamics Division. 12.10.2004. <*http://www.cgd.ucar.edu/~jhurrell/nao.stat. winter.html*>

Oksanen, T. 1999. *Suomen lumipeitteen alueellinen vaihtelu*. Master's Thesis. University of Helsinki.

Omstedt, A. 1990. A coupled one-dimensional sea ice-ocean model applied to a semi-enclosed basin. *Tellus*. 42A. 568-582.

Quervain, M.DE. 1950. Die Festigkeitseigenschaften der Schneedecke und ihre Messung. *Geofisica pura e applicata*. Bd. XVIII.

Paterson, W. S. B. 1994. *The physics of glaciers*. Pergamon.

Palosuo, E., Keinonen, J., Suominen, H., Jokitalo, R. 1979. Lumen ja suksenpohjamuovien välisen kitkan mittauksia. Osa 2. *Report Series in Geophysics*. No. 13. University of Helsinki.

Perla, R. I. 1978. *Snow Crystals*. NHRI Paper No. 1. National Hydrology Research Institute, Environment Canada, Ottawa.

Perälä, J. and M. Reuna. 1990. Lumen vesiarvon alueellinen ja ajallinen vaihtelu Suomessa. *Vesi- ja ympäristöhallinnon julkaisuja*. A 56.

Pfeffer, W.T and Mrugala, R. 2002. Temperature gradient and initial snow density as controlling factors in the formation and structure of hard depth hoar. *Journal of Glaciology*. Vol. 48. No. 163. 485-494.

Pomeroy, J. and Brun, E. 2001. Physical properties of snow. In Jones, H., Pomeroy, J., Walker, D. and Hoham, R. (Edt.) *Snow ecology*. Cambridge University Press. 201. USA.

Pomeroy, J. W. and Gray, D. M. 1990. Saltation of snow. *Water Resources Res*. Vol. 26. No. 7. 1583-1594.

Pruitt, W. 1959. Snow as a factor in the winter ecology of the barren-ground caribou (Rangifer arcticus). *Arctic.* 12. 158-179.

Rasmus, K., H. Granberg, K. Kanto, E. Kärkäs, C. Lavoie and M. Leppäranta. 2003. Seasonal snow in Antarctica. Data report. *Report Series in Geophysics* No 47. University of Helsinki, Division of Geophysics.

Rasmus, S., Räisänen, J. and Lehning, M. 2005. Estimating snow conditions in Finland in the late 21st century using the SNOWPACK –model with regional climate scenario data as input. *Annals of Glaciology*. 38. (in press).

Reimers, E. 1982. Winter mortality and population trends of reindeer on Svalbard, Norway. *Arctic and Alpine Research*. 14. 295-300.

Roeckner, E., L. Bengtsson, J. Feichter, J. Lelieveld and H. Rodhe. 1999. Transient climate change simulations with a coupled atmosphere--ocean GCM including the tropospheric sulfur cycle. *J. Climate*, Vol. 12. No. 10. 3004-3032.

Räisänen, J. 2001. CO_2-induced climate change in CMIP2 experiments: quantification of agreement
and role of internal variability. *J. Climate*, Vol. 14. No. 9. 2088-2104.

Räisänen, J. and 8 others. 2003. *GCM driven simulations of recent and future climate with the Rossby Centre coupled atmosphere --- Baltic Sea regional climate model RCAO*. Norrköping, Sveriges Meteorologiska och Hydrologiska Institut. (SMHI Reports of Meteorology and Climatology 101.)

Saarnisto, M. and 10 others. 2002. Modelling past global change – forecasting the future. In Käyhkö, J and Talve, L. (eds) *Understanding the Global System. The Finnish Perspective*. Figare 1999-2002. Turku 2002.

Sato, A., Adams, E. E. and Brown, R. L. 1994. Effect of microstructure on heat and vapor transport in snow composed of uniform ice spheres. *Proceedings of the International Snow Science Workshop*. Snowbird, Utah. 176-184.

Satyawali, P.K. 2000. Diffusivity and vapour flow into snow during the phase change. *Annals of Glaciology*. Vol. 32. 445-450.

Seligman, G. 1936. *Snow Structure and Ski Fields*. Macmillan, London.

Seppänen, M. 1967. Average depth of snow in undulating land in Finland. *Geophysica*. Vol. 9, No. 4, 277-285.

Shapiro, L.H., Johnson, J.B., Sturm, M. and Blaisdell, G.L. 1997. Snow Mechanics: Review of the state of knowledge and applications. CRREL Report. 97-3.

Shook, K. and Gray, D. 1994. Determining the snow water equivalent of shallow prairie snowcovers. *Proceedings of 51st Eastern Snow Conference*, Dearborn, Michigan.

Shook, K. and Grey, D. M. 1996. Small-scale spatial structure of shallow snow covers. *Hydrological Processes*. Vol. 10. 1283-1292.

Simojoki, H. and Seppänen, M. 1963. On the vertical distribution of the density of the snow cover. *Geophysica*. Vol. 7. No. 4.

Singh. A.K. 1999. An investigation of the thermal conductivity of snow. *Journal of Glaciology*. Vol. 45. No. 150. 346-351.

Solantie, R. 2000. Snow depth on January 15th and March 15th in Finalnd 1919-98, and its implications for soil frost and forest ecology. *Meteorologisia julkaisuja* 42. Finnish Meteorological Institute, Helsinki

Solantie, R. 1998. Occurence of Unfrozen Ground in Finland. *Geophysica.* Vol. 34. No. 3. 141-157.

Solantie, R., A. Drebs, E. Hellsten and P. Saurio. 1996. Lumipeitteen tulo-, lähtö- ja kestoajoista Suomessa talvina 1960/61--1992/1993. *Meteorologisia julkaisuja* 34. Finnish Meteorological Institute, Helsinki

Solantie, R. and Junila, P. 1995. Sademäärien korjaaminen Tretjakovin ja Wildin sademittarien vertailumittausten avulla. *Meteorologisia julkaisuja* 33. Finnish Meteorological Institute, Helsinki

Solantie, R. 1981. Lumipeitteen vesiarvon vuotuinen maksimi ja sen ajankohta. *Vesitalous.* No. 5/1981.

Solantie, R. 1978. On the variation of snow depth on 15th March in Finland. *Nordic Hydrological Conference, Hanasaari. Papers of sessions II.*

Sommerfeld, R. A. and LaChapelle, E. 1970. The classification of snow metamorphism. *Journal of Glaciology*. Vol. 9. No. 45. 3-17.

Sturm, M. and Benson, C.S. 1997. Vapour transport, grain growth and depth-hoar development in the subarctic snow. *Journal of Glaciology*. Vol. 43. No. 143. 42-59.

Sturm, M., Holmgren, J. and Liston, G. E. 1995. A seasonal snow cover classification scheme for local to global applications. *J. Climate*, 8(5), Part 2, 1261-1283.

Sturm, M., Holmgren, J., König, M. and Morris, K. 1997. The thermal conductivity of seasonal snow. *Journal of Glaciology*. Vol. 43. No. 143. 26-41.

Sturm, M. and Holmgren, J. 1998. Differences in compaction behaviour of three climate classes of snow. *Annals of Glaciology*. 26. 125-130.

Vehviläinen, B. 1992. *Snow cover models in operational watershed forecasting*. Publications of Water and Environment Research Institute. 11.

Venäläinen, A. 1994. *The spatial variation of mean monthly global radiation in Finland*. Licentiate Thesis. University of Helsinki.

Vesala, T., Haataja, J., Aalto, P., Altimir, N. and Buzorius, G. And others. 1998. Long-term field measurements of atmosphere-surface interactions in boreal forest ecology, micrometeorology, aerosol physics and atmospheric chemistry. *Trends in Heat, Mass and Momentum Transfer*. 4. 17-35.

Vesihallitus. 1984. *Hydrologiset havainto- ja mittausmenetelmät*. Vesihallituksen julkaisuja 47.

Wolley, J. 1858. *Report of the British Association.* Part II. 40-41.

Yamazaki, T., Kondo, J., Sakuraoka, T. and Nakamura, T. 1993. A one-dimensional model of the evolution of snow-cover characteristics. *Annals of Glaciology*. Vol. 18. 22-26.

Yosida, Z. and others. 1955. Physical studies on deposited snow: thermal properties. *Contrib. Inst. Low Temperture Sci*., Ser. A. 27. 19-74.

Appendix I :
List of symbols

Appendix II:
Sorted table of slope values of the time-density curves in the snow zonation testing

Appendix III:
Structure of the SNOWPACK -model

Appendix IV:
Agreement scores, an objective snow profile comparison method

Appendix V:
Overall agreement scores between observations from Hyytiälä 2000/2001 and the different test runs

Appendix I. List of symbols

In the order of appearance (symbols used only in appendices not included):

Symbol	Description and value	Unit
ΔQ	total energy exchange	Wm^{-2}
Q_{sw}	incoming short wave radiation	Wm^{-2}
α	albedo	
Q_{La}	atmospheric long wave radiation	Wm^{-2}
Q_{Lo}	long wave radiation emitted by the snow cover	Wm^{-2}
Q_c	sensible heat flux	Wm^{-2}
Q_e	latent heat flux	Wm^{-2}
Q_{pc}	melting/refreezing heat	Wm^{-2}
ρ_s	snow density	kgm^{-3}
c_s	specific heat capacity of snow	$Jkg^{-1} K^1$
T_s	snow bulk temperature	K
t	time	s
k_e	effective thermal conductivity of snow	$Wm^{-1}K^1$
z	vertical coordinate	m
h	snow depth	m
F_d	cold content of the snow cover	Jm^{-2}
F_m	energy needed for melt	Jm^{-2}
L	latent heat of melting	Jkg^{-1}
Θ	thermal quality of the snow cover	
θ_w	volume fraction of liquid water in snow	
θ_a	volume fraction of air in snow	
θ_i	volume fraction of ice in snow	
σ_s	stress	Pa
g	gravitational acceleration	ms^{-2}
ϕ	slope angle	°
ε	total strain	
ε_e	elastic strain	
ε_v	viscous strain	
η	viscosity	Pa s
J_v	water vapour flux	$kgm^{-2}s^{-1}$
M_{mm}	water vapour deposition/sublimation mass	kg
J_w	liquid water flux	$kgm^{-2}s^{-1}$
ρ_i	density of ice	kgm^{-3}
ρ_w	density of water	kgm^{-3}
ρ_a	density of air	kgm^{-3}
p_a	water vapour partial pressure	Pa
p_s	water vapour saturation pressure	Pa
T_A	air temperature	K
T_{ss}	surface temperature	K
T_g	ground temperature	K
T_h	temperature at depth h	K
RH	relative humidity	
VW	wind velocity	ms^{-1}
DW	wind direction	°
P	precipitation, in water equivalent	mm
u_i	displacement	m
q_h	vapour mass flux at the snow pack surface	kg
RB	bond radius	mm
RG	crystal radius	mm
DN	dendricity of snow crystals (0-1)	
SP	sphericity of snow crystals (0-1)	
FR	categorical variable indicating previous melt and refreeze (0 or 1)	
n	days from the latest snow fall	
ρ_n	new snow density	kgm^{-3}

Appendix II. Sorted table of slope values of the time-density curves from the different snow surveys

Snow survey location	Slope	Correct?
IITTOVUOMA 2	0,6511	
YLIJOKI, RANUA	0,6664	Yes
SYVÄOJA, SAVONLINNA	0,6916	
KOTIOJA, RANUA	0,7028	Yes
IITTOVUOMA 3	0,7065	
Savukoski, Ainijärvi	0,7793	Yes
Pesiö, Joutenvaara	0,785	Yes
ANSOPURO, SOTKAMO	0,8063	Yes
MYLLYOJA, SAVUKOSKI	0,8211	Yes
Salla, Kelloselkä	0,8314	Yes
IITTOVUOMA 4	0,8536	
Inari, Nellim	0,8747	Yes
Sodankylän observatorio	0,9006	Yes
Ylitornio, Meltosjärvi	0,9253	Yes
Puolanka	0,9318	Yes
Orimattila, Keituri	0,9329	
Siilinjärvi	0,9753	
Kalanti	0,9759	
Puumala, Heiska	1,0029	
Kittilä, Hormakumpu	1,0046	Yes
Savitaipale	1,0292	Yes
Sodankylä, Vuotso	1,0296	
Vuolijoki, Saaresmäki	1,0385	Yes
Lappi, Kaukola	1,0664	
Sonkajärvi, Uura	1,0853	Yes
Anjalankoski, Mämmälä	1,1109	
Kuhmo, Jonkeri	1,1392	
Haukivuori	1,1596	Yes
Hyrynsalmi, Paljakka	1,1655	
Taivalkoski, Inget	1,1996	
Varpaisjärvi, Kärsämäki	1,2127	Yes
Turku	1,2145	
Sotkamo, Laaka	1,2192	
Kemijärvi, Halosenranta	1,2386	
Suomussalmi, Ruhtinansalmi	1,2387	
Rovaniemi, Olkkajärvi	1,2436	
Sodankylä, Unari	1,2451	
Salla, Naruska	1,2488	
Utsjoki	1,2544	
Tohmajärvi, Kemie	1,2662	Yes
Rautavaara, Alaluosta	1,2691	Yes
Konginkangas, Kivetty	1,2764	Yes
Pihtipudas, Luomala	1,2766	Yes
Ilomantsi	1,3298	Yes
Ilomantsi, Naarva	1,3344	Yes
Kuusamo, Teeriranta	1,3349	
Pudasjärvi, Korpinen	1,3482	
SIUKOLANPURO, ORIVESI	1,353	Yes
KOHISEVANPURO, KARTTULA	1,3696	Yes
Kuhmo, Varajoki	1,4128	
Pudasjärvi, Jonku	1,431	
Jalasjärvi	1,4353	Yes
Temmes	1,4443	
Jokioinen	1,4509	Yes
JUONISTONOJA, HAUKIVUORI	1,4527	Yes
Urjala, Valajärvi	1,4607	Yes
Pudasjärvi, Sarakylä	1,4938	
Kuhmo, Lentua	1,531	
Karleby	1,5323	
Pulkkila, Jylhänranta	1,557	Yes
Saarijärvi, Pyhäjärvi	1,6606	Yes
NORRSKOGSDIKET, NÄRPES	1,7336	
Pielavesi, Säviä	1,9048	Yes

Zone	Slope (kgm^-3/d)
Maritime	1.03-2.04
Taiga	0.43-0.72

Appendix III. Structure of the SNOWPACK –model

In this appendix the use of governing equations introduced in Chapters 2 and 4 in the SNOWPACK –model are gone through in detail. The equations are bulk temperature equation (energy equation), vapour diffusion equation (mass conservation of air phase), water transport equation (mass conservation of water phase) and the settlement equation (momentum conservation of ice phase). The parameterisation of thermal conductivity and viscosity, as well as of grain size and shape development for equilibrium growth, kinetic growth and wet snow metamorphoses are gone through. In the last section of this appendix the boundary conditions of the SNOWPACK –model are discussed in detail. Most of the contents of this appendix can be found in the articles by Bartelt and Lehning (2002) and Lehning and others (2000, 2002a and 2002b).

1. Bulk temperature equation

The conservation of energy leads to following equation:

$$P_s(z,\ t)c_s(\theta,\ z,\ t)\frac{\partial T_s(z,\ t)}{\partial t} - k_e(\theta,\ z,\ t)\frac{\partial^2 T_s(z,\ t)}{\partial z^2} = Q_{pc}(z,\ t) + Q_{sw}(z,\ t) + Q_{mm}(z,\ t). \tag{1}$$

where P_s is the snow density and c_s is the specific heat capacity of snow at constant pressure,

$$P_s c_s = P_i c_i \theta_i + P_w c_w \vartheta_w + P_a c_a \theta_a. \tag{2}$$

Q_{pc} is an energy sink or source term accounting for melting and melt water refreezing, Q_{sw} the short wave radiation energy source term and Q_{mm} a vapour diffusion energy sink or source term representing the latent heat contribution of sublimation and deposition of water vapour. (Bartelt and Lehning, 2002)

<u>Q_{pc}</u>

A link between meteorological energy input and surface and subsurface melting is needed. Melt water refreezing and subsurface melting are treated as volumetric heat sources and sinks, that correspond to changes in an element's volumetric ice and water contents. Subsurface melting is treated as a constraint on the temperature field. Even if the numerical heat transfer solution produces temperatures higher than 0°C at certain depth and time, the snow temperature has to remain at 0°C. The excess energy is used to melting.

ΔT is the difference between the calculated snow temperature T_s' and the melting temperature, T_m=0 °C,

$$\Delta T = T_s' - T_m. \tag{3}$$

The mass of melt water Δm_w that can be produced is

$$\Delta m_w = \frac{c_i m_i \Delta T_s}{L_f} \qquad (4)$$

Because the volumetric ice and water contents are used to describe the snow matrix, the above equation can also be written:

$$\Delta \theta_w = \frac{c_i \theta_i P_i \Delta T_s}{L_f P_w} \qquad (5)$$

The change in volumetric ice content is then

$$\Delta \theta_i = \frac{P_w \Delta \theta_w}{P_i}. \qquad (6)$$

The latent heat energy per unit volume required for the phase change is

$$Q_{pc} = L_f \Delta \vartheta_i P_i. \qquad (7)$$

This term is added to the governing differential energy equation at the next time step to enforce the temperature constraint. Melt water refreezing is treated similarly, but this time ΔT is negative, $\Delta \theta_i$ is positive and Q_{pc} is a heat source that raises the bulk temperature of the snow pack. Since the viscosity and heat conduction are functions of the volumetric ice and water contents phase changes will influence the settlement velocities. (Bartelt and Lehning, 2002)

<u>Q_{sw}</u>

Q_{sw} equals the amount of short wave energy absorbed by the snow cover,

$$Q_{sw} = \mathrm{RSWR}(1/A-1) \qquad (8)$$

where RSWR is measured reflected short wave radiation and A is albedo, or when the incoming short wave radiation, SWR, is measured, SWR(1-A).

$$Q_{sw} = \mathrm{SWR}(1-A) \qquad (9)$$

(Bartelt and Lehning, 2002)

<u>Q_{mm}</u>

The calculated vapour pressure cannot be greater than the saturation pressure. The saturation pressure is a constraint on the vapour pressure field.

The difference between the calculated vapour pressure (p_v') and saturation pressure is:

$$\Delta p = p_v' - p_s. \qquad (10)$$

The excess mass of vapour in the pore air (Δm_v) that must be deposited on the ice lattice (Δm_i) to enforce the saturation constraint is

$$\Delta m_v = -\Delta m_i = -\frac{V_a \mu_v}{R T_s} \Delta p. \tag{11}$$

The change per unit volume over the time step Δt is

$$M_{mm} = \frac{\Delta m_v}{V_a \Delta t} = -\frac{\theta_a \mu_v}{R T_s} \frac{\Delta p}{\Delta t}. \tag{12}$$

The associated energy exchange is

$$Q_{mm}=L_s M_{mm}. \tag{13}$$

For the case when the $p_v<p_s$ (undersaturated), $M_{mm}=Q_{mm}=0$. The change in volumetric ice content is

$$\Delta \theta_i = \frac{\theta_a \mu_v}{P_i R T_s} \Delta p. \tag{14}$$

(Bartelt and Lehning, 2002)

2. Thermal conductivity:

k_e is the bulk conductivity, which is usually written as,

$$k_e=k_i\theta_i+k_w\theta_w+k_a\theta_a. \tag{15}$$

To solve the equation 1 an estimation of the thermal conductivity of snow is needed. It must be parameterised including all heat transfer processes not explicitely modelled, like vapour transport across a pore space or ventilation. The effective heat conduction model included in SNOWPACK is extended version of works by Adams and Sato (1993), Sato et al. (1994) and Edens and Brown (1995). In these works snow is modelled as a system of ice grains and pores in series and parallel with each other. The heat conduction is divided into three parts: solid ice conduction from one grain through a bond into a neighbouring grain; series conduction of heat through a grain, then across a pore and again into another grain and conduction purely across a pore. In SNOWPACK also series conduction of heat through a grain, then across a pore filled with water and again into another grain is included. (Lehning et al., 2002a)

The effective conductivity is written as:

$$k_e = \frac{n_{ca}}{n_{cl}} \left[\frac{\pi^2 r_b k_i N_3 F_k}{32} + \frac{k_a k_{ap} A_{ip}}{L_{is} k_{ap} + L_{ps} k_i} + \frac{k_a k_w A_{iw}}{L_{is} k_w + L_{ws} k_i} + \frac{k_{ap} A_p}{L_p} \right]. \tag{16}$$

There are two changes made compared to the original Adams and Sato (1993) model: the effect of transport of latent heat has been added to conductivity of air in the pore conduction term – so any conduction of heat in the pore includes the transport of vapour - and the effect of liquid water is introduced.

The empirical correction factor F_k had to be included in the first term, which describes the heat conduction grain–bond–grain. The factors are discussed in detail later with viscosity modelling.

$$F_k = 3.5 + 1.6\frac{e^{-x}}{1+e^{-x}}. \tag{17}$$

Here x is:

$$x = \frac{0.3 - \Theta_i}{0.05} \tag{18}$$

(Lehning et al., 2002a)

3. Vapour diffusion equation, mass conservation of air phase

The pore air pressure P_a is the sum of the partial pressures of the dry air Pd and water vapour P_w. The air density is similarly the sum of the water vapour density and dry air density. The relations between densities and pressures can be given as, assuming that the air is ideal gas:

$$P_v = \frac{p_v \mu_v}{RT_s} \tag{19}$$

and

$$P_d = \frac{p_d \mu_d}{RT_s}. \tag{20}$$

The partial pressure of water vapour in air, relative humidity, is

$$\mathrm{rh} = \frac{p_v}{p_s}100. \tag{21}$$

The saturation pressure of water vapour is defined using an approximation for the Clausius-Clayperon equation:

$$p_s(T) = p_{s0}\exp\left[\frac{L}{R_v}\left(\frac{1}{T_0} - \frac{1}{T}\right)\right]. \tag{22}$$

The water vapour flux is given by Fick's law, and diffusion of a gas in a binary mixture:

$$J_v = -D_e\left(\frac{\partial P_v}{\partial z} - \alpha_{th}\left[\frac{P_v P_d(\mu_v + \mu_d)^2}{(P_v + P_d)\mu_v\mu_d}\frac{1}{T_s}\frac{\partial T_s}{\partial z}\right]\right) \tag{23}$$

Conservation of mass on the air phase leads to a differential equation:

$$\theta_a(z,t)\frac{\partial(P_v)}{\partial t} + \theta_a(z,t)\frac{\partial J_v}{\partial z} = M_{mm}(z,t). \tag{24}$$

Here M_{mm} is a mass sink or source term due to the deposition or sublimation of water vapour onto the ice matrix.

By combining equations 23 and 24 the following equation is obtained:

$$\theta_a\frac{\partial P_v}{\partial t} - \theta_a D_e\frac{\partial^2 P_v}{\partial z^2} + \theta_a D_e\frac{\partial}{\partial z}\left(\alpha_{tb}\left[\frac{P_v P_d(\mu_v+\mu_d)^2}{(P_v+P_d)\mu_v\mu_d}\frac{1}{T_s}\frac{\partial T_s}{\partial z}\right]\right) = M_{mm}. \tag{25}$$

(Bartelt and Lehning, 2002)

4. Water transport equation

The water phase mass conservation equation is written as

$$\frac{\partial\theta_w}{\partial t} - \frac{\partial J_w}{\partial z} = M_{pc}. \tag{26}$$

Where M_{pc} is a phase change sink or source term due to the melt water refreezing or subsurface melting. The rate of water flow per unit area, J_w is often described using Darcy's law relating water flow and matrix pressure, but the snow is normally unsaturated, and water flow through the snow is not homogenous. So the gradient in water flow is defined as

$$\frac{\partial J_w}{\partial z} = 0 \quad \text{for} \quad \theta_w \le \theta_r. \tag{27}$$

with

$$\frac{\partial J_w}{\partial z} = \dot{\theta}_f \quad \text{for} \quad \theta_w > \theta_r. \tag{28}$$

and

$$\dot{\theta}_f = \frac{\partial(\theta_w - \theta_r)}{\partial t}. \tag{29}$$

where ϑ_r is the residual water content (at the moment 0.05; in the operational version 5.0); that is, below this water remains fixed within the ice matrix. Above this value, excess water is transported to the layer below with rate defined in equation 29.

(Bartelt and Lehning, 2002).

5. Momentum conservation of ice phase

The settlement equation is

$$\frac{\partial \sigma_s(z,\ t)}{\partial z} + P_s(z,\ t)g\cos\phi = 0. \tag{30}$$

In an n layer snow pack, the stress in layer l is given by (layers are numbered from the bottom up)

$$\sigma_s(z) = \left[P_l g(z_l - z) + \sum_{j=l+1}^{n} P_j g(z_j - z_{j-1}) \right] \cos\phi. \tag{31}$$

where P_l is the density of layer l. On an infinite slope of constant slope angle ϕ, the shear stress is defined as

$$\tau_s(z) = \left[P_l g(z_l - z) + \sum_{j=l+1}^{n} P_j g(z_j - z_{j-1}) \right] \sin\phi. \tag{32}$$

Snow is deforming all the time, and the deformations are large and instationary. The state of stress is known, but the rate of deformation and the state of strain are unknown. (Bartelt and Lehning, 2002)

Given a snow layer with height h_l and original height h_0, the total strain, ε, is defined as

$$\epsilon = \int_{h_0}^{h_l} \frac{dh}{h} = \ln\left(\frac{h_l}{h_0}\right) \cdot \tag{33}$$

The total strain is divided into an elastic, ε_e, and viscous, ε_v, parts,

$$\varepsilon = \varepsilon_e + \varepsilon_v. \tag{34}$$

The constitutive law relates the elastic mean stress to the elastic strain,

$$\sigma_s = E_s \varepsilon_e = E_s(\varepsilon - \varepsilon_v), \tag{35}$$

where E_s is the density- and temperature-dependent bulk modulus of elasticity of snow. A simple rheological Maxwell law relates the viscous strain rate, $\dot{\epsilon}_v$ to the mean stress,

$$\dot{\epsilon}_v = \frac{\sigma_s}{\eta_s}. \tag{36}$$

where η_s is the snow viscosity. (Bartelt and Lehning, 2002)

6. Viscosity:

The material viscosity, η, relates the stress σ to the strain rate $d\varepsilon/dt$, when elastic deformations are small as in the case of snow settling:

$$\dot{\varepsilon} = -\sigma_s / \eta_s. \tag{37}$$

where σ_s is the applied snow pressure, here the self-weight of the snow pack.

Constitutive relationship for snow relates volumetric strain rate to hydrostatic pressure. It is a simplified version of the formulation by Mahajan and Brown (1993) including combined effects of pressure sintering, intergranular glide, bond fracture with resultant intergranular slip and elastic response. The portion describing bond fracture and the one representing intergranular glide are dropped in SNOWPACK, but the latter is expressed with empirical adjustment. Only the elastic and viscous part of the ice behaviour are employed, because the stress states in snow covers normally change slowly or are steady. (Lehning et al., 2002a)

There is a nonlinear and linear range in the calculation of viscosity. The critical stress of 0.4 MPa dividing the ranges is an ice property. So the behaviour of snow – linear or nonlinear – is determined by the stress applied to the ice in the necks, not to the snow as a whole. At low stresses the strain rate takes the form:

$$\dot{\varepsilon}_i = \sigma / \eta_i. \tag{38}$$

In the nonlinear range, the relationship between stress and strain rate is:

$$\dot{\varepsilon}_i = \sigma^n / \eta_i^t. \tag{39}$$

where the exponent n is assumed to be 3. (Lehning et al., 2002a)

Nonlinear range:

The steady state uniaxial strain rate of ice is determined by:

$$\dot{\varepsilon}_i = \frac{\sigma^n}{\eta_i} = \frac{\sigma}{\eta_i^p} = \dot{\varepsilon}_1(T_R, \sigma_1) e^{\left[\frac{Q}{R}\left(\frac{1}{T_R} - \frac{1}{T}\right)\right]} \left(\frac{\sigma}{\sigma_1}\right)^3. \tag{40}$$

Here $\dot{\varepsilon}_1(T_R,\sigma_1)$ is the strain rate at the reference temperature T_R and at the unit stress σ_1 and η_i^p is a pseudo-linear ice viscosity masking the nonlinear stress dependency. These are determined by experiments.

The above equation can be used to determine the strain rate in the necks, but before that the stresses in the neck can be related to the stresses applied to the snow. The relationship between the neck stress and the snow stress can be derived:

$$\sigma_n = \frac{4}{N_3 \theta_i} \left(\frac{r_g}{r_b}\right)^2 \sigma_s. \tag{41}$$

Here a hydrostatic pressure, σ_s, is applied to the snow. The neck stress, σ_n, is related to the snow stress by the square of the ratio of the grain size to bond size, the 3-D coordination number N_3 and the snow volume fraction.

Combining the two equations the strain rate in the neck is:

$$\dot{\varepsilon}_n = \dot{\varepsilon}_1(T_R, \sigma_1) e^{\left[\frac{Q}{R}\left(\frac{1}{T_R}-\frac{1}{T}\right)\right]} \left[\frac{4\sigma_s}{N_3\theta_i\sigma_1}\left(\frac{r_g}{r_b}\right)^2\right]^3. \tag{42}$$

The rate of bond growth due to pressure sintering $\dot{r}_b^{PS}$ is:

$$\dot{r}_b^{PS} = C_{PR} r_b \dot{\varepsilon}_n. \tag{43}$$

Here C_{PR} is the plastic Poisson's ratio which is set to

The definition of the deformation velocity gradient is needed to relate the strain rate in the necks to the volumetric strain rate of the snow. A small but finite strain is assumed:

$$\dot{\varepsilon} = \frac{du}{dz} \approx \frac{\Delta u}{\Delta z} \approx \frac{l_n \dot{\varepsilon}_n}{\Delta z} \approx \frac{l_n \dot{\varepsilon}_n}{2r_g + l_n}. \tag{44}$$

Here u is the deformation velocity. The resulting volumetric constitutive relation becomes:

$$\dot{\varepsilon} = \left[\frac{l_n}{2r_g + l_n}\right] \dot{\varepsilon}_1(T_R, \sigma_1) e^{\left[\frac{Q}{R}\left(\frac{1}{T_R}-\frac{1}{T}\right)\right]} \left[\frac{4F_\eta\sigma_s}{N_3\theta_i\sigma_1}\left(\frac{r_g}{r_b}\right)^2\right]^3. \tag{45}$$

The term $F\eta$ is an empirical constant used to fit the equation to the experimental data. It is used to take into account the intergranular gliding, lattice imperfections and also the effect of liquid water. The experimental data suggests the nonlinear dependency of $F\eta$ on the density of snow:

$$F_\eta = \frac{0.4}{\theta_i} + 3.2\frac{e^x}{1+e^x} + 35\theta_w, \qquad \text{where } x = \frac{0.3-\theta_i}{0.05}. \tag{46}$$

The viscosity then becomes:

$$\eta_s = \left\{\left[\frac{l_n}{2r_g + l_n}\right] \dot{\varepsilon}_1(T_R, \sigma_1) e^{\left[\frac{Q}{R}\left(\frac{1}{T_R}-\frac{1}{T}\right)\right]} \left[\frac{4F_\eta}{N_3\theta_i\sigma_1}\left(\frac{r_g}{r_b}\right)^2\right]^3 \sigma_s^2\right\}^{-1} \tag{47}$$

(Lehning et al., 2002a)

<u>*Linear range:*</u>

The ice is assumed to behave as a linear viscoelastic material, when the stress in the necks drops below 0.4 MPa. The steady-state strain rate of the ice in the necks is:

$$\dot{\varepsilon}_n = \frac{\sigma_n}{\eta_0} \quad (48)$$

where the linear ice viscosity is given by η_0 and is not stress dependent. The snow viscosity in the linear range becomes:

$$\eta_s = \frac{N_3\theta_1}{4}\left(\frac{r_b}{r_g}\right)^2\left(\frac{l_n+2r_g}{l_n}\right)\eta_0. \quad (49)$$

The value of η_0 can be determined by requiring a smooth transition in viscosity from the linear to nonlinear range:

$$\eta_0 = \frac{\sigma_1^3}{\dot{\varepsilon}_1(T_R,\sigma_1)F_\eta^3\sigma_{ncrit}^2}e^{-\frac{Q}{R}\left[\frac{1}{T_R}-\frac{1}{T}\right]}. \quad (50)$$

The viscosity described above is applied to the old dry and wet snow, that means to the snow that has lost its dendricity. For new snow an empirical relationship is employed:

$$\eta_s=0.007\rho^{(4.75-T_C/40)}. \quad (51)$$

(Lehning et al., 2002a)

Laboratory triaxial tests by Bartelt and Von Moos (2000) have been used to develop the viscosity not only as a function of density but microstructure as well. See also Brown et al. (2001) for microstructure based viscosity law development.

7. Equilibrium growth metamorphism

The equilibrium growth metamorphism is defined as the snow development under small temperature gradient (less than –5 °Cm^{-1}). A mixture theory has been used to model this metamorphism, validation of the theory is presented in Brown et al. (2001). See also Baunach et al. (2001). The growth and decay of bonds and grains are determined by differences between equilibrium vapour pressures of the different ice surfaces. Temperature differences between the ice surfaces develop because mass transfer between grains and necks involve heat transfer. (Brown et al., 2001)

The grain growth rate is given as function of sphericity, snow temperature, melting temperature and grain radius:

$$\dot{r}_g(T,t) = sp\left(A_1+\frac{A_2}{r_g}\right)e^{A_3(1/T_R-1/T)}. \quad (52)$$

Where A_1 is 5.9×10^{-12} (m s^{-1}), $A_2=9.4\times10^{-17}$ (m^2 s^{-1}) and $A_3=2.9\times10^3$ (K).

Mixture theory also suggests a bond growth equation of the following form:

$$\dot{r}_b(T,t) = B_1 \left(e^{\frac{-B_2}{r_b}} - e^{\frac{-B_2}{r_g}} \right) e^{B_3(1/T_R - 1/T)}. \quad (53)$$

where B_1=1.4×10^{-7} (m s^{-1}), B_2=1.9×10^{-9} (m) and B_3=4.7×10^3 (K). r_n is the thermodynamic neck radius, which determines the vapour pressure over the ice surface. It is given by:

$$\frac{2}{r_n} = \frac{1}{r_b} - \frac{1}{r_c}, \quad (54)$$

where r_c is the concave radius:

$$r_c = \frac{r_b^2}{2\left(r_g - r_b\right)}. \quad (55)$$

When the snow becomes fully faceted and after that come under low temperature gradient conditions, the grain growth will cease, because faceted surfaces are quite stable. When the grain has a high degree of sphericity, the mean grain size will continue to increase. The bonds will continue to grow regardless of the faceting. (Lehning et al., 2002a)

8. Kinetic growth metamorphism

Water vapour gradients between the ice matrix and the pores play a leading role at higher growth rates, and recrystallization occurs. Because supersaturation is low, the kinetic growth metamorphism is thought to be diffusion limited. The empirical Marbouty (1980) formulation has been quite successful in modelling faceted crystal growth, but in SNOWPACK a new approach is included in the model. (Baunach et al, 2001; Fierz and Baunach, 2000)

The water vapour flux associated to water vapour gradient between ice matrix and pore spaces is assumed to obey Fick's law:

$$J_v = -D \frac{\partial \rho_v}{\partial z}. \quad (56)$$

The vapour fluxes are vertical fluxes between snow layers and between grains within one snow layer. These formulations are local estimations, not integrated with the global vapour transport equation.

For saturated conditions the flux can be expressed:

$$J_v \left(T, \frac{\partial T}{\partial z} \right) = -D_{vs} \frac{p_S(T)}{RT^2} \left[\frac{L}{RT} - 1 \right] \frac{\partial T}{\partial z} \quad (57)$$

Here it is assumed that water vapour is an ideal gas, and the Clausius-Clayperon equation is used.

Two sources of water vapour supply are taken into account here: layer-to-layer transport calculated from the flux from the previous equation, and intra-layer or grain-to-grain flux calculated using a temperature gradient at the centre of the layer. For the latter, the ice matrix is considered to be a body-centered cubic lattice, where all grains are cubes. The central grain acts as a source and the vertex grains as sinks. Grains are allowed to grow as plates, and the growth rate is expressed using the geometrical parameters of the model:

$$\dot{r}_g(t) = \frac{a^2(t)J_L(t) + \frac{a^3(t)}{\Delta z}\Delta J_{L2L}(t)}{2f_{gg}\rho_i r_g(0) r_g(t)}. \tag{58}$$

Value 2 was given to f_{gg} to get good agreement between simulations and laboratory work results.

The growth of the bonds is calculated determining the vapour flux using a temperature gradient along the bonds.

$$\frac{\partial T}{\partial z}_{\text{bond}} = \frac{Ak_e}{A_g k_i}\frac{\partial T}{\partial z}. \tag{59}$$

The cubes are replaced by rounded grains, which are connected with vertical bonds. It is assumed, that the bonds grow due to vapour transport from the neighbouring grains. Here, *A* is an average cross-sectional area:

$$A = \frac{1}{3}(A_g + A_b + A_p) = \frac{1}{3}(\pi r_g^2 + \pi r_b^2 + A_p). \tag{60}$$

Using again Equation 57, the following rate of bond growth is finally obtained:

$$\dot{r}_b(t) = f_{gb}\frac{D_{va}}{\rho_i}\frac{p_v(T)}{RT^2}\left[\frac{L}{RT} - 1\right]\frac{\partial T}{\partial z}_{\text{bond}}. \tag{61}$$

The density-dependent geometrical factor for bond growth, f_{gb}, can be theoretically predicted for a cubic packing of grain–bond–grain units as assumed above:

$$f_{gb} = \frac{r_g^2}{r_b l_a} - \frac{r_b}{2l_a}. \tag{62}$$

F_{gb} has been given a value 0.35. (Lehning et al., 2002a)

Baunach and Fierz (2001) have adjusted the kinetic grain growth routine using the laboratory experiments. Because thermal conductivity depends on bond size, it is adjusted concurrently to bond growth rate. Viscosity was adjusted next by comparing the settlement measurements with model outputs. The reliability of the adjusted set of parameters is seen in correct simulation of temperature and density during long term runs. Settlement of new snow under high loading rates is not well reproduced, but new and fragmented type of snow are treated separately in SNOWPACK. There is found rather peculiar behaviour of conductivity and viscosity under heavy load conditions. While the layer remains near the surface large temperature gradients cause grains to grow. Viscosity is reduced, but conductivity is not affected a lot. Under load however, pressure sintering causes bonds to grow increasing the ratio of bond to grain size until the resulting increase in viscosity slows the process down. So, even if the density dos not grow, conductivity increases. (Fierz and Lehning, 2001)

9. Wet snow metamorphism

Grain growth and changes in shape are much faster in the wet than dry snow. The grain radius growth rate is based on the Brun et al. (1992) formulation:

$$\dot{r}_g(t) = \frac{4\pi(C_1 + C_2\theta_w^m(t)^3)}{r_g(t)^2}. \tag{63}$$

where the two empirical constants are: C_1=1.1 10^{-3} mm day^{-1} and C_2=3.7 10^{-5} mm day^{-1}. No data or theoretical considerations are currently available for wet snow bond growth. Therefore it is assumed that the wet snow bond growth is dominated by pressure sintering. The fast grain growth together with the low viscosity of ice at the melting temperature will cause a significant bond growth due to pressure sintering:

$$\dot{r}_b^{PS} = C_{PR} r_b \dot{\varepsilon}_n. \tag{64}$$

The change in dendricity and sphericity for new wet snow are assumed to be:

$$\dot{dd}(t) = -\frac{\theta_w^m(t)^3}{16} \text{ and } \dot{sp}(t) = -0.5\dot{dd}(t). \tag{65}$$

For old wet snow we have:

$$\dot{sp}(t) = \frac{\theta_w^m(t)^3}{16}. \tag{66}$$

(Lehning et al., 2002a)

10. Grain shape development

The rate of change in dendricity depends on the temperature gradient:

$$\dot{dd}(t) = \begin{cases} -2 \times 10^8 e^{\frac{-6000}{T}}, & \left|\frac{\partial T}{\partial z}\right| \le 5\frac{K}{m} \\ -2 \times 10^8 e^{\frac{-6000}{T}} \left|\frac{\partial T}{\partial z}\right|^{0.4}, & \left|\frac{\partial T}{\partial z}\right| > 5\frac{K}{m} \end{cases}. \tag{67}$$

Here $\dot{dd}(t)$ has the unit (1/s). The change of sphericity is made dependent on the change of dendricity:

$$\dot{sp}(t) = \begin{cases} -0.3\dot{dd}(t), & \left|\frac{\partial T}{\partial z}\right| \le 5\frac{K}{m} \\ 0.3\dot{dd}(t), & \left|\frac{\partial T}{\partial z}\right| > 5\frac{K}{m} \end{cases}. \tag{68}$$

In old and dry snow, the change of sphericity is assumed to be:

$$\dot{sp}(t) = \begin{cases} 5 \times 10^8 e^{\frac{-6000}{T}} \left(5 - \left|\frac{\partial T}{\partial z}\right|\right), & \left|\frac{\partial T}{\partial z}\right| \le 5\frac{K}{m} \\ -1 \times 10^8 e^{\frac{-6000}{T}} \left|\frac{\partial T}{\partial z}\right|^{0.4}, & \left|\frac{\partial T}{\partial z}\right| > 5\frac{K}{m} \end{cases} \tag{69}$$

The sharp transition between the two regimes in the latter equation is not supported by theoretical consideration or observational data.

Some of the observed snow changes cannot be represented by grain size or shape parameters only. So a snow type marker that tracks the history of grain development is introduced. For new snow (sphericity 0.5) the marker is set to 0. If the sphericity first reaches 1 (grains fully rounded), 2 is added to the marker; if it first reaches 0 (grains fully faceted), 1 is added to the marker. The first wetting of the grain adds 10 to the marker and the first refreezing another 10. Surface hoar or ice lenses are not part of the classification scheme. The surface hoar is modelled, but it is treated as a layer boundary consisting of grains with certain size and density (100 kgm^{-3}). Buried surface hoar layers persist in the model, and only disappear during melt process. The symbol for ice lens is used, when the volumetric ice content exceeds 0.7. (Lehning et al., 2002a)

11. Boundary conditions

Wind pumping

A simplified wind pumping model is included to find the effect on snow cover, that is effect on increase in heat and vapour transport. The thermal conductivity and the water vapour diffusivity are increased in the SNOWPACK model because of wind pumping. These will consequently have effect on grain and bond growth.

To deal with wind pumping the SNOWPACK –model has a wind speed description analogous to canopy flow is chosen: the wind speed does not vanish at the snow surface. This is a new principle in the snow cover modelling. The vertical coordinate z is zero at the snow surface, and the displacement depth d is defined first from:

$$\int_{-d}^{0} \rho(z)dz = 0.5 \text{ kg m}^{-2}. \tag{70}$$

Now a logarithmic wind profile is assumed:

$$u(z) = \frac{u_*}{k} \ln \frac{z+d}{z_0}. \tag{71}$$

Using the measured wind speed, u(z), and knowing the displacement height, d, it is possible to solve for the friction velocity, u_*, and the roughness length, z_0. (Lehning et al., 2002b)

Sensible heat flux

It is assumed, that the scalar surface layer profiles are still valid in the presence of wind pumping. The gradient of the scalar quantity temperature, T, takes the form:

$$\frac{\partial T}{\partial z} = \frac{-0.74}{kzu_*}\frac{Q_s(z)}{\rho_a c_p}. \tag{72}$$

As the surface is not entirely smooth, the measured surface temperature is set to be the temperature at the temperature at z_0: $T(z_0)=T(0)$. We can now integrate the equation above from z_0 to the height of the measured air temperature to receive:

$$T(z) - T(0) = \frac{-0.74}{ku_*}\frac{Q_s(z)}{\rho_a c_p}\ln\frac{z}{z_0}. \tag{73}$$

and the surface sensible heat flux, $Q_s(0)$ can be obtained from the measurement of wind speed and temperature at any height, z, and the surface temperature, $T(0)$:

$$Q_s(0) = \frac{-ku_*}{0.74\ln\frac{z}{z_0}}\rho_a c_p(T(z) - T(0)). \tag{74}$$

(Lehning et al., 2002b)

Latent heat

The development for the latent heat flux is identical resulting to:

$$Q_l = -C\frac{0.622L^{w/i}}{R_a T(z)}[e_s^w(T(z))rH - e_s^i(T(0))] = -C\frac{0.622L^{w/i}\rho_a}{p_a}[e_s^w(T(z))rH - e_s^i(T(0))]. \tag{75}$$

The transfer coefficient C here is obtained from the equation:

$$C = \frac{ku_*}{0.74\ln\frac{z}{z_0}}. \tag{76}$$

The exchange of latent heat determines the amount of surface hoar formed, and the observations show that best results with bulk transfer models of latent heat are obtained if surface hoar formation is taken as latent heat exchange with wind speeds lower than 3 ms^{-1}. (Lehning et al., 2002b)

Rain

The flux of energy added to the snow cover by rain is given by:

$Q_r = r_r C_p(\text{TA}–\text{TSS})$. (77)

The rain mass is added to the uppermost element of the snow cover and the water will then undergo phase changes or will be transported downwards. (Lehning et al., 2002b)

Long wave radiation

If the measured surface temperature is available it is used as an upper boundary conditions as long as it is below –1.3 °C. Above this and when the surface temperature data is not available the complete energy exchange including the long wave radiation has to be known. Cloudiness is neglected at the moment, and the atmospheric emissivity is estimated (Brutsaert, 1975):

$$\mathrm{ea} = 1.24\left(\frac{e_s(\mathrm{TA})\mathrm{RH}}{\mathrm{TA}}\right)^{\frac{1}{7}}. \qquad (78)$$

The net longwave radiation, R^{l}_{n}, is then:

$$R_l^n = -\sigma(\mathrm{eaTA}^4 - \mathrm{TSS}^4). \qquad (79)$$

(Lehning et al., 2002b)

Short wave radiation

Short wave radiation dominates the energy balance of Alpine snow packs as well as the one in the boreal zone during the spring. So it is very important to have correct formulation of snow surface albedo in the model. Two statistical models were developed using three year continuous measurements in Swiss Alps. One is based on measured meteorological parameters only, the second one includes also snow pack parameters.

The models of the optimal albedo function A have the form:

$$A = \alpha + \ln(1+x). \qquad (80)$$

The parameterisation of function x is discussed in the Chapter 5.

The amount of shortwave energy absorbed by the snow cover,

$$R_s^a = \mathrm{RSWR}(1/A - 1), \qquad (81)$$

is treated as a body (volume) source. At the layer/element boundaries, the residual radiation is calculated,

$$R_s^r(l) = R_s^a e^{-k_{ext} l}, \qquad (82)$$

where l (m) is the distance from the snow cover surface and k_{ext} is the extinction coefficient (m^{-1}). The amount of energy absorbed in the snow layer between $l2$ and $l1$ is then

$R_s^r(l1)$-$R_s^r(l2)$. (83)

The extinction coefficient varies linearly with snow density:

$$k_{ext} = \frac{\rho}{c1} + c2. \qquad (84)$$

The parameters are $c1$=3 kg m^{-2} and $c2$=50 m^{-1}.

If the measured incoming short wave radiation is given as input, it is naturally used as R_s^a.

(Lehning et al., 2002b)

<u>*Snowdrift*</u>

Deposition of snow and redistribution of already deposited snow are governed by the interaction between topography, vegetation and wind. A simple model of snowdrift has been implemented to SNOWPACK. A logarithmic wind profile is assumed. The friction velocity and roughness length are solved using grain size measurement height and measured wind speed in the calculations. The roughness length increases in the presence of snow drift and is proportional to the height of the saltation layer. (Lehning et al., 2000)

A threshold friction velocity for erosion of the snow pack is determined based on microstructural parameters: grain size, bond size, coordination number and sphericity of the uppermost snow element. From this it is possible to determine a threshold wind velocity using the equation for friction velocity and comparing the threshold wind speed to the measured one. If the measured wind speed is below the threshold, no erosion is assumed. If there is erosion, a mass flux or transport rate is calculated. (Lehning et al., 2000)

Saltation of snow particles is distinguished from transport in suspension. For the mass flux in saltation the Pomeroy and Gray (1990) parameterization is used. The mass flux in suspension is calculated integrating the product of measured wind profile and the snow particle mass concentration profile, where parameterization of Liston and Sturm (1998) of concentration at the height of the saltation layer is used. (Lehning et al., 2000)

For each time step the erodibility of the uppermost layer is checked, and the layer is eroded if the threshold wind speed, dependent on snow properties, is reached. The same procedure is then applied to the layers below. The current implementation does not take into account the drift contribution from snow precipitation. Also because of the new snow estimation procedure, possible deposition due to wind drift cannot be distinguished from snowfall. The drift index should however indicate this mass flux if the threshold friction velocity is reached. (Lehning et al., 2000)

Comparison between observed and modelled snow drifts was done in two locations in Swiss Alps. Most of the drift events were well represented by this formulation. In some cases there was an underestimation of snowdrift. This may be due to the fact that

SNOWPACK metamorphism routines tend to overestimate the development of faceted crystals; this may prevent the erosion of the layers. It is also important to remember the following shortcomings and assumptions of the snowdrift model: the index represents only local conditions; the index does not yet take drift from erosion into account; the formulation of mass flux assumes equilibrium conditions in the atmosphere; a logarithmic wind profile is assumed without influence of the surrounding topography. (Lehning et al., 2000)

Appendix IV. Agreement scores, an objective snow profile comparison method

An algorithm to objectively compare snow pit profile to simulated SNOWPACK profile is presented here. This method can also be used to compare different model profiles. The comparison is made for temperature, density, snow type, snow liquid water content and grain size. A quantitative agreement-disagreement score is calculated for each parameter. These are combined to give an overall score of profile agreement. The method is developed in the Swiss Federal Institute for Snow and Avalanche Research (SLF) in Davos. This appendix is based on the article by Lehning et al. (2001).

For the purposes of this study minor changes were made to the procedure described here. Liquid water content was not taken into account in calculations, and weighing factors for all of the studied properties were kept as 1.

1. Comparison algorithm

The modelled profile has a much higher resolution and finer structure than the observed profile and an error in the calculated settling rate might have shifted the layers. Because of these reasons it is necessary to perform a mapping. The first step in the mapping is to adjust for potentially different snow heights in the modelled and observed profiles.

1.1 Stretching

The model profile is stretched linearly to compensate for the snow depth differences. Let $z_i'^{\mathrm{mod}}$ describe the nodes (layer boundaries) of the model profile and $z_{nM}'^{\mathrm{mod}}$ and z_{nO}^{obs} the total snow heights of the model and observed profiles, respectively. The mapping into the new coordinates z_i^{mod} is done:

$$z_i^{\mathrm{mod}} = z_i'^{\mathrm{mod}} \frac{z_{nO}^{obs}}{z_{nM}'^{\mathrm{mod}}} =: z_i'^{\mathrm{mod}} s \tag{1}$$

Here, s is the stretch factor which is constant for all layers. The index of the nodes or layer boundaries is i: $0 \leq i \leq nM$. All model profile quantities keep their identical values, except for the density and the volumetric fractions. It can be used for the new layer density, ρ_l^{mod}:

$$\rho_l^{\mathrm{mod}} = \frac{\rho_l'^{\mathrm{mod}}}{s} \tag{2}$$

Here, l is the layer index ($0<l<=nM$). The same stretch factor can be used for the volumetric contents of ice and water:

$$\theta_l^{water} = \frac{\theta_l'^{water}}{s} \tag{3a}$$

and

$$\theta_l^{ice} = \frac{\theta_l^{'ice}}{s} \tag{3b}$$

1.2 Mapping

Next step is the mapping of individual layers of the observed profile onto layers of the model profile. The mapping function determines for each observed layer a selection of one or more layers in the model profile. A normalized agreement score will be calculated between the observed layer and this selection of model layers.

Layer characteristics:

For layer characteristics such as grain type, grain size or the volumetric water content the observed profile is chosen to be the master profile and try to find for each observed layer the best correspondence in the model profile. For the layer *i* in the observed profile between $z_{i\text{-}1}^{\text{obs}}$ and z_i^{obs}, a height range is determined for the corresponding model profile in which the parameters are compared. An increased tolerance range is allowed for layers in the middle of the snow cover:

$$z_{\text{upper}}^{\text{mod}}=z_{\text{i}}^{\text{obs}}+\text{Wt}_{\text{i}};\ z_{\text{lower}}^{\text{mod}}=z_{\text{i-1}}^{\text{obs}}\text{-Wt}_{\text{i-14}} \tag{4}$$

With

$$t_i = \frac{(z_{nO}^{obs} - z_i^{obs})z_i^{obs}}{z_{nO}^{obs}} \tag{5}$$

The tolerance functions that have a maximum in the middle of the snow cover. The maximum range of the tolerance is determined by the factor, *W*. Here *W*=0.2.

Point measurements:

For point measurements such as temperature or sometimes density, the mapping is less complicated. For the series of point measurements, T^{obs}, at snow depths z_j^{obs}, we make a linear interpolation. Temperature is interpolate between the two model nodes above and below z_j^{obs}:

$$T^{\text{mod}}(z_j^{obs}) = \frac{z_i^{\text{mod}} - z_j^{\text{mod}}}{z_i^{\text{mod}} - z_{i=1}^{\text{mod}}} T_i^{\text{mod}} + \frac{z_j^{obs} - z_{i-1}^{\text{mod}}}{z_i^{\text{mod}} - z_{i=1}^{\text{mod}}} T_{i-1}^{\text{mod}} \tag{6}$$

Bulk measurements:

For the series of bulk measurements (such as density), R^{obs}, with interface depths, z_j^{obs}, corresponding values are constructed from the model profile by introducing artificial model nodes at the heights, z_j^{obs}:

$$R_j^{\mathrm{mod}} = \frac{1}{z_j^{obs} - z_{j-1}^{obs}} \left(R_m^{\mathrm{mod}} (z_m^{\mathrm{mod}} - z_{j-1}^{obs}) + \sum_{i=1}^{n-1} R_{m+1}^{\mathrm{mod}} (z_{m+1}^{\mathrm{mod}} - z_{m+i-1}^{\mathrm{mod}}) + R_n^{\mathrm{mod}} (z_j^{obs} - z_{n-1}^{\mathrm{mod}}) \right) \quad (7)$$

where $z_{m-1}^{\mathrm{mod}} < z_{j-1}^{\mathrm{obs}} \leq z_m^{\mathrm{mod}}$ and $z_{n-1}^{\mathrm{mod}} \leq z_j^{\mathrm{obs}} < z_n^{\mathrm{mod}}$.

A bulk portion of the model profile is selected exactly matching the height range over which the bulk measurement has been performed. The model parameter is averaged over this height range.

2. Agreement scores

The comparison between the measured and modelled profiles leads to a non-dimensional quantitative measure of agreement for each parameter. A score of 1 is the maximum and 0 stands for no agreement.

2.1 Grain type

The comparison is based on the international classification by Colbeck et al. (1990). Each layer is characterized by two basic grain shapes $F1$ and $F2$, the latter standing for the minority type.

For all model layers k within the tolerance borders (equation 4), the difference to the observed layer l is determined as follows:

$$\begin{aligned} d_{lk}^{11} &= d(F1_l^{\mathrm{obs}}, F1_k^{\mathrm{mod}}) \\ d_{lk}^{22} &= d(F2_l^{\mathrm{obs}}, F2_k^{\mathrm{mod}}) \\ d_{lk}^{12} &= d(F1_l^{\mathrm{obs}}, F2_k^{\mathrm{mod}}) \\ d_{lk}^{21} &= d(F2_l^{\mathrm{obs}}, F1_k^{\mathrm{mod}}), \end{aligned} \quad (8)$$

where Table 1 below gives F. The four scores between the basic grain shapes need to be combined into one distance number for the combination observed layer l and model layer k. We define therefore:

$$d_{lk}^{straight} = \frac{d_{lk}^{11} + d_{lk}^{22}}{2} \quad (9a)$$

and

$$d_{lk}^{cross} = \max(0.\frac{d_{lk}^{12} + d_{lk}^{21}}{2} - 0.1) \quad (9b)$$

Table 1. Measure of agreement d() for all combinations of basic grain types

Norm. distance		INTL.	1	2	3	4	5	6	7	4c
Grain types		SLF	1	2	3	4	5	7	6	9
INTL.	SLF	SYMB	+	/	•	□	Λ	○	V	∩
1	1	+	1	0.8	0.5	0.2	0	0	0	0.2
2	2	/	0.8	1	0.8	0.4	0	0	0	0.4
3	3	•	0.5	0.8	1	0.4	0.1	0	0	0.5
4	4	□	0.2	0.4	0.4	1	0.8	0	0	0.8
5	5	Λ	0	0	0.1	0.8	1	0	0	0.7
6	7	○	0	0	0	0	0	1	0	0
7	6	V	0	0	0	0	0	0	1	0
4c	9	∩	0.2	0.4	0.5	0.8	0.7	0	0	1

Now it is possible to calculate the measure of agreement d_{lk}^{type} for each model layer k as:

$$d_{lk}^{type}=\max(d_{lk}^{straight}, d_{lk}^{cross}). \qquad (10)$$

Now the actual score for the observed layer is calculated, which corresponds to one or more model layers. The difference is defined as the weighted average of the differences over the extent of the observed layer. It is assumed that the model height range as determined by equation 4 starts with z_m^{mod} and ends with z_n^{mod}. Introducing the layer thickness, L, a normalized score for each observed layer can be defined as:

$$d^{type_l^{obs}} = \max_{\substack{z_{l2}^{mod}\le z_n^{mod} \\ z_{l1}^{mod}\ge z_m^{mod}}} \left(\frac{1}{\sum_{l=l1}^{l2} L_l^{mod}} \sum_{l=l1}^{l2} d^{type_l^{mod}} L_l^{mod}\right) \qquad (11)$$

with $l1$, $l2$ such that:

$$\sum_{l=l1}^{l2} L_l^{mod} \le L_l^{obs} \qquad (12a)$$

and

$$\sum_{l=l1}^{l2+1} L_l^{mod} \rangle L_l^{obs} \qquad (12b)$$

The equation above states that we take a window of depth z_n^{mod} and slide it through the height range to find the best correspondence.

Finally, the score for the whole profile is obtained. The normalized measure of the quality of the model grain type profile is calculated by a weighted average over all observed layers:

$$d_{profile}^{type} = \frac{1}{z_{nO}^{obs}} \sum_{l=1}^{nO} d^{type_l^{obs}} L_l^{obs} \qquad (13)$$

A simple average over the number of observed layers can also be performed:

$$d^{type}_{profile} = \frac{1}{nO}\sum_{l=1}^{nO} d^{type_l^{obs}} \tag{14}$$

2.2 Grain size

For grain size, a relative deviation is defined by assuming that the difference in the largest grains between the model profile and the observed profile is only due to a different definition of the grain size. So the layer grain sizes *rg* are normalized by the size of the largest grains in each profile:

$$rg_n = \frac{rg}{\max(rg)} \tag{15}$$

A normalized agreement measure:

$$d^{size}{}_l^{\mathrm{mod}} = 1 - |rg_n^{\mathrm{obs}} - rg_n^{\mathrm{mod}}|, \tag{16}$$

The overall normalized score for each observed layer and finally the whole profile is obtained identically using equations 11 and 14.

2.3. Liquid water content

Only three classes of liquid water content are needed to distinguish for the comparison: dry, wet and saturated. The comparison values are listed in the Table 2, where the model liquid water content (MLWC) and the manually observed snow moisture (OC) are translated into moisture comparison values (cv). The normalized score is:

$$d^{wet_l^{\mathrm{mod}}} = 1 - \frac{|cv^{obs} - cv^{\mathrm{mod}}|}{2} \tag{17}$$

and the overall score for each observed layer and finally the whole profile is again obtained in analogy to equations 11 and 14.

Table 2. Comparison values for snow moisture.

MLWC (%)	cv	OC (1-5)
0	0	1
0<MLWC<5	1	1-2, 2, 2-3
>5	2	3, 4, 5

2.4. Temperature and density

Because temperature and density in the field are usually measured at regular intervals, the vectors with an equal and identical spacing of length *N* are obtained from the mapping of point as well as bulk measurements, and the layer depth weighting does not has to be performed again. In order to receive an agreement measure between 0 and 1 the normalizing has to be done. The maximum and minimum values for normalization are used. Since a possible offset is also of interest, one maximum and minimum value is determined for the combined observation/model data set. This approach will create small scores for systematic deviations:

$$d_{profile}^{T,\rho} = \frac{1}{N} \frac{N - \sum_{1=1}^{N} \left| T, \rho_l^{obs} - T, \rho_i^{\mathrm{mod}} \right|}{\max(T, \rho^{obs/\mathrm{mod}}) - \min(T, \rho^{obs/\mathrm{mod}})} \tag{18}$$

3. Overall agreement score

The scores of the individual parameters all describe the agreement between two profiles as a number between 0 and 1. These individual scores can be combined in a weighted sum to yield a single number that describes the overall score between two profiles:

$$d_{profile} = \frac{1}{\sum_{i=type,size,wet,T,\rho} w^i} \sum_{i=type,size,wet,T,\rho} w^i d_{profile}^i \tag{19}$$

The weights of 35, 25, 25, 10 and 5 for grain type, temperature, density, grain size and liquid water content, respectively, are normally used in SLF studies in order to get an agreement score.

Appendix V. Overall agreement scores between observations and the different test runs.

	19.1.		1.2.		16.2.		5.3.		17.3.		4.4.
Dirilecht	0,61	addDepth	0,8	Dirilecht	0,65	addWS	0,85	Precipitat	0,78	dimTG	0,65
IL precip	0,6	addGlob	0,79	Iqbal	0,65	addGlob	0,85	Dirilecht	0,7	Precipitat	0,64
addDepth	0,59	density	0,79	Precipitat	0,65	addTsnow	0,85	dens_old	0,69	dimGlob	0,64
addWS	0,57	albedo	0,79	IL precip	0,64	addTG	0,85	addTsnow	0,68	addRH	0,62
alb_old	0,57	Dirilecht	0,78	IL snow	0,63	dimGlob	0,85	addTG	0,68	dimRH	0,62
dimTsnow	0,56	Iqbal	0,78	addDepth	0,63	density	0,85	dimGlob	0,68	addTsnow	0,61
density	0,55	addTG	0,78	3h	0,63	new_alb	0,85	density	0,68	dimTsnow	0,61
Iqbal	0,52	dimTair	0,78	6h	0,63	albedo	0,85	new_alb	0,68	dens_old	0,61
addTair	0,52	dimGlob	0,78	addWS	0,62	Control	0,85	Control	0,68	addWS	0,6
addGlob	0,52	new_alb	0,78	addGlob	0,61	dimTair	0,84	addRH	0,67	addGlob	0,6
addTsnow	0,52	water	0,78	addTG	0,61	dimRH	0,84	dimTsnow	0,67	alb_old	0,6
addTG	0,52	Control	0,78	dimGlob	0,61	dimTsnow	0,84	water	0,67	water	0,6
dimTair	0,52	IL precip	0,77	dimTsnow	0,61	dimTG	0,84	6h	0,67	Dirilecht	0,59
dimGlob	0,52	dimRH	0,77	new_alb	0,61	dens_old	0,84	dimWS	0,66	dimDepth	0,58
new_alb	0,52	dimTsnow	0,77	alb_old	0,61	6h	0,84	dimTG	0,66	IL precip	0,5
albedo	0,52	3h	0,77	albedo	0,61	Longwave	0,83	alb_old	0,64	Iqbal	0,25
3h	0,52	Precipitat	0,76	Control	0,61	addTair	0,83	IL precip	0,63	Longwave	0,25
Control	0,52	addWS	0,76	addTsnow	0,6	alb_old	0,83	addDepth	0,61	IL snow	0,25
Precipitat	0,51	new_grsz	0,76	dimTair	0,6	water	0,83	Iqbal	0,6	addTair	0,25
dimRH	0,51	Longwave	0,74	dimRH	0,6	dimWS	0,82	IL snow	0,6	addTG	0,25
water	0,51	alb_old	0,71	dimTG	0,6	new_grsz	0,81	addTair	0,6	addDepth	0,25
6h	0,51	IL snow	0,7	new_grsz	0,6	IL precip	0,79	addWS	0,6	dimTair	0,25
IL snow	0,5	addTsnow	0,7	water	0,6	Dirilecht	0,77	dimTair	0,6	dimWS	0,25
addRH	0,5	addTair	0,68	Longwave	0,59	IL snow	0,75	dimRH	0,59	density	0,25
dimTG	0,5	dimWS	0,68	density	0,59	Iqbal	0,74	albedo	0,59	new_alb	0,25
dens_old	0,5	dimTG	0,68	dimDepth	0,58	addRH	0,73	new_grsz	0,57	new_grsz	0,25
new_grsz	0,49	dens_old	0,68	dens_old	0,58	3h	0,73	addGlob	0,56	albedo	0,25
dimWS	0,47	6h	0,67	addRH	0,57	Precipitat	0,71	dimDepth	0,56	3h	0,25
dimDepth	0,45	addRH	0,66	addTair	0,56	addDepth	0,71	3h	0,56	6h	0,25
Longwave	0,44	dimDepth	0,66	dimWS	0,56	dimDepth	0,7	Longwave	0,54	Control	0,25

REPORT SERIES IN GEOPHYSICS

1. Noponen, I., 1974: Comparison of crust and upper mantle structure between shield and arc areas.
2. Palosuo, E. 1975: Pintaveden lämpötila- ja suolaisuuskartasto Pohjanlahdella, I. Kesäkausi. Atlas of surface water temperatures and salinities on the Gulf of Bothnia, I. Summerperiod.
3. Hiltunen, T., Huttula, T., 1976: Vanajaselän virtausoloista talvella. (Current measurements in the ice covered water of Vanajanselkä).
4. Hiltunen, T., 1976: Vesimassojen liikkuminen Vanajanselällä kesällä 1975. Käsiluotaushavainnot. (The movement of water in Lake Vanajanselkä in summer 1975. Part I).
5. Uusitalo, S., 1976: Mean surface velocities on southern Bothnian Bay determined by an indirect method.
6. Palosuo, E., Hiltunen, T., Jokinen, J., Teinonen, M., 1977: Lumen kitkan vaikutus suksen luistoon. The effect of friction between snow and skis.
7. Virta, J., 1978: A rainfall-runoff model for catchment areas with an abundance of lakes.
8. Tyrväinen, M., 1978: Lämpötilaolot Suomenlahdella sekä mallisovellutuksia. Temperature conditions and simulation in the Gulf of Finland.
9. Mäki-Lopez, M.-L., 1978: Geomagnetic variation study in Hidalgo and Grant counties, southwestern New Mexico, USA.
10. Keinonen, J., Palosuo, E., Korhonen, P., Suominen, H., 1978: Lumen ja suksenpohjanmuovien välisen kitkan mittauksia. Measurements of friction between snow and sliding materials of ski.
11. Palosuo, E., 1978: Hiihtokauden ajoittumisesta Suomessa. The length of the skiing season in Finland.
12. Pellinen, R., 1979: Induction model and observations of onset of magnetospheric substorms.
13. Palosuo, E., Keinonen, J., Suominen, H., Jokitalo, R., 1979: Lumen ja suksenpohjamuovien välisen kitkan mittauksia. Osa 2. Measurements of friction between snow and ski running surfaces. Part 2.
14. Nevanlinna, H., 1980: Geomagnetic secular variation described by dipole models.
15. Kahma, K. K., 1981: On the growth of wind waves in fetch-limited conditions.
16. Palosuo, E., 1982: Jään vahvistaminen Finlandia-82 hiihdon lähtöpaikalla. Strengthening of the ice at start of the Finlandia-82 ski event.
17. Pihkala, P., Spring, E., 1982: A simple dilatometer for determination of the free water of the snow.
18. Leino, M. A. H., Spring, E., Suominen, H., 1983: Coefficients of kinetic friction of skis on snow determined from sliding length and velocity of the skier.
19. Leino, M. A. H., Spring, E., 1984: Determination of the coefficient of kinetic friction between ski and snow from the gliding velocity of a skier.
20. Pihkala, P., Spring, E., 1985: A practical method for photographing snow samples.
21. Erkkilä, J., Hämäläinen, T., Pihkala, P., Savolainen, S., and Spring, E., 1985: A cinematographic method for determination of the kinetic friction of skis on snow.
22. Pihkala. P., Spring, E., 1986: Determination of the contact area between ski and snow using a simple thermal conductivity meter.
23. (Distribution limited)
24. Pulkkinen, K., 1989: Calibration and basic manipulation of SC-ADCP data.
25. Pulkkinen, K., 1991: Water sample -based calibration of VARIOSENS turbidity meter with some comparisons with other soundings.
26. Simojoki, H., 1992: Geofysiikan tulo oppiaineeksi Helsingin yliopistossa (2nd ed.).
27. Leppäranta, M., Haapala, J. (eds.), 1993: Proceedings of the first workshop on the Baltic sea ice climate, Tvärminne, Finland, 22-26 August 1993.
28. Vihma, T. (ed.), 1994: Evening sessions of the summer school on physics of ice-covered seas, Savonlinna, Finland, 6-17 June 1994.
29. Pulkkinen, K., 1995: STD-12 mini-CTD:n käyttö ja datan kalibrointi (English summary: The use of STD-12 mini-CTD and calibration of data).
30. Pulkkinen, K., (ed.), 1995: Underwater optical measurements made during the first concentrated field effort (CFE 1) of NOPEX - A data report.
31. Multala, J., Hautaniemi, H., Oksama, M., Leppäranta, M., Haapala, J., Herlevi, A., Riska, K., and Lensu, M., 1995: Airborne electromagnetic surveying of Baltic sea ice.
32. Pulkkinen, K., (ed.), 1995: Proceedings of the 2nd Finnish-Estonian seminar on underwater optics with applications, Helsinki, 10-12 April 1995.
33. Launiainen, J., and Cheng, B., 1995: A simple non-iterative algorithm for calculating turbulent bulk fluxes in diabatic conditions over water, snow/ice and ground surface.
34. Stipa, T., 1996: Water renewal and vertical circulation of Pohja Bay.
35. Haapala, J., Alenius, P., Dubra, J., Klyachkin, S. V., Kõuts, T., Leppäranta, M., Omstedt, A., Pakstys, L., Schmelzer, N., Schrum, C., Seinä, A., Strübing, K., Sztobryn, M., and Zaharchenko, E., 1996: IDA. Ice data bank for Baltic Sea climate studies.
36. Leppäranta, M., (ed.), 1996: AISA lake experiment 1993-94. Final Report.
37. Haapala, J., Leppäranta, M. (eds.), 1997: ZIP-97 data report.
38. Pulkkinen, K., (ed.), 1998: Proceedings of the 4th Finnish-Estonian seminar on underwater optics with applications, Lammi, 22-24 April 1997.
39. Saloranta, T. M., 1998: Snow and snow ice in sea ice thermodynamic modelling.
40. Leppäranta, M., (ed.), 1998: Downscaling in sea ice geophysics.
41. Herlevi, A., (ed.), 1999: The optics ground truth of the Finnish SALMON experiment.
42. Haapala, J., 2000: Modelling of the seasonal ice cover of the Baltic sea.
43. Zhang, Z., 2000: On modelling ice dynamics of semi-enclosed seasonally ice-covered seas.
44. Jevrejeva S., V.V. Drabkin, J. Kostjukov, A. A. Lebedev, M. Leppäranta, Ye. U. Mironov, N. Schmelzer and M. Sztobryn, 2002: Ice time series of the Baltic Sea.
45. Herlevi, A. 2002: Inherent and apparent optical properties in relation to water quality in Nordic waters.
46. Leppäranta, M. (ed.), 2003, Proceedings of the seminar “Sea Ice Climate and Marine Environments in the Okhotsk and Baltic Seas – The Present Status and Prospects”.
47. Rasmus, K., H. Granberg, K. Kanto, E. Kärkäs, C. Lavoie and M. Leppäranta, 2003: Seasonal snow in Antarctica data report.

ISBN 952-10-2378-3
ISSN 0355-8630

Helsinki 2005
Yliopistopaino
Pikapaino